NANYANG TECHNOLOGICAL UNIVERSITY

DESIGN AND SYNTHESIS OF CHIRAL ORGANOPALLADIUM-AMINE COMPLEXES

YAP SEE LENG JEANETTE

SCHOOL OF PHYSICAL AND MATHEMATICAL SCIENCES

2013

DESIGN AND SYNTHESIS OF CHIRAL ORGANOPALLADIUM-AMINE COMPLEXES

YAP SEE LENG JEANETTE

School of Physical & Mathematical Sciences

A thesis submitted to the Nanyang Technological University
in fulfillment of the requirement for the degree of
Doctor of Philosophy

2013

ACKNOWLEDGEMENTS

I would like to express my sincere gratitude to my supervisor, Professor Leung Pak Hing for his support and patient guidance throughout the course of my study.

I would also like to thanks Dr. Sumod, for offering his helps and support. I really appreciate your encouragements.

I am extremely grateful to all the administration and technical Support staffs in CBC especially, Ms Celine Hum, Ms Tan Wei Ting, Ms Tan Shi Min, Ms Goh Ee Ling, Ms Zhu Wen Wei, Ms Pui Pang Yi, Ms Seow Ai Hua and Mr Hendra for kind assistances and advices.

I would like to extend my genuine appreciation to Dr. Li Yongxin for carrying out the X-ray crystallographic studies on the complexes I have synthesized. I am truly very indebted to Dr. Li Yongxin for his contributions.

I would also like to express my gratitude to my former senior co-workers in Professor Leung's research group: Dr. Ding Yi, Dr. Chiang Mingyi, Dr. Xu Chang, Dr. Cheow, Dr. Luo Ding, Dr. Zhang Yi, Dr. Tan Kien-Wee, Dr Chen Shuli, and Dr. Huang Yinhua who have provided generous help and invaluable advices. I am also very thankful to my lovely laboratory mates and friends Kim Hong, Kennard, Xiang Yuan, Esther, Feny and Bin Bin for bringing lots of laughter and joy to brighten up my life in the laboratory. I would like to thank all summer, FYP and exchange students especially, Emma, Jeremy, Jonathan, Duy and Vinod for lending their helping hands.

I would also like to acknowledge the Nanyang Technological University for awarding the research scholarship to pursue my Ph.D. study.

Last but not least, my deepest gratitude to my family members for providing their unquestionable support and understanding throughout my study.

TABLE OF CONTENTS

CHAPTER 1: INTRODUCTION

CHAPTER 2: SYNTHESIS OF 1-(2,5-DI-TERT-BUTYLPHENYL)-*N*,*N*-DIMETHYLETHANAMINE AND ITS ORTHO-PALLADATED STUDIES, AN UNEXPECTED N–C BOND CLEAVAGE

Abbreviations and Symbols

acac	acetylacetonate
AccuTOF	Accurate Time of Flight
Aq	aqueous
Ar	aryl
ax	axial
Bn	benzyl
Bu	butyl
br	broad
c	concentration for optical rotation analysis
calcd	calculated
conc.	concentrated
$CDCl_3$	chloroform-d_1
CD_2Cl_2	dichloromethane-d_2
$CHCl_3$	chloroform
CH_3CN	acetonitrile
Claisen's alkali	a strong base prepared by 8.81 g KOH dissolved in 6 ml of water and diluted to 25 ml with methanol
d	doublet
DART	Direct Analysis in Real Time
dba	dibenzylideneacetone
DCM	dichloromethane
dd	doublet of a doublet
de	diastereomeric excess
dec	decomposed
dm	decimetre
DMAD	dimethyl acetylene dicarboxylate
DMPP	3,4-dimethyl-1-phenylphosphole
dppe	1,2-bis(diphenylphosphino)ethane
eq	equatorial
ESI	Electrospray Ion Source
Et	ethyl
g	gram(s)
h	hour(s)
HCl	hydrochloric acid
Hex	hexyl

HRMS	High Resolution Mass Spectroscopy
Hz	hertz
i	iso
m	multiplet
Me	methyl
MeOH	methanol
MeCN	acetonitrile
mg	milligram(s)
mmol	millimole(s)
M.p.	melting point
nm	nanometer
NMR	Nuclear Magnetic Resonance
Noe	Nuclear Overhauser effect
o	ortho
p	para
Pr	propyl
Ph	phenyl
ppm	parts per million
q	quartet
qn	quintet
rt	room temperature
R	rectus (Latin: right absolute configuration)
ROESY	2D rotating frame Nuclear Overhauser Enhancement
S	sinister (Latin: left absolute configuration)
s	singlet
t	triplet
t	tertiary
TFA	trifluoroacetic acid
THF	tetrahydrofuran
tol	tolyl
Å	angstrom(s)
δ	NMR chemical shift in ppm
$[\alpha]_D$	specific rotation measured at sodium D line (589 nm)

List of Figures

List of Tables

Summary

This thesis describes the design and synthesis of chiral organopalladium-amine complexes and their applications in stoichiometric asymmetric synthesis.

A brief introduction on the organopalladium-amine complexes, the research development and the objective of this project were presented in Chapter 1.

In Chapter 2, a functionalized amine, 1-(2,5-di-*tert*-butylphenyl)-*N*,*N*-dimethylethanamine was designed and synthesized, but the *ortho*-palladation reaction did not give the desired palladacycle. An unexpected C–N bond cleavage was observed and gave two C–N bond cleavage complexes. The mechanistic studies on the formation of C–N bond cleavage complex was carried out, but no substantial conclusion can be made yet. The initial step is likely *β*-hydride elimination and it is a base promoted reaction.

Chapter 3 describes the synthesis of slightly less bulky amine ligand, 1-(2,5-di-*iso*-propylphenyl)-*N*,*N*-dimethylethanamine from *p*-di-iso-propylbenzene. By optimizing the reaction conditions including replacement of some of the reagents, it resulted in increased of the overall yield of the amine ligand. The *ortho*-palladation reaction gave the desired palladacycle and C–N bond cleavage complex by varying the palladating agent used. The racemic dimeric complex was resolved by separation of the (*S*)-prolinate diastereomeric derivatives *via* column chromatography. The efficiency of the palladacycle was assessed *via* the asymmetric intramolecular *endo*-cycloaddition reaction and a better stereoselectivity was obtained.

In chapter 4 describes the synthesis of an electron-withdrawing group functionalized benzyl palladacycle to investigate the electronic effect of the palladacycle in asymmetric Diel-Alder reaction. The amine ligand, 1-(2,5-dichlorophenyl)-*N*,*N*-dimethylethanamine was synthesized *via* three step synthetic

route with high overall yield and *ortho*-palladation with $Pd(OAc)_2$ to give the acetate-bridged dimeric palladacycle. The racemic dimer was resolved with optically active sodium prolinate and by treatment of the corresponding diastereomer with aqueous 1M HCl produced the chiral chloro-bridged dimer. The efficiency of the palladacycle was examined *via* Diels-Alder reaction between DMPP-coordinated complex and ethyl vinyl ketone, however poor stereoselectivity was observed. The chiral dimeric complex was converted to the cationic complex and used in asymmetric hydrophosphination reaction between diphenylphosphine and DMAD to give one diastereomeric product.

Chapter 1: Introduction

1.1 Palladacycles

Palladacycles or cyclopalladated complexes are commonly defined as any palladium complexes containing a Pd–C bond, wherein the carbon atom is part of a chelate ligand and the chelate is stabilized further by the presence of one or two neutral donor atoms (i.e N, P, As, O, or S). In this thesis, the palladacycles would represent functionalized benzyl- or naphthyl-amine cyclopalladated such as complexes **1** and **2**.

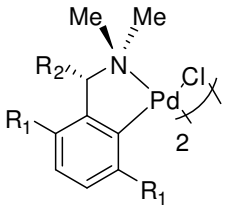

(*S*)-**1**

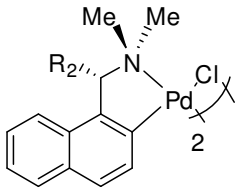

(*S*)-**2**

R_1,R_2 = alkyl, aryl, halogen *etc*.

Palladacycles can be generally classified by their chelating ligand into two categories, the anionic four-electron donor ligand (CY-type) palladacycle **3** or the anionic six-electron donor ligand (YCY pincer type) palladacycle **4**. The CY type palladacycles exist as halogen or acetate bridged dimers in either *cisoid* or *transoid* conformations. The metalated ring size can vary from three to eleven members, with the five- or six-membered rings being the most common ones. The YCY pincer type palladacycles are further divided into symmetrical metalated rings and the unsymmetrical metalated rings. Symmetrical type consist of two equivalent size rings and unsymmetrical type is the mixture of two different metalated ring sizes.[1]

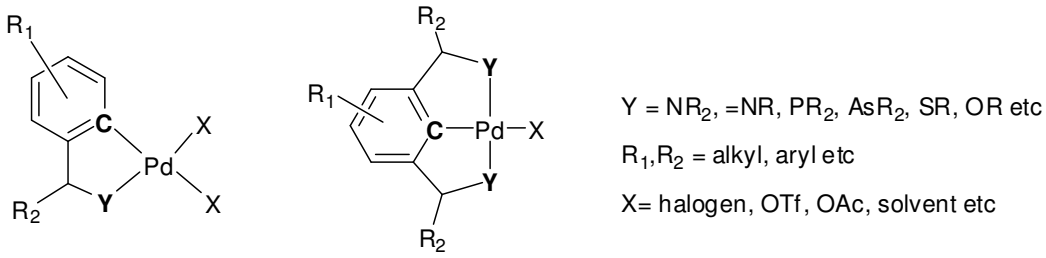

3 **4**

In mid 1960s, Cope and Siekman[2] discovered and characterized the first palladacycle **5** generated from azobenzene and palladium(II) chloride (Scheme 1.1).

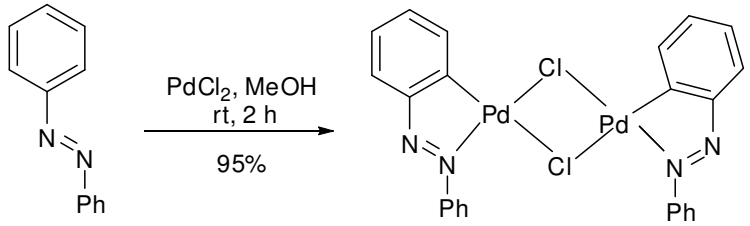

5

Scheme 1.1

Palladacycles only started to gain prominence in the 1990s after Herrmann *et al.* highlighted the use of palladated complex **6**, synthesized from tris(*o*-tolyl)phosphine (Scheme 1.2), as a catalyst precursor in palladium-catalyzed Heck reactions.[3]

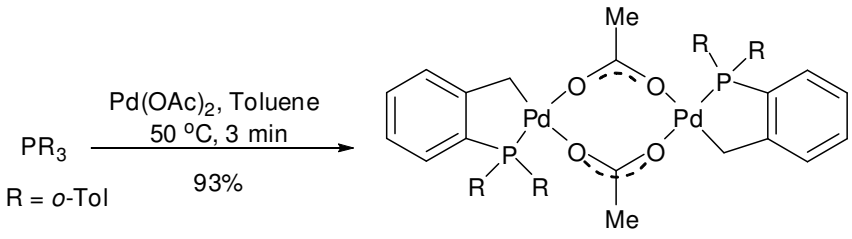

6

Scheme 1.2

The cyclopalladated complexes are also applicable in many aspects such as optical resolution of racemic ligands[4], highly versatile catalytic reactions, organic and asymmetric synthesis.[1,5-7]

1.2 Nitrogen-Donor Complexes

Majority of the palladacycles contain heteroatoms such as N, P or S. The following discussion will be focused mainly on aromatic nitrogen-donor palladacyles.

The cyclopalladation of nitrogen-donor ligands have gained great awareness due to their versatility and potential in many applications.[1,5-7] They are categorized by the functional group of the N atom for example amine, ferrocenylmethylamine, pyridine, quinoline, benzoquinoline, amide, imine, iminophosphorane and benzylideneamines *etc* functionalized ligands.

1.2.1 Amine Functionalized Ligands

In 1968, Cope and Friedrich had reported the first benzylamine cyclopalladated complex **7**, di-μ-chlorobis(*N*,*N*-dimethylbenzylamine-C,N) dipalladium(II). Complex **7** is obtained in high yield as shown in Scheme 1.3.[8]

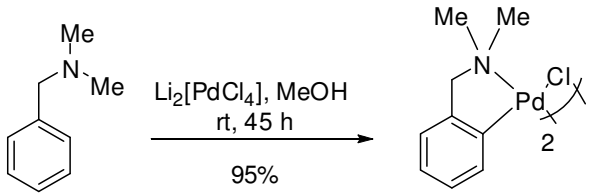

7

Scheme 1.3

In their report, both *N*,*N*-dimethylbenzylamine and *p*-methoxy-*N*,*N*-dimethylbenzylamine reacted successfully with $Li_2[PdCl_4]$ to give the desired cyclopalladated complexes. However, unsubstituted benzylamine, secondary benzylamine *N*-methylbenzylamine and *p*-nitro-*N*,*N*-dimethylbenzylamine did not give the desired cyclopalladated complexes, the coordination complexes, dichlorobis(amine)palladium(II), $[(Pd_2Cl_2(amine)_2)]$ were obtained instead. The

findings of Cope and Friedrich suggested the following general requirements for successful cyclopalladation for amine ligands.

(i) The nitrogen must be tertiary, (ii) the palladacycle formed should be a five-membered ring; and (iii) the carbon on the aromatic ring which hydrogen is displaced by palladium must not be deactivated towards electrophilic attack.

In the early 1970s, the first chiral benzylamine cyclopalladated complex was prepared by Otsuka and co-workers using chiral amine ligand (*S*)-*N*,*N*-dimethyl-α-methylbenzylamine as shown in Scheme 1.4. This chiral palladacycle (*S*)-**8** was applied in kinetic resolutions of tertiary phosphines.[9]

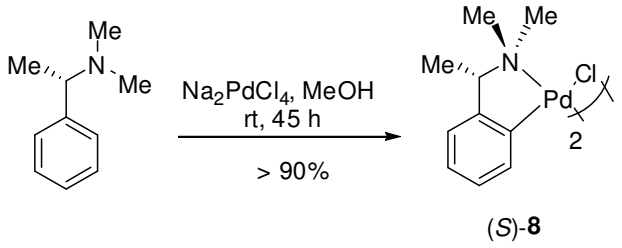

(*S*)-**8**

Scheme 1.4

In 1975, Julia *et al*. used naphthalenylmethanamine ligands to successfully synthesize palladacycles **9**, **10** and **11**.[10]

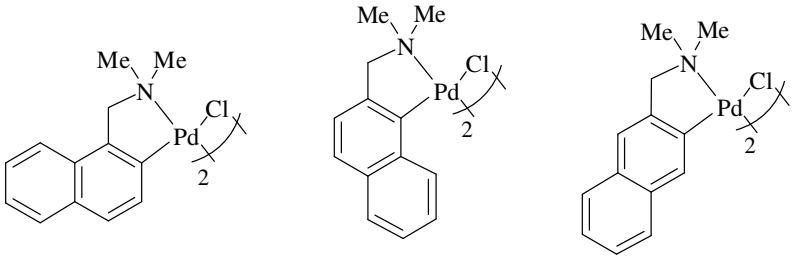

9 **10** **11**

Two years later, Tani and co-workers synthesized chiral naphthalenylethanamine complex (*R*)-**12** by reacting $Na_2[PdCl_4]$ with (+)-(*R*)-*N*,*N*-dimethyl-α-(2-naphthyl)ethylamine in the presence of triethylamine (Scheme 1.5).[11]

The chiral complex (*R*)-**12** was found to be effective in the resolution of racemic tertiary phosphines.

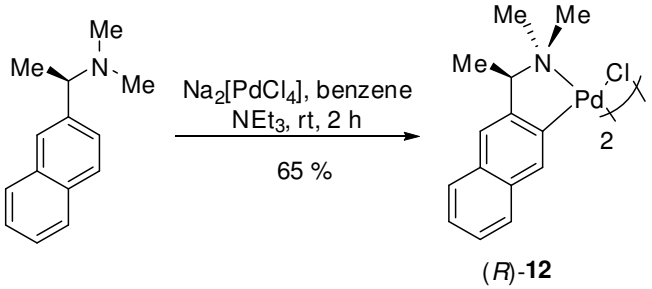

(*R*)-**12**

Scheme 1.5

Subsequently in 1982, Wild *et al.* synthesized chiral naphthalenylethanamine complex (*R*)-**13** with chiral ligand, (+)-(*R*)-*N*,*N*-dimethyl-(2-naphthyl)ethylamine shown in Scheme 1.6.[12] This complex (*R*)-**13** was successfully used to resolve methylphenyl(8-quinolyl)phosphine and its arsenic analogue.

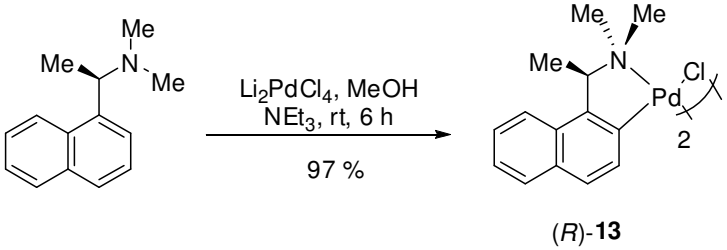

(*R*)-**13**

Scheme 1.6

From 2002 onwards Leung *et al.* had reported several chiral derivatives of benzylamine and naphthalenylethanamine based palladium complexes such as (*S*)-**14**[13a], (*S*)-**15**[13b], (*S*)-**16**[13c] and (*S*)-**17**[13d] by using $[Pd(NCMe)_4](ClO_4)_2$ for (*S*)-**14** to (*S*)-**16**, and $Li_2[PdCl_4]$ for (*S*)-**17** as palladium source. These optically active complexes are designed and synthesized to improve the selectivity in asymmetric cycloaddition reaction of DMPP with a variety of dienophiles.

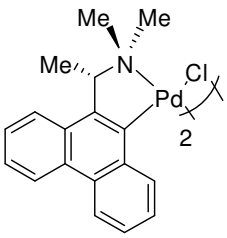
(*S*)-**14**

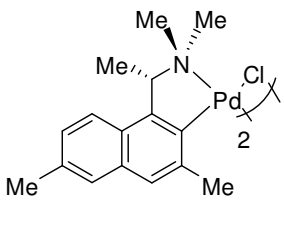
(*S*)-**15**

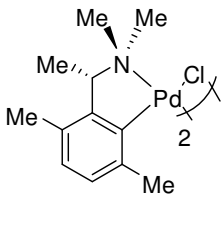
(*S*)-**16**

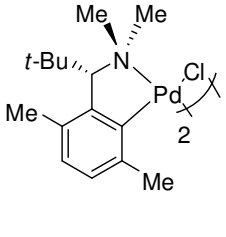
(*S*)-**17**

There are several exceptions to the general requirements outlined by Cope and Friedrich for cyclopalladation. For example, when the ligand is 8-methylquinoline the resultant palladacyle has the palladium centre bonded to the aliphatic carbon instead of the aromatic carbon.[14] Although it was in the requirement outlined by Cope and Friedrich, the nitrogen has to be tertiary for successful cyclopalladation, it has been demonstrated that under suitable condition (For example, changing palladating agent), even primary amine can be successfully cyclopalladated.[15]

For example Lewis *et al.* demonstrated the cyclopalladation with a primary amine **18**, under Cope's reaction conditions to give the *ortho*-palladated complex **19** in 1973 (Scheme 1.7). This reaction is likely promoted by the presence of sterically hindered substituent at the α-carbon.[15,16]

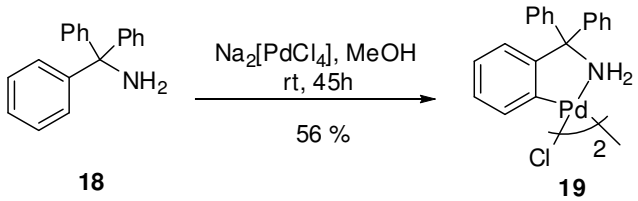

18 **19**

Scheme 1.7

In another example Avshu *et al.*, successful prepared *ortho*-palladated complex **21** from a diiodobis(amine)palladium(II) complex **20** (Scheme 1.8).[17]

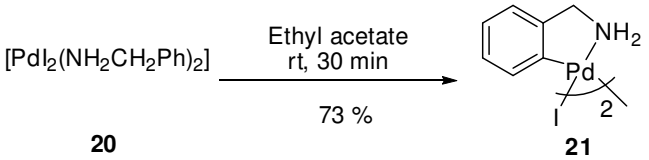

20 **21**

Scheme 1.8

Other palladating agents like $Pd(acac)_2$ and $Pd(OAc)_2$ are also able to promote successful cyclopalladation of primary amines. The *ortho*-palladation of benzylamine with $Pd(acac)_2$ to give complex **22**was reported by Baba *et al*. in 1975[18] (Scheme 1.9) and in 1993, Fuchita *et al*. use $Pd(OAc)_2$ reacting with benzylamine to give the acetate-bridged complex **23** (Scheme 1.9).[19] Since Fuchita's discovery, $Pd(OAc)_2$ has become the popular palladating agent for synthesis of primary amine palladacycles.

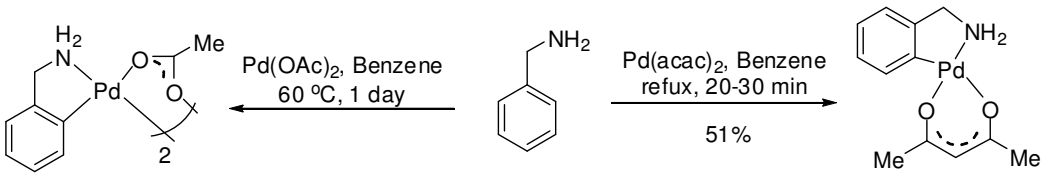

23 **22**

Scheme 1.9

In 1995, Vincete *et al*. reported the first palladacycle benzylamine that is substituted with an electron-withdrawing group on the aromatic ring as shown in Scheme 1.10.[20] Vincete continued to expand the scope to bioactive primary amines and derivatives such as phentermine, (*S*)-tryptophan methyl ester[21a], (*S*)-phenylalanine methyl ester[21b], homoveratrylamine and (*S*)-tyrosine methyl ester[21c], with $Pd(OAc)_2$ as the palladating agent.

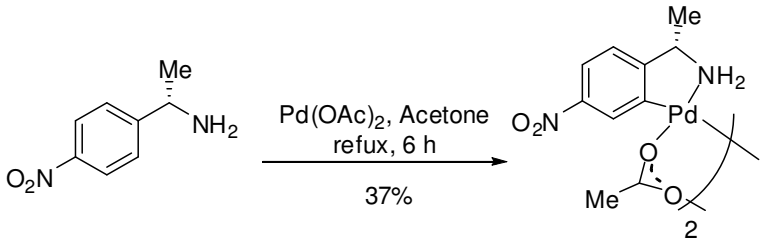

24 **25**

Scheme 1.10

1.2.2 Iminphosphoranes ligands

Iminphosphoranes are any imino derivative of a phosphorane with a general formula of $R_3P{=}NR'$ where R,R' = alkyl, aryl, acyl, *etc*. In 1997, Alper reported the

first example of cyclopalladation of iminphosphoranes **26** with $Na_2[PdCl_4]$ to give the dimeric cyclopalladated complexe **27** (Scheme 1.11).[22]

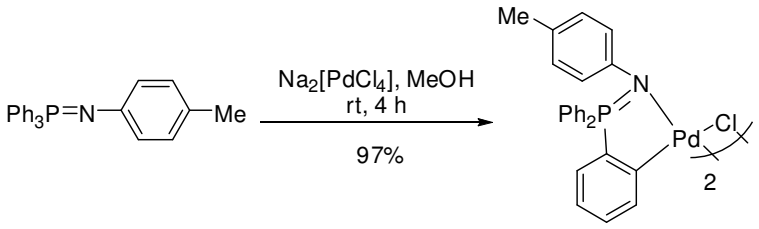

26 **27**

Scheme 1.11

In 2003, Vincete *et al*. cyclopalladated iminophosphoranes **28** using $Pd(OAc)_2$ in THF to give the palladacycles **29** (Scheme 1.12).[23]

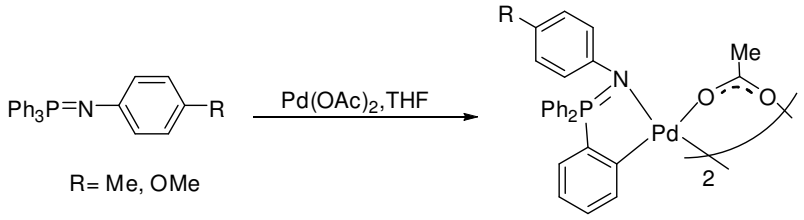

28 **29**

Scheme 1.12

It was not until 2005 where Bielsa *et al*. demonstrated that the presence of neutral and anionic complexes by reaction of the dimeric complex **31** (Scheme 1.13) with thallium acetylacetonate [TI(acac)], triphenylphosphine (PPh_3), and silver perchlorate ($AgClO_4$) in acetonitrile (NCMe) to give monomeric complexes **32**, **33** and **34** respectively.[24]

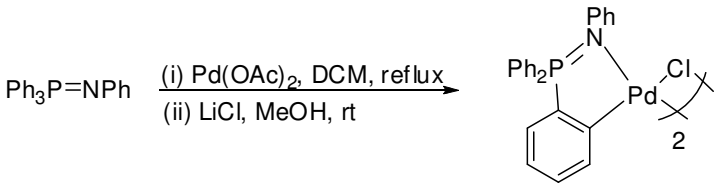

30 **31**

Scheme 1.13

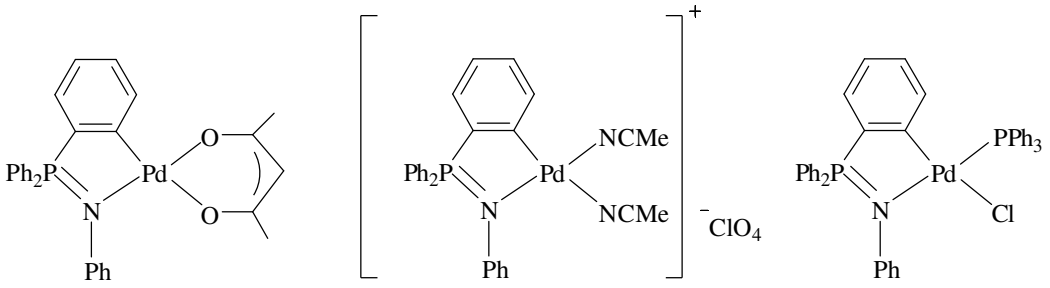

32 **33** **34**

1.2.3 NCN Pincer-type Ligands

The first pincer-type palladium complex **35** was reported by Moulton and Shaw in 1976.[25] While the first NCN pincer-type ligand, palladium complex, **36**, was reported by Koten and Noltes in 1978.[26] These complexes are the most important class of ligand in organometallic chemistry due to it extraordinary thermal stability. They are useful catalyst such as Heck and Suzuki–Miyaura coupling reactions, catalyst immobilisation, optical devices and sensor materials.[27]

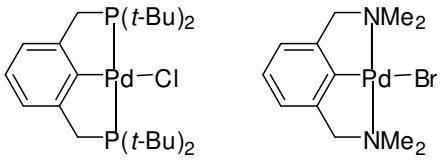

35 **36**

In 2003, van Koten *et al.* synthesized *p*-functionalized NCN-pincer palladium complex **37** to study the electronic influences of the *p*-substituent. The *p*-functionalized NCN-pincer palladium complexes were applied as Lewis acid catalysts in the double Michael reaction between methyl vinyl ketone and ethyl α-cyanoacetate, and small differences in their catalytic activities were observed.[27b]

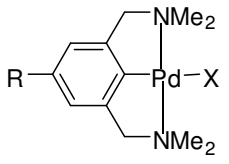

R= H, NO_2, NMe_2, C(O)Me, OCH_2Ph, Ph, $SiMe_3$
X= Cl, Br

37

In 2004, Uozumi *et al*. reported a NCN pincer palladium complex **39** (Scheme 1.14) bearing pyrroloimidazolone groups that was found to catalyze Heck reaction between aryl iodide and methyl acrylate at high catalytic activity (TON: 520 x10^6).[27d]

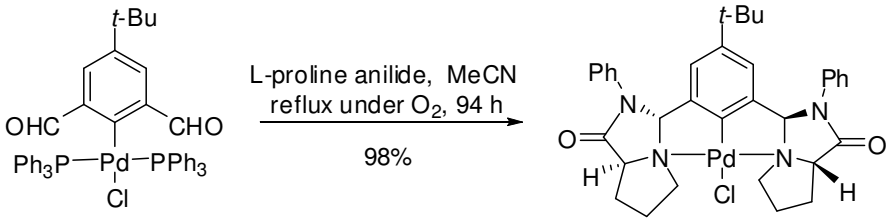

38 **39**

Scheme 1.14

This year, Arai *et al*. have reported the use of NCN pincer palladium complex **40** as catalyst for the asymmetric synthesis conjugate addition of malononitrile to nitroalkenes in reasonably good yield and enantiomeric excess (Scheme 1.15). [27g]

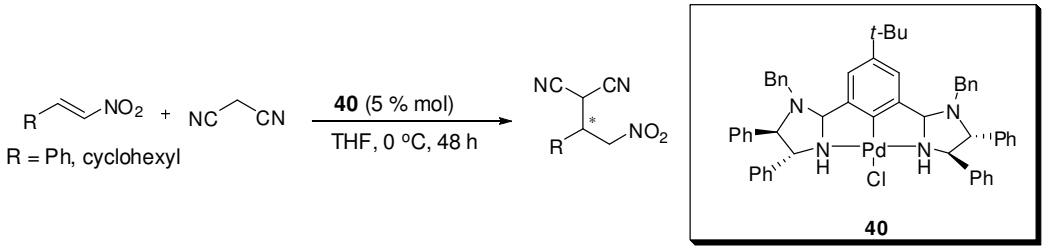

Scheme 1.15

1.2.4 Other Nitrogen-Donor Complexes

Cyclopalladated complexes (**41**-**60**) can be generated from other nitrogen-donor ligands such as benzylideneamines, ferrocenylmethylamines, pyridine, quinoline, benzoquinoline, and amide, with different palladation sources.[28-45]

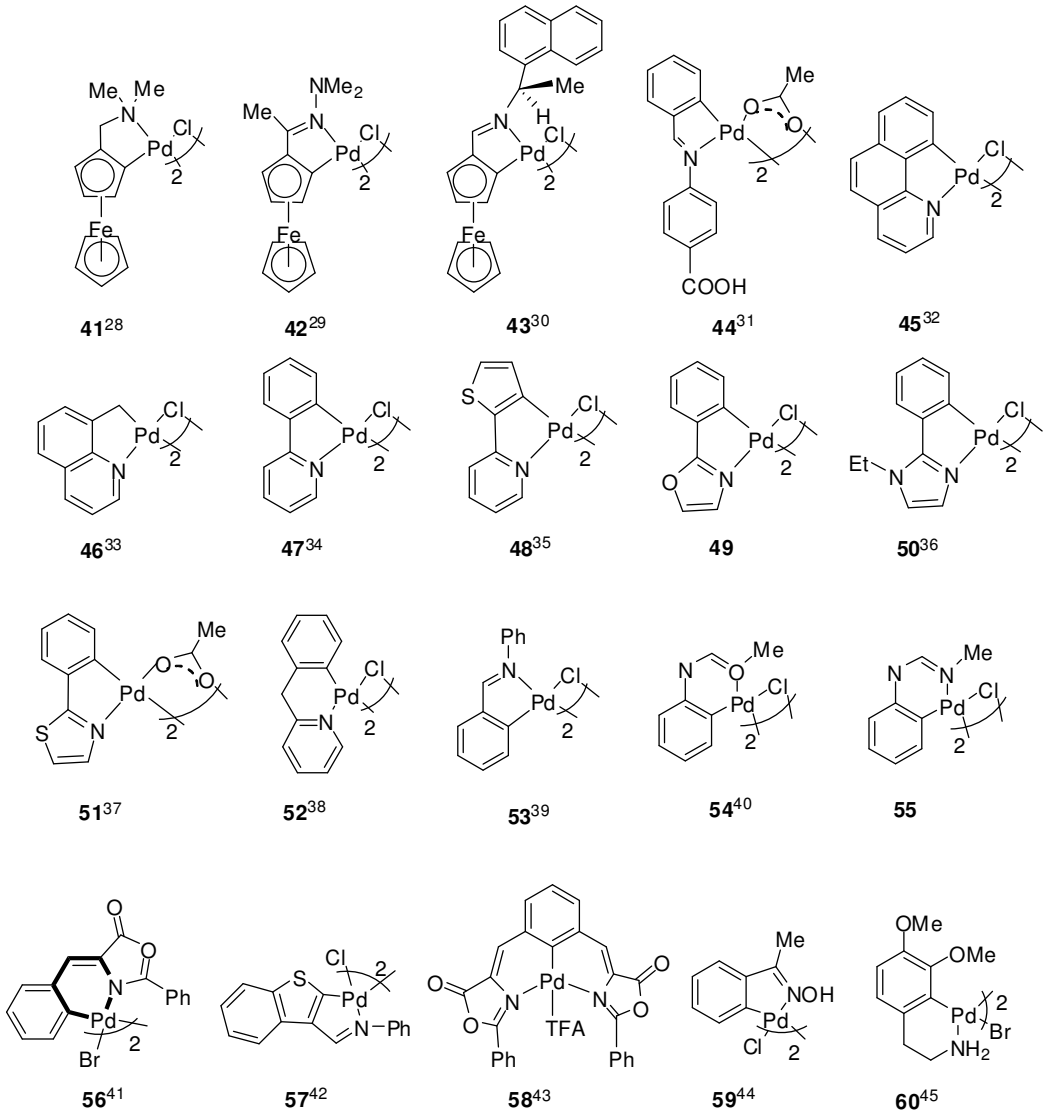

41[28] **42**[29] **43**[30] **44**[31] **45**[32]

46[33] **47**[34] **48**[35] **49** **50**[36]

51[37] **52**[38] **53**[39] **54**[40] **55**

56[41] **57**[42] **58**[43] **59**[44] **60**[45]

1.3 Methods of Preparation

There are several methods available for the synthesis of palladacycles. They are C–H activation, ligand exchange, transmetalation and oxidative addition.

1.3.1 C–H Activation (*ortho*-Palladation)

The simplest, most direct and most representative approach for the preparation of palladacycles is *via* C–H activation also known as *ortho*-palladation. It is generally accepted, base on Cope's work that the palladium center behaves as electrophile.[2,8]

Direct *ortho*-palladation, which is also an aromatic substitution reaction, involves the interaction of the palladium source (such as $Pd(OAc)_2$, $Li_2[PdCl_4]$) with the organic ligand. Base is occasionally added to the reaction to facilitate the cleavage of the C–H bond of the ligand for the formation of the C–Pd σ bond.

Commonly used palladating agents include palladium acetate ($Pd(OAc)_2$), tetrachloropalladate salts ($M_2[PdCl_4]$, M = Li or Na) or tetrachloropalladated salts with bases such as triethylamine and sodium acetate. Lithium and/or sodium tetrachloropalladate are the mildest and therefore by default are the initial choices. If the desired palladacyle is not formed, and instead results in the formation of the coordination complex, $[PdCl_2(amine)_2]$, $Pd(OAc)_2$ will be the next preferred option. $Pd(OAc)_2$ adopts multiple roles when it is used as a palladating agent. It can palladate with aromatic, pseudo-aromatic and aliphatic ligands. In addition, it aids the solvolysis process. It also acts as an intramolecular base for deprotonation of the C–H bond. Finally, $Pd(OAc)_2$ also enhances the electrophilicity of the palladium center.

Other important factors in the *ortho*-palladation reaction are

(i) the molar ratio of amine to palladium source; (ii) the type of palladation agent; (iii) the polarity of solvent; and (iv) the reaction temperature.

Polar solvent such as methanol, acetone, acetonitrile as well as in binary water-organic mixtures are preferred in cyclopalladation. Generally, cyclopalladation will occur readily at ambient temperature; however, heating might be required in certain cases.

1.3.2 Ligand Exchange (Transcyclopalladation)

Ligand exchange reactions involve reaction of the cyclopalladated complex (chloro- or acetato-bridged complex) with an organic ligand with donor center (*eg.* N or P donor) to form a new palladacycle in the present of acetic acid.[46] This method is

employed when either C–H activation failed or the yield obtained *via* C–H activation is not quantitative. For instance, the direct *ortho*-palladation of ligand, 1,3-bis(methylthiomethy1)benzene **61** with $Pd(OAc)_2$ give a palladacycle **62** of yield less than 10% yield, but *via* ligand exchange method, the yield increase dramatically to 97% (Scheme 1.16). [47]

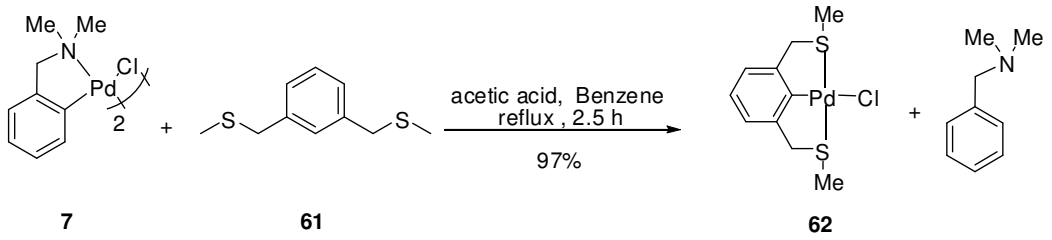

7 **61** **62**

Scheme 1.16

1.3.3 Transmetalation

Transmetalation reaction is a methodology to prepare palladacycles *via* transmetalating agents, such as organolithium or organomercurial regents with palladium source. For example, by reacting the transmetalating agent, **63** with $[PdCl_2(SEt_2)_2]$ under refluxing benzene for 24 h genterated palladacycle **64** (Scheme 1.17).[48]

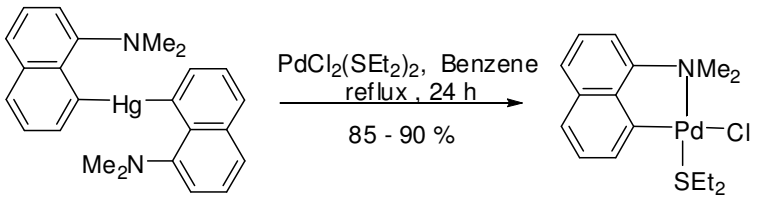

63 **64**

Scheme 1.17

Another example shown in scheme 1.18 is the reaction of organomercury compound **65** with zero-valent palladium complex $Pd_2(dba)_3$ to give the cyclopalladated complex **66**.[49]

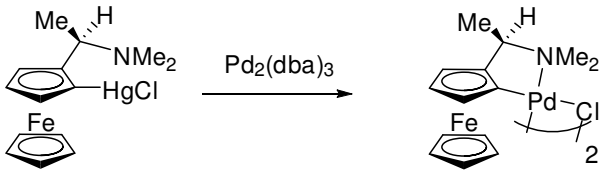

65 **66**

Scheme 1.18

1.3.4 Oxidative Addition

Oxidative addition to a C–X bond (where C = aryl or alkyl and X = halogen or triflate) is another useful method used for synthesis of various palladacycles, when cyclopalladated complexes are not accessible *via* direct *ortho*-palladation. The commonly used palladium source for oxidative addition is $Pd(dba)_2$, $Pd_2(dba)_3$ and $Pd(PPh_3)_4$. This method was successfully applied for the preparation of three- and four-membered ring cyclopalladated complexes, which are not accessible by the C–H bond activation methodology due to their high ring strain about the metal site. For example oxidative addition of aryl halide **67** to Pd(0) source, $Pd(PPh_3)_4$ gave PPh_3-bound monomeric complex **68** (Scheme 1.19).[50]

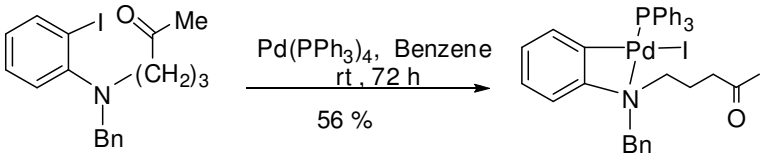

67 **68**

Scheme 1.19

1.4 Applications of Palladacycles

Chiral cyclopalladated complexes have gained attention over the past two decades due to their versatility and significant contribution in many aspects of synthetic chemistry. For instance, they have been used as efficient resolving agents, highly sensitive diamagnetic shift reagents for the determination of enantiomeric

purities of organic compound by NMR spectroscopy, highly versatile catalyst for organic reaction and asymmetric reactions.[1]

1.4.1 Catalysis

The use of palladacycles as catalyst precursors have only intensively studied in recent years. The first application of a palladacycle as catalyst in hydrogenation of the C=C double bond was first reported by Lewis in 1986.[51]

1.4.1.1 Heck Coupling Reactions

Heck reaction is a palladium-catalyzed C–C coupling between unsaturated aryl or vinyl halide or triflates with activated alkenes in the presence of a base to form a substituted alkene (Scheme 1.20). Due to the synthetic potential for C–C bond formation, Heck coupling reactions have gained popularity and have become an important tool in the synthesis of organic molecules. It is an important methodology for peparation of aryl-functionalized alkene with outstanding *trans* selectivity.[52]

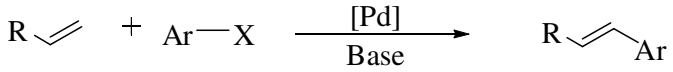

Scheme 1.20

Some examples of nitrogen-containing palladacycles (**69**-**73**) that were used as active catalyst precursors for promotion of Heck coupling reaction (mainly reaction of aryl iodides with acrylic esters). [53-55]

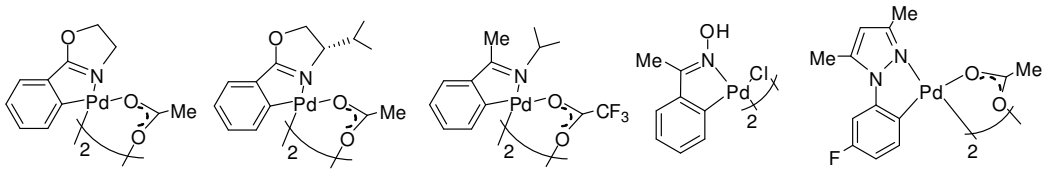

69[53] **70**[53] **71**[53] **72**[54] **73**[55]

1.4.1.2 Cross-Coupling Reactions

Palladacycles are used as catalyst precursors for cross-coupling reactions such as Suzuki, Stille and Sonogashira.

1.4.1.2.1 Suzuki Coupling

Suzuki coupling reactions make use of a palladium catalyst to form C–C bond between an unsaturated (aryl or vinyl) boronic acid with an unsaturated halide or triflate. Boronic esters and organotrifluoroborate salts may be used instead of boronic acids. It is widely used to synthesize conjugated olefins, poly-olefins, styrenes, and substituted biaryls that are useful in the synthesis of natural products and polymers.[56] For example, complex **74** efficiently catalyzes the coupling of aryl bromides with phenylboronic acid (Scheme 1.21).[57]

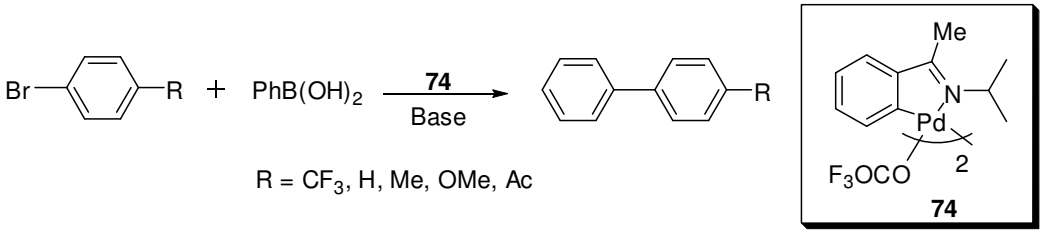

Scheme 1.21

1.4.1.2.2 Stille Coupling

Stille coupling reaction is a C-C bond forming reaction between organotin compound and halides or pseudohalides (such as triflate). The reaction is usually performed under inert atmosphere using anhydrous and degassed solvent. An example is illustrated in scheme 1.22.[58]

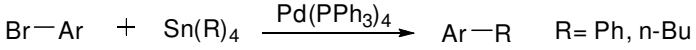

Scheme 1.22

1.4.1.2.3 Sonogashira Reactions

Sonogashira reaction involved the coupling of terminal alkynes with unsaturated halide or triflate, catalyzed by a palladium catalyst with a CuI co-catalyst in the presence of an amine base to give disubstituted alkynes. For example, cyclopalladated ferrocenylimines **75**, was used as catalyst in the decarboxylative coupling of alkynyl carboxylic acids with aryl chlorides (Scheme 1.23).[59]

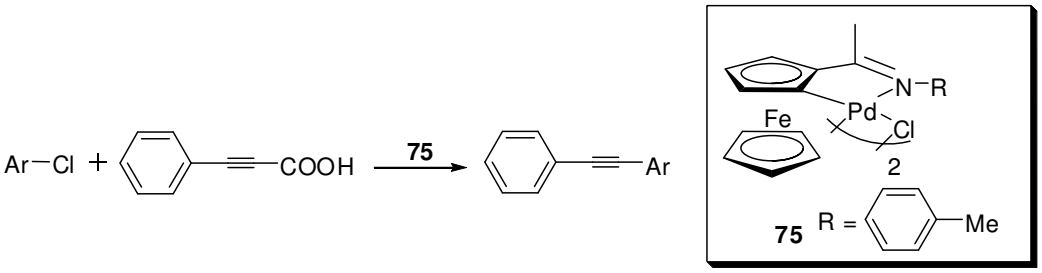

Scheme 1.23

1.4.2 Resolution of Phosphines and Arsines

Palladacylcles, in particular chiral cyclopalladated complexes have been used widely for the resolution of racemic ligands. The resolution of racemic ligands remains an active area of research due to the usefulness of the enantiomerically pure compounds in asymmetric catalysis.[60-61]

The use of chiral cyclopalladeted complexes as resolving agents for resolution of phosphines and arsines have being employed by Wild *et al.*[62-66] and Leung *et al.*[67-69]. The chiral dimeric palladacycles (*R*)-**13** derived from optically pure tertiary amines, interacts with the racemic ligands *via* cleavage of the halo-bridged to give a diastereomeric mixtures that can be separated *via* column chromatography or fractional crystallization in high yield. The absolute configuration of the diastereomers can be easily determined by X-ray crystallography and in some cases NMR spectroscopy. Subsequently, enantiopure ligands can be liberated from the metal

center in the presence of chelating ligand such as dppe or a hard donor ligand such as cyanide. A series of enantiomerically pure ligands (**76**-**81**) have being resolved using chiral palladacycle **13** (Scheme 1.24).[62-69]

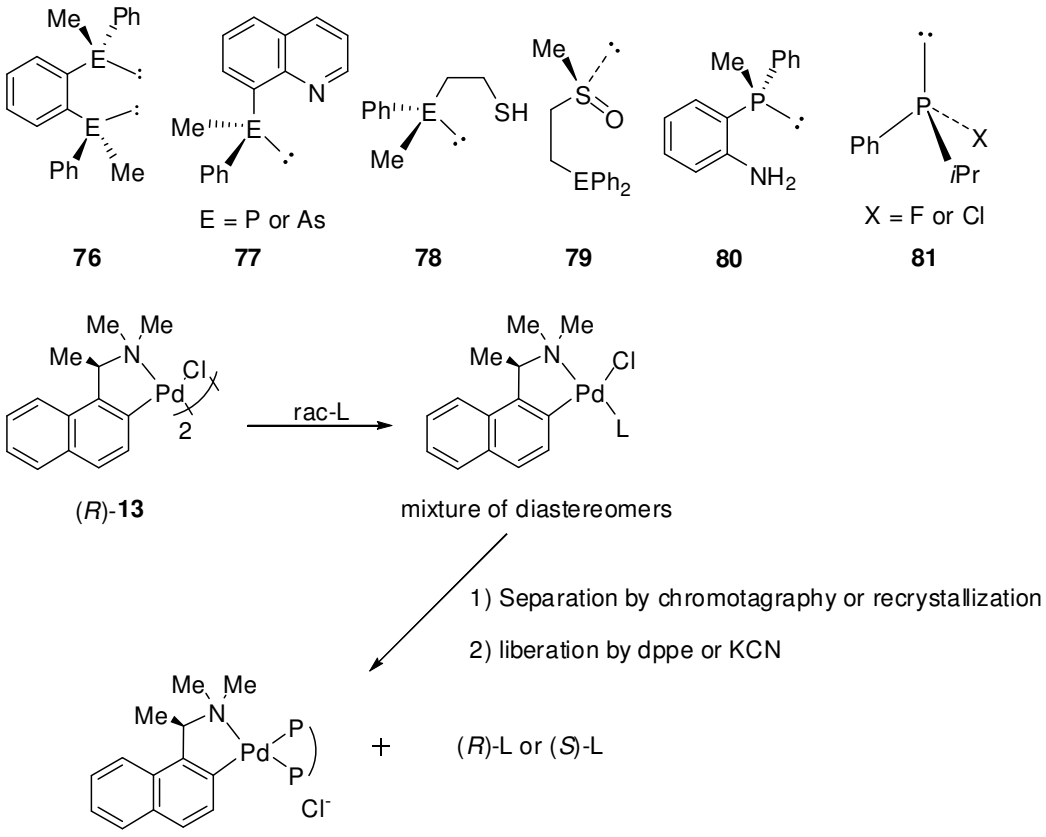

Scheme 1.24

1.4.3 Determination of Enantiomeric Excess

Chiral cyclopalladated complexes can be used to determine the enantiomeric excess of various species in solution similar to the way the chiral ligands such as amino acid, used to determine the enantiomeric excess of the chiral cyclopalladated complexes. Chiral cyclopalladated complexes have being used as chiral agents to facilitate the determination of enantiomeric purity of optically active phosphine, arsines, 1,2-diamines *via* the use of NMR spectroscopy (NOE of ROESY and NOESY,

$^{31}P\{^{1}H\}$ NMR, ^{1}H NMR *etc*). The chiral ligand interacts with the chiral dimeric cyclopalladated complex to give a pair of diastereomers which display distinct NMR signals.

Leung *et al.* commonly used chiral cyclopalladated complex **13** to obtain the enantiomeric excess of a chiral phosphine. For example, complex **13** is use to determine the enantiomeric excess of the chiral tertiary phosphine obtained from the palladacycle-catalyzed asymmetric hydrophosphination of enones[70] (Scheme 1.25).

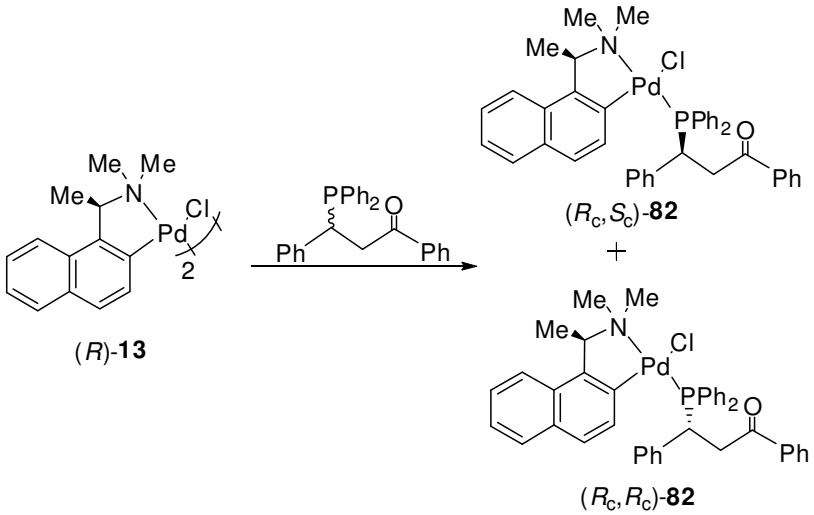

Scheme 1.25

1.4.4 Asymmetric Synthesis

Cyclopalladated compounds have proven to be useful stoichiometric chiral templates for the synthesis of P-chiral phosphines *via* cycloaddition, hydrophosphination *etc*. By systematic manipulation of the subtle stereoelectronic properties of the chiral amine moiety and the metal centers, the palladacycle properties can be modified in order to enhance the stereoselectivity.

1.4.4.1 Asymmetric Diels–Alder reactions

A series of optically pure norbornene-based P-chiral phosphines can be synthesized by asymmetric Diels–Alder reaction. The chiral templates **13** can react with a diene like DMPP, resulting in the formation of the chiral DMPP coordinated complex **83**. Subsequent reaction with a dienophile such as ethyl vinyl ketone or *N,N*-dimethylacrylamide resulted in the formation of *endo*-cycloaddition products (R_C,R_P)- and (R_C,S_P)-**84** (Scheme 1.26).[1,71] The selectivity of the two products obtained at room temperature after 6 days using ethyl vinyl ketone as dienophile is 2.5:1. When the dienophile was replaced by *N,N*-dimethylacrylamide, the ratio obtained after reacting at room temperature for 32 days is 1:2. The major isomer can be isolated *via* column chromatography.

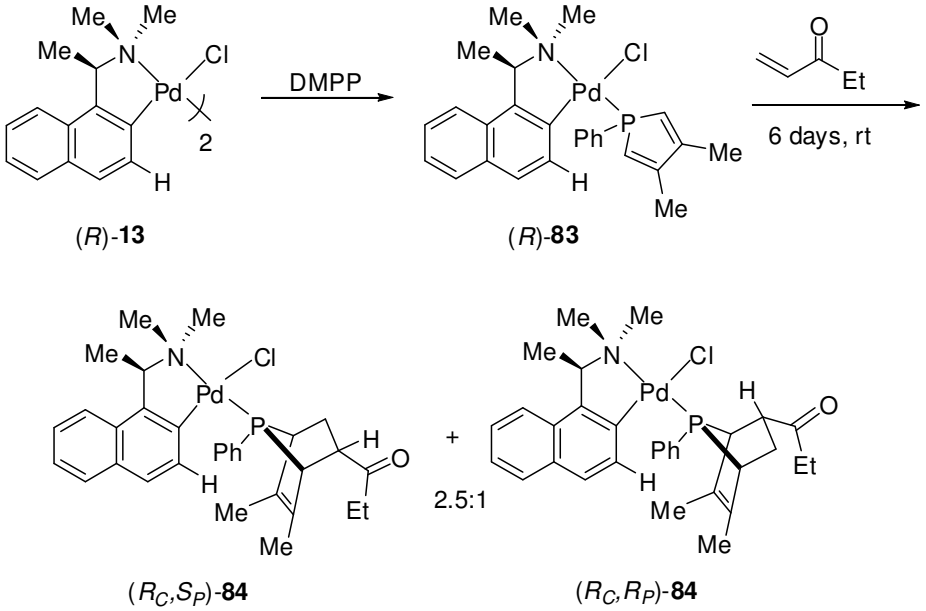

Scheme 1.26

The *exo*-cycloaddition products can also be obtained *via* activation with a chloride scavenger. Firstly, the chloride on the metal center is removed to give complex (*R*)-**85**, followed by addition of the dienophile (Scheme 1.27). This reaction

exhibits high stereoselectivity, resulting in a single product (R_C,S_P)-**86**, the free phosphine ligand is obtained *via* the liberation with dppe or KCN. [1,71]

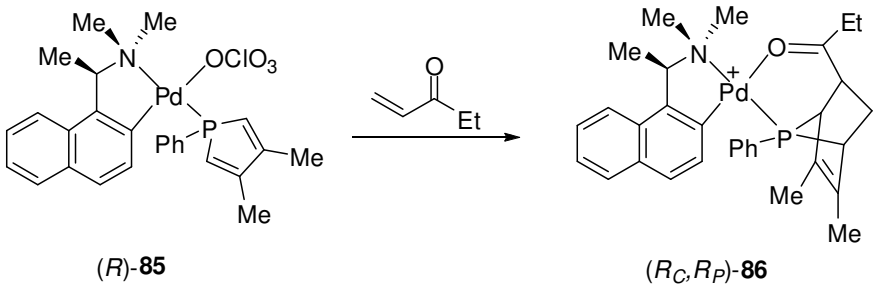

(*R*)-**85** (R_C,R_P)-**86**

Scheme 1.27

As the stereoselectivity of the *endo*-cycloaddition products is relatively low with chiral palladacyle **13**, other chiral palladacycles **14** and **16** were synthesized to improve the stereoselectivity. They react with DMPP to form complexes **87** and **88**.

Similar cycloaddition was conducted with complexes **87** and **88** with *N,N*-dimethylacrylamide (Scheme 1.28) or ethyl vinyl ketone as dienophile (Scheme 1.29). The selectivity of the *endo*-cycloaddition products increases for both from 1:2 to 6:1 for chiral palladacycle (*R*)-**14** and from 2.5:1 to 3.5:1 for chiral palladacycle (*R*)-**16** as compared to complex (*R*)-**13**.

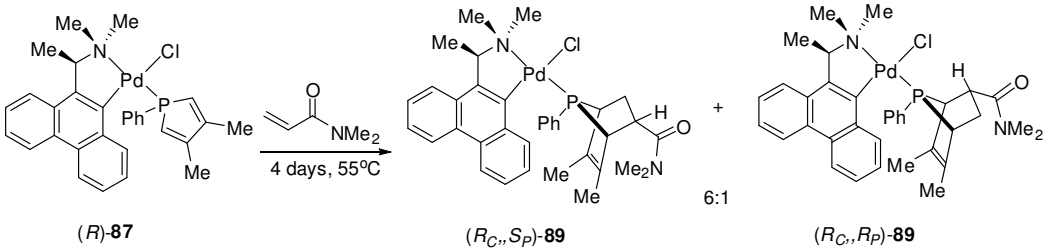

(*R*)-**87** (R_C,,S_P)-**89** (R_C,,R_P)-**89**

Scheme 1.28

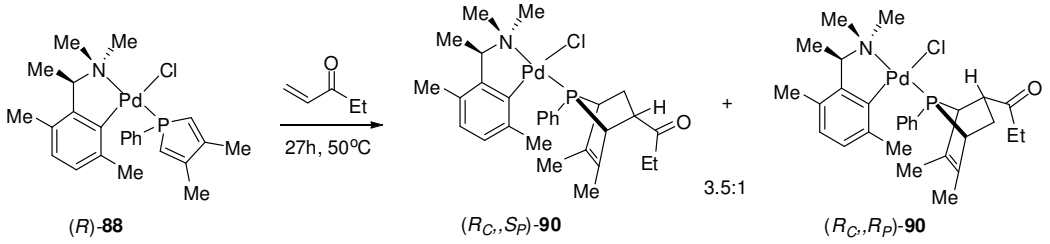

(*R*)-**88** (R_C,,S_P)-**90** (R_C,,R_P)-**90**

Scheme 1.29

1.4.4.2 Hydrophosphination Reaction of Diphenylphosphine with DMAD

The asymmetric synthesis of functionalized optically active phosphines *via* the addition of P–H bond to C–C multiple bonds is an important reaction in organophosphorus chemistry. As the development of enantiomerically pure diphosphines bearing chirality on the carbon backbone, such as chiraphos and prophos, have played important roles in transition metal catalyzed reactions.[72] Despite their vital roles, the preparations of these oxygen-sensitive, highly reactive and potentially unstable chiral ligands are tedious and remain a major challenge. Hydrophosphination reaction can proceed with the assistance of thermal,[73] acid,[74] base,[75] free radical,[76] transition metal catalyst[77] and transition metal palladacycle.[78]

The chiral cyclometalated-amine complex (*S*)-**13** service as efficient chiral template for promoting hydrophosphination reactions between diphenylphosphine and DMAD in the presence of base. The stable bridging chloro ligands in the chiral dimeric complex (*S*)-**13** were replaced by the weakly coordinating acetonitrile ligands to generate a monomeric bis-acetonitrile species (*S*)-**91**. It then reacted with diphenylphosphine and DMAD in the presence of base (NEt_3), resulted in the formation of two diastereomeric products (*S*,*SS*)- and (*S*,*RR*)-**92** in the ratio of 1:6 (Scheme 1.30).[78a] The mixture showed two sets of doublet on $^{31}P\{^{1}H\}$ NMR spectrum at δ 36.6, 57.4 (J_{PP} = 37.8 Hz, minor) and 36.1, 55.3 (J_{PP} = 39.0 Hz, major).

Theoretically, there should be four diastereomeric products from the two newly generated chiral carbon centers, adopting the (*SR*), (*SS*), (*RR*) and (*RS*) configuration. However, for (*SR*) and (*RS*) configuration, one of the ester groups must occupy a sterically unfavourable axial position, regardless of the conformation of the organometallic ring on the naphthylamine moiety. On the other hand, for (*SS*) and (*RR*) configuration, the two ester groups can occupy the favourable equatorial position.

Since the five-membered ring of the naphthylamine moiety is locked in λ conformation, the newly generated bidentate P–P five-membered ring at the palladium center will prefer to adopt the same λ ring conformation. This is due to inter-chelating repulsion between the amine naphthylamine moiety and the bidentate diphosphine. Therefore, resulting in (*S*,*RR*)-**92** as the major product.

The two diastereomeric products cannot be fully separated by column chromatography. The mixture is treated with concentrated HCl and the racemic dichloro complex (*RR*)-**93** was obtained after repeated crystallisation. The complex (*RR*)-**93** shows a singlet resonance signal at δ 58.1 in the $^{31}P\{^{1}H\}$ NMR spectrum. Further treatment of the complex (*RR*)-**93** with aqueous cyanide liberated the symmetrical bidentate diphosphine ligand (*RR*)-**94**. The free ligand shows a singlet resonance signal at δ -6.2 in the $^{31}P\{^{1}H\}$ NMR spectrum.

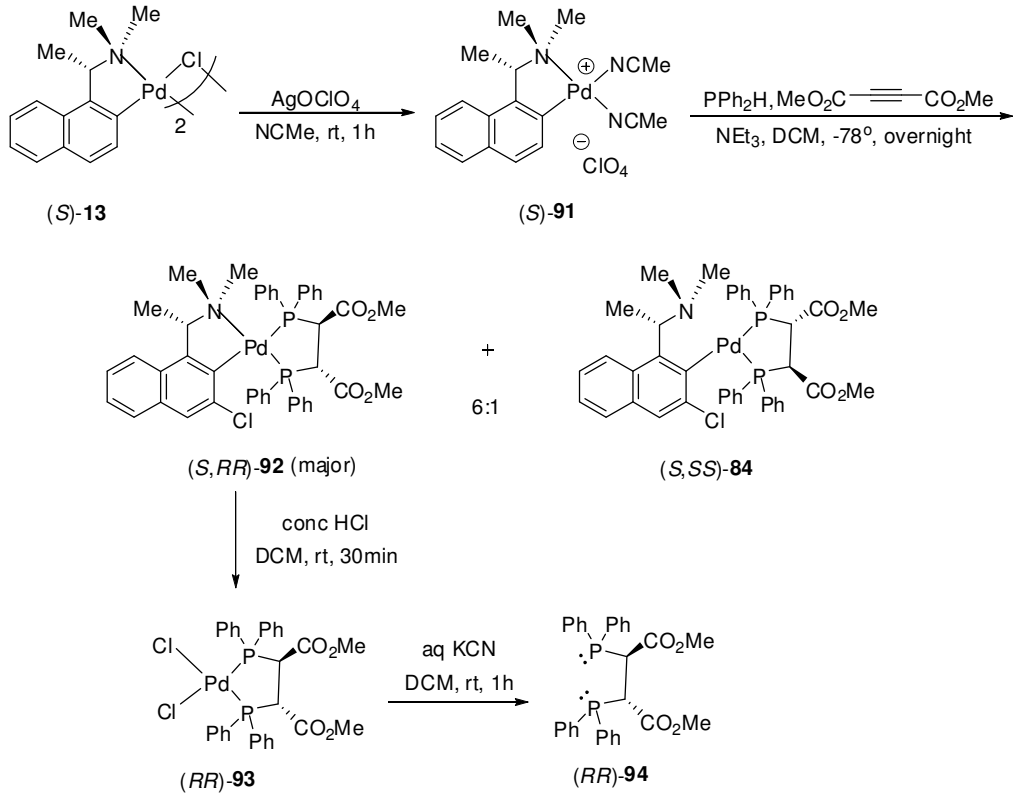

Scheme 1.30

1.5 Aim of the Work

The above studies show that the chiral palladacycle **13** exerts a weak stereochemical influence on the *endo*-cycloaddition reaction, and through the addition of steric hindrance, a spacer group to the aromatic ring adjacent to the Pd–C bond can improve the stereoselectivity of the cycloaddition products. Taking into account of these findings, this project aims to develop novel chiral *ortho*-palladated complexes with bulkier spacer group and also to explore the electronic effect on the stereoselectivity of the cycloaddition.

CHAPTER 2

SYNTHESIS OF 1-(2,5-DI-*TERT*-BUTYLPHENYL)-*N*,*N*-DIMETHYLETHANAMINE AND ITS *ORTHO*-PALLADATED STUDIES, AN UNEXPECTED N–C BOND CLEAVAGE

2.1 Introduction

Recognizing the relevance of optically pure palladacycles in the field of catalysis, we have been inspired toward the design and synthesis of novel, chiral *ortho*-palladated complexes, notably (*S*)-**8** and (*S*)-**13**. Both auxiliaries have been successfully implemented as catalysts for hydrophosphination, hydroarsination and hydroamination, providing yields and selectivity of up to 99 %.

Both (*S*)-**8** and **13** have similar electronic properties; with one coordination site disposed *trans* to the *ortho*-metalated C atom of the strong π accepting aromatic ring and another *trans* to the prochiral σ donating NMe_2 group.

However, it has been seen that (*S*)-**13** gave better stereoselectivity when compared to (*S*)-**8** in various asymmetric applications.[71] The steric interaction between H8 and the *methyl* group on the stereogenic carbon center confines the methyl group to the axial position and hence locking the organometallic five-membered ring into the stable and non- interconvertible λ conformation in both solid and solution. This locking aids in the efficient transmission of chirality onto the neighbouring coordination site. The absence of ring lock in (*S*)-**8** allows dynamic interconversion between the λ and δ conformations in solution, thus leading to flipping of the organometallic five-membered ring in solution and subsequent diminished stereoselectivity.

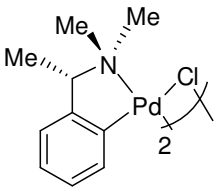

(*S*)-**8**

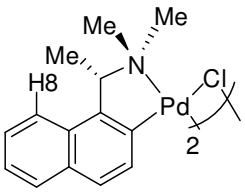

(*S*)-**13**

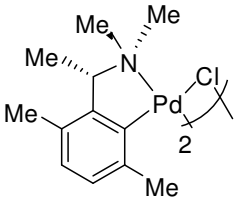

(*S*)-**16**

Hence, the naphthylamine palladacycle (*S*)-**13** was chosen for the asymmetric *endo* [4+2] cycloaddition reaction between cyclic diene DMPP with a series of dienophiles to give phosphanorbornene cycloadducts.[71] Yet poor stereoselectivity was observed with some dienophiles such as ethyl vinyl ketone and *N*,*N*-dimethylacrylamide. The reaction of the DMPP coordinated naphthylamine palladacycle, (*S*)-**83** with ethyl vinyl ketone, gave two diastereomeric *endo*-cycloadducts mixture ((*S*$_C$,*S*$_P$)- and (*S*$_C$,*R*$_P$)-**84**) of 1:2.5 ratio at room temperature for 6 days (Scheme 1.26). This chiral naphthylamine chiral palladacycle (*S*)-**13** exerted weak influences on the reaction site as the coordinated DMPP group experiences a certain degree of free rotation around the P–Pd bond in the transition state. Therefore, another chiral *ortho*-palladated complex (*S*)-**16** with two spacer groups (methyl) introduced on the aromatic ring was developed.[13c] This chiral palladacycle (*S*)-**16** aims to retain the advantages of (*S*)-**13** and also strive to improve the stereoselectivity of the asymmetric *endo* [4+2] cycloaddition reaction. One of the methyl spacer groups will interact with the methyl group at the stereogenic carbon center to fix the conformation of the organometallic five-membered ring. And the second methyl group is introduced on the α–position next to the C–Pd bond to improve the stereochemical influence on the neighbouring reaction site. The cycloaddition reaction between complex (*S*)-**88** and ethyl vinyl ketone, resulted in improvement in the stereoselectivity (Scheme 1.29).

2.2 Research Objectives

We appreciate that a spacer present at the α–position of C–Pd bond will enhance the stereochemical influence on the reaction site. Hence, to increase the stereoselectivity, a novel chiral palladacycle (*S*)-**95** with bulky spacer groups (*t*-butyl) was designed and synthesised. The steric interaction of the bulky *t*-butyl group and the methyl group on the stereogenic carbon was expected to lock the organometallic five-member ring and the *t*-butyl group introduced on the aromatic carbon next to the C–Pd bond to exert more stereochemical influence on the neighbouring reaction site. This influence will likely increase the stereoselectivity of asymmetric *endo* [4+2] cycloaddition reaction as the steric interaction of the *t*-butyl group with the DMPP group will either restrict or reduce the free rotation of the P–Pd bond.

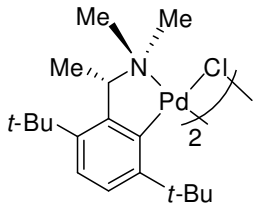

(*S*)-**95**

2.3 Result and Discussion

2.3.1 Synthesis of 1-(2,5-di-*tert*-butylphenyl)-*N*,*N*-dimethylethanamine

As illustrated in Scheme 2.1, 2,5-di-*tert*-butylbromobenzene, **96**[79] reacted with magnesium in dried THF to generated the Grignard reagent **97**. Next, the Grignard reagent **97** reacted with the acetaldehyde to obtain the desired racemic alcohol (±)-**98** in 95 % yield. The racemic alcohol (±)-**98** then reacted with CH_3CN *via* Ritter reaction[80] in strong acid (acetic acid and sulfuric acid) to form amide compound (±)-**99** in 75 % yield. Followed by, the reductions of the amide compound (±)-**99** to primary amine (±)-**100** via the use of Claisen's alkali[81] in 76 % yield. To overcome the poor solubility of the amide in the Claisen's alkali, the reaction temperature was

increased to 125 °C. Lastly, the tertiary amine (±)-**101** was obtained in a 78 % yield *via* Eschweiler-Clarke reaction by treating the primary amine (±)-**100** with formaldehyde and formic acid. The overall yield of this synthesis route is 42%.

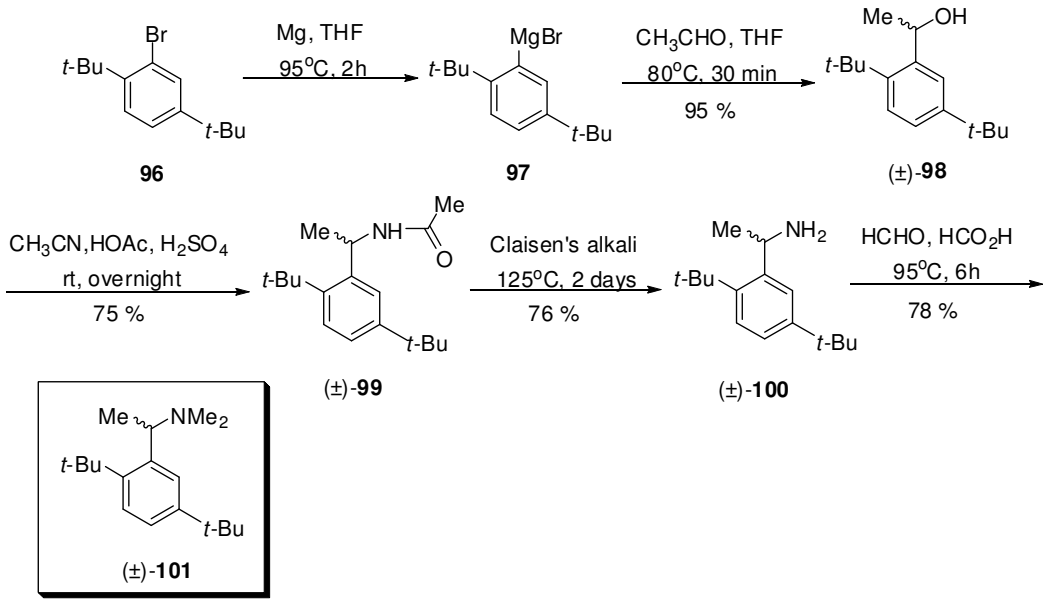

Scheme 2.1

In an attempt to increase the overall yield, another synthetic route was proposed involving the replacement of the Ritter reaction and Claisen's alkali reduction by nucleophillic substitution by sodium azide and resultion by LAH respectively. The racemic alcohol was treated with sodium azide in the presence of CF_3CO_2H at room temperature to give the azide compound (±)-**102**.[82] The azide compound (±)-**102** was immediately reduced with LAH in dried THF and the solution heated under reflux condition to give the racemic primary amine (±)-**100** in 85% yield. Lastly, the tertiary amine (±)-**101** was obtained *via* Eschweiler-Clarke reaction. The overall yield of the synthesis can be improved to 54% using this protocol (Scheme 2.2)

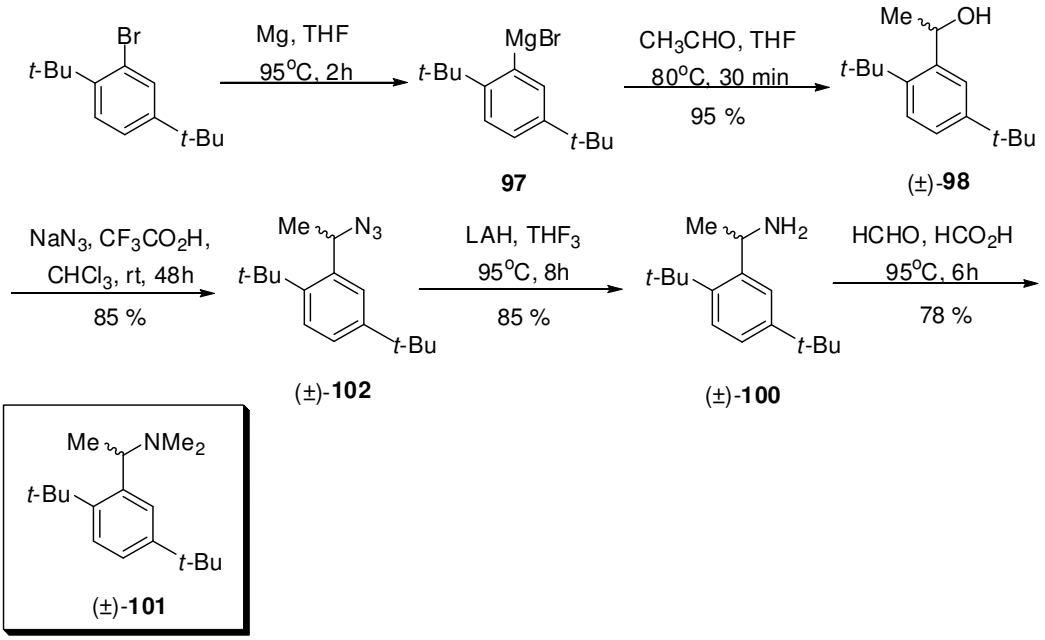

Scheme 2.2

2.3.2 *ortho*-Palladation of Amine Ligand (±)-101

The *ortho*-palladation of amine (±)-**101** posed a complication due to the steric hindrance present due to the bulky *t*-Butyl group. As such, a series of palladating agents, bases and solvents were screened. But, none of the conditions tested provided the desired *ortho*-palladated complex **95** (Scheme 2.3).

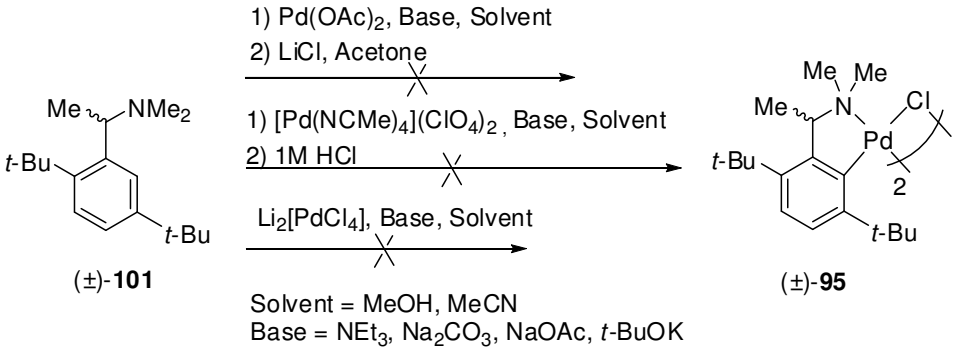

Scheme 2.3

2.3.3 Unexpected C–N Bond Cleavage Complex

Although the above palladation studies did not yield the desired racemic dimeric palladacycle (±)-**95**, a C–N bond cleavage complex **103** was obtained in 53% yield during the cyclopalladated using $Pd(OAc)_2$ (Scheme 2.4). Changing the solvent to CH_3CN gave slight deviation in yield (50%). However, the modification of the molar ratio of the reactants affects the yield of the complex **103**. When the molar ratio of reactants (amine: $Pd(OAc)_2$) is altered from 1:1 to 2:1, the yield of the C–N bond cleavage complex **103** obtained was lowered to 34%. When the reaction was conducted at room temperature, C–N bond cleavage complex **103** was obtained but the reaction was incomplete. From the results obtained, the optimal conditions for formation of the complex **103** are ligand-to-palladium ratio of 1:1 and reaction temperature of 55 °C.

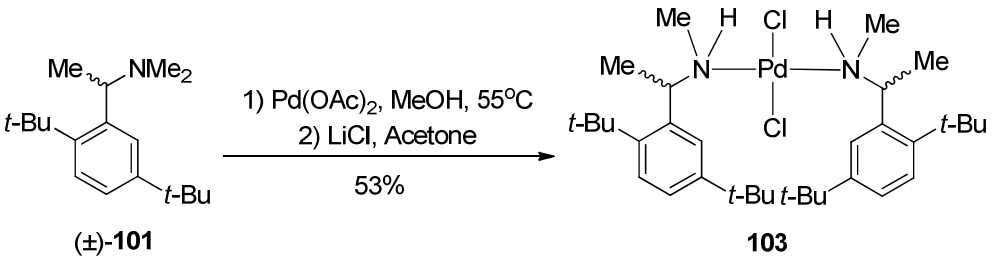

(±)-**101** **103**

Scheme 2.4

2.3.4 Molecular Structure of Complex 103

Yellow crystals were obtained from a DCM/ *n*-hexane solution and the structure of complex **103** was reaffirmed crystallographically. The molecular structure of complex **103** is depicted in Figure 2.1 and selected bond lengths and angles are presented in Table 2.1. The coordination geometry is a perfect square planar. The two nitrogen donor atoms are *trans* to each other and one of the methyl groups on each of the nitrogen atom (N1, N1A) is cleaved. And both C(15) and C(15A) are of opposite configuration.

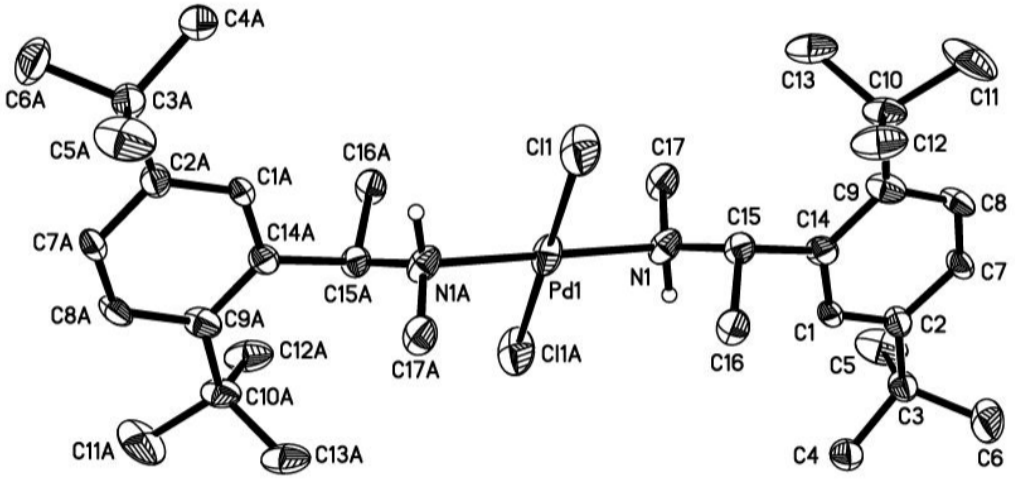

Figure 2.1 Molecular Structure of Complex **103**, all hydrogen was omitted for clarity.

Table 2.1 Selected bond lengths (Å) and angles (°) for complex **103**

Pd(1)-N(1)	2.075(7)	Pd(1)-N(1A)	2.071(2)
C(17)-N(1)	1.471(8)	C(17A)-N(1A)	1.508(15)
Pd(1)-Cl(1)	2.308(1)	N(1A)-Pd(1)-N(1)	19.4(3)
N(1)#1-Pd(1)-N(1)	180.0(4)	N(1A)#1-Pd(1)-N(1A)	180.0(12)
N(1A)#1-Pd(1)-N(1)	160.6(3)	N(1A)-Pd(1)-N(1)#1	160.6(3)
N(1)-Pd(1)-Cl(1)	92.2(2)	N(1)-Pd(1)-Cl(1)#1	87.8(2)
N(1A)-Pd(1)-Cl(1)	95.8(5)	N(1A)-Pd(1)-Cl(1)#1	84.2(5)
C(15)-N(1)-Pd(1)	114.7(4)	C(15A)-N(1A)-Pd(1)	114.3(10)
C(17)-N(1)-Pd(1)	109.1(5)	C(17A)-N(1A)-Pd(1)	110.3(14)

2.3.5 Formation and Isolation of Complex 104

In addition to complex **103**, another C–N bond cleavage complex **104** was isolated during the cyclopalladated step using $Pd(OAc)_2$ in the presence of slight excess of NEt_3 (1.2 molar equivalent). In this reaction, when the amine (±)-**101** reacted with $Pd(OAc)_2$ in the presence of a base, NEt_3 at 55°C, two C–N bond cleavage products **103** and **104** was obtained after column purification. The major product **104**

was isolated in 23 % yield and the minor product **103** in 8 % yield (Scheme 2.5). The amount of NEt_3 and the reaction temperature was found to affect the yield of the products formed (Table 2.2). At room temperature, the yields of **104** and **103** were lowered to 10% and 3% respectively (entry 2). When large excess of NEt_3 (10 molar equivalent) was added, the yields of **104** and **103** were 13% and 3% respectively (entry 3). The best results were obtained when a slight excess of NEt_3 (1.2 molar equivalent) was added and the reaction temperature is 55 °C (entry 1).

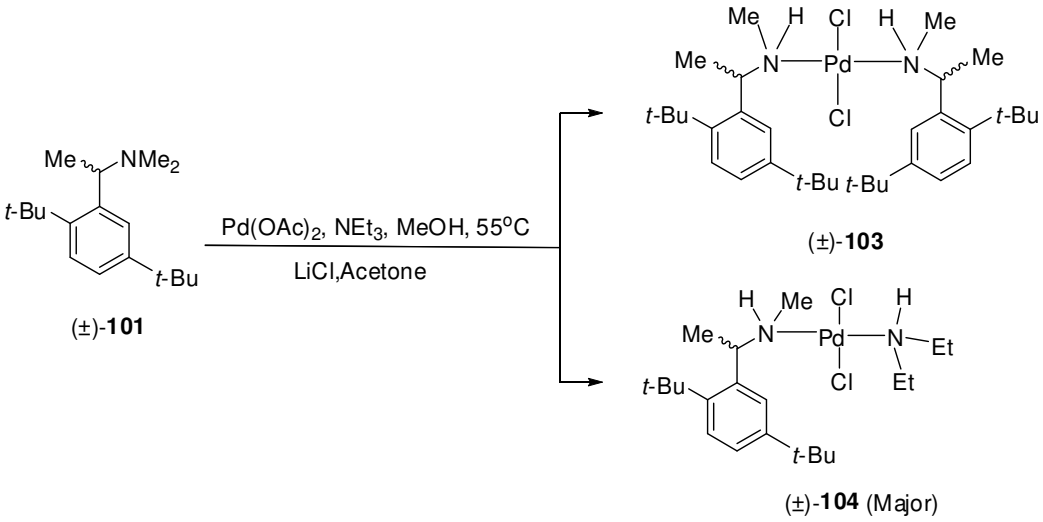

Scheme 2.5

Table 2.2 Conditions for formation of complexes **103** and **104**

Entry	(±)-**101**	$Pd(OAc)_2$	NEt_3	Reaction Temperature (°C)	% Yield [a]	
					104	**103**
1	1	1	1.2	r.t.	10	3
2	1	1	1.2	55	23	8
3	1	1	10	55	13	3

[a] Isolated yields following column chromatography.

2.3.6 Molecular Structure of Complex 104

Light yellow single crystals of complex **104** were formed from a solution of DCM and *n*-hexane of complex **104**. The X-ray diffraction study of complex **104** was performed (Figure 2.2) and the selected bond lengths and angles are provided in Table 2.3. All hydrogen except H(N1) and H(N2) were omitted for clarity. The coordination geometry of the complex **104** is in a slightly distorted square planar geometry. The dihedral angle between the two coordination plane {N(1) –Pd(1) –Cl(1)} and {N(2) –Pd(1) –Cl(2)} is 2.54°. In this molecule, the two nitrogen donor atoms are *trans* related. One of the methyl groups on the nitrogen atom (N1) has been cleaved. Moreover, one of the ethyl groups of the NEt_3 has also been cleaved from the nitrogen atom (N2) as shown below.

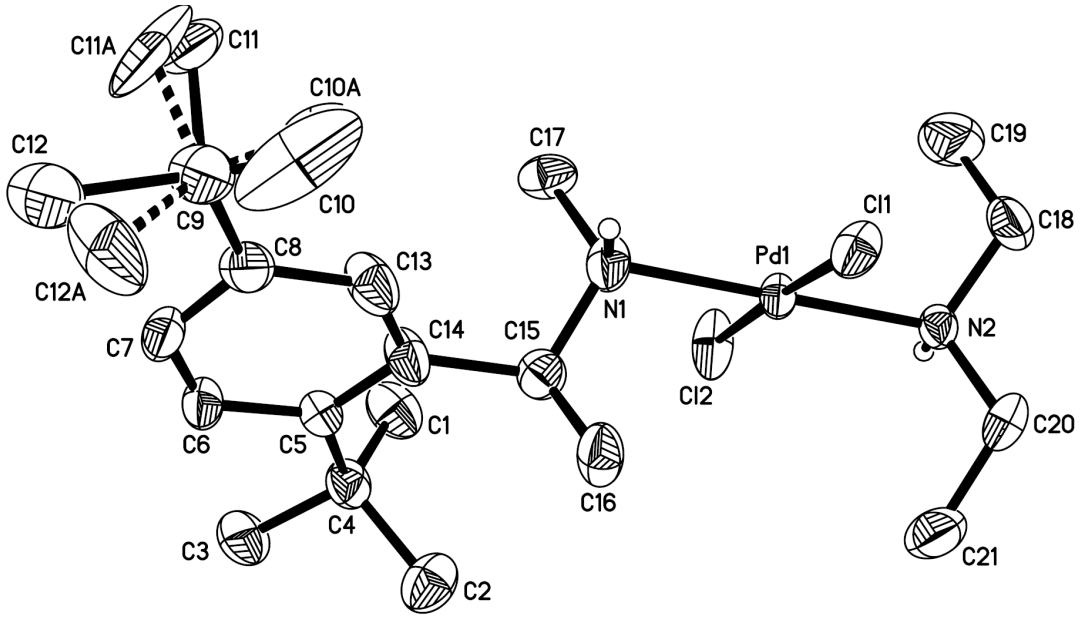

Figure 2.2 Molecular Structure of Complex **104** all hydrogen except H(N1) and H(N2) were omitted for clarity.

Table 2.3 Selected bond lengths (Å) and angles (°) for complex **104**

Pd(1)-N(1)	2.063(3)	Pd(1)-N(2)	2.049(2)
Pd(1)-Cl(1)	2.309(7)	Pd(1)-Cl(2)	2.295(8)
C(15)-N(1)	1.475(5)	C(18)-N(2)	1.486(4)
C(17)-N(1)	1.564(5)	C(20)-N(2)	1.481(4)
N(2)-Pd(1)-N(1)	177.6 (1)	Cl(2)-Pd(1)-Cl(1)	177.4(4)
N(1)-Pd(1)-Cl(1)	90.8(8)	N(2)-Pd(1)-Cl(1)	91.4(7)
N(1)-Pd(1)-Cl(2)	90.3(8)	N(2)-Pd(1)-Cl(2)	87.5(7)
C(15)-N(1)-Pd(1)	110.3(2)	C(17)-N(1)-Pd(1)	113.3(2)
C(18)-N(2)-Pd(1)	113.9(2)	C(20)-N(2)-Pd(1)	114.3(2)

2.3.7 Mechanism Studies

2.3.7.1 Assumption from Reported Reaction Mechanism using $Pd(OAc)_2$

$Pd(OAc)_2$ is often used as the palladating agent due to the properties of the acetate ligand. The acetate enhances the electrophilicity of the palladium(II) center which results in higher reactivity and yield. It also acts as an intramolecular base for deprotonation. In 2007, Vicente Jose[83a] reported the reaction mechanism (Scheme 2.6) when $Pd(OAc)_2$ is used as the palladation agent for primary amine ligands.

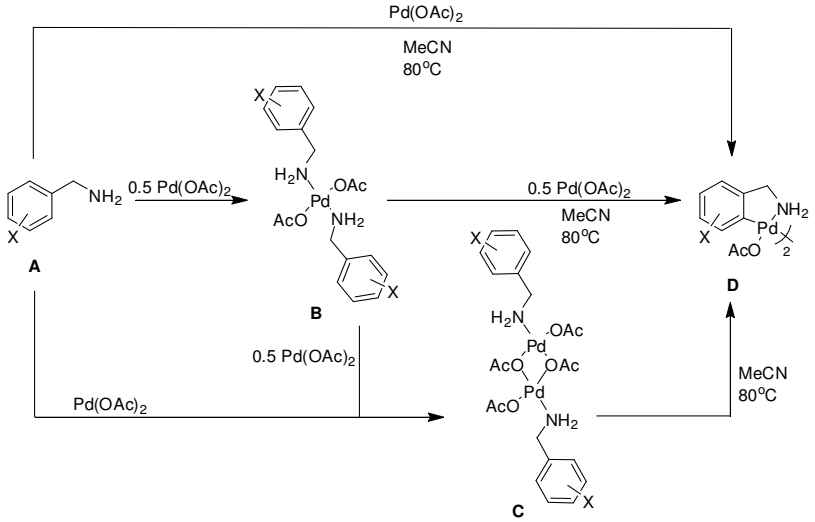

Scheme 2.6

According to the mechanism proposed by Vicente Jose[83a], firstly the ligand will react with 0.5 molar equivalent of $Pd(OAc)_2$ at room temperature to give amine coordinated complex **B**. Following which, it will react with another 0.5 molar equivalent of $Pd(OAc)_2$ to give the bridging complex **C**. Followed by, heating of the complex **C** to give the dimeric complex **D**. Secondly, the amine coordinated complex **B** will react with another 0.5 molar equivalent of $Pd(OAc)_2$ together with heating to obtain dimeric complex **D**.

Hence it was assumed that the amine ligand (±)-**101** will follow the similar mechanism, except that when the complex was heated, it will not form the dimeric product. Instead, the acetate group and one of the methyl groups on the amine will cleave off with the acetate group to give methyl acetate.

Several NMR scale experiments were conducted to determine if the mechanism can be fully applied to the C–N bond cleavage reaction. The reaction conditions were altered by varying different ratios of ligand-to-palladium acetate and reaction temperatures (55 °C and room temperature). As no trace of methyl acetate found in the ^1H NMR analysis, it rules out that the mechanism above is not applicable to C–N bond cleavage reaction complex formation.

2.3.7.2 Use of $PdCl_2$ as Palladium Source

$PdCl_2$ was used in place of $Pd(OAc)_2$ to examine if $Pd(OAc)_2$ is important to the formation of complex **103**. Under similar reaction condition complex **103** is obtained in 37% yield. The reaction with $PdCl_2$ was repeated in presence of LiOAc, give complex **103** in 43% yield. This shows that both $PdCl_2$ and $Pd(OAc)_2$ can be used to generate complex **103** and the presence of a base will aid in the formation of complex **103**.

2.3.7.3 Basicity Effect of Amine Base Presence

The *ortho*-palladation of the amine ligand (±)-**101** in the presence of NEt_3, will lead to formation of **104** with cleavage of one of the ethyl group. Investigation with various amines of different pKa was conducted to determine if basicity will affect the formation of complex **103** (Table 2.4). The pKa of the conjugated acid of various amine bases is presented in Table 2.4. The reaction was conducted with ligand-to-palladium-to-amine base of 1:1:1, at reaction temperature of 55 ^oC. The presence of the amines, except triphenylamine, resulted in the formation of the cleavage products complex **103**. Among the amine base tested, diisopropylamine is the strongest base and gave the highest yield. This shows that basicity will affect the formation of the cleavage complex **103**. In additional, the bulkiness of the amine base also plays a part, diphenylamine being the one of the weakest base obtained one of the high yield. And the triphenylamine, being the weakest and the most bulky resulted in no cleavage complex **103** formed.

Table 2.4 Basicity effect on formation of complex **103**

Conjugated acid of Amine	pKa	Yield of 103 (%)
Triethylamine	10.8	8
Tri(*n*-propyl)amine	10.3	7
Tri(*n*-butyl)amine	9.9	20
Tri(*n*-hexyl)amine	10.5	9
Diisopropylamine	38	58
Diphenylamine	0.8	40
Triphenylamine	-5	0
Aniline	4.6	19

2.3.7.4 Catalytic Amount of Palladium(II) Salt

Knowing that the addition of excess the palladium(II) salts will result in increase in the yield of the C–N bond cleavage complexes. The use of catalytic amount (5% or 10%) of palladium(II) salts was investigated to check if the tertiary ligand (±)-**101** was converted to secondary amine before coordinating to the metal. The reaction was conducted at room temperature between 5-13 days with $PdCl_2$ or $Pd(OAc)_2$ as the palladium source. Indeed, it resulted in formation of secondary amine compound (±)-**105**, in good yield (Scheme 2.7).

Since both palladium(II) salts give secondary amine compound (±)-**105** in similar yield of 70%, $PdCl_2$ was chosen due to the simpler workup procedure. The catalytic reaction was completed in 5 days when 10% of $PdCl_2$ was used whereas for 5% of $PdCl_2$, the reaction was incomplete with conversion of 80% over the same time period. And both gave the secondary amine (±)-**105** in similar yield. However, the formation of C–N bond cleavage complexes **103**, is twice the amount for 10% of $PdCl_2$ catalytic reaction. Therefore, 5% $PdCl_2$ was used for further investigations.

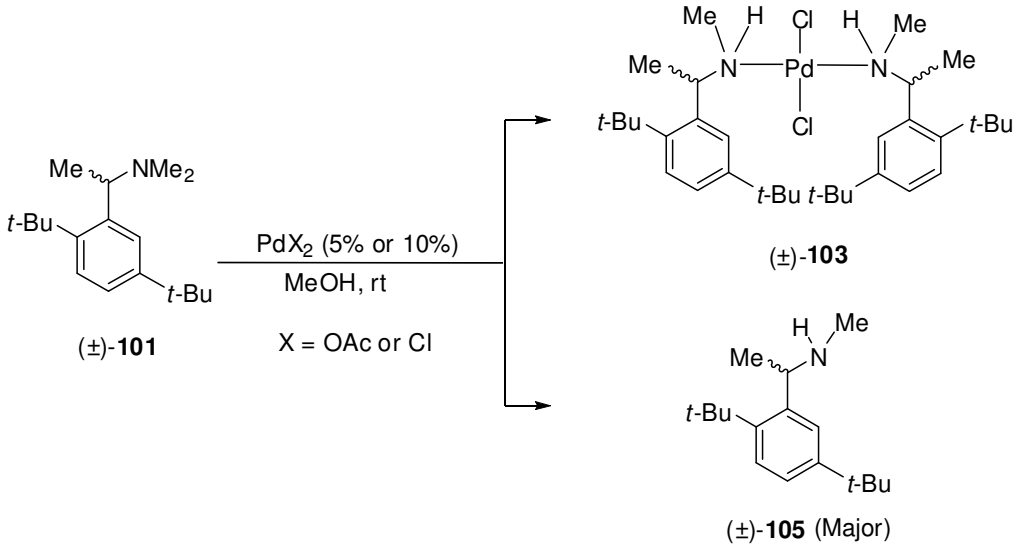

Scheme 2.7

Further investigation with addition of amine base to the reaction was conducted. When NEt_3 was added, it resulted in formation of three products, C–N bond cleavage complexes **103**, **104** and secondary amine (±)-**105** (Scheme 2.8). Although the conversion of the reaction increases from 21% (5 days) to 27% (13 days), the yield of the secondary amine decreases from 14% to 10%.

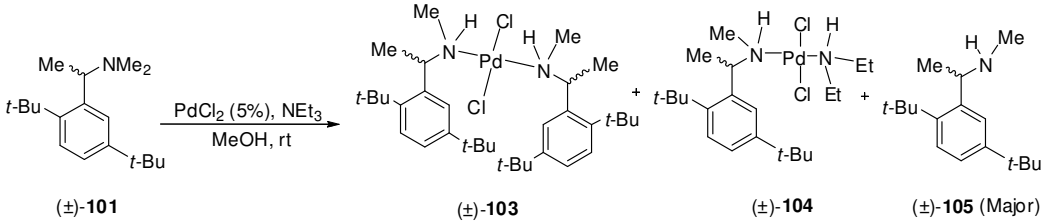

Scheme 2.8

Other amine [such as tri(*n*-propyl)amine, tri(*n*-butyl)amine and tri(*n*-hexyl)amine] with similar pKa values as NEt_3 was chosen to conduct the catalytic reaction with 5% $PdCl_2$ at room temperature within 5-13 days. When tri(*n*-propyl)amine was used, formation of two products, **103** and (±)-**105** was observed. Surprisingly, for both amine (tri(*n*-butyl)amine and tri(*n*-hexyl)amine), only the secondary amine (±)-**105** was formed. Unlike the case for NEt_3, the conversion of the tertiary amine to the secondary amine decreases with the increase reaction time. Out of the four amine bases, in the presence of tri(*n*-hexyl)amine resulted in the highest yield 72% with conversion of 80% (Table 2.5).

This shows that the presence of the amine base will compete with the (±)-**101** for the formation of the secondary amine, (±)-**105**. And the size of the R group on the amine base presence will affect the yield of the (±)-**105** formed. This is probably due to the presence of an equilibrium step in formation of (±)-**105**.

Table 2.5 Conversion and yield of (±)-**98** with various amine bases

Entry	Amine Base	Conversion (%)		Yield of (±)-**105** (%) [a]	
		5 days	13 days	5 days	13 days
1	Triethylamine	21	27	14	10
2	Tri(*n*-propyl)amine	56	30	38	12
3	Tri(*n*-butyl)amine	49	30	45	15
4	Tri(*n*-hexyl)amine	80	-	72	-

[a] Isolated yields following column chromatography

2.3.7.5 Reduction of Palladium

It is noteworthy that such type of C–N bond cleavage is not usually observed in analogous naphthyl- and benzyl-amine ligands and it is difficulty to rationalize the dealkylation of tertiary arylamines. Pfeffer *et al*. reported the Li_2PdCl_4-mediated dealkylation of *N*,*N*-dialkylanilines and 9-(diethylamino)naphthalene, [83b] and the mechanism of this dealkylation remains unclear. Interestingly, in our case, the use of Li_2PdCl_4 as palladium source does not afford the *N*-dealkylated complex **103**.

It is notable that the chemoselectivity of cyclometallation will also be decreased when such C–N cleavage occurred. Such precedents of C–N bond cleavage during cycloplatination[83c] and C–C bond cleavage during cyclopalladation of bulky benzylamines were known in literature.[83d]

In 2002, Trzeciak *et al*.[83e] reported a proposed mechanism of reduction of palladium ($PdCl_2(P(OPh)_3)_2$) with NEt_3 in the presence of water. The C–H bond of NEt_3 coordinated on palladium was activated *via* hydride elimination to form a Pd–C bond, followed by nucleophillic attack of hydroxide ion (from water) on the α-carbon of the intermediate complex. Then the intermediate complex underwent reductive elimination to give aldehyde (rearrangement of $-CH_2CH_2OH$) and secondary amine (Scheme 2.9).

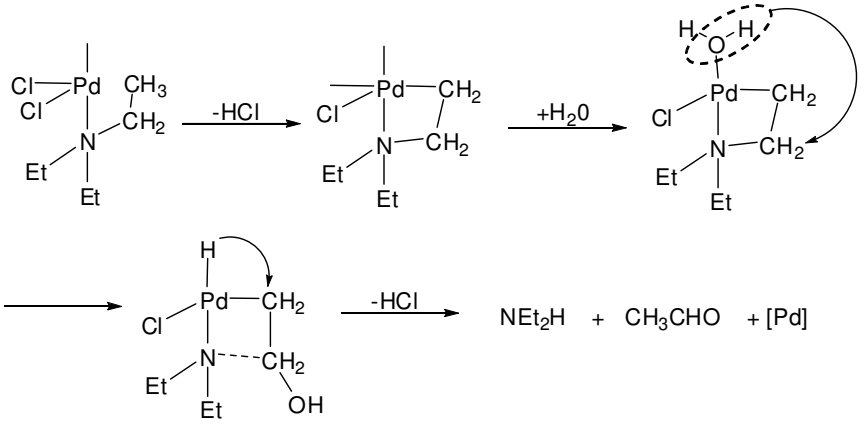

Scheme 2.9

Assume similar mechanism took place in this work, formaldehyde and the secondary amine (±)-**105** should be obtained. But formaldehyde has a boiling point of -19 ^{o}C; it is not possible to isolate it from the reaction. The stoichiometric reaction of (±)-**101** and $PdCl_2$ with molar ratio of 1:1 was carried out in CD_3OD at room temperature. As the proposed mechanism includes elimination of HCl, pH of the mixture before (neutral) and after (acidic) the reaction was tested using pH paper. This shows there is elimination of acid as side product in the reaction. However, the ^{1}H NMR spectrum of the crude product shows no proton resonance at 9-10 ppm (aldehyde proton range) and in crude $^{13}C\{^{1}H\}$ NMR spectrum revealed a peak at 209 ppm (C=O peak range for a ketone). No other side product besides complex **103** and starting material (±)-**101** was isolated after column chromatography. This shows that the initial step is likely hydride elimination, and intermediate species is most likely not a three-membered ring, probably, there is a formation of the iminium ions instead. And the side product is likely a ketone compound.

2.3.8 Conclusion

In this part of the work, the novel 1-(2,5-di-*tert*-butylphenyl)-*N*,*N*-dimethylethanamine, (±)-**101** was designed and synthesized *via* a multi-step synthesis. During the *ortho*-palladation reaction, the desired product palladacycle (*S*)-**87** was not obtained, due to the presence of bulky *t*-butyl group protruding uncompromisingly into the space near the donor atoms (N and C). An unexpected C–N bond cleavage was observed in place of *ortho*-palladation. Much effort has been put in attempting to study its mechanism. Although substantial conclusion on the mechanism cannot be made as yet, we know with the use of $PdCl_2$ or $Pd(OAc)_2$ as palladating source will result in the C–N bond cleavage products and the addition of base will increase the yield of complex **103** formed. The C–N bond cleavage involved the formation of the secondary amine 1-(2,5-di-*tert*-butylphenyl)-*N*-methylethanamine, (±)-**105** initially before coordinating with the metal to give complex **103** giving higher yield in the presence of a base. The conceivable mechanism for this *N*-dealkylation, will probably be *β*-hydride elimination upon coordination of the amine ligand, result in the iminium ions produced *in situ*, followed by methanolysis or hydrolysis, by traces of water to give the secondary amine. The secondary amine then coordinates to the palladium to give the C–N bond cleavage complexes.

2.4 Experimental

Reactions involving air-sensitive compounds were performed under positive pressure of purified nitrogen by using standard Schlenk techniques. Proton nuclear magnetic resonance (^{1}H NMR) and carbon nuclear magnetic resonance (^{13}C{^{1}H} NMR) spectroscopies were performed on Bruker Avance 300, 400 and 500 NMR Spectrometers. Multiplicities are given as: s (singlet); br (broad singlet); d (doublet); t (triplet); q (quartet); qn (quintet); dd (doublets of doublet); m (multiplets) and *etc*. The number of protons (n) for a given resonance is indicated by nH. Coupling constants are reported as a *J* value in Hz. Chemical shifts are reported as δ in units of parts per million (ppm) downfield from tetramethylsilane (δ 0.0) and relative to the signal of chloroform-*d* (^{1}H at δ 7.26, singlet and ^{13}C{^{1}H} NMR δ 77.00, triplet). Unless stated otherwise, all NMR spectroscopic experiments were performed at room temperature (300 K). Mass spectra were recorded on a Finnigan Trace GC Ultra instrument at 70 Ev with EI mode. Melting points were determined on SRS-Optimelt MPA-100 apparatus and were uncorrected. 2,5-di-tert-butylbromobenzene, **96** was prepared according to procedures as reported in literature.[79]

2.4.1 Synthesis of *1-(2,5-di-tert-butylphenyl)ethanol*, (±)-98

One small crystal of iodine was added to a RBF containing magnesium (2.5 g, 0.103 mol) and dried THF (10 mL), followed by addition of **96** (2 mL) to initiate the formation of Grignard reagent **97**. After initiation, a solution of **96** (20.23 g, 0.075 mol) in THF (50 mL) was added dropwise. The suspension was heated to 95 °C and stirred for 2 hours. The Grignard reagent **97** obtained was cooled to 0°C and acetaldehyde (10 mL, 0.18 mol) was added in dropwise. The solution was refluxed at 85 °C for 30 min, followed by addition to a beaker containing ice and conc. hydrochloric acid (2mL)

and stirred for 10 min. This is followed by extraction with DCM (100 mL × 3). The organic layer obtained was dried over $MgSO_4$, filtered and concentrated under vacuum. The product was obtained as dark yellow oil, (±)-**98** (16.67 g, 95 % yield). ^{1}H NMR (300 MHz): δ = 1.35 (s, 9H, CC*H*$_3$), 1.44 (s, H, CC*H*$_3$), 1.55 (d, $^3J_{H,H}$ = 6.3 Hz, 3 H, CHC*H*$_3$), 1.81 (br, 1H, OH), 6.66 (q, $^3J_{H,H}$ = 6.3 Hz, 1H, CH_3C*H*), 7.24 (dd,1 H, $^4J_{H,H}$ = 2.3 Hz, $^3J_{H,H}$ = 8.4 Hz, aromatic), 7.30 (d, 1H, $^3J_{H,H}$ = 8.4 Hz, aromatic), 7.68 (d, 1H, $^4J_{H,H}$ = 2.2 Hz, aromatic). ^{13}C{^{1}H} NMR (75 MHz): δ = 25.05 (***C***H_3CH), 31.32 (C***C***H_3), 32.27 (C***C***H_3), 34.37 (***C***CH_3), 35.05 (***C***CH_3), 66.49 (CH_3***C***H), 124.22 (Ar-C4), 124.48 (Ar-C6), 125.34 (Ar-C3) , 143.15 (Ar-C5), 144.31 (Ar-C1), 149.15 (Ar-C2). HRMS (EI, m/z) calcd for $C_{16}H_{26}O$ 234.1978, found 234.1979.

2.4.3 Synthesis of *N-(1-(2,5-di-tert-butylphenyl)ethyl)acetamide*, (±)-99

A solution of acetic acid (25 mL) and sulfuric acid (3 mL) was added to (±)-**98** (15.8 g, 0.067 mol) in acetonitrile (6 mL) and the mixture stirred overnight. The solution is cooled to 0°C, followed by slow addition of sodium hydroxide solution to neutralize the acid. The pH of the resulting mixture must be controlled at pH 7. The solution was extraction with DCM (100 mL × 3) and washed with water (100mL). The organic layer was concentrated and separated using silica column, the product was eluted using (acetone: DCM, (V/V = 1:1). The solvent was removed under reduced pressure to give an orange colour solid, (±)-**99** (14.69 g, 75 % yield). M.p. 169–171 °C. ^{1}H NMR (400 MHz): δ = 1.35 (s, 9H, CC*H*$_3$), 1.42 (s, 9H, CC*H*$_3$), 1.53 (d, $^3J_{H,H}$ = 6.5 Hz, 3H, CHC*H*$_3$), 1.96 (s, 3H, COC*H*$_3$), 5.74 (qn, $^3J_{H,H}$ = 6.6 Hz, 1H, CH_3C*H*), 5.87 (d, $^3J_{H,H}$ = 6.3 Hz , 1H, NH), 7.23 (dd, 1H, $^4J_{H,H}$ = 2.0 Hz, $^3J_{H,H}$ = 8.4 Hz, aromatic), 7.33 (d, 1H, $^3J_{H,H}$ = 8.4 Hz, aromatic), 7.38 (d, 1H, $^4J_{H,H}$ = 1.2 Hz, aromatic). ^{13}C{^{1}H} NMR (100 MHz): δ = 22.89 (***C***H_3CH), 23.46 (***C***H_3C=O) 31.34 (C***C***H_3), 31.80 (C***C***H_3),

34.37 (***C***CH_3), 35.10 (***C***CH_3), 46.58 (CH_3***C***H), 123.87(Ar-C4), 124.87 (Ar-C3), 126.11 (Ar-C6), 141.59 (Ar-C5), 144.11 (Ar-C1), 149.29 (Ar-C2), 169.11 (C=O). HRMS (ESI, m/z (M + H)]$^+$ calcd for $C_{18}H_{30}NO$ 276.2327, found 276.2321.

2.4.4 Synthesis of *1-(2,5-di-tert-butylphenyl)ethanamine*, (±)-**100**

Method 1:

The Claisen's alkali (8.81 g KOH dissolved in 6 mL of water and diluted to 25 mL with MeOH) was added to (±)-**99** (1.00 g, 0.36 mmol) and the solution heated at 125 °C for two days. The methanol was removed under vacuum. Extraction using DCM (40 mL × 3) was performed. The organic layer was dried with $MgSO_4$, filtered and then removal of solvent to give the product as yellow oil, (±)-**100** (0.61 g, 76 % yield).

Method 2:

A solution of azide compound (±)-**102** (2.16 g, 8.33 mmol) in dry THF (10 mL) was added dropwise to a stirred solution of LAH (0.33 g, 8.70 mmol) in the same solvent (5 mL) at 0 °C. The reaction mixture was heated for 8 h at 95 °C before it was cooled to 0 °C. The excess LAH was quenched by the dropwise addition of ice H_2O and ethyl acetate in ratio of 1:2 until effervescence ceased. The thick white precipitate was then removed by filtration under vacuum. The filtrate was dried with $MgSO_4$, filtered and evaporated to dryness, affording yellow oil, (±)-**100** (1.84 g, 95 % yield). ^{1}H NMR (300 MHz): δ = 1.35 (s, 9H, CCH_3), 1.43 (d, $^3J_{H,H}$ = 6.1 Hz, 3H, CHCH_3), 1.45 (s, 9H, CCH_3), 1.66 (br, 2H, NH_2), 4.85 (q, $^3J_{H,H}$ = 6.5 Hz, 3 H, CH_3C*H*), 7.19 (dd, 1H, $^4J_{H,H}$ = 2.3 Hz, $^3J_{H,H}$ = 8.4 Hz, aromatic), 7.29 (d, 1 H, $^3J_{H,H}$ = 8.4 Hz, aromatic), 7.58 (d, 1 H, $^4J_{H,H}$ = 2.2 Hz, aromatic). ^{13}C{^{1}H} NMR (75 MHz): δ = 25.60 (***C***H_3CH), 31.35 (C***C***H_3), 32.15 (C***C***H_3), 34.36 (***C***CH_3), 35.05 (***C***CH_3), 46.75 (CH_3***C***H), 123.27 (Ar-C4),

124.12 (Ar-C3), 125.31 (Ar-C6), 143.00 (Ar-C5), 146.51 (Ar-C1), 148.92 (Ar-C2). HRMS (ESI, m/z (M + H)]$^+$ calcd for $C_{16}H_{28}N$ 234.2222, found 234.2231.

2.4.5 Synthesis of *1-(2,5-di-tert-butylphenyl)-N,N-dimethylethanamine*, (±)-**101**

The formic acid (5 mL) and formaldehyde (10 mL) was added to (±)-**100** (9.46 g, 0.041 mol) and the mixture was heated at 95 °C for 6 hours. Hydrochloric acid (5 mL) was added to the stirred solution. The solution was then evaporated to remove the hydrochloric acid, followed by addition of concentrated sodium hydroxide to the solution, pH =14. The solution was extracted with DCM (40 mL × 5). The organic layer was then dried with $MgSO_4$ and removal of solvent under vacuum. The product was obtained as yellow solid, (±)-**101** (8.26 g, 78 % yield). M.p. 71–73 °C. ^{1}H NMR (300 MHz): δ = 1.34 (s, 9H, CCH_3), 1.36 (d, 3H, $^3J_{H,H}$ = 6.3 Hz, CHCH_3), 1.45 (s, 9H, CCH_3), 2.29 (s, 6H, N(CH_3)$_2$), 3.90 (q, $^3J_{H,H}$ = 6.2 Hz, 1H, CH_3CH), 7.17 (dd, 1H, $^4J_{H,H}$ = 2.4 Hz, $^3J_{H,H}$ = 8.4 Hz, aromatic), 7.29 (d, 1H, $^3J_{H,H}$ = 8.4 Hz, aromatic), 7.58 (d, 1 H, $^4J_{H,H}$ = 2.3 Hz, aromatic). ^{13}C{^{1}H} NMR (75 MHz): δ = 23.72 (***C***H_3CH), 31.35 (C***C***H_3), 32.33 (C***C***H_3), 34.29 (***C***CH_3), 35.37 (***C***CH_3), 44.37 (N(***C***H_3)$_2$), 61.99 (CH_3***C***H), 122.74 (Ar-C4), 125.37 (Ar-C3), 125.80 (Ar-C6), 143.10 (Ar-C5), 144.81 (Ar-C1), 148.86 (Ar-C2). HRMS (ESI, m/z (M + H)]$^+$ calcd for $C_{18}H_{32}N$ 262.2535, found 262.2530.

2.4.6 Synthesis of *2-(1-azidoethyl)-1-tert-butyl-4-methylbenzene*, (±)-**102**

A mixture of racemic alcohol (±)-**98** (3.00 g, 12.8 mmol) and sodium azide (1.70 g, 26.1 mmol) in chloroform (13 mL) was cooled to 0 ºC. A solution of CF_3CO_2H (5 mL) in chloroform (13 mL) was added in dropwise. The mixture was stirred for 48 h at room temperature. The mixture is cooled to 0 ºC and dilute sodium hydroxide solution

was added slowly until the pH = 7. The resulting solution was extracted with DCM (50 mL x 2) and washed with H_2O (10 mL). The organic layer obtained was dried over $MgSO_4$, filtered and evaporated to dryness to give the product, (±)-**102** as yellow oil (2.33 g, 85 % yield). ^{1}H NMR (300 MHz): δ = 1.32 (s, 9H, CC*H*$_3$), 1.44 (s, 9H, CC*H*$_3$) 1.54 (d, $^3J_{H,H}$ = 6.7 Hz, 3H, CHC*H*$_3$), 5.42 (q, $^3J_{H,H}$ = 6.7 Hz, 1H, CH$_3$C*H*), 7.27 (dd, $^4J_{H,H}$ = 2.2 Hz, $^3J_{H,H}$ = 8.9 Hz, 1H, aromatic), 7.33 (d, $^3J_{H,H}$ = 8.4 Hz, 1H, aromatic), 7.47 (d, $^4J_{H,H}$ = 2.2 Hz, 1H, aromatic). ^{13}C{^{1}H} NMR (100 MHz): δ = 22.52 (***C***H$_3$CH), 31.22 (C***C***H$_3$), 31.29 (C***C***H$_3$), 34.43 (***C***CH$_3$), 35.10 (***C***CH$_3$), 57.34 (CH$_3$***C***H), 124.18 (Ar-C4), 124.65 (Ar-C3), 125.19 (Ar-C6), 125.70, 146.56. HRMS (ESI, m/z (M – N$_3$)]$^+$ calcd for 217.1956, found 217.1956.

2.4.7 *Synthesis of trans*-dichlorobis[1-(2,5-di-*tert*-butylphenyl)-*N*-methylethanamine]- palladium(II), 103

A solution of (±)-**101** (0.10 g, 0.38 mmol) dissolved in MeOH (5 mL) was added to $Pd(OAc)_2$ (0.085 g, 0.38 mmol) in MeOH (5 mL). The mixture was stirred and was heated at 55 °C overnight. LiCl (0.06 g, 1.41 mmol) in acetone (2 mL) was added. After 1 hour, the mixture was filtered through Celite. After removing the solvent, the residue was then dissolved in DCM and washed with H_2O (10 mL). The organic layer was then dried ($MgSO_4$), filtered and the solvent removed under vacuum. The product was then separated by silica column using n-hexane: DCM, (V/V = 1:1) as mobile phase. Removal of solvent obtained the product as yellow solid, (±)-**101**, 0.0675 g (53 % yield). M.p. 250–253 °C (dec). ^{1}H NMR (400 MHz): δ = 1.30 (s, 9H, CC*H*$_3$), 1.44 (s, 9H, CC*H*$_3$), 2.11−2.14 (m, 3H, CHC*H*$_3$), 2.37 (d, $^3J_{H,H}$ = 6.4 Hz, 3 H, NC*H*$_3$), 3.66 (br, 1 H, NH), 4.69 (m, 1H, CH$_3$C*H*), 7.08 (d, 1H, $^4J_{H,H}$ = 2.0 Hz, aromatic), 7.23 (dd, 1 H, $^4J_{H,H}$ =2.0 Hz, $^3J_{H,H}$ = 8.4 Hz, aromatic), 7.33 (d, 1 H, $^3J_{H,H}$ = 8.4 Hz, aromatic).

$^{13}C\{^{1}H\}$ NMR (100 MHz): δ = 25.72 (***C***H_3CH), 31.21 (C***C***H_3), 32.01 (C***C***H_3), 34.29 (***C***CH_3), 35.32 (***C***CH_3), 38.09 N(***C***H_3), 57.56 (CH_3***C***H), 121.53 (Ar-C6), 124.56 (Ar-C4), 126.51 (Ar-C3), 139.16 (Ar-C1), 145.28 (Ar-C5), 149.77 (Ar-C2). HRMS (ESI, m/z (M - Cl)]$^+$ calcd for $C_{34}H_{58}N_2ClPd$ 635.3327, found 635.3323.

Same complex (±)-**101** was obtained when the reaction was repeated with acetonitrile as solvent; or when the palladium source was changed to $PdCl_2$; or when bases (Na_2CO_3, NaOAc and *t*-BuOK) were added.

2.4.8 *Synthesis of trans*-dichloro-(diethylamine)-[1-(2,5-di-tert-butylphenyl)-N-methylethanamine]- palladium(II), 104

A solution of **104** (0.10 g, 0.38 mmol) dissolved in MeOH (5 mL) was added to $Pd(OAc)_2$ (0.085 g, 0.38 mmol) in MeOH (5 mL). A base, NEt_3 (0.044 g, 0.44 mmol) was then added to the mixture. The mixture was stirred at 55 °C overnight. Subsequently, LiCl (0.06 g, 1.41 mmol) in acetone (2 mL) was added to the reaction mixture. The workup method was the same as mentioned above. After column chromatography two major products, (±)-**101** and **104** were separated. Using DCM as mobile phase, removal of solvent afforded **104** was as a yellowish solid, M.p. 174–177 °C (dec). ^{1}H NMR (300 MHz): δ = 1.32 (s, 9H, CCH_3), 1.41 (s, 9H, CCH_3), 1.64–1.69 (m, 6H, NCH_2CH_3), 2.02–2.08 (m, 3H, CHCH_3), 2.31 (d, $^{3}J_{H,H}$ = 6.1 Hz, 3H, NCH_3), 2.38–2.42 (m, 2H, NCH_2CH_3), 3.00–3.05 (m, 3H, NCH_2CH_3, $NH(CH_2CH_3)_2$), 3.62 (br, 1H, NH), 4.80–4.86 (m, 1H, CH_3CH), 7.05 (d, 1H, $^{4}J_{H,H}$ = 2.1 Hz, aromatic), 7.21 (dd, 1 H, $^{4}J_{H,H}$ =2.1 Hz, $^{3}J_{H,H}$ = 8.4 Hz, aromatic), 7.32 (d, 1H, $^{3}J_{H,H}$ = 8.5 Hz, aromatic). $^{13}C\{^{1}H\}$ NMR (100 MHz): δ = 15.17 (NCH_2***C***H_3), 25.46 (***C***H_3CH), 31.19 (C***C***H_3), 31.98 (C***C***H_3), 34.25 (***C***CH_3), 35.28 (***C***CH_3), 37.79 (N***C***H_3), 48.42(N***C***H_2CH_3), 57.38 (CH_3***C***H), 121.52 (Ar-C6), 124.49 (Ar-C4), 126.44 (Ar-C3), 139.23 (Ar-C1), 145.21

(Ar-C5), 149.71 (Ar-C2). HRMS (ESI, m/z (M - Cl)]$^+$ calcd for $C_{21}H_{40}N_2ClPd$ 461.1889, found 461.1891.

2.4.9 *Synthesis of 1-(2,5-di-tert-butylphenyl)-N-methylethanamine*, (±)-**105**

Catalytic amount of palladium(II) salt, 5 mmol % $PdCl_2$ (4.00 mg, 0.021 mmol) was added to (±)-**101** (0.11 g, 0.42 mmol) in MeOH and stirred at room temperature for 5 days. The workup method was the same as mentioned above. After column chromtography, **103** and (±)-**105** were separated. With DCM: ethyl acetate (V/V = 1:1) as mobile phase, (±)-**105** was obtained as yellow oil. The reaction was not complete after 5 working days. ^{1}H NMR (400MHz): δ =1.28 (s, 9H, CCH_3), 1.33 (d, 3H, $^3J_{H,H}$ = 6.3 Hz, CHCH_3), 1.40 (s, 9H, CCH_3), 1.64 (s, 1H, NH), 2.36 (s, 3H, NCH_3), 4.37 (q, 1H, CHCH_3, $^3J_{H,H}$ = 6.3 Hz), 7.14 (dd, 1H, $^4J_{H,H}$ = 2.3 Hz, $^3J_{H,H}$ = 8.4 Hz, aromatic), 7.25 (d, 1H, $^3J_{H,H}$ = 8.4 Hz, aromatic), 7.51 (d, 1 H, $^4J_{H,H}$ = 2.3 Hz, aromatic). ^{13}C{^{1}H} NMR (100 MHz): δ = 23.57 (***C***H$_3$CH), 31.55 (C***C***H$_3$), 32.35 (C***C***H$_3$), 34.52 (***C***CH$_3$), 34.75 (N***C***H$_3$), 35.38 (***C***CH$_3$), 55.46 (CH$_3$***C***H), 123.40 (Ar-C4), 124.66 (Ar-C3), 125.53 (Ar-C6), 144.00 (Ar-C5), 144.43 (Ar-C1), 149.08 (Ar-C2). HRMS (ESI, m/z (M + H)]$^+$ calcd for $C_{17}H_{30}N$ 248.2386, found 248.2378.

The reaction was repeated with $Pd(OAc)_2$ as pallading agent; when the 10 mmol % palladium(II) salt were used; when bases (triethylamine, tripropylamine, tributylamine and trihexylamine) were added; or when the reaction time was increased to 13 days, gave the same compound (±)-**105**.

CHAPTER 3

CHIRAL *ORTHO*-PALLADATED 1-(2,5-DI-ISOPROPYLPHENYL)-*N*,*N*-DIMETHYLETHANAMINE

3.1 Introduction

The commonly used naphthylamine palladacycle (*S*)-**13** is chosen for the asymmetric *endo* [4+2] cycloaddition reaction between DMPP and ethyl vinyl ketone. The stereoselectivity is observed with two diastereomeric *endo*-cycloadducts mixture ((S_C,S_P)- and (S_C,R_P)-**84**) generated in a ratio of 1:2.5. [71] As discussed in the earlier chapters, the stereoselectivity of the cycloaddition will increase with the presence of bulky spacer group. For instance, chiral *ortho*-palladated complex (*S*)-**16** with two spacer groups (methyl) introduced on the arylamine ring. The methyl spacer groups can interact with the methyl group at the stereogenic carbon center to lock the conformation of the organometallic five-membered ring and also exert more stereochemical influence on the reaction site. The cycloaddition reaction between the DMPP-coordinated chiral *ortho*-palladated complex (*S*)-**88** and ethyl vinyl ketone, showed an improvement in the stereoselectivity ratio of the two diastereomeric mixture ((S_C,S_P)- and (S_C,R_P)-**90**) to 1:3.5. [13c]

It is worthy to note that the spacer group cannot be too bulky, as it will hinder the C–H activation reaction for formation of the *ortho*-palladated complex. In the case of *t*-butyl spacer groups introduced on the aromatic ring, it had resulted in formation of C–N cleavage complexes (**103** and **104**) instead of cyclopalladated complex.

3.2 Research Objectives

We know that the presence of spacer group like methyl group at the α–position of C–Pd bond will enhanced the stereochemical influence on the reaction sites.

However, the size of the spacer group must be carefully controlled to avoid it from hindering the formation of the *ortho*-palladated complex. Hence, we designed and synthesized a novel chiral *ortho*-palladated complex (*S*)-**106** with slightly less bulky spacer groups (*i*-propyl) on the aryl ring. This chiral *ortho*-palladated complex (*S*)-**106** retained all the desired stereoelectronic properties of the (*S*)-**16**. The steric repulsion between the *i*-propyl group and the the methyl group on the stereogenic carbon will lock the five-membered ring in fixed λ conformation in both solid and solution state. Furthermore, the *i*-propyl group adjacent to the C–Pd bond will exert additional stereochemical influence on the reaction site *trans* to N donor atom. The application of this new template on the Diels–Alder reaction was also examined.

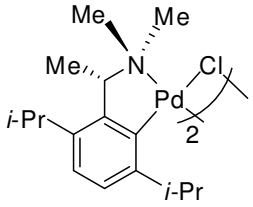

(*S*)-**106**

3.3 Result and Discussion

3.3.1 Synthesis of 1-(2,5-di-*iso*-propylphenyl)-*N*,*N*-dimethylethanamine

The amine ligand is synthesized *via* 4 step approach, beginning with 2,5-di-*iso*-propylbenzaldehyde **107**[84] (Scheme 3.1). The starting material reacted with methyl magnesium bromide to form a racemic alcohol product (±)-**108** in 86% yield. The racemic alcohol was further reacted with sodium azide in the presence of CF_3CO_2H to yield the azide compound (±)-**109** in 97% yield.[83] Next, compound (±)-**109** was reduced using LAH in dried THF to obtain the racemic primary amine (±)-**110** in 97% yield. Finally, the primary amine was converted to the tertiary amine (±)-**111** *via*

Eschweiler-Clarke reaction with the addition of 5% formic acid and formaldehyde with a success rate of 74%. The synthesis provided an overall yield of 60%.

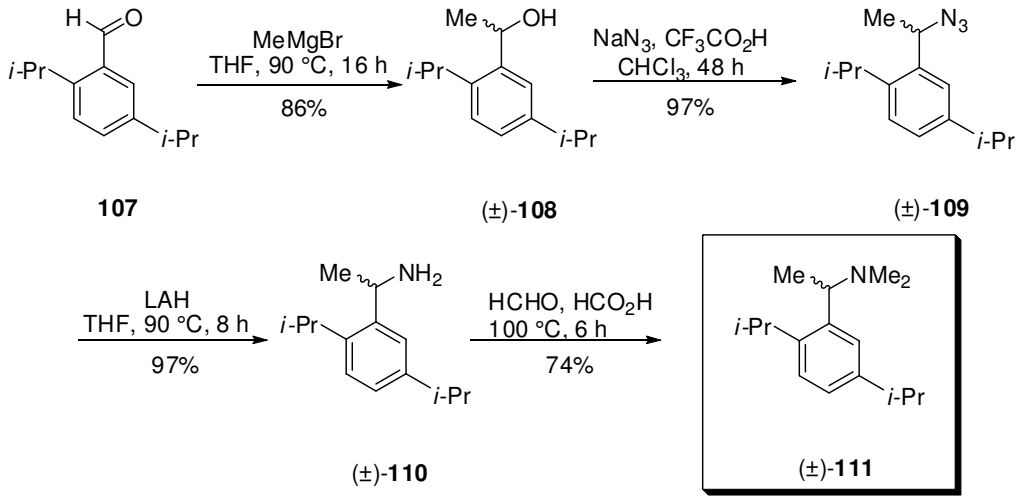

Scheme 3.1

With the intention to increase the overall yield, and to make the route more environmental friendly, an alternate pathway was introduced (Scheme 3.2). The new synthetic method uses a 3 step approach. The overall yield can be enhanced by using optimized conditions for alkylation, eliminating the use of hazardous substances such as NaN_3 with strong acid and LAH and the Eschweiler-Clarke reaction was replaced with nucleophilic substitution with dimethylamine.

Methylation with methylmagnesium bromide at room temperature to afford the racemic alcohol (±)-**108** in 98% yield, followed by the treatment with PBr_3 in degassed DCM to give the bromo compound (±)-**112** in 99% yield. Subsequent amination with aqueous dimethylamine under rapid stirring afforded the desired product (±)-**111** in 96% yield. An overall yield of 93% was obtained for the improved synthesis (Scheme 3.2).

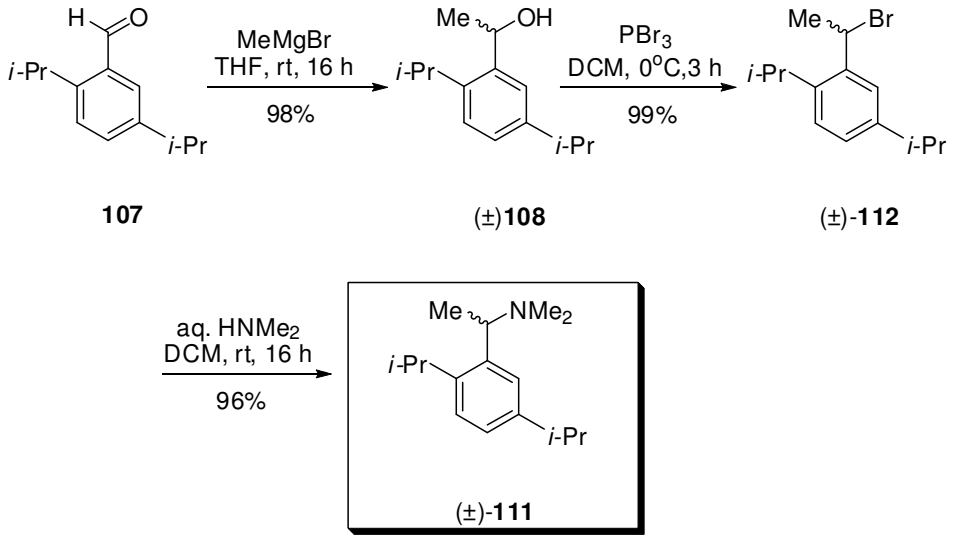

107 (±)**108** (±)-**112** (±)-**111**

Scheme 3.2

3.3.2 *ortho*-Palladation of Amine Ligand (±)-111

The *ortho*-palladation of amine ligand (±)-**111** resulted in formations of two possible products when different palladium sources were used (Scheme 3.3). The reaction conditions and the yields are presented in Table 3.1.

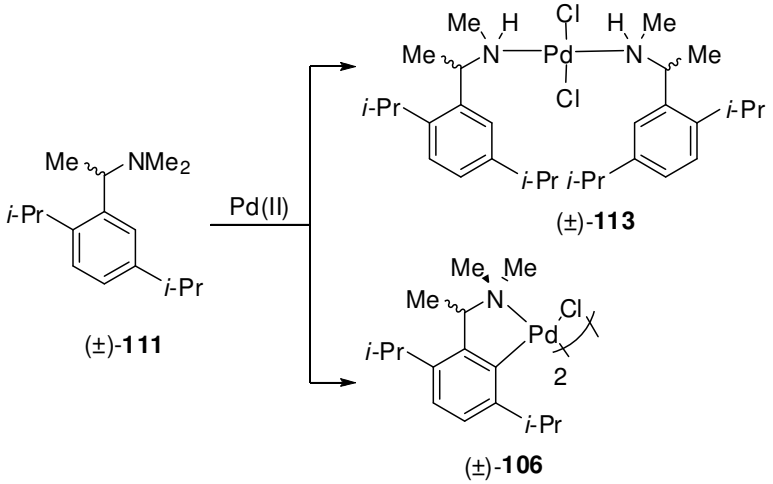

(±)-**111** (±)-**113** (±)-**106**

Scheme 3.3

Table 3.1 Optimization of conditions for palladation of tertiary amine (±)-**111**

	Conditions[a]				% yield[b]	
	Palladating Agent	Solvent	Base	T (°C)	(±)-**106**	(±)-**113**
1	$PdCl_2$	MeOH	-	55	23	29
2	$Pd(OAc)_2$[c]	MeOH	-	55	16	2
3	$Li_2(PdCl_4)$	MeOH	NaOAc	r.t.	78	0
4	$Li_2[PdCl_4]$	MeOH	NaOAc	55	20	0
5	$PdCl_2(NCMe)_2$	MeOH	-	55	19	0
6	$[Pd(NCMe)_4](ClO_4)_2$	MeCN	-	r.t.	-[d]	-[d]
7	$PdCl_2$	MeOH	-	80	10	23
8	$PdCl_2$	Benzene	-	55	43	11
9	$PdCl_2$	DMF	-	55	39	0

[a] Unless otherwise specified, reaction employed 1 equivalent of palladating agent and 16 h reaction time. [b] Isolated yields following column chromatography. [c] Use of $Pd(OAc)_2$ as palladating agent yielded μ-acetato dimer instead of μ-chloro dimer. [d] No reaction.

The racemic dimeric complex (±)-**106** was obtained in 78% yield directly from the treatment of tertiary amine (±)-**111** with $Li_2[PdCl_4]$ (entry 3) in the presence of NaOAc at room temperature (Scheme 3.4). When the reaction was repeated at elevated temperature (entry 4) or the palladating agent was changed to $PdCl_2(NCMe)_2$ (entry 5), the yield was dramatically lowered. It is worthy to note that *ortho*-palladation of such a sterically-hindered amine proved to be difficult as steric hindrance will hinder the C–H bond activation and possibility of formation of C–N bond cleavage complex as reported previously in chapter 2.

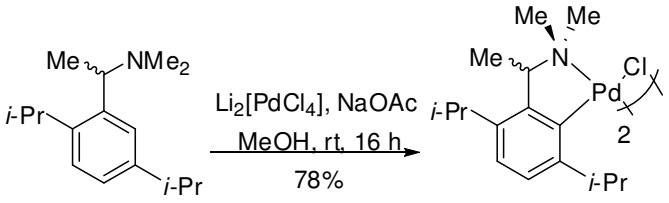

(±)-**111** (±)-**106**

Scheme 3.4

The *ortho*-palladation with $[Pd(NCMe)_4](ClO_4)_2$ (entry 6) showed no reaction at ambient temperature, with the amine ligand (±)-**111** fully recoverable by column chromatography.

In contrast, when $Pd(OAc)_2$ and $PdCl_2$ were used, a mixture of products, dimeric complex (±)-**106** and of C–N bond cleavage complex (±)-**113** were obtained. The initial treatment of the tertiary amine (±)-**111** with stoichiometric $PdCl_2$ in MeOH at 55 °C yielded both palladacycle (±)-**106** and complex (±)-**113** in low yields. In order to raise the production of (±)-**113**, various temperatures and solvents were conducted (entry 7-9). When the reaction temperature was raised to 80 °C, the yield of the dimeric complex (±)-**106** dropped more than 50% and the C–N bond cleavage complex (±)-**113** was lowered by 20%. Solvents were found to play a vital role in product outcome of these reactions. Employment of benzene and DMF as solvents favors the production of palladacycle (±)-**106**, with significant decrease in yields of complex (±)-**113**. This shows that non-polar and polar aprotic solvent will not favour the formation of complex (±)-**113**. Despite efforts to promote the formation of complex (±)-**113**, the conditions of entry 1 resulted in the best yield.

3.3.3 Characterization of C–N Bond Cleavage Complex (±)-113

Bright yellow prisms were grown from the yellow powder of complex (±)-**113** in a solution of DCM/diethyl ether. The structural analyses of the complex confirmed that a C–N bond cleavage indeed occurred during the coordination process. Selected bond lengths and angles are provided in Table 3.2. The palladium center exhibits a typical square-planar coordination geometry with the bond angles of N(1)–Pd(1)–N(1A) and Cl(1)–Pd(1)–Cl(1A) both being 180.0° with standard deviations of 2 and 4, respectively. The two nitrogen donor atoms are *trans* to each other with each of the

nitrogen atoms bearing only one methyl substituent as a consequence of the C–N cleavage. The relative stereochemistry of asymmetric nitrogen and carbon atoms of complex (±)-**113** in solid state was (R_CS_N,R_CS_N)*. The ^{1}H NMR of complex (±)-**113** shows only one resonance observed for every chemically non-equivalent proton. The presence of the bulky *iso*-propyl groups on the aromatic ring have prevented the asymmetric nitrogen and carbon atoms to isomerize to other isomers as in the case of the unsubstituted aromatic ring.[85]

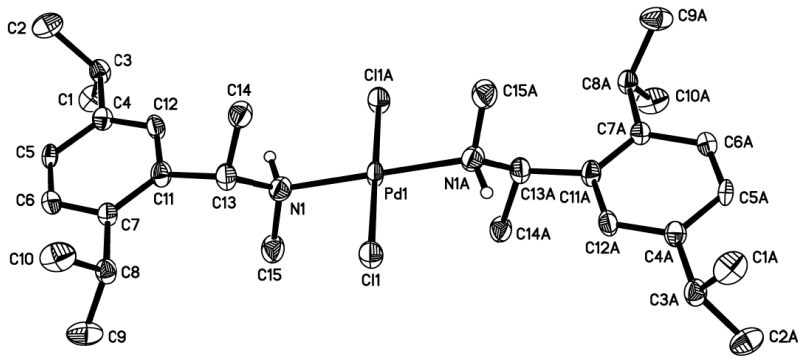

Figure 3.1 Molecular structure of complex (±)-**113**. All hydrogen atoms except H(N1) and H(N1A) were omitted for clarity.

Table 3.2 Selected bond lengths (Å) and angles (°) for complex, (±)-**113**

Pd(1)–N(1)	2.057(4)	Pd(1)–N(1A)	2.057(4)
Pd(1)–Cl(1)	2.302(1)	Pd(1)–Cl(1A)	2.302(1)
N(1)–C(13)	1.486(7)	N(1A)–C(13A)	1.486(7)
N(1) – C(15)	1.479(7)	N(1A)–C(15A)	1.479(7)
N(1)–Pd(1)–Cl(1)	93.0(1)	N(1)–Pd(1)–Cl(1A)	87.0(1)
Cl(1A)–Pd(1)–N(1A)	93.0(1)	N(1A)–Pd(1)–Cl(1)	87.0(1)
N(1)–Pd(1)–N(1A)	180.0(2)	Cl(1)–Pd(1)–Cl(1A)	180.0(4)
C(13)–N(1)–Pd(1)	115.9(3)	C(13A)–N(1A)–Pd(1)	115.9(3)
C(15)–N(1)–Pd(1)	112.6(3)	C(15A)–N(1A)–Pd(1)	112.6(3)
C(15)–N(1)–C(13)	112.1(4)	C(15A)–N(1A)–C(13A)	112.1(4)

3.3.4 Characterization of Racemic *ortho*-Palladated Complex (±)-106

3.3.4.1 Molecular Structure of Complex (±)-106

The needle-like bright yellow single crystals of palladacycle (±)-**106** were obtained *via* vapour diffusion method (DCM/diethyl ether). In the solid state, structural investigations confirmed that no C–N bond cleavage occurred during the cyclopalladation reaction with each nitrogen atom bearing two methyl groups (Figure 3.2). Selected bond lengths and bond angles of complex are given in Table 3.3. In addition, the dimer exists in the crystal in its *transoid* configuration with the two chiral organometallic units adopting the same relative configurations. The palladium atoms, Pd(1) and Pd(1A), were found to adopt a distorted square-planar coordination geometry, the dihedral angles between the planes {Cl(1)–Pd(1)–Cl(1A)} and {N(1)–Pd(1)–C(1)}, and between the planes {Cl(1)–Pd(1A)–Cl(1A)} and {N(1A)–Pd(1A)–C(1A)} were both equal to 13.6°. As predicted, the iso-propyl substituent (C(8) and C(8A)) interacts with the methyl groups (C(14) and C(14A)) at the stereogenic center thus forcing the methyl group to take up the axial position instead of the relatively more favorable equatorial position.

The four-membered ring bridged by the chlorine atoms to the palladium centers, Cl(1)–Pd(1)–Cl(1A)–Pd(1A), were found to be non-coplanar, with a bent angle of 27.8° about the Cl(1)–Cl(1A) axis. In addition, torsion angles for Cl(1)–Pd(1)–C(1)–C(2) and Cl(1A)–Pd(1A)–C(1A)–C(2A) were both calculated to be -45.0°. Such twisting of the rings was partly a consequence of the internal steric repulsions between the iso-propyl substituent and the bridged chlorine atoms. Furthermore, the distance between the bridged chlorine atom and the hydrogen of the isopropyl spacer is 2.46 Å, which is considerably lower than the summation of their

Van der Waals radii of 2.95 Å.[86] This provided stronger evidence that the isopropyl spacers are projected away from the chloro bridges.

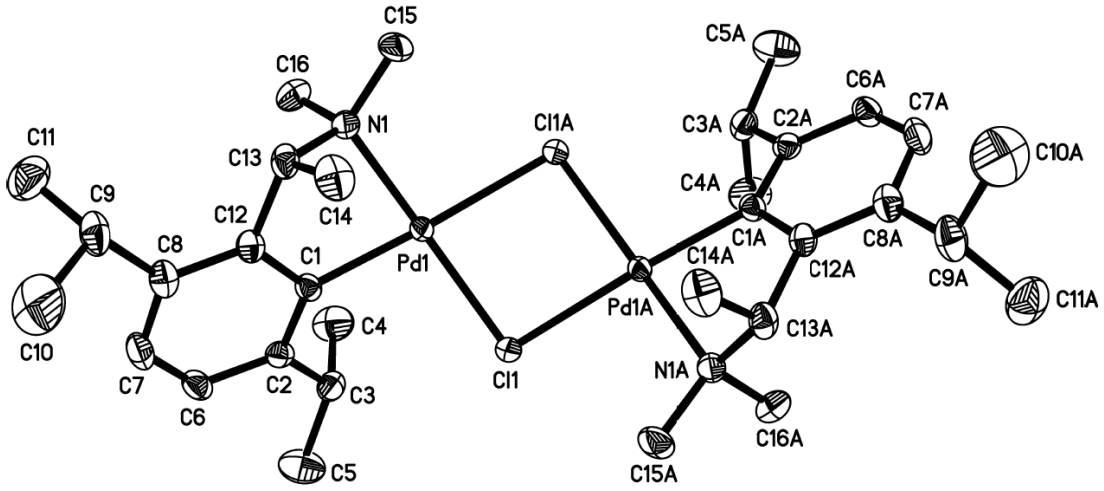

Figure 3.2 Molecular structure of dimeric complex (±)-**106**. All hydrogen atoms were omitted for clarity.

Table 3.3 Selected bond lengths (Å) and angles (°) for dimeric complex (±)-**106**.

Pd(1)–C(1)	1.993(2)	Pd(1A)–C(1A)	1.993(2)
Pd(1)–N(1)	2.071(2)	Pd(1A)–N(1A)	2.071(2)
Pd(1)–Cl(1)	2.347(4)	Pd(1A)–Cl(1A)	2.347(4)
Pd(1)–Cl(1A)	2.463(4)	Pd(1A)–Cl(1)	2.463(4)
C(1)–Pd(1)–N(1)	80.2(7)	C(1A)–Pd(1A)–N(1A)	80.2(7)
C(1)–Pd(1)–Cl(1)	98.8(5)	C(1A)–Pd(1A)–Cl(1A)	98.8(5)
N(1)–Pd(1)–Cl(1A)	97.9(4)	N(1A)–Pd(1A)–Cl(1)	97.9(4)
Cl(1)–Pd(1)–Cl(1A)	83.8(2)	Cl(1A)–Pd(1A)–Cl(1)	83.8(2)
C(1)–Pd(1)–Cl(1A)	176.3(5)	C(1A)–Pd(1A)–Cl(1)	176.3(5)
N(1)–Pd(1)–Cl(1)	167.2(5)	N(1A)–Pd(1A)–Cl(1A)	167.2(5)

3.3.4.2 Synthesis of Monomeric Complex (±)-114

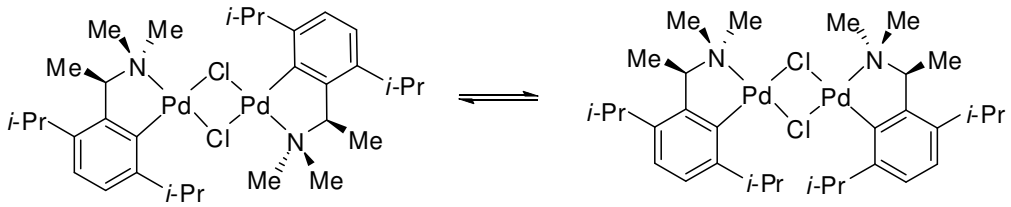

anti-(*R*,*R*)-**106** *syn*-(*R*,*R*)-**106**

In the ^{1}H NMR spectrum at room temperature, complex (±)-**106** showed broad and poorly resolved resonance signals. The phenomenon can be attributed to the well-documented dynamic *syn-anti* interconversion of such dimeric complexes in solution.[87] The broadness of the ^{1}H NMR signals makes the identification difficult. Hence, the dimeric complex (±)-**106**, was converted to monomeric complex (±)-**114** by addition of PPh_3 (Scheme 3.5).

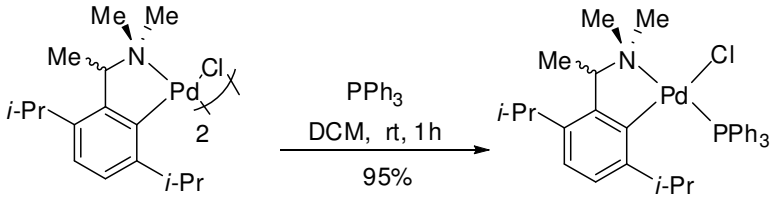

(±)-**106** (±)-**114**

Scheme 3.5

3.3.4.3 Molecular Structure of Monomeric Complex (±)-114

The monomeric complex (±)-**108** could be isolated as yellow prisms from DCM/ *n*-hexane. The coordination chemistry of the complex was confirmed by X-ray structural analysis. Interestingly, four crystallographically unique molecules were found in the unit cell with each differing only slightly in bond lengths and bond angles (Table 3.4). For clarity, only one of these molecules (molecule A) is depicted in Figure 3.3. The coordination geometry at palladium is distorted square-planar and the chiral five-membered ring adopts an envelope-like conformation in the solid state. More importantly, complex (±)-**114** adopts the highly unfavourable *trans* N–Pd–P geometry

in which the bulky *iso*-propyl spacer and the PPh_3 ligand were located at the adjacent positions of the square-planar complex. The *trans* effect (transphobia) for the C–Pd–P geometry is larger than that of the N–Pd–P geometry resulting in a greater degree of destabilisation for the C–Pd–P geometry. Clearly, the strong electronic directing effects must be the dominating influence, even in such sterically demanding complexation scenarios.[88] As a consequence of these strong steric repulsions, the palladium center exhibits a large dihedral angles of 21.8° between the planes {P(1)–Pd(1)–Cl(1)} and {N(1)–Pd(1)–C(1)}.

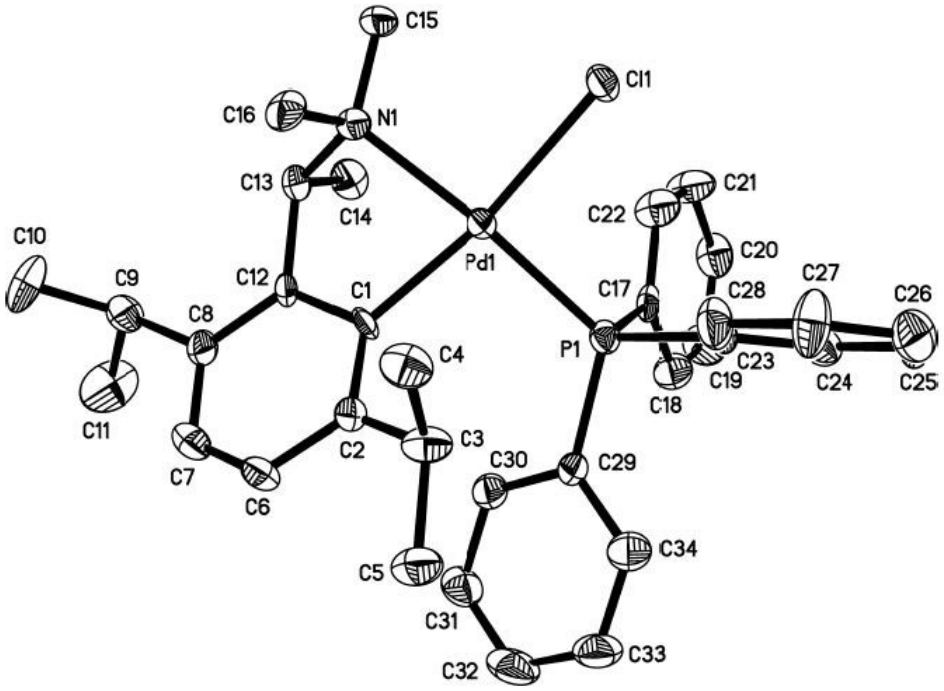

Figure 3.3 Molecular structure of monomeric complex (±)-**114**. All hydrogen atoms were omitted for clarity.

Table 3.4 Selected bond lengths (Å) and angles (°) for monomeric complex (±)-**114**

Molecule A		Molecule B	
Pd(1)-C(1)	1.996(7)	Pd(2)-C(35)	1.999(1)
Pd(1)-N(1)	2.135(8)	Pd(2)-N(2)	2.143(8)
Pd(1)-P(1)	2.265(2)	Pd(2)-P(2)	2.274(2)
Pd(1)-Cl(1)	2.396(2)	Pd(2)-Cl(2)	2.403(2)
C(1)-Pd(1)-N(1)	78.5(3)	C(35)-Pd(2)-N(2)	78.7(3)
C(1)-Pd(1)-P(1)	96.7(3)	C(35)-Pd(2)-P(2)	97.7(3)
N(1)-Pd(1)-Cl(1)	93.9(2)	N(2)-Pd(2)-Cl(2)	95.3(2)
P(1)-Pd(1)-Cl(1)	93.9(8)	P(2)-Pd(2)-Cl(2)	89.5(9)
N(1)-Pd(1)-P(1)	160.1(2)	N(2)-Pd(2)-P(2)	162.4(2)
C(1)-Pd(1)-Cl(1)	166.9(3)	C(35)-Pd(2)-Cl(2)	172.3(3)
Molecule C		Molecule D	
Pd(3)-C(69)	1.980(9)	Pd(4)-C(103)	2.011(8)
Pd(3)-N(3)	2.140(8)	Pd(4)-N(4)	2.136(8)
Pd(3)-P(3)	2.262(3)	Pd(4)-P(4)	2.262(2)
Pd(3)-Cl(3)	2.413(2)	Pd(4)-Cl(4)	2.414(2)
C(69)-Pd(3)-N(3)	77.6(4)	C(103)-Pd(4)-N(4)	78.6(3)
C(69)-Pd(3)-P(3)	96.3(3)	C(103)-Pd(4)-P(4)	97.3(3)
N(3)-Pd(3)-Cl(3)	95.0(2)	N(4)-Pd(4)-Cl(4)	96.1(2)
P(3)-Pd(3)-Cl(3)	94.2(1)	P(4)-Pd(4)-Cl(4)	88.5(1)
N(3)-Pd(3)-P(3)	159.6(2)	N(4)-Pd(4)-P(4)	163.7(2)
C(69)-Pd(3)-Cl(3)	166.7(3)	C(103)-Pd(4)-Cl(4)	174.3(3)

3.3.5 Optical Resolution of Racemic Dimeric Complex (±)-106

The optical resolution of racemic dimeric complex (±)-**106**, was performed using optically active sodium prolinate as the resolving agent (Scheme 3.6).

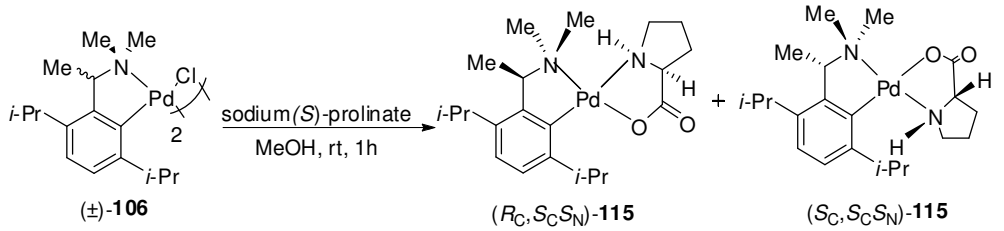

Scheme 3.6

The racemic dimer was treated with two molar equivalents of sodium (*S*)-prolinate to give a mixture of 1:1 diastereomers, (R_C,S_CS_N)-**115** and (S_C,S_CS_N)-**115**. The diastereomeric adducts were separated *via* column chromatography. The less polar diastereomer (R_C,S_CS_N)-**115** was eluted out first with acetone/DCM (V/V = 1:1). And the more polar diastereomer (S_C,S_CS_N)-**115** was eluted out with MeOH as mobile phase. The diastereomeric ratio of both fractions was verified with ^{1}H NMR spectroscopy. The (R_C,S_CS_N)-**115** was crystallized using ethyl acetate and diethyl ether yielding pale yellow plate-like crystal in 82% yield (based on half equivalent of dimer used) with $[\alpha]^{23.4}$ +43.4° (*c* 0.02, DCM) and >99% *de* (according to ^{1}H NMR data). Another diastereomeric adduct was crystallized from a solution of (S_C,S_CS_N)-**115** in DCM/ *n*-hexane to give colourless needle-like crystal with $[\alpha]^{23.4}$ +196.9° (*c* 0.02, DCM) and >99% *de* (according to ^{1}H NMR data). The absolute configuration and the solid structure of both diastereomeric adducts (R_C,S_CS_N)-**115** and (S_C,S_CS_N)-**115** were concluded by X-ray single crystal diffraction investigation. Their structures in solution were studied by 2D ^{1}H-^{1}H ROESY NMR spectroscopy.

3.3.5.1 Molecular Structure of Diastereomer (R_C,S_CS_N)-115

The molecular structure of the complex (R_C,S_CS_N)-**115** is shown in Figure 3.4 The absolute configuration of the stereogenic carbon center within the organometallic ring is *R*. The torsion angle for C(1)–Pd(1)–N(1)–C(13) is +40.9°. The methyl group

at the chiral center occupies the expected axial position and the absolute conformation of the five-membered ring is *δ* (Figure 3.5).[89] The secondary stereogenic nitrogen atom from the prolinato group is in *S* absolute configuration.

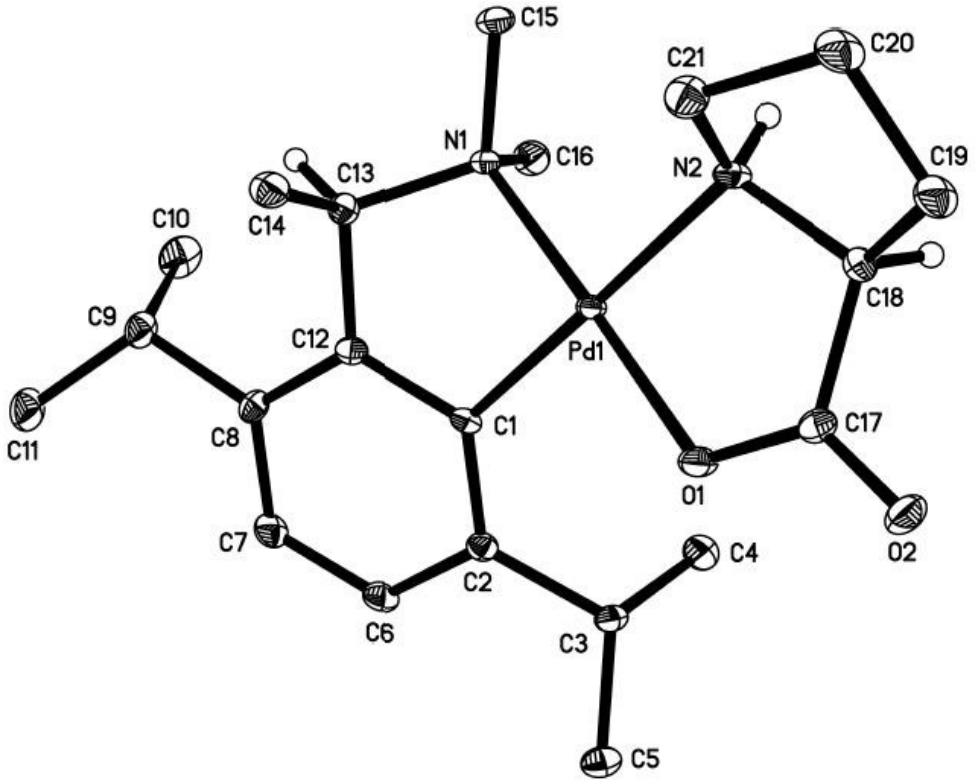

Figure 3.4 Molecular structure of diastereomer (R_C,$S_C$$S_N$)-**115**. All hydrogen atoms except H(C13), H(C18) and H(N2) were omitted for clarity.

The palladium center adopts a slightly distorted square planar coordination geometry with tetrahedral distortion of 2.8°. The organometallic five-membered ring is in an envelope conformation wherein N(1) is 0.803 Å below the mean plane formed by C(1)–C(12)–C(13)–Pd(1). The two coordinated nitrogen groups are in unusual *cis*-(*N*,*N*)-geometry.[13b,13c] This phenomenon can be attributed to the steric interaction between the protruding *iso*-propyl spacer adjacent to the Pd–C bond and the nitrogen of the prolinato group which forces the complex to adopt the sterically more

favourable *cis*-(*N*,*N*)-geometry and the requirement of the crystal lattice. The angle between the mean plane of the organometallic five-membered ring C(1)–C(12)–C(13)–N(1)–Pd(1) and the mean plane formed from O(1)–C(17)–C(18)–N(2)–Pd(1) of the prolinato ligand is 13.10°. The bond length of Pd(1)–N(2) is 2.140 Å and is comparable to reported values of the *cis*-(*N*,*N*)-geometry. [13b,13c] On the other hand, the distance is much longer than the reported value of 2.037-2.083 Å for the *trans*-(*N*,*N*)-geometry.[13a,89a] The bond lengthening is an expected result of the *trans* influence caused by the aryl-carbon and the repulsion between the C(15) on the NMe and the C(21) of the prolinate moiety.

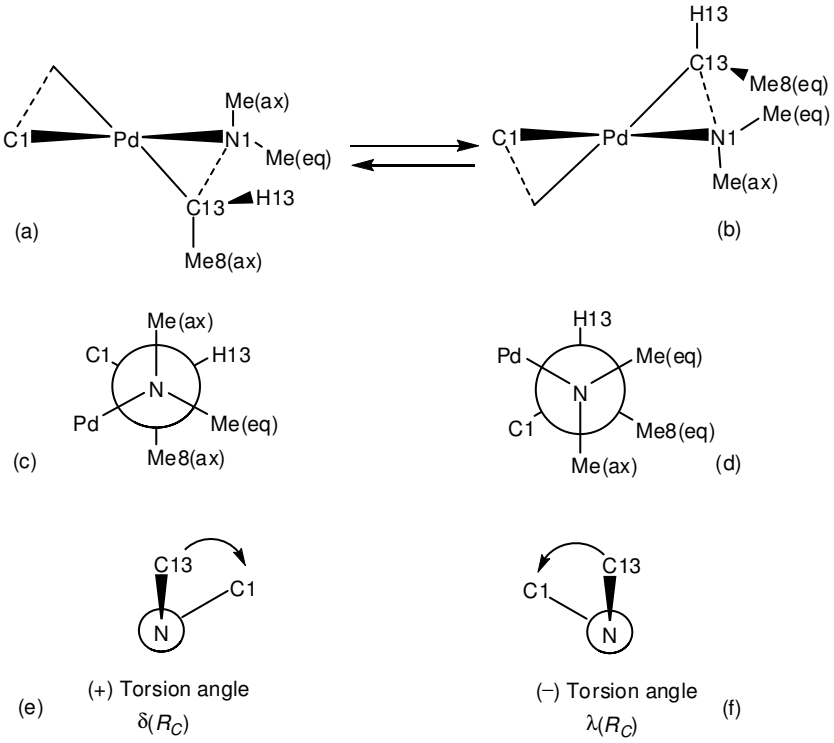

Figure 3.5 Chiral $\delta(R_C)$ (a, c, e) and $\lambda(R_C)$ (b, d, f) conformations of the (R_C,$S_C$$S_N$)-**115** five-membered ring in projections to the plane orthogonal to the {C(1)–Pd(1)–N(1)} plane (a, b); in the Newman projections relative the N(1)–C(13) bond (c, d) and in the Newman projections relative the N(1)–Pd(1) bond (e, f).

Table 3.5 Selected bond lengths (Å) and angles (°) for diastereomer (R_C,$S_C$$S_N$)-**115**

Pd(1)-C(1)	2.014(2)	Pd(1)-O(1)	2.046(2)
Pd(1)-N(1)	2.053(2)	Pd(1)-N(2)	2.140(2)
C(17)-O(1)	1.283(3)	C(17)-O(2)	1.235(3)
C(1)-Pd(1)-O(1)	99.6 (9)	C(1)-Pd(1)-N(1)	80.5(9)
O(1)-Pd(1)-N(1)	177.4(8)	C(1)-Pd(1)-N(2)	178.5(10)
O(1)-Pd(1)-N(2)	80.5(8)	N(1)-Pd(1)-N(2)	99.3(9)

3.3.5.2 Solution Structure of Diastereomer (R_C,$S_C$$S_N$)-115

There are two possible geometric isomers for each diastereomer (Figure 3.6) due to the different arrangements of the coordinating atoms around the palladium center. Isomers of type II, where the two nitrogen atom *trans* to each other were usually observed. [13d,89a]

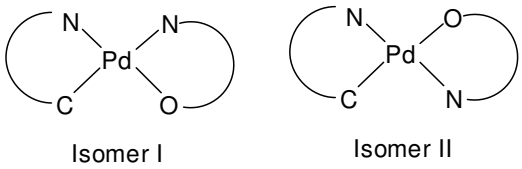

Figure 3.6 Two possible geometric isomers of (R_C,$S_C$$S_N$)-**115**

However, for diastereomer (R_C,$S_C$$S_N$)-**115** the solid state conformation shows that the two nitrogen atoms are in *cis*-(*N*,*N*) arrangement (Figure 3.4). In solution, on the other hand the molecules of the complex will enjoy less restriction and more freedom. Hence, the solution behavior of the complex was examined using the ^{1}H NMR and 2D ^{1}H-^{1}H ROESY NMR experiments.

The ^{1}H NMR spectrum of the complex (R_C,S_CS_N)-**115** conducted at room temperature in $CDCl_3$, shows only one resonance observed for every chemically non-equivalent proton. Hence, concluded that there is only one geometric isomer present in solution. The numbering scheme of the diastereomer (R_C,S_CS_N)-**115** use for NMR study and the 2D ^{1}H-^{1}H ROESY NMR spectrum is shown in in Figure 3.7 and Figure 3.8 respectively.

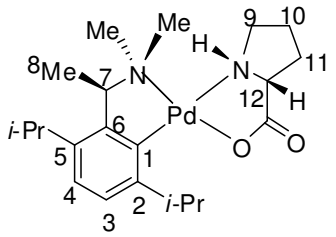

Figure 3.7 Numbering scheme of complex (R_C,S_CS_N)-**115** for NMR assignment

As showed the expanded 2D ^{1}H-^{1}H ROESY NMR spectrum of complex (R_C,S_CS_N)-**115** (Figure 3.8). The interaction between H10/H11 of the prolinato group and NMe(*eq*), represented by signal A, depicts that the two nitrogen groups are *cis* to each other in solution as observed in the solid state investigations. The presence of NOE signals between Me8 and the equatorially disposed NMe group (B) and the interactions of H7 with NMe(*ax*), NMe(*eq*) and Me8 (E, F and G respectively) shows that the methyl group (Me8) at the stereogenic center is axially positioned and the five-membered organometallic ring is locked in δ conformation in solution (Figure 3.5).[89] The distance between the Me8 carbon, C(14) and the NMe(*eq*) carbon, C(15) is 2.876 Å, and is smaller than the summation of the Van der Waals radii of 3.40 Å[86] which indicates the steric repulsion between them. These signals were consistent with the assignment shown in the solid state investigations wherein the organometallic ring is adopting exclusively the δ conformation. The inter-ligand and intra-ligand

interactions of the CH (*iso*-propyl) group with the NH of the prolinato group and H7 were represented by NOE signals C and D, respectively.

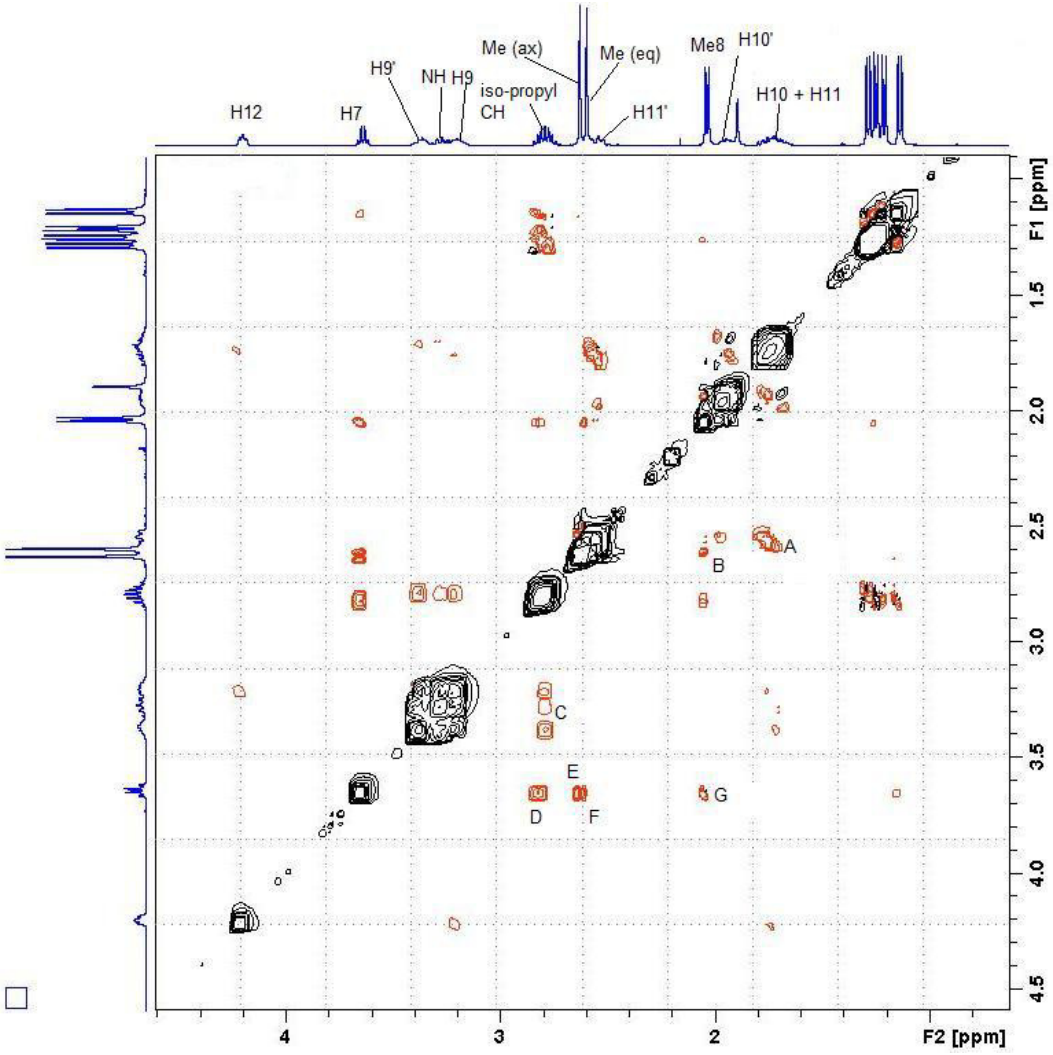

Figure 3.8 Expanded 2D ^{1}H-^{1}H ROESY NMR spectrum of the complex (R_C,$S_C S_N$)-**115** in $CDCl_3$. ROESY Interactions: (A) NMe(eq)−H10/H11; (B) Me8−NMe(eq); (C) NH−CH(iso-propyl); (D) H7−CH(iso-propyl); (E) H7–NMe(ax); (F) H7–NMe(eq); (G) H7–Me8.

3.3.5.3 Molecular Structure of Diastereomer (S_C,$S_C S_N$)-115

Similarly, X-ray crystallographic studies on the other diastereomer (S_C,$S_C S_N$)-**115** were performed and five crystallographically unique molecules were observed in

the asymmetric unit cell. These molecules adopt the same stereochemistry, only differing slightly in bond lengths and bond angles (Table 3.6). For clarity, only one of these molecules (Molecule A) is shown in Figure 3.9. The crystallographic study showed that the absolute stereochemistry at the stereogenic carbon within the organometallic ring is *S*. Similarly, the secondary stereogenic nitrogen atom in the prolinato moiety also adopted the *S* absolute configuration. The torsion angle for C(1)–Pd(1)–N(1)–C(13) is -43.5° with the skewed five-membered ring locked in λ conformation.[89] The five-member ring is in an envelope conformation with N(1) 0.7845 Å above the plane C(1)–C(12)–C(13)–Pd(1). The coordination geometry at palladium is distorted square-planar. The dihedral angles between the planes {N(1)–Pd(1)–C(1)} and {O(1)–Pd(1)–N(2)} is 5.5°. The two coordinated nitrogen groups adopt the *trans*-(*N*,*N*) arrangement. The angle between the mean plane of the organometallic five-membered ring C(1)–C(12)–C(13)–N(1)–Pd(1) and the mean plane formed from O(1)–C(18)–C(19)–N(2)–Pd(1) of the prolinato ligand is 27.26°.

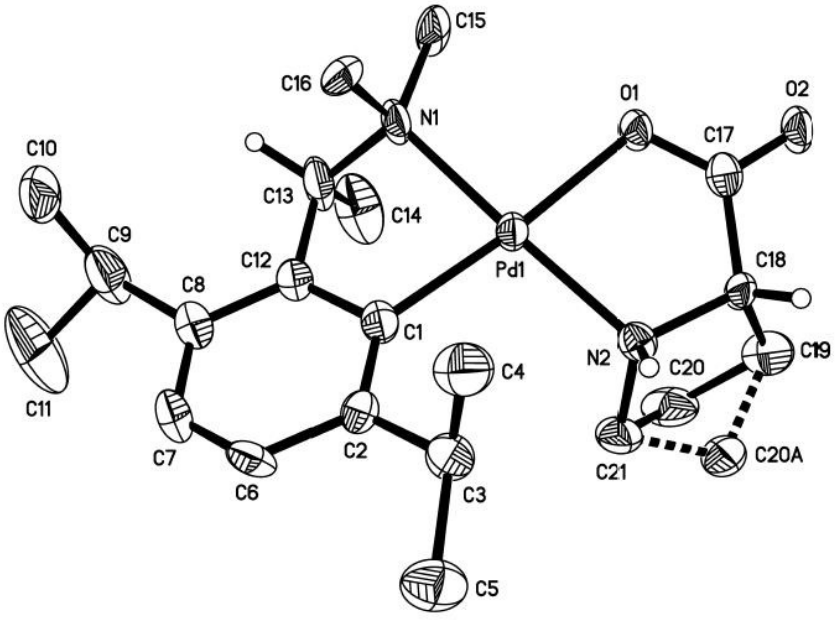

Figure 3.9 Molecular structure of diastereomer (S_C,S_CS_N)-**115**. All hydrogen atoms except H(C13), H(C18) and H(N2) were omitted for clarity

Table 3.6 Selected bond lengths (Å) and angles (°) for diastereomer (S_C,S_CS_N)-**115**

Molecule A		Molecule B		Molecule C	
Pd(1)-C(1)	2.020(7)	Pd(1)-C(1)	2.020(7)	Pd(3)-C(43)	1.984(8)
Pd(1)-N(1)	2.046(7)	Pd(1)-N(1)	2.046(7)	Pd(3)-N(5)	2.060(6)
Pd(1)-N(2)	2.078(6)	Pd(1)-N(2)	2.078(6)	Pd(3)-N(6)	2.058(6)
Pd(1)-O(1)	2.100(5)	Pd(1)-O(1)	2.100(5)	Pd(3)-O(5)	2.108(5)
C(1)-Pd(1)-N(1)	79.9(3)	C(1)-Pd(1)-N(1)	79.9(3)	C(43)-Pd(3)-N(5)	80.3(3)
C(1)-Pd(1)-N(2)	103.4(3)	C(1)-Pd(1)-N(2)	103.4(3)	C(43)-Pd(3)-N(6)	101.7(3)
N(1)-Pd(1)-O(1)	94.6(2)	N(1)-Pd(1)-O(1)	94.6(2)	N(5)-Pd(3)-O(5)	95.4(2)
N(2)-Pd(1)-O(1)	81.8(2))	N(2)-Pd(1)-O(1)	81.8(2))	N(6)-Pd(3)-O(5)	82.0(2)
N(1)-Pd(1)-N(2)	173.9(3)	N(1)-Pd(1)-N(2)	173.9(3)	N(6)-Pd(3)-N(5)	173.4(3)
C(1)-Pd(1)-O(1)	173.9(3)	C(1)-Pd(1)-O(1)	173.9(3)	C(43)-Pd(3)-O(5)	173.4(3)

Molecule D		Molecule E	
Pd(3)-C(64)	1.992(7)	Pd(5)-C(85)	2.023(7)
Pd(3)-N(7)	2.056(6)	Pd(5)-N(10)	2.058(6)
Pd(3)-N(8)	2.058(6)	Pd(5)-N(9)	2.063(6)
Pd(3)-O(7)	2.105(5)	Pd(5)-O(9)	2.094(5)
C(64)-Pd(4)-N(7)	80.6(3)	C(85)-Pd(5)-N(10)	102.8(2)
C(64)-Pd(4)-N(8)	103.4(3)	C(8)5-Pd(5)-N(9)	80.4(3)
N(7)-Pd(4)-O(7)	94.4(2)	N(10)-Pd(5)-O(9)	82.4(2)
N(8)-Pd(4)-O(7)	81.4(2)	N(9)-Pd(5)-O(9)	94.0(2)
N(7)-Pd(4)-N(8)	172.9(3)	N(10)-Pd(5)-N(9)	173.7(3)
C(64)-Pd(4)-O(7)	174.5(3)	C(85)-Pd(5)-O(9)	173.2(3)

3.3.5.4 Solution Structure of Diastereomer (S_C,S_CS_N)-115

The structure in solution and signal assignment of the diastereomer (S_C,S_CS_N)-**115** is determined by the ^{1}H NMR and 2D ^{1}H-^{1}H ROESY NMR experiments. Similarly, the ^{1}H NMR spectrum of the complex (S_C,S_CS_N)-**115** conducted at room temperature in $CDCl_3$, also shows only one geometric isomer in solution. The numbering scheme of the diastereomer (S_C,S_CS_N)-**115** use for NMR assignment and the 2D ^{1}H-^{1}H ROESY NMR spectrum is presented in Figure 3.10 and Figure 3.12 respectively

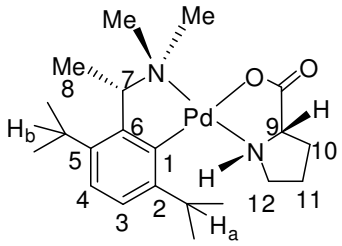

Figure 3.10 Numbering scheme of complex (S_C,S_CS_N)-**115** for NMR assignment

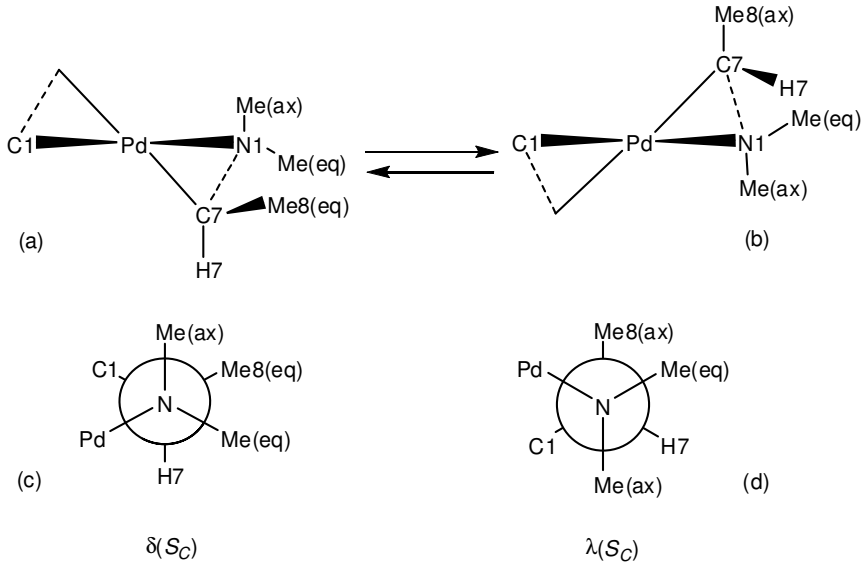

Figure 3.11 Chiral δ(S_C) (**a**, **c**) and λ(S_C) (**b**, **d**) conformations of the (S_C,S_CS_N)-**115** five-membered ring in projections to the plane orthogonal to the {C(1)–Pd(1)–N(1)} plane (**a**, **b**) and in the Newman projections relative the N–C(7) bond (**c**, **d**)

Figure 3.12 depicts the expanded 2D ^{1}H-^{1}H ROESY NMR spectrum of the diastereomeric complex (S_C,$S_C S_N$)-**115**. The presence of interaction of Me8 with NMe(eq) represented by NOE signal A and the interactions of H7 with the Hb, NMe(eq), NMe(ax) and Me8 (correspond to NOE signals D to G) indicated that the five-membered organometallic ring is locked in λ conformation and the Me8 take up the axial position in solution (Figure 3.11).[89] The distance between the Me8 carbon, C(14) and the NMe(*eq*) carbon, C(15) and the distance between the H7 proton H(13) and the Hb proton H(9) is 2.925 Å and 2.072 Å respectively. Both are smaller than the summation of the corresponding Van der Waals radii of 3.40 Å and 2.40 Å.[82] The NOE signals in solution matches the interactions of the complex in solid state investigations. The presence of inter-ligand interaction between Ha and NH is denoted as C which indicates that the two nitrogen groups are *trans* to each other. This is further supported by solid state investigations where the distance between the Ha proton H(3) and the NH proton N(2) is 1.962 Å.[82]

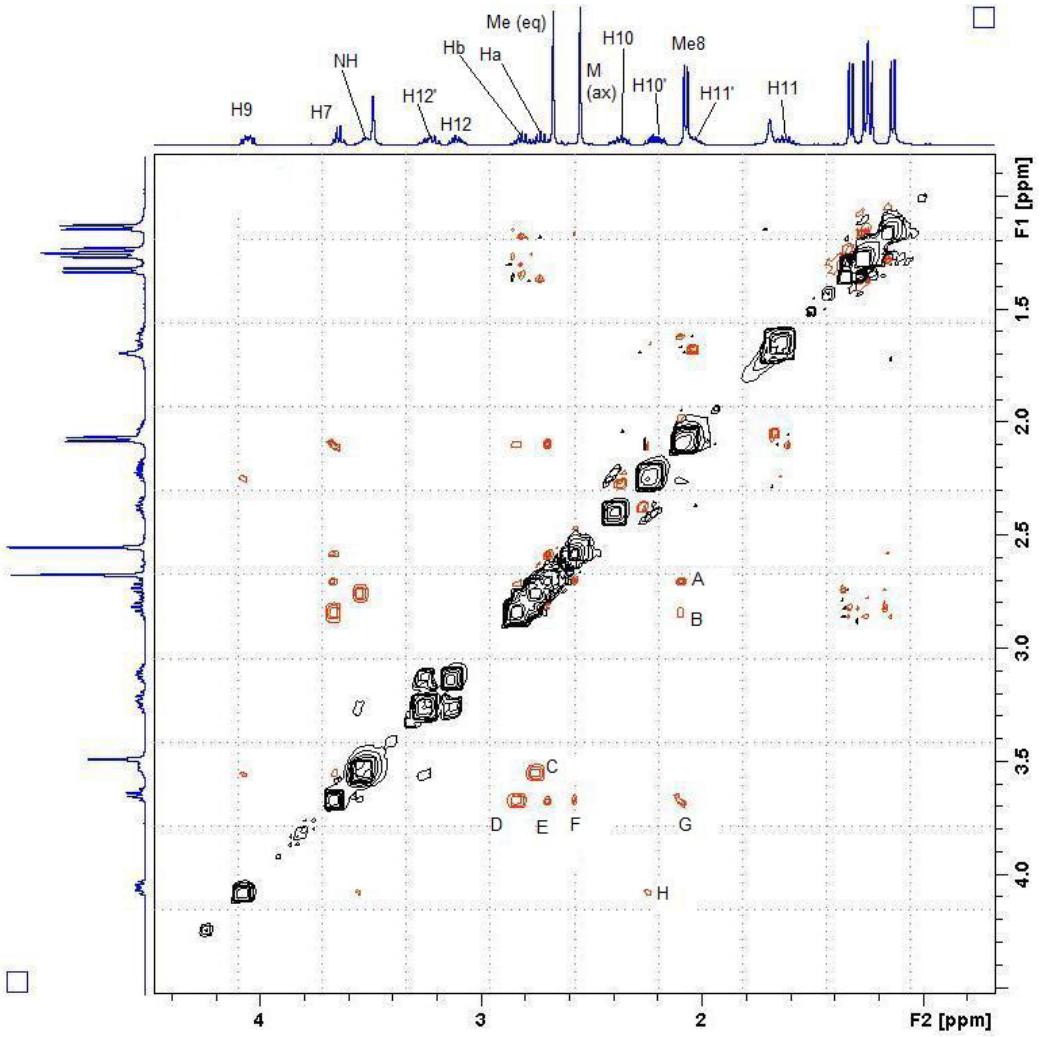

Figure 3.12 Expanded 2D ^{1}H-^{1}H ROESY NMR spectrum of the complex (S_C,$S_C S_N$)-**115** in $CDCl_3$. ROESY Interactions: (A) Me8−NMe(eq); (B) Hb–Me8; (C) Ha–NH; (D) H7–Hb; (E) H7–NMe(eq); (F) H7–NMe(ax); (G) H7–Me8; (H) H9–H10'

3.3.6 Synthesis of Optically Active Dimeric Complex (*R*)-106

The optically active dimeric complex, (*R*)-**106** was in 90% isolated yield with $[\alpha]^{25.0}$ -210.2^{o} (*c* 0.02, DCM) by the removal of the prolinate ligand using 1M aqueous hydrochloric acid in two-phase conditions (Scheme 3.7).

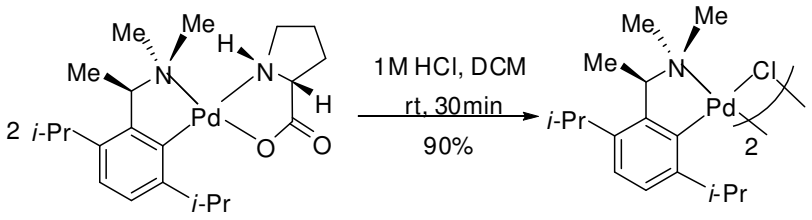

(R_C,$S_C$$S_N$)-**115** (*R*)-**106**

Scheme 3.7

The other dimeric complex, (*S*)-**106** was also prepared in same way by treating the diastereomer (S_C,$S_C$$S_N$)-**115** with 1M aqueous hydrochloric acid to give the dimeric complex (*S*)-**106** in 90% yield as yellow solid, $[\alpha]^{23.8}$ +180.7° (*c* 0.02, DCM) (Scheme 3.8). The dimeric complex (*S*)-**106** did not crystallized out after several attempts.

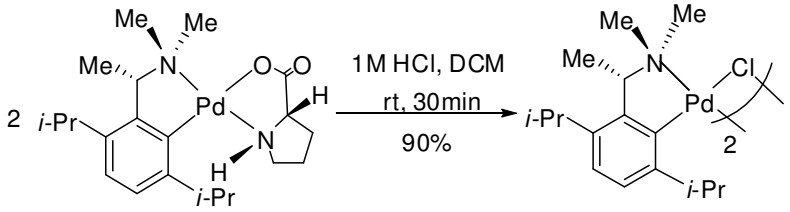

(S_C,$S_C$$S_N$)-**115** (*S*)-**106**

Scheme 3.8

3.3.6.1 Molecular Structure Optically Active Dimeric Complex (*R*)-106

Yellow plate-like single crystals obtained from a solution of (*R*)-**106** in DCM/ *n*-hexane solution and the solid state structure of complex was determined crystallographically. The X-ray study confirms the absolute *R* configuration of the α-carbon stereocenter of the palladacycle and the molecular structure of complex (*R*)-**106** is depicted in Figure 3.13. Selected bond lengths and angles are tabulated in Table 3.7. The coordination geometry of both palladium centers are distorted square planar. The dihedral angle of distortion on Pd(1) and Pd(2) is 9.9° and 9.3°, respectively. The five-membered ring is in enveloped conformation with N(2) being 0.895 Å below the

plane {C(1)–C(12)–C(13)–Pd(1)} and N(1) is 0.874 Å below the plane {C(17)–C(28)–C(29)–Pd(2)}. The two nitrogen donor atoms are *trans* to each other. The chloro bridging and palladium centers formed a four-membered ring that is bent 50.6° along the Cl(1)–Cl(2) axis. The bond lengths and the bond angles are comparable to the reported values.[13b]

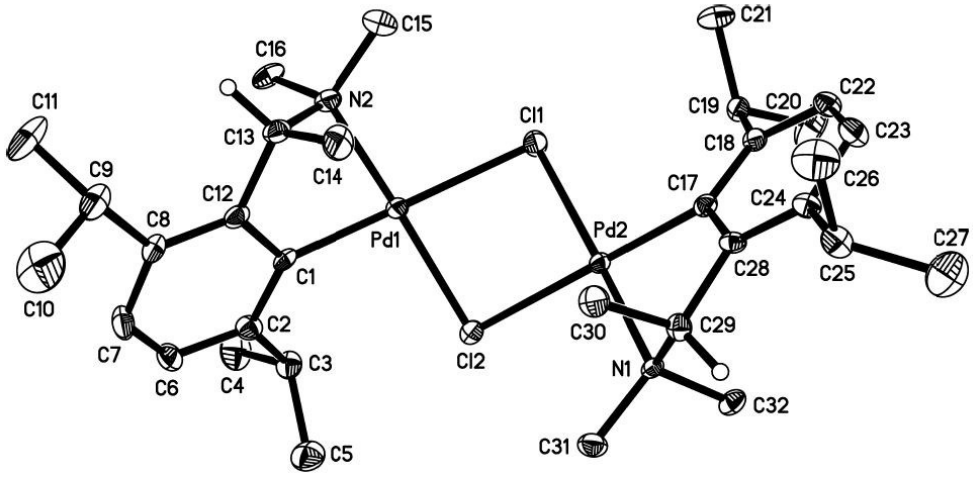

Figure 3.13 Molecular structure of complex (*R*)-**106**. All hydrogen atoms except H(C13), and H(C29) in were omitted for clarity.

Table 3.7 Selected bond lengths (Å) and angles (°) for complex (*R*)-**106**

Pd(1)-C(1)	1.987(5)	Pd(1)-N(2)	2.087(4)
Pd(1)-Cl(2)	2.3368(12)	Pd(1)-Cl(1)	2.4674(12)
Pd(2)-C(17)	1.994(4)	Pd(2)-N(1)	2.072(4)
Pd(2)-Cl(1)	2.3443(13)	Pd(2)-Cl(2)	2.4684(12)
C(1)-Pd(1)-N(2)	79.24(17)	C(1)-Pd(1)-Cl(2)	97.21(13)
N(2)-Pd(1)-Cl(2)	169.60(13)	C(1)-Pd(1)-Cl(1)	177.20(14)
N(2)-Pd(1)-Cl(1)	99.68(12)	Cl(2)-Pd1-Cl(1)	83.41(4)
C(17)-Pd(2)-N(1)	80.06(16)	C(17)-Pd(2)-Cl(1)	98.09(13)
N(1)-Pd(2)-Cl(1)	170.90(11)	C(17)-Pd(2)-Cl(2)	175.99(12)
N(1)-Pd(2)-Cl(2)	98.03(11)	Cl(1)-Pd(2)-Cl(2)	83.24(4)

3.3.7 Regio-selective Formation of the DMPP Complex (*S*)-116 and its *endo*-Cycloaddition Reactions with Ethyl Vinyl Ketone

In order to assess the effectiveness and the effect of the bulky *i*-propyl group of the new palladacycle (*S*)-**106** synthesized, the asymmetric [4+2] *endo*-cycloaddition reaction between DMPP and ethyl vinyl ketone promoted by the new palladacycle (*S*)-**106** is conducted. The DMPP-coordinated complex (*S*)-**116** is obtained by cleavage of the optically pure dimeric complex (*S*)-**106** with two molar equivalents of DMPP in 90% yield, $[\alpha]^{23.4}$ +431.5° (*c* 0.0121, DCM) (Scheme 3.9).

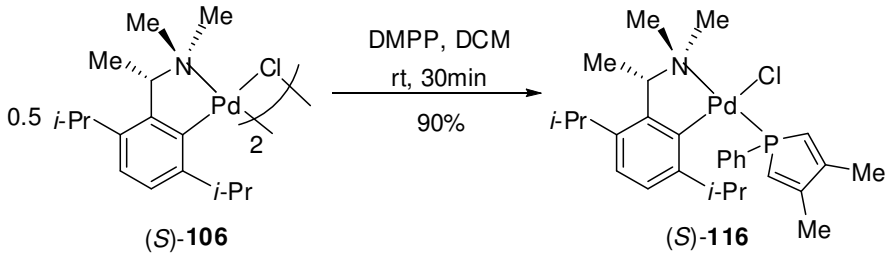

(*S*)-**106** (*S*)-**116**

Scheme 3.9

3.3.7.1 Molecular Structure of DMPP Complex (*S*)-116

The solid-state structural study on the yellow single crystal obtained from slow evaporation of the complex (*S*)-**116** in DCM/ *n*-hexane solution is investigated using X-ray crystallography (Figure 3.14). Selected bond lengths and angles of (*S*)-**110** are presented in Table 3.8. The palladium center of complex (*S*)-**110** is in distorted square planar coordination geometry with tetrahedral distortion of 20.68° and the nitrogen group is *trans to* phosphole group. The Pd(1)–P(1) bond length is slightly longer than that of DMPP-coordinated complex (*S*)-**88**.[13c] This shows that the Pd–P bond is weaker than DMPP-coordinated complex (*S*)-**88**. The bond angle of C(1)-Pd(1)-P(1) is also bigger than DMPP complex (*S*)-**88** which shows that the steric repulsion between *i*-propyl group and the DMPP group in complex (*S*)-**116** is larger.

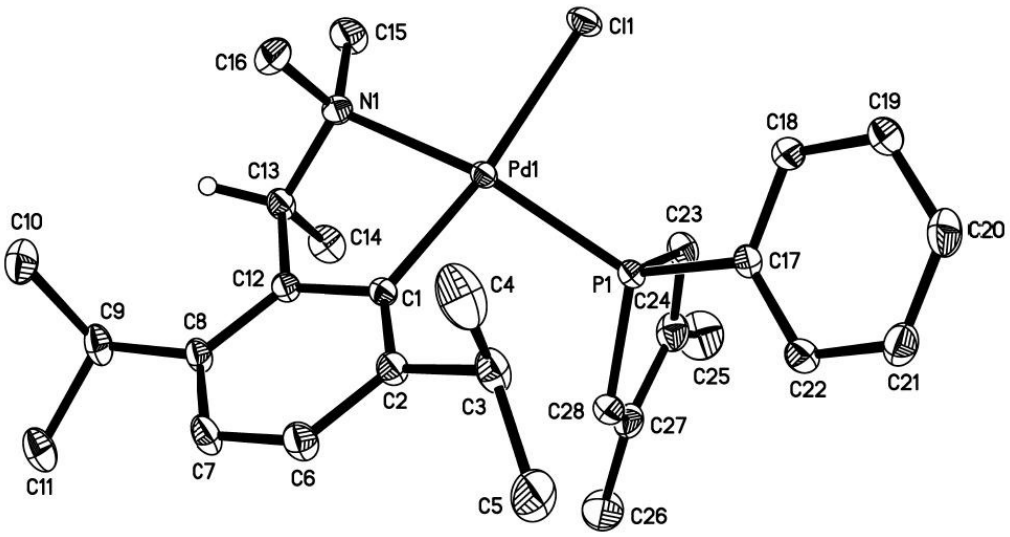

Figure 3.14 Molecular structure of DMPP complex (*S*)-**116**. All hydrogen atoms except H(C13) were omitted for clarity.

Table 3.8 Selected bond lengths (Å) and angles (°) for complex (*S*)-**116**

Pd(1)-C(1)	2.020(2)	Pd(1)-N(1)	2.141(2)
Pd(1)-P(1)	2.2390(7)	Pd(1)-Cl(1)	2.4195(6)
C(1)-Pd(1)-N(1)	80.48(9)	C(1)-Pd(1)-P(1)	96.63(7)
N(1)-Pd(1)-P(1)	160.37(7)	C(1)-Pd(1)-Cl(1)	171.56(7)
N(1)-Pd(1)-Cl(1)	94.49(6)	P(1)-Pd(1)-Cl(1)	90.36(2)

3.3.7.2 Solution Structure of DMPP Complex (*S*)-116

The $^{31}P\{^{1}H\}$ NMR spectrum of DMPP complex (*S*)-**116** in CD_3CN in room temperature gave only one singlet at δ 28.9. This indicates that there is only one isomer present in the solution. ^{1}H NMR and 2D ^{1}H-^{1}H ROESY NMR experiments were conducted to determine the solution structure and signal assignment of the complex (*S*)-**116**. The numbering scheme of the DMPP complex (*S*)-**110** used for

NMR study and the 2D ^{1}H-^{1}H ROESY NMR spectrum is presented in Figure 3.15 and Figure 3.16, respectively.

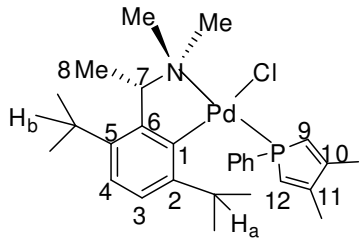

Figure 3.15 Numbering scheme of DMPP complex (*S*)-**116**

In Figure 3.16, the presence of strong interaction between the Me8 with NMe(eq) symbolized as A, proves that the Me8 is position in axial position and the five-membered organometallic ring is locked in λ conformation in solution. In addition, there is no interaction of the Me8 with the axially disposed NMe group further confirmation. NOE signal B represents the interaction of both NMe groups on the amine moiety. ROESY correlations C to F correspond to the interactions between H7 with Hb, NMe(eq), NMe(ax) and Me8, respectively. The absence of interactions between the proton on the phosphole and the NMe groups further confirm that they are *trans* to each other.

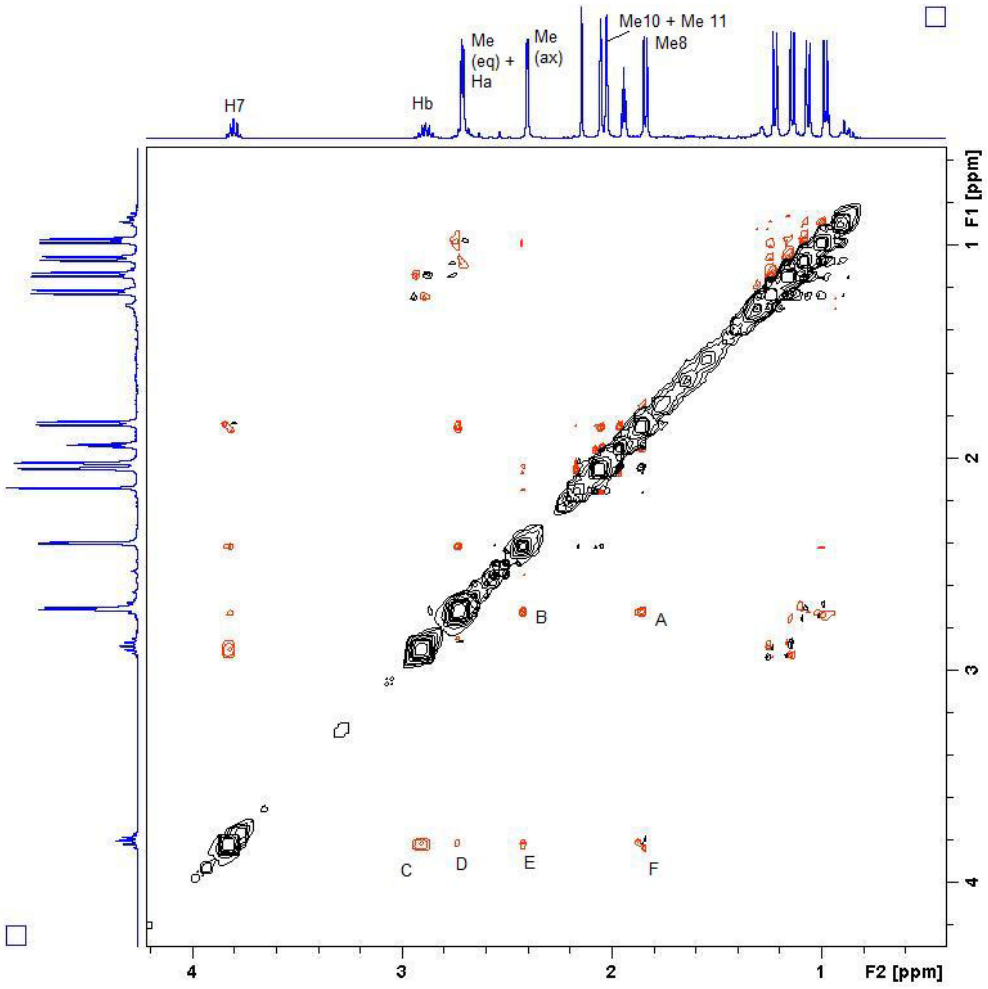

Figure 3.16 Expanded 2D ^{1}H-^{1}H ROESY NMR spectrum of the complex (*S*)-**116** in CD_3CN. Selected ROESY Interactions: (A) Me8–NMe(eq); (B) NMe(ax)–NMe(eq); (C) H7– Hb; (D) H7–NMe(eq); (E) H7–NMe(ax); (F) H7– Me8

3.3.7.3 Asymmetric Intramolecular *endo*- Cycloaddition Reactions between DMPP Complex (*S*)-116 and Ethyl Vinyl Ketone

Complex (*S*)-**116** was treated with excess of ethyl vinyl ketone in chloroform and stirred at room temperature. The reaction was monitored using ^{31}P{^{1}H} NMR. After 14 days, the reaction was not completed and a diastereomeric ratio of 1:5.6 was observed. In order to increase the reactivity of the reaction, the reaction temperature was increased to 50 ^{o}C. The reaction was completed after five days, the peak at δ 28.9

disappeared and two new sharp singlets δ 118.2 and 119.4 in a 1:4.4 diastereomeric ratio were observed. Other unknown by-products peaks at δ 21.2 (s), 67.4 (d), 71.6 (s) were also observed. The stereoselectivity of the cycloaddition reaction at 50 ^{o}C is slightly lower than the stereoselectivity of the reaction at room temperature. The presence of the protruding *i*-propyl group did exert more stereochemical influence on the reaction site than the presence of methyl group.[13c] After column chromatography, the major product, *(*S_C,R_P*)*-**117** was eluted together with the impurities (δ 21.2 and 67.4) using DCM as eluent in low yield (Scheme 3.10). Unfortunately, the *(*S_C,R_P*)*-**117** complex did not crystallized after several attempt with various solvent.

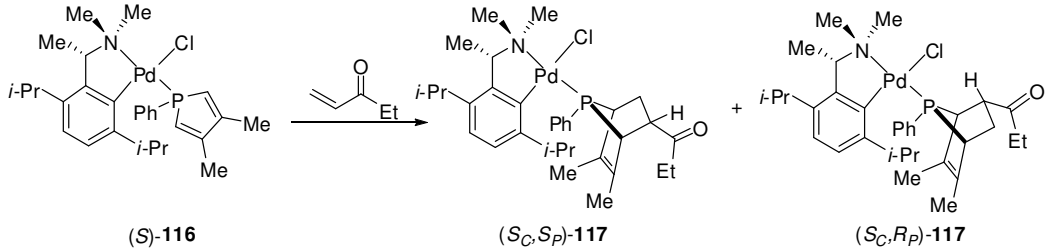

(*S*)-**116** (S_C,S_P)-**117** (S_C,R_P)-**117**

Scheme 3.10

3.3.8 Conclusion

In this chapter, the novel palladacycle **106** was successfully synthesized. The amine ligand (±)-**105** was synthesized from *p*-di-iso-propylbenzene *via* two synthetic routes. The second synthetic route improves the greenness and also increased the overall yield from 46% to 89%. The *ortho*-palladation of the amine ligand (±)-**111** generated two products, C–N bond cleavage complex (±)-**113** and palladacycle (±)-**106**. The palladacycle (±)-**106** was successfully resolved *via* separation of (*S*)-prolinate diastereomeric derivatives. It was confirmed *via* X-ray crystallography and 2D ^{1}H-^{1}H ROESY NMR spectroscopy that the (*S*)-prolinate diastereomeric derivatives exist in one conformation, (*R*)δ or (*S*)λ and methyl group on the stereogenic carbon is in axial position. This affirmed that the chiral palladacycle is rigid in both solid state and in solution. Investigation on the effectiveness of the bulky *i*-propyl group of the complex in asymmetric [4+2] *endo*-cycloaddition reaction, results in better stereoselectivity obtained than the methyl substituted benzyl chiral template.

3.4 Experimental

Reactions involving air-sensitive compounds were performed under positive pressure of purified nitrogen by using standard Schlenk techniques. Proton nuclear magnetic resonance (^{1}H NMR), carbon nuclear magnetic resonance (^{13}C{^{1}H} NMR) spectroscopy and phosphorus nuclear magnetic resonce (^{31}P{^{1}H} NMR) spectroscopy were performed on a Bruker Avance III 400 Spectrometer (1H at 400 MHz, ^{13}C{^{1}H} at 100 MHz, ^{31}P{^{1}H} at 162MHz). Multiplicities are given as: s (singlet); br (broad singlet); d (doublet); t (triplet); q (quartet); qn (quintet); sep (septet); dd (doublets of doublet); m (multiplets) and *etc*. The number of protons (n) for a given resonance is indicated by nH. Coupling constants are reported as a *J* value in Hz. Chemical shifts are reported as δ in units of parts per million (ppm) downfield from tetramethylsilane (δ 0.0) and relative to the signal of chloroform-*d* (^{1}H at δ 7.26, singlet and ^{13}C{^{1}H} NMR δ 77.00, triplet). unless otherwise stated. All NMR spectroscopic experiments were performed at room temperature (300 K). Mass spectra were recorded on a Finnigan Trace GC Ultra instrument at 70 Ev with EI mode. Melting points were determined on SRS-Optimelt MPA-100 apparatus and were uncorrected. Optical rotations were measured using a 0.1-dm cell at 589 nm with Atago automatic polarimeter model (AP-300). 2,5-Di-*iso*-propylbenzaldehyde, **107** was prepared according to procedures as reported in literature. [84]

3.4.1 Synthesis of *1-(2,5-diisopropylphenyl)ethanol*, (±)-**108**

A colourless solution of MeMgBr (3 M, 7.9 mL, 23.70 mmol) in dry THF (10 mL) was added dropwise to a stirred solution of (±)-**107** (2.25 g, 11.82 mmol) dissolved in the same solvent (10 mL) at 0 °C. The reaction mixture was heated under reflux for 16 h at 90 °C and then cooled to room temperature. The pale yellow mixture was poured

into a mixture of ice water (20 mL) and concentrated HCl (1 mL) and left to stir for 5 min. The resulting mixture was then extracted with DCM (3 x 50 mL), concentrated, followed by purification with column chromatography on silica gel using *n*-hexane/DCM (v/v = 1:1) as eluent. After removal of solvent, gave colourless oil. Yield: 2.10 g (86%). ^{1}H NMR (400 MHz, $CDCl_3$): δ = 1.24 (d, $^{3}J_{H,H}$ = 7.2 Hz, 6H, CH(CH_3)$_2$), 1.26 (d, $^{3}J_{H,H}$ = 6.8 Hz, 1H, CH(CH_3)$_2$), 1.49 (d, $^{3}J_{H,H}$ = 6.4 Hz, 3H, CHCH_3), 1.86 (br, 1H, O*H*), 2.89 (sep, $^{3}J_{H,H}$ = 6.9 Hz, 1H, C*H*(CH$_3$)$_2$), 3.19 (sep, $^{3}J_{H,H}$ = 6.8 Hz, 1H, C*H*(CH$_3$)$_2$), 5.25 (q, $^{3}J_{H,H}$ = 6.4 Hz, 1H, C*H*CH$_3$), 7.12 (dd, $^{3}J_{H,H}$ = 8.0 Hz, $^{4}J_{H,H}$ = 2.0 Hz, 1H, aromatic), 7.20 (d, $^{3}J_{H,H}$ = 8.0 Hz, 1H, aromatic), 7.38 (d, $^{4}J_{H,H}$ = 2.0 Hz, 1H, aromatic) . ^{13}C{^{1}H} NMR (100 MHz, $CDCl_3$): δ = 23.96 (CH(***C***H$_3$)$_2$), 24.01 (CH(**C**H$_3$)$_2$), 24.41 (CH(***C****H*$_3$)$_2$), 25.02 (CH***C***H$_3$), 27.82 (***C***H(CH$_3$)$_2$), 33.82 (***C***H(CH$_3$)$_2$), 66.30 (***C***HCH$_3$), 122.81 (Ar-C6), 125.27 (Ar-C3), 125.53 (Ar-C4), 142.12 (Ar-C1), 142.52 (Ar-C5), 142.47 (Ar-C2). HRMS (ESI, m/z (M + Na)]$^{+}$ calcd for $C_{14}H_{22}O$ 229.1568, found 229.1559.

The reaction was repeated at room temperature to give 98% yield.

3.4.2 Synthesis of *2-(1-azidoethyl)-1,4-diisopropylbenzene*, (±)-**109**

A pale yellow solution of CF_3CO_2H (4 mL) in dry chloroform (5 mL) was added dropwise to the stirring mixture of racemic alcohol (±)-**108** (2.0 g, 9.69 mmol) and sodium azide (1.26 g, 19.38 mmol) in same solvent (10 mL) at 0 °C. The reaction mixture was then stirred at room temperature for 48 h. Dilute NaOH solution was added to the reaction mixture until pH 7. The organic layer was separated, washed with H_2O, dried with $MgSO_4$, filtered and evaporated to dryness, affording colourless oil. Yield: 2.18 g (97%) ^{1}H NMR (400 MHz, $CDCl_3$): δ = 1.26 (d, $^{3}J_{H,H}$ = 6.3 Hz, 6H, CH(CH_3)$_2$), 1.28 (d, $^{3}J_{H,H}$ = 7.0 Hz, 6H, CH(CH_3)$_2$), 1.67 (d, $^{3}J_{H,H}$ = 6.6 Hz, 3H,

CHCH_3), 2.90 (sep, $^3J_{H,H}$ = 6.9 Hz, 1H, CH(CH_3)$_2$), 3.19, (sep, $^3J_{H,H}$ = 6.9 Hz, 1H, CH(CH_3)$_2$), 4.97 (q, $^3J_{H,H}$ = 6.8 Hz, 1H, CH(CH_3), 7.15 (dd, $^3J_{H,H}$ = 8.1 Hz, $^4J_{H,H}$ = 1.9 Hz, 1H, aromatic), 7.19 (d, $^3J_{H,H}$ = 8.2 Hz, 1H, aromatic), 7.23 (d, $^4J_{H,H}$ = 1.8 Hz, 1H, aromatic) . $^{13}C\{^1H\}$ NMR (100 MHz, $CDCl_3$): δ = 21.85 (CH***C***H_3), 24.20 (CH(***C***H_3)$_2$), 24.30 (CH(***C***H_3)$_2$), 24.53 (***C***H(CH_3)$_2$), 28.49 (CH(***C***H_3)$_2$), 33.97 (CH(***C***H_3)$_2$), 57.14 (***C***HCH_3), 124.18 (Ar-C4), 125.82 (Ar-C3), 126.37 (Ar-C6), 137.32 (Ar-C1), 143.43 (Ar-C5), 146.79 (Ar-C2). HRMS (ESI, m/z (M + H)]$^+$ calcd for $C_{14}H_{22}N_3$ 232.1814, found 232.1824.

3.4.3 Synthesis of *1-(2,5-diisopropylphenyl)ethanamine*, (±)-110

A colourless solution of azide compound (±)-**109** (2.16 g, 9.34 mmol) in dried THF (10 mL) was added dropwise to a stirred solution of LAH (0.36 g, 9.48 mmol) in the same solvent (5 mL) at 0 °C. The reaction mixture was heated under reflux for 8 h at 90 °C before it was cooled to 0 °C. The excess LAH was quenched by the dropwise addition of ice H_2O (1.2 mL), then diluted NaOH solution (3 wt.%, 0.8 mL), followed by more ice H_2O (0.4 mL) again. The thick white precipitate was then removed by filtration under vacuum. The filtrate was extracted with ethyl acetate (3 x 50 mL), dried with $MgSO_4$, filtered and evaporated to dryness, affording colourless oil. Yield: 1.86 g (97%). ^1H NMR (400 MHz, $CDCl_3$): δ = 1.24 (d, $^3J_{H,H}$ = 6.8 Hz, 6H, CH(CH_3)$_2$), 1.26 (d, $^3J_{H,H}$ = 6.8 Hz, 6H, CH(CH_3)$_2$), 1.38 (d, $^3J_{H,H}$ = 6.6 Hz, 3H, CHCH_3), 1.65 (br, 2H, NH), 2.90 (sep, $^3J_{H,H}$ = 6.9 Hz, 1H, CH(CH_3)$_2$), 3.25 (sep, $^3J_{H,H}$ = 6.9, 1H, CH(CH_3)$_2$), 4.49 (q, $^3J_{H,H}$ = 6.5, 1H, C$H$$CH_3$), 7.09 (dd, $^3J_{H,H}$ = 8.0 Hz, $^4J_{H,H}$ = 1.9 Hz, 1H, aromatic), 7.20 (d, $^3J_{H,H}$ = 8.0 Hz, 1H, aromatic), 7.33 (d, $^4J_{H,H}$ = 1.9 Hz, 1H, aromatic) . $^{13}C\{^1H\}$ NMR (100 MHz, $CDCl_3$): δ = 23.96 (CH***C***H_3), 24.03 (CH(***C***H_3)$_2$), 24.07 (CH(***C***H_3)$_2$), 24.38 (CH(***C***H_3)$_2$), 25.50 (CH(***C***H_3)$_2$), 27.77

(***C***H(CH$_3$)$_2$), 33.81 (***C***H(CH$_3$)$_2$), 45.85 (***C***HCH$_3$), 122.59 (Ar-C4), 124.64 (Ar-C3), 125.11 (Ar-C6), 142.42 (Ar-C1), 143.91(Ar-C5), 146.31 (Ar-C2). HRMS (ESI, m/z (M + H)]$^+$ calcd for $C_{14}H_{24}N$ 206.1909, found 206.1909.

3.4.4 Synthesis of *1-(2,5-diisopropylphenyl)-N,N-dimethylethanamine*, (±)-111

Method A:

A mixture of primary amine (±)-**109** (1.80 g, 8.77 mmol) in formic acid (1.7 mL, 43.85 mmol) was treated with formaldehyde (37%, 1.1 mL, 29.54 mmol) at 0 °C. The reaction mixture was heated at 100 °C for 6 h and then cooled to room temperature. Concentrated HCl was added and the mixture was stirred for 15 min. After removal of the HCl under reduced pressure, the residual oil was treated with NaOH solution until pH 14 for liberation of amine. The liberated amine was extracted with ethyl acetate (3 x 50 mL), dried with $MgSO_4$, filtered and evaporated to dryness, affording colourless oil. Yield: 1.52 g (71%).

Method B:

A solution of aqueous dimethylamine (40 wt.%, 19.3 mL, 17.1 mmol) was added to a solution of bromo compound (±)-**112** (3.08 g, 11.4 mmol) in DCM (20 mL) and the mixture was then left to stir at room temperature for 16 h. The organic layer was separated and the aqueous layer was extracted with DCM (2 x 25 mL). The clear organic solution was then washed with brine (50 mL), dried with $MgSO_4$, filtered and evaporated to dryness. The crude product was then purified by column chromatography on silica gel using DCM/ethyl acetate (v/v = 2:1) as eluent affording colourless oil. Yield: 2.62g (98%). ^{1}H NMR (400 MHz, $CDCl_3$): δ = 1.22 (d, $^3J_{H,H}$ = 6.8 Hz, 6H, CH(C*H*$_3$)$_2$), 1.24 (d, $^3J_{H,H}$ = 6.8 Hz, 6H, CH(C*H*$_3$)$_2$), 1.32 (d, $^3J_{H,H}$ = 6.4 Hz, 3H, CHC*H*$_3$), 2.22 (s, 6H, NC*H*$_3$), 2.88 (sep, $^3J_{H,H}$ = 6.9 Hz, 1H, C*H*(CH$_3$)$_2$), 3.34

(sep, $^{3}J_{H,H}$ = 6.9 Hz, 1H, C*H*(CH_3)$_2$), 3.47 (q, $^{3}J_{H,H}$ = 6.5 Hz, 1H, C*H*CH_3), 7.07 (dd, $^{3}J_{H,H}$ = 8.0 Hz, $^{4}J_{H,H}$ = 2.0 Hz, 1H, aromatic), 7.18 (d, $^{3}J_{H,H}$ = 8.0 Hz, 1H, aromatic), 7.31 (d, $^{4}J_{H,H}$ = 2.0 Hz, 1H, aromatic) . $^{13}C\{^{1}H\}$ NMR (100 MHz, $CDCl_3$): δ = 21.85 (CH***C***H_3), 24.24 (CH(***C***H_3)$_2$), 24.26 (CH(***C***H_3)$_2$), 24.27 (CH(***C***H_3)$_2$), 24.29 (CH(***C***H_3)$_2$), 27.86 (***C***H(CH_3)$_2$), 33.94 (***C***H(CH_3)$_2$), 44.32 (N(***C***H_3)$_2$), 61.44 (***C***HCH_3), 124.51 (Ar-C4), 125.13 (Ar-C3), 125.16 (Ar-C6), 142.04 (Ar-C1), 143.33 (Ar-C5), 146.36 (Ar-C2). HRMS (ESI, m/z (M + H)]$^{+}$ calcd for $C_{16}H_{28}N$ 234.2222, found 234.2220.

3.4.5 Synthesis of *2-(1-Bromoethyl)-1,4-diisopropylbenzene*, (±)-112

A solution of PBr_3 (1.3 mL, 13.9 mmol) dissolved in the DCM (10 mL) was added dropwise to a solution of racemic alochol (±)-**108** (2.39 g, 11.6 mmol) in dry DCM (10 mL) at 0 °C. The mixture was left to stir at room temperature for 3 h. The excess PBr_3 was quenched by addition of H_2O (10 mL) dropwise. The mixture was extracted with DCM (3 x 10 mL). The organic layer obtained was then dried with $MgSO_4$, filtered and evaporated to dryness, affording a colourless solution. Yield: 3.08 g (99%); ^{1}H NMR (400 MHz, $CDCl_3$): δ = 1.24-1.32 (m, 12H, CH(C*H*$_3$)$_2$), 2.09 (d, $^{3}J_{H\text{-}H}$ = 6.8 Hz, 3H, CH(C*H*$_3$)Br), 2.91 (sep, $^{3}J_{H\text{-}H}$ = 6.9 MHz, 1H, C*H*(CH_3)$_2$), 3.30 (sep, $^{3}J_{H\text{-}H}$ = 6.8 MHz, 1H, C*H*(CH_3)$_2$), 5.59 (q, $^{3}J_{H\text{-}H}$ = 6.9 MHz, 1H, C*H*(CH_3)Br), 7.15 (dd, $^{3}J_{H,H}$ = 8.0 Hz, $^{4}J_{H,H}$ = 1.6 Hz, 1H, aromatic), 7.20 (d, $^{3}J_{H,H}$ = 8.0 Hz, 1H, aromatic), 7.42 (d, $^{4}J_{H,H}$ = 1.2 Hz, 1H, aromatic) . $^{13}C\{^{1}H\}$ NMR (100 MHz, $CDCl_3$): δ = 23.27 (CH(***C***H_3)$_2$), 23.90 (CH(***C***H_3)$_2$), 23.94 (CH(***C***H_3)$_2$), 24.50 (CH(***C***H_3)$_2$), 26.72 (CH***C***H_3), 28.13 (***C***H(CH_3)$_2$), 33.73 (***C***H(CH_3)$_2$), 45.77 (***C***HCH_3), 124.62 (Ar-C6), 125.50 (Ar-C3), 126.57 (Ar-C4), 139.34 (Ar-C1), 142.91 (Ar-C5), 146.53 (Ar-C2). HRMS (ESI, m/z (M + H)]$^{+}$ calcd for $C_{16}H_{28}N$ 234.2222, found 234.2220.

3.4.6 General procedure for palladation of amine, (±)-111

A solution of (±)-**111** (0.10 g, 0.43 mmol) in the preferred solvent (3 mL) was added to a stirred mixture of palladating agent (0.43 mmol, 1.0 equivalent) in the presence of base (0.43 mmol, 1.0 equivalent) if required in the same solvent (5 mL). The reaction mixture was then stirred at the desired temperature for 16 h. The mixture was filtered through a plug of Celite and concentrated. The crude product was then washed with H_2O, dried with $MgSO_4$, filtered and dried before purification by column chromatography on silica gel. Complexes (±)-**113** and palladacycle (±)-**106** were eluted out using *n*-hexane/DCM (V/V = 1:1) and DCM as mobile phase, respectively.

3.4.7 Synthesis of *(±)-trans-dichlorobis[1-(2,5-diisopropylphenyl)-N-methylethanamine]- palladium(II),* (±)-113

The complex (±)-**113** was obtained from $PdCl_2$ as palladating agent in MeOH at 55 °C. (29% yield). M.p. 193–196 °C. ^{1}H NMR (400 MHz, $CDCl_3$): δ = 1.17-1.27 (m, 12H, CH(CH_3)$_2$), 2.09 (d, $^3J_{H,H}$ = 6.7 Hz, 3H, CHCH_3), 2.34 (d, $^3J_{H,H}$ = 6.0 Hz, 3H, NHCH_3), 2.89 (sep, $^3J_{H\text{-}H}$ = 6.6 MHz, 1H, CH(CH$_3$)$_2$), 3.17 (sep, $^3J_{H\text{-}H}$ = 6.8 MHz, 1H, CH(CH$_3$)$_2$), 3.45 (br, 1H, NHCH$_3$), 4.51 (br, 1H, CHCH$_3$), 6.90 (d, $^4J_{H,H}$ = 1.6 Hz, 1H, aromatic), 7.14 (dd, $^3J_{H,H}$ = 8.2 Hz, $^4J_{H,H}$ = 1.6 Hz, 1H, aromatic), 7.22 (d, $^3J_{H,H}$ = 8.2 Hz, 1H, aromatic), . ^{13}C{^{1}H} NMR (100 MHz, $CDCl_3$): δ = 23.36 (CH(***C***H$_3$)$_2$), 23.89 (CH(***C***H$_3$)$_2$), 24.06 (CH(***C***H$_3$)$_2$), 24.62 (CH(***C***H$_3$)$_2$), 25.02 (CH***C***H$_3$), 28.03 (***C***H(CH$_3$)$_2$), 33.75 (***C***H(CH$_3$)$_2$), 38.17 N***C***H$_3$, 56.04 (***C***HCH$_3$), 121.85 (Ar-C6), 125.81 (Ar-C3), 125.96 (Ar-C4), 136.91 (Ar-C1), 144.40 (Ar-C5), 147.33 (Ar-C2). HRMS (ESI, m/z (M − Cl)]$^+$ calcd for $C_{30}H_{50}N_2ClPd$ 581.2701, found 581.2690.

3.4.8 Synthesis of *(±)-di-μ-chlorobis[1-[1-(dimethylamino)ethyl]-2,5-diisopropyl-6-phenyl-C,N]-di-palladium(II),* (±)-106

The complex (±)-**106** was obtained from the reaction of $Li_2[PdCl_4]$ with amine (±)-**105** dissolved in MeOH in the presence of NaOAc at rt to give a yield of 78%. M.p. 189–190 °C. ^{1}H NMR (400 MHz, $CDCl_3$): δ = 1.12-1.25 (m, 12H, CH(CH_3)$_2$), 2.28-2.29 (m, 3H, CHCH_3), 2.59-2.62 (m, 6H, NCH_3), 2.78 (br, 1H, CH(CH$_3$)$_2$), 3.61 (br, 1H, CH(CH$_3$)$_2$), 3.86 (br, 1H, CHCH$_3$), 6.76-6.87 (m, 2H, aromatic) . ^{13}C{^{1}H} NMR (100 MHz, CD_2Cl_2): δ = 23.39 (CH(***C***H$_3$)$_2$), 24.34 (CH***C***H$_3$), 25.04 (CH(***C***H$_3$)$_2$), 26.84 (CH(***C***H$_3$)$_2$), 31.22 (***C***H(CH$_3$)$_2$), 33.92 (***C***H(CH$_3$)$_2$), 50.71 (N(***C***H$_3$)$_2$), 75.28 (***C***HCH$_3$), 122.24 (Ar-C3), 124.05 (Ar-C4), 140.56 (Ar-C5), 149.12 (Ar-C1), 151.03 (Ar-C2). HRMS (ESI, m/z (M − Cl)]$^+$ calcd for $C_{32}H_{52}N_2ClPd_2$ 713.1893, found 713.1901.

3.4.9 Synthesis of *(±)-Chloro[1-[1-(dimethylamino)ethyl]-2,5-diisopropyl-6-phenyl-C,N] (triphenylphosphine-P)palladium(II),* (±)-114

Triphenylphosphine (0.35 g, 1.33 mmol) was added to a solution of racemic dimer (±)-**106** (0.50 g, 0.67 mmol) dissolved in DCM (10 mL). The mixture was left to stir for 1 h at rt, followed by removal of solvent to give complex (±)-**114** in 95% yield. (0.20 g) M.p. 178–181 °C. ^{31}P{^{1}H} NMR (161 MHz, $CDCl_3$): δ 30.7 (s). ^{1}H NMR (400 MHz, $CDCl_3$): δ = 0.22 (d, $^3J_{H,H}$ = 6.8 Hz, 3H CH(CH_3)$_2$), 1.16 (d, $^3J_{H,H}$ = 6.8 Hz, 3H CH(CH_3)$_2$), 1.25-1.28 (m, 6H, CH(CH_3)$_2$), 2.08 (d, $^3J_{H,H}$ = 6.4 Hz, 3H CHCH_3), 2.43 (d, $^4J_{P,H}$ = 2.0 Hz, 3H, NCH_3 (eq)), 2.48-2.53 (m, 1H, CH(CH$_3$)$_2$), 2.81 (d, $^4J_{H,P}$ = 3.6 Hz, 3H, NCH_3 (ax)), 2.84-2.90 (m, 1H, CH(CH$_3$)$_2$), 3.73 (qn, $^3J_{H,H}$ = 6.4 Hz, 1H, CHCH$_3$), 6.39-7.64 (m, 16H, aromatic). ^{13}C{^{1}H} NMR (100 MHz, CD_2Cl_2): δ = 19.72 (CH(***C***H$_3$)$_2$), 22.50 (CH***C***H$_3$), 23.38 (CH(***C***H$_3$)$_2$), 24.61 (CH(***C***H$_3$)$_2$), 29.25 (CH(***C***H$_3$)$_2$), 30.44 (***C***H(CH$_3$)$_2$), 37.84 (d, $J_{C,P}$ = 11.8 Hz, ***C***H(CH$_3$)$_2$), 49.09

(N***C***H_3(ax)), 50.47 (N***C***H_3(eq)), 74.31 (d, $J_{C,P}$ = 3.1 Hz, ***C***HCH_3), 121.08 (Ar-C4), 122.98 (Ar-C3), 127.69-134.70 (6C, Ph), 139.95 (Ar-C2), 148.27 (Ar-C1), 148.69 (Ar-C5), 158.81 (d, $J_{C,P}$ = 2.0 Hz, Ar-C6). HRMS (ESI, m/z (M − Cl)]$^+$ calcd for $C_{34}H_{41}N_2PPd$ 600.2011, found 600.1981.

3.4.10 Synthesis of *(R_C,$S_C$$S_N$)-Prolinato-[1-[1-(dimethylamino)ethyl]-2,5-diisopropyl-6-phenyl-C,N]palladium(II),* (R_C,$S_C$$S_N$)-115

A solution of sodium prolinate (0.65 g, 4.74 mmol) in MeOH (20 mL) was add to a solution of racemic dimer, (±)-**106** (1.79 g, 2.39 mmol) dissolved in MeOH (20 mL). The mixture was stirred for 1 h, and the solvent was removed under reduced pressure. The residue was dissolved in DCM and washed with water (3 x 100 mL). The organic layer was dried over anhydrous $MgSO_4$, filtered and concentrated. The (R_C,$S_C$$S_N$)-**115** diastereomer was separated by flash column chromatography over silica using DCM/acetone v/v: 1:1). The complex was crystallized from a DCM/diethyl ether solution to give yellow plate-like single crystals (0.44 g, 82% yield, based on half equivalent of dimer used). M.p. 200–201 (dec) °C. $[\alpha]^{23.4}$ +43.4° (*c* 0.0161, DCM). ^{1}H NMR (400 MHz, $CDCl_3$): δ = 1.13-1.29 (m, 12H, CH(C***H***$_3$)$_2$), 1.67-1.96 (m, 3H, CH_2C***H***$_2$$CH_2$, COCHC***H***$_2$), 2.03 (d, $^3J_{H,H}$ = 6.4 Hz, 1H, CHC***H***$_3$), 2.52-2.58 (m, 1H, COCHC***H***$_2$), 2.59 (s, 3H, NC***H***$_3$ (eq)), 2.63 (s, 3H, NC***H***$_3$ (ax)), 2.79 (sep, $^3J_{H,H}$ = 6.7 Hz, 2H, CH(C***H***$_3$)$_2$), 3.20-3.36 (m, 3H, N***H***, NHC***H***$_2$), 3.63 (q, $^3J_{H,H}$ = 6.4 Hz, 1H, C***H***CH_3), 4.20 (br, 1H, COC***H***CH_2), 6.89 (dd, , $^3J_{H,H}$ = 8.0 Hz, $^3J_{H,H}$ = 8.0 Hz, 2H, aromatic). ^{13}C{^{1}H} NMR (100 MHz): δ = 22.78 (CH(***C***H_3)$_2$), 23.17 (CH_2***C***H_2CH_2), 23.65 (CH***C***H_3), 23.78 (CH(***C***H_3)$_2$), 24.84 (CH(***C***H_3)$_2$), 26.24 (CH(***C***H_3)$_2$), 28.84 (COCH***C***H_2), 30.40 (***C***H$(CH_3)_2$), 33.73 (***C***H$(CH_3)_2$), 48.51 (N***C***H_3(eq)), 50.92 (NH***C***H_2), 53.33 (N***C***H_3(ax)), 66.98 (CO***C***HCH_2), 73.14 (***C***HCH_3), 121.73 (Ar-C3),

122.48 (Ar-C4), 140.40 (Ar-C2), 144.06 (Ar-C6), 149.44 (Ar-C5), 150.09 (Ar-C1), 177.89 (C=O). HRMS (ESI, m/z (M + H)]$^+$ calcd for $C_{21}H_{35}N_2O_2Pd$ 453.1733, found 453.1742.

3.4.11 Synthesis of *(S_C,$S_C$$S_N$)-Prolinato-[1-[1-(dimethylamino)ethyl]-2,5-diisopropyl-6-phenyl-C,N]palladium(II),* (S_C,$S_C$$S_N$)-115

The other diastereomer (S_C,S_C,S_N)-**109** was obtained by using MeOH as mobile phase, in 80% yield (0.43 g). $[\alpha]^{23.4}$ +196.9° (*c* 0.0198, DCM). ^{1}H NMR (400 MHz, $CDCl_3$): δ = 1.13-1.33 (m, 12H, CH(CH_3)$_2$), 1.60-2.05 (m, 2H, $CH_2CH_2CH_2$), 2.07 (d, $^3J_{H,H}$ = 6.4 Hz, 1H, CHCH_3), 2.17-2.39 (m, 2H, COCHCH_2), 2.55 (s, 3H, NCH_3 (ax)), 2.67 (s, 3H, NCH_3 (eq)), 2.72 (sep, $^3J_{H,H}$ = 6.8 Hz, 1H, CH(CH_3)$_2$), 2.81 (sep, $^3J_{H,H}$ = 6.8 Hz, 1H, CH(CH_3)$_2$), 3.10-3.25 (m, 2H, NHCH_2), 2.51-2.53 (m, 1H, N*H*), 3.63 (q, $^3J_{H,H}$ = 6.2 Hz, 1H, C*H*CH$_3$), 4.06 (br, 1H, COC*H*CH$_2$), 6.87 (dd, , $^3J_{H,H}$ = 8.0 Hz, $^3J_{H,H}$ = 8.4 Hz, 2H, aromatic). ^{13}C{^{1}H} NMR (100 MHz): δ = 22.75 (CH(***C***H$_3$)$_2$), 23.07 (CH***C***H$_3$), 23.93 (CH(***C***H$_3$)$_2$), 24.89 (CH(***C***H$_3$)$_2$), 25.09 (CH_2***C***H_2CH_2), 26.34 (CH(***C***H$_3$)$_2$), 29.77 (COCH***C***H$_2$), 30.45 (***C***H(CH$_3$)$_2$), 34.28 (***C***H(CH$_3$)$_2$), 48.30 (N***C***H$_3$(eq)), 52.92 (N***C***H$_3$(ax)), 53.43 (CO***C***HCH$_2$), 65.41 (CO***C***HCH$_2$), 73.22 (***C***HCH$_3$), 121.34 (Ar-C3), 122.79 (Ar-C4), 140.05 (Ar-C2), 145.60 (Ar-C6), 149.40 (Ar-C5), 149.89 (Ar-C1), 179.84 (C=O). HRMS (ESI, m/z (M + H)]$^+$ calcd for $C_{21}H_{35}N_2O_2Pd$ 453.1733, found 453.1742.

3.4.12 Synthesis of *R-μ-chloro-[1-[1-(dimethylamino)ethyl]-2,5-diisopropyl-6-phenyl-C,N dipalladium(II),* (*R*)-106.

The complex (R_C,$S_C$$S_N$)-**115** (0.40 g, 0.90 mmol) dissolved in DCM (10 mL) was treated with 1 M HCl (5 mL) and left to stir at rt. After vigorous stirring for 30 min,

the organic layer was separated, washed with water, dried over $MgSO_4$, followed by removal of solvent under vacuum to give the dimeric complex (*R*)-**106**. Yield: 0.30 g (90%). M.p. 188-190°C (dec). $[\alpha]^{25.0}$ -210.2° (*c* 0.0224, DCM).

The other optically pure (*S*)-**106** was prepared using the same method with (S_C,$S_C S_N$)-**115** (0.41 g, 0.93 mmol). Yield: 0.31 g (90%). $[\alpha]^{23.8}$ +180.7° (*c* 0.0166, DCM). ^{1}H NMR (400 MHz, $CDCl_3$): δ = 1.14-1.25 (m, 12H, CH(CH_3)$_2$), 2.28 (d, $^3J_{H,H}$ = 6.0 Hz, 3H, CHCH_3), 2.59-2.62 (m, 6H, NCH_3), 2.78 (sep, $^3J_{H,H}$ = 6.8 Hz, 1H, CH(CH$_3$)$_2$), 3.61 (br, 1H, CH(CH$_3$)$_2$), 3.60-3.85 (br, 2H, CHCH$_3$, CH(CH$_3$)$_2$), 6.76-6.87 (m, 2H, aromatic) . ^{13}C{^{1}H} NMR (100 MHz, $CDCl_3$): δ = 22.96 (CH(***C***H$_3$)$_2$), 23.88 (CH(***C***H$_3$)$_2$), 24.81 (CH***C***H$_3$), 26.64 (CH(***C***H$_3$)$_2$), 30.67 (***C***H(CH$_3$)$_2$), 50.18 (N(***C***H$_3$)$_2$), 74.61 (***C***HCH$_3$), 121.64 (Ar-C3), 123.62 (Ar-C4), 123.76 (Ar-C6), 139.90 (Ar-C5), 150.36 (Ar-C2). HRMS (ESI, m/z (M − Cl)]$^+$ calcd for $C_{32}H_{52}N_2ClPd_2$ 713.1893, found 713.1901.

3.4.13 Synthesis of *S-chloro-[1-[1-(dimethylamino)ethyl]-2,5-diisopropyl-6-phenyl-C,N][3,4-dimethyl-1-phenylphosphole-P]palladium(II),* (*S*)-116.

A solution of the dimeric complex (*S*)-**106** (1.0 g, 1.3 mmol) dissolved in degassed DCM (5 mL) was added to a mixture DMPP (0.49 g, 2.6 mmol) in the same solvent (5 mL) under positive pressure of nitrogen. The mixture was stirred for 30 min at rt, followed by the removal of solvent. The crude product was then purified by column chromatography on silica gel using DCM as eluent affording yellow solid. Yield: 1.35 g (90 %). M.p. 158-161°C (dec). $[\alpha]^{23.4}$ +431.5° (*c* 0.0121, DCM). ^{31}P{^{1}H} NMR (162 MHz, $CDCl_3$): δ = 28.4 (s) . ^{1}H NMR (400 MHz, $CDCl_3$): δ = 0.96-1.24 (m, 12H, CH(CH_3)$_2$), 1.87 (d, $^3J_{H\text{-}H}$ = 6.4 Hz, 3H, CH(CH_3), 1.98 (s, 3H, CH=CCH_3), 2.01 (s, 6H, CH=CCH_3), 2.43 (d, $^4J_{P,H}$ = 2.0 Hz, 3H, NCH_3 (ax)), 2.71 (sep, $^3J_{H,H}$ = 6.4 Hz, 1H,

C*H*(CH_3)$_2$), 2.67 (d, $^4J_{P,H}$ = 3.6 Hz, 3H, NC*H*$_3$ (eq)), 2.83 (sep, $^3J_{H,H}$ = 6.8 Hz, 1H, CH(C*H*$_3$)$_2$), 2.67 (qn, $^3J_{H,H}$ = 6.4 Hz, 1H, C*H*(CH_3), 6.06 (d, $^2J_{H,P}$ = 32.4 Hz, 1H, C*H*=CCH_3), 6.76 (d, $^2J_{H,P}$ = 31.6 Hz, 1H, C*H*=CCH_3), 6.80-7.84 (m, 7H, aromatic) . $^{13}C\{^1H\}$ NMR (100 MHz, $CDCl_3$): δ = 17.26 (d, $J_{C,P}$ = 20.2 Hz, CH=C***C***H$_3$), 17.76 (d, $J_{C,P}$ = 19.7 Hz, CH=C***C***H$_3$), 20.75 (CH(***C***H$_3$)$_2$), 22.83 (CH***C***H$_3$), 23.08 (CH(***C***H$_3$)$_2$), 24.75 (CH(***C***H$_3$)$_2$), 28.55 (CH(***C***H$_3$)$_2$), 30.42 (***C***H(CH_3)$_2$), 37.79 (d, $J_{C,P}$ = 20.1 Hz, ***C***H(CH_3)$_2$), 48.62 (N***C***H$_3$(eq)), 50.54 (d, $J_{C,P}$ = 4.6 Hz, N***C***H$_3$(ax)), 73.44 (d, $J_{C,P}$ = 5.3 Hz, ***C***HCH_3), 121.16 (Ar-C4), 122.11 (Ar-C3), 125.69 (d, $J_{C,P}$ = 49.5 Hz, ***C***H=CCH_3), 127.87-133.20 (6C, Ph), 129.33 (d, $J_{C,P}$ = 50.9 Hz, ***C***H=CCH_3), 140.66 (Ar-C2), 148.31 (d, $J_{C,P}$ = 9.4 Hz, CH=***C***CH_3), 149.71 (Ar-C1), 150.42 (d, $J_{C,P}$ = 4.4 Hz, Ar-C5), 152.14 (Ar-C6), 152.86 (d, $J_{C,P}$ = 10.6 Hz, CH=***C***CH_3). HRMS (ESI, m/z (M – Cl)]$^+$ calcd for $C_{28}H_{39}NPPd$ 526.1855, found 526.1874.

4.4.14 Asymmetric *endo*- Cycloaddition Reactions between Complex (*S*)-116 and Ethyl Vinyl Ketone Formation of Complex (*S*C,*Rp*)-117 and (*S*C,*Sp*)-117.

A mixture of the DMPP-coordinated complex (*S*)-**106** (83.8 mg, 0.15 mmol) and ethyl vinyl ketone (0.1 mL, 1.00 mmol) in chloroform (3 mL) was left to stir at room temperature and was monitored by $^{31}P\{^1H\}$ NMR spectroscopy. After 14 days the reaction was incomplete, two new singlets with a diastereomeric ratio of 5.6:1 were observed. The reaction was repeated at 50 °C, and was completed after 5 days and two new peaks with a diastereomeric ratio of 4.4:1 were observed. The reaction mixture was then filtered through a plug of celite and the concentrated. The major product was eluted using DCM as yellow oil in 6.8 mg. Yield = 7.4%. $^{31}P\{^1H\}$ NMR (161 MHz, $CDCl_3$): δ = 119.4 (s, 1P) ; other unknown by-products peaks at δ 21.2 (s) and 67.4 (d)) were also observed. ^1H NMR (400 MHz, $CDCl_3$): δ = 0.69-0.76 (m, 3H, $COCH_2CH_3$),

1.16-1.42 (m, 12H, CH(C*H*$_3$)$_2$), 1.55 (s, 3H, C=CC*H*$_3$), 1.60 (s, 3H, C=CC*H*$_3$), 1.91-2.06 (m, 3H, COC*H*$_2$CH$_3$, C*H*$_2$CHCO), 2.08 (d, $^3J_{H,H}$ = 6.4 Hz, 3H, CHC*H*$_3$), 2.41 (s, 3H, 2.71 (sep, $^3J_{H,H}$ = 6.4 Hz, 1H, C*H*(CH$_3$)$_2$), 2.41 (d, $^4J_{P,H}$ = 1.6 Hz, 3H, NC*H*$_3$ (ax)), 2.64 (sep, $^3J_{H,H}$ = 6.4 Hz, 1H, C*H*(CH$_3$)$_2$), 2.76 (d, $^4J_{P,H}$ = 3.2 Hz, 3H, NC*H*$_3$ (eq)), 2.82-2.90 (m, 1H, C*H*(CH$_3$)$_2$), 3.73 (qn, $^3J_{H,H}$ = 6.4 Hz, 1H, C*H*(CH$_3$), 6.87-7.92 (m, 5H, aromatic) .

CHAPTER 4

CHIRAL *ORTHO*-PALLADATED 1-(2,5-DICHLOROPHENYL)-*N*,*N*-DIMETHYLETHANAMINE

4.1 Introduction

As discussed in the earlier chapters, the stereoselectivity in asymmetric [4+2] *endo*-cycloaddition will increase with the presence of bigger spacer groups.[71] The introduction of bulky spacer groups on the aromatic ring of the amine moiety will aid in the locking of the organometallic five-membered ring and will also exert stereochemical influence on the neighbouring reaction site. However, the spacer group cannot be too bulky (*t*-butyl); it will hinder the C–H activation reaction to give the *ortho*-palladated complex.

4.2 Research Objectives

In earlier chapters, the steric hindrance was always being the main focus to improve the stereoselectivity in asymmetric [4+2] *endo*-cycloaddition but the electronic influence of the group substituted on the aromatic ring has not being investigated. Therefore, in this chapter an electron-withdrawing group was introduced to the arylamine, in order to investigate the electronic effect. Thus, a novel chiral palladacycle (*S*)-**118** was designed. The internal steric repulsion between the chloro group and the methyl substituent on the stereogenic carbon is expected to lock the conformation of the organometallic five-membered ring in the solid state and solution. The application of this new template on the asymmetric *endo* [4+2] cycloaddition reaction and hydrophosphination was also examined.

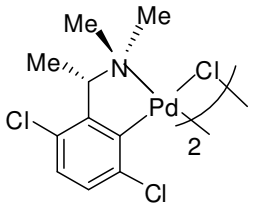

(*S*)-**118**

4.3 Result and Discussion

4.3.1 Synthesis and Characterization of Racemic *ortho*-Palladated Complex

4.3.1.1 Synthesis of Racemic *ortho*-Palladated Complex (±)-119

The ligand (±)-**120** was synthesized from 1-(2,5-dichlorophenyl)ethanone **121** *via* a three step synthetic route as illustrated in Scheme 4.1. Firstly, the 1-(2,5-dichlorophenyl)ethanone **121**, was reduced by $NaBH_4$ in MeOH to give the racemic alcohol, (±)-**122** in 99% yield. The alcohol is then brominated with PBr_3 in DCM, to give (±)-**123** with a yield of 90%. Next, the bromo compound (±)-**123**, undergoes direct alkylamination with aqueous dimethylamine to afford the target *N*,*N*-dimethylamine ligand (±)-**119** in 92% yield. The overall yield of this synthetic route is 83%. Lastly, the acetate-bridged dimeric palladated complex (±)-**119** was obtained in high yield by treatment of the amine ligand (±)-**120** with $Pd(OAc)_2$.

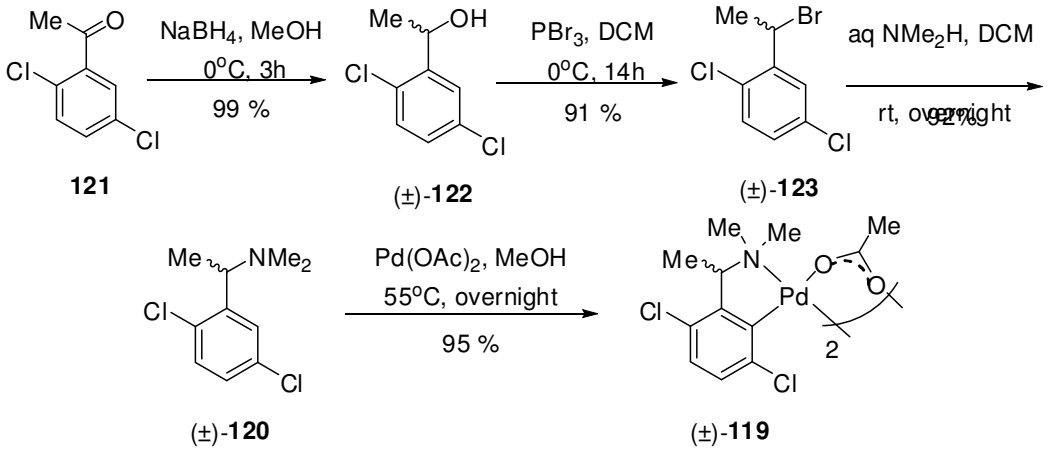

121 (±)-**122** (±)-**123** (±)-**120** (±)-**119**

Scheme 4.1

4.3.1.2 Molecular Structure of Complex (±)-119

The dynamic *cis-trans* interconversion of the dimeric complex (±)-**119** in solution during the characterization *via* ^{1}H NMR spectroscopy is not detected at room temperature. Thus, the dimeric complex is not converted to monomeric form like the previous chapter. The complex (±)-**119** was crystallized through slow evaporation of the DCM/ *n*-hexane solution of (±)-**119** give bight yellow single crystals. The solid state structure is confirmed crystallographically and shown in Figure 4.1, while selected bond lengths and angles are presented in Table 4.1.

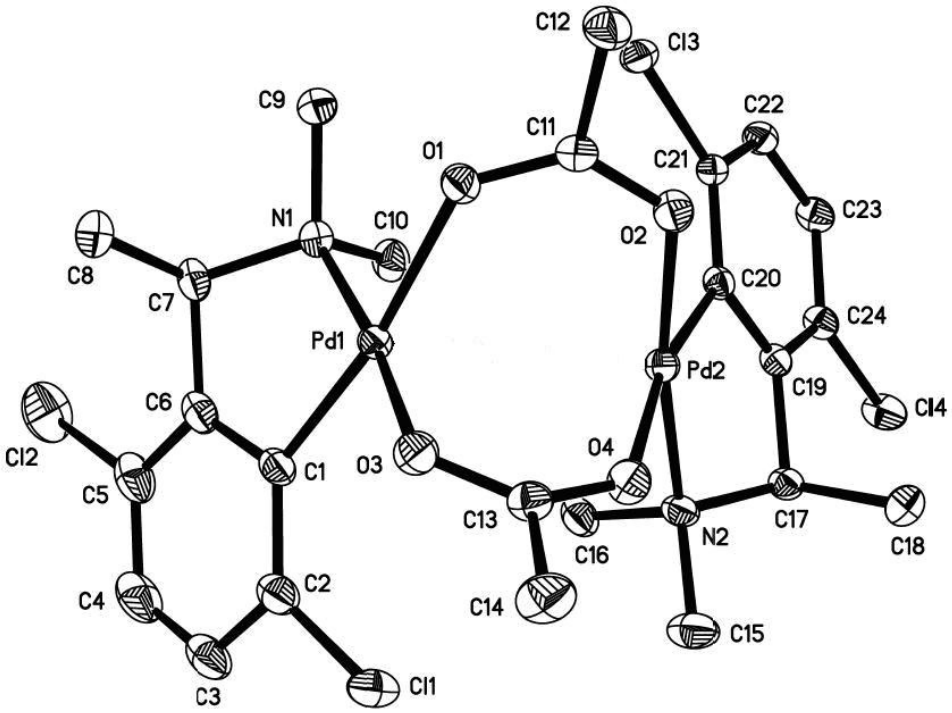

Figure 4.1 Molecular Structure of Complex (±)-**119**. All hydrogen atoms were omitted for clarity.

The complex (±)-**119** adopted distorted square planar coordination geometry about the palladium center. The two arylamine units are located *trans* to each to other, adopting the "butterfly" geometry with the organometallic units linked by the bridging acetate ligands. The dihedral angles between the two palladium coordination planes at

the Pd(1) and Pd(2) units are 9.8° and 12.6°, respectively. The acetate bridge and the palladium center form an eight-membered ring in boat-boat conformation with an interplanar angle between planes {O(1)–C(11)–O(2)} and {O(3)–C(13)–O(4)} of 84.3°. The average bond length of the four C−O bonds in the acetate bridge is 1.258 Å, which is consistent with the delocalized C−O bond length of 1.254 Å[90] The Pd(1)–Pd(2) distance in the solid state is 3.161 Å.

Table 4.1 Selected bond lengths (Å) and angles (°) for complex (±)-**119**

Pd(1)-C(1)	1.989(2)	Pd(1)-N(1)	2.047(2)
Pd(1)-O(1)	2.111(1)	Pd(1)-O(3)	2.026(2)
Pd(2)-C(20)	1.993(2)	Pd(2)-N(2)	2.066(2)
Pd(2)-O(2)	2.034(1)	Pd(2)-O(4)	2.101(2)
C(11)-O(1)	1.249(2)	C(11)-O(2)	1.265(2)
C(13)-O(3)	1.264(3)	C(13)-O(4)	1.253(2)
C(1)-Pd(1)-N(1)	81.8(1	C(1)-Pd(1)-O(3)	96.7(1)
O(3)-Pd(1)-O(1)	87.9(1)	N(1)-Pd(1)-O(1)	92.7(1)
C(1)-Pd(1)-O(1)	171.4 (1)	O(3)-Pd(1)-N(1)	172.5(1)
C(20)-Pd(2)-N(2)	82.1(1)	C(20)-Pd(2)-O(2)	95.9(1)
O(2)-Pd(2)-O(4)	88.1(1)	N(2)-Pd(2)-O(4)	92.4(1)
C(20)-Pd(2)-O(4)	169.2 (1)	O(2)-Pd(2)-N(2)	171.0(1)
O(1)-C(11)-O(2)	126.8(2)	O(4)-C(13)-O(3)	126.4 (2)
O(1)-C(11)-C(12)	117.5(2)	O(2)-C(11)-C(12)	115.7(2)
O(4)-C(13)-C(14)	117.4(2)	O(3)-C(13)-C(14)	116.2(2)

4.3.2 Optical Resolution of Racemic Dimeric Complex (±)-119

The optical resolution of racemic dimeric complex (±)-**119**, was performed using optically active sodium (*S*)-prolinate as the resolving agent (Scheme 4.2).

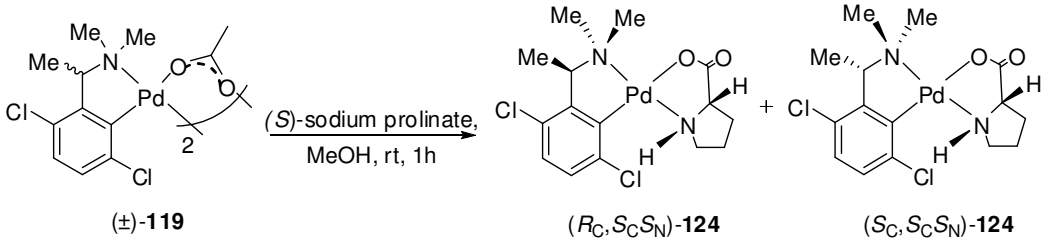

Scheme 4.2

The racemic dimer was treated with two molar equivalents of sodium (*S*)-prolinate to give a 1:1 mixture of diastereomers, (R_C,S_CS_N)-**124** and (S_C,S_CS_N)-**124**. The diastereomeric adducts were separated *via* column chromatography as the initial attempt to separated them by fractional crystallization was unsuccessful. The diastereomer (R_C,S_CS_N)-**124** was eluted out first with acetone/ *n*-hexane (V/V = 1:1) as mobile phase. The other diastereomer (S_C,S_CS_N)-**124** was eluted out with acetone as mobile phase. The optical purities of both fractions were verified with ^{1}H NMR spectroscopy. The (R_C,S_CS_N)-**124** was crystallized using ethyl acetate and diethyl ether yielding pale yellow flakes in 73% yield (based on half equivalent of dimer used) with $[\alpha]^{23.2}$ +28.5° (*c* 0.03, DCM) and >99% *de* (according to ^{1}H NMR data). Another diastereomeric adduct (S_C,S_CS_N)-**124** was crystallized from acetone and *n*-heptane to give pale yellow needle-like crystal in 77% yield with $[\alpha]^{23.2}$ +306.4° (*c* 0.02, DCM). The absolute configuration and the solid structure of both diastereomeric complexes (R_C,S_CS_N)-**124** and (S_C,S_CS_N)-**124** were confirmed by single crystal X-ray diffraction investigation. Their structures in solution were also studied by their 2D ^{1}H-^{1}H ROESY NMR spectroscopy.

4.3.2.1 Molecular Structure of Diastereomer (R_C,S_CS_N)-124

The pale yellow colored single crystals of diastereomer (R_C,S_CS_N)-**124** was obtained from slow evaporation of ethyl acetate/diethyl ether solution. The X-ray

diffraction study of the complex (R_C,$S_C$$S_N$)-**124** was performed (Figure 4.2) and selected bond lengths and angles are provided in Table 4.2.

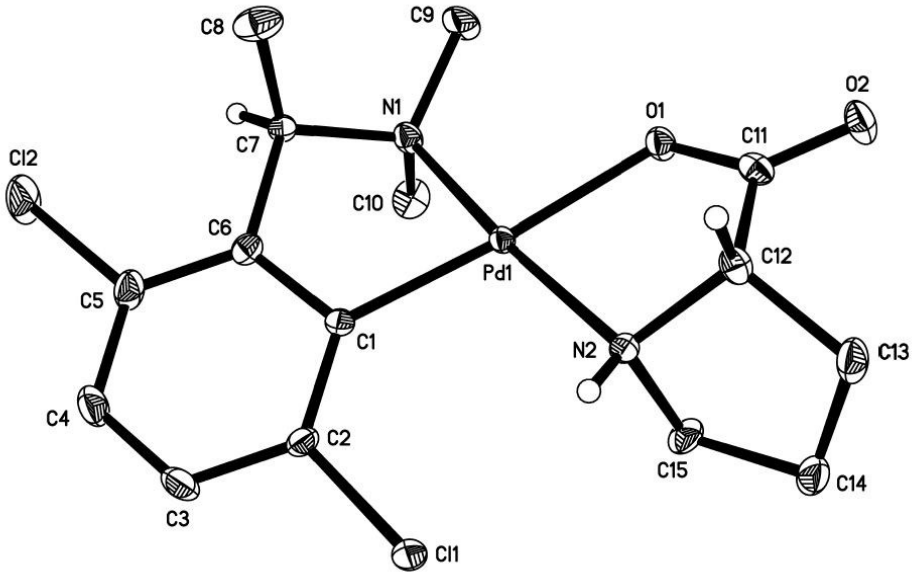

Figure 4.2 Molecular structure of complex (R_C,$S_C$$S_N$)-**124**. All hydrogen atoms except H(C7), H(C12) and H(N2) in were omitted for clarity.

The crystallographic study revealed the *R*-configuration at the α-carbon stereocenter within the five-membered organometallic ring. The secondary stereogenic nitrogen atom from the prolinato group is in the expected *S* absolute configuration. The distance between the chloro atom, Cl(2) and the proton, H(7) on the α-carbon stereocenter is 2.685 Å, which is smaller than the summation of the Van der Waals radii of the two atoms (2.95 Å).[86] This steric repulsion locked the five-membered organometallic ring. The torsion angle for C(1)–Pd(1)–N(1)–C(7) is +31.9°, showing that the C–methyl group occupies an axial position and the five-membered organometallic ring adopts the δ conformation (Figure 4.3).[89] The two coordinated nitrogen atoms are located *trans* to each other. The coordination geometry around the palladium center is distorted square planar. The dihedral angle between planes {N(1)–

Pd(1)–C(1)} and {O(1)–Pd(1)–N(2)} is 4.7°. The organometallic five-membered ring is in an envelope conformation with N(1) 0.626 Å below the plane C(1)–C(6)–C(7)–Pd(1). There is an angle of 22.1° between the mean plane formed from C(1)–C(6)–C(7)–N(1)–Pd(1) and the mean plane of the five membered ring prolinato ligand , O(1)–C(11)–C(12)–N(2)–Pd(1).

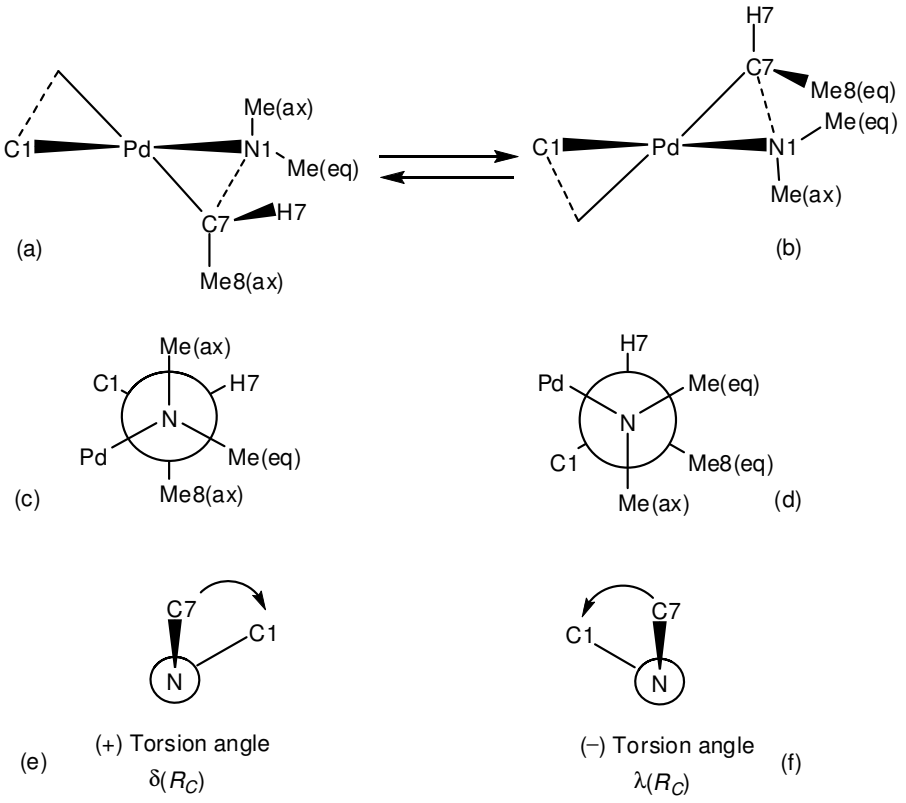

Figure 4.3 Chiral $\delta(R_C)$ (**a**, **c, e**) and $\lambda(R_C)$ (**b**, **d, f**) conformations of the (R_C,$S_C$$S_N$)-**124** five-membered ring in projections to the plane orthogonal to the {C(1)–Pd(1)–N(1)} plane (**a**, **b**); in the Newman projections relative to N(1)–C(7) bond (**c**, **d**) and in the Newman projections relative to N(1)–Pd(1) bond (**e**, **f**).

Table 4.2 Selected bond lengths (Å) and angles (°) for complex (R_C,S_CS_N)-**124**

Pd(1)-C(1)	2.003(3)	Pd(1)-N(1)	2.054(2)
Pd(1)-N(2)	2.051(2)	Pd(1)-O(1)	2.086(2)
C(11)-O(1)	1.291(3)	C(11)-O(2)	1.232(3)
C(1)-Pd(1)-N(1)	81.6(1)	C(1)-Pd(1)-N(2)	104.6(1)
N(1)-Pd(1)-O(1)	94.1(1)	N(2)-Pd(1)-O(1)	79.7(1)
C(1)-Pd(1)-O(1)	175.6(1)	N(2)-Pd(1)-N(1)	172.5(1)

4.3.2.2 Solution Structure of Diastereomer (R_C,S_CS_N)-124

From the ^{1}H NMR and 2D ^{1}H-^{1}H ROESY NMR experiments, the solution structure and signal assignment of the diastereomer (R_C,S_CS_N)-**124** was determined. The ^{1}H NMR spectrum of the complex (R_C,S_CS_N)-**124** conducted at room temperature in $CDCl_3$, shows the presence of one geometric isomer in solution. The numbering scheme of the diastereomer (R_C,S_CS_N)-**124** used for NMR study and the 2D ^{1}H-^{1}H ROESY NMR spectrum are shown in figure 4.4 and figure 4.5, respectively.

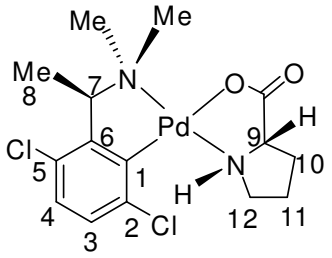

Figure 4.4 Numbering scheme of complex (R_C,S_CS_N)-**124** for NMR assignment

A key feature observed in Figure 4.5 is the signal (A) due to the strong interaction between Me8 and the equatorially disposed NMe group. This observation comply with the crystallographic findings where the distance between the Me8 carbon, C(8) and the NMe(*eq*) carbon, C(9) (2.825 Å) is smaller than the summation of the Van der Waals radii of 3.40 Å.[86] ROESY correlations C to E correspond to the

interactions of H7 with the Me8, NMe(eq) and NMe(ax) respectively. These clearly indicated that the Me8 is axially positioned and the five-membered organometallic ring is locked into the single static δ conformation in solution, Figure 4.3.[89] Furthermore, intra-ligand interactions of the prolinato ligand include H10–H11; H11'–H12'; H11–H12; and H9–H10' were also observed. This observation is consistent with the solid state investigation in which the two nitrogen groups adopt the *trans*-(*N*,*N*)-geometry.

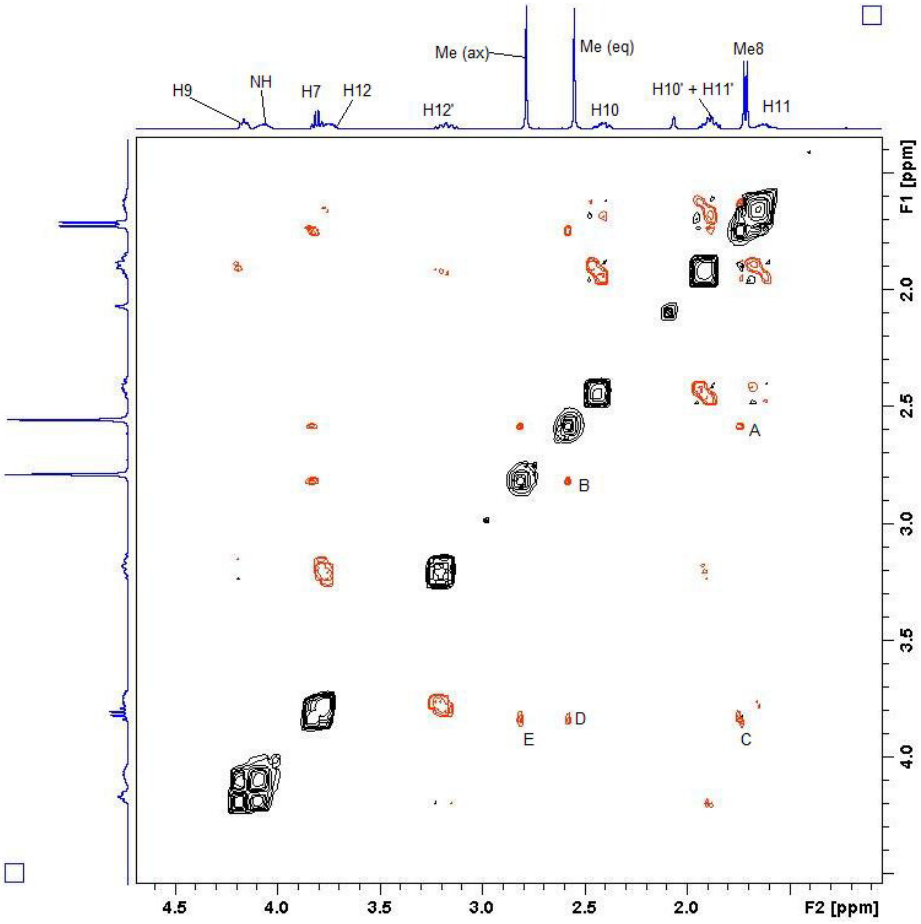

Figure 4.5 Expanded 2D ^{1}H-^{1}H ROESY NMR spectrum of the complex ((*R*$_C$,*S*$_C$*S*$_N$)-**124** in $CDCl_3$. Selected ROESY Interactions: (A) Me8 - NMe(eq); (B) NMe(eq)–NMe(ax); (C) H7– Me8; (D) H7–NMe(eq); (E) H7–NMe(ax)

4.3.2.3 Molecular Structure of Diastereomer (S_C,S_CS_N)-124

The X-ray diffraction study of the complex (S_C,S_CS_N)-**124** was performed. The molecular structure is shown in Figure 4.6 while selected bond lengths and angles are provided in Table 4.3. The X-ray crystallographic study shows that the α-carbon stereocenter of the arylamine ligand and the secondary stereogenic nitrogen atom from the prolinato ligand are both in *S* absolute configuration. The organometallic five-membered ring is locked in λ configuration (Figure 4.7) with torsion angle of -36.7° for C(1)–Pd(1)–N(1)–C(7). [89] And the ring is in an envelope conformation with N(1) 0.742Å above the plane C(1)−C(6)−C(7)−Pd(1). The coordination geometry of the palladium center is distorted square-planar and the tetrahedral distortion between the triangular planes {N(1)−Pd(1)−C(1)} and {O(1)−Pd(1)−N(2)} is 9.7°. The two coordinated nitrogen donors are *trans* to each other. The angle between the mean plane of the organometallic five-membered ring C(1)−C(6)−C(7)−N(1)−Pd(1) and the mean plane formed from O(1)−C(11)−C(12)−N(2)−Pd(1) of the prolinato ligand is 19.99°.

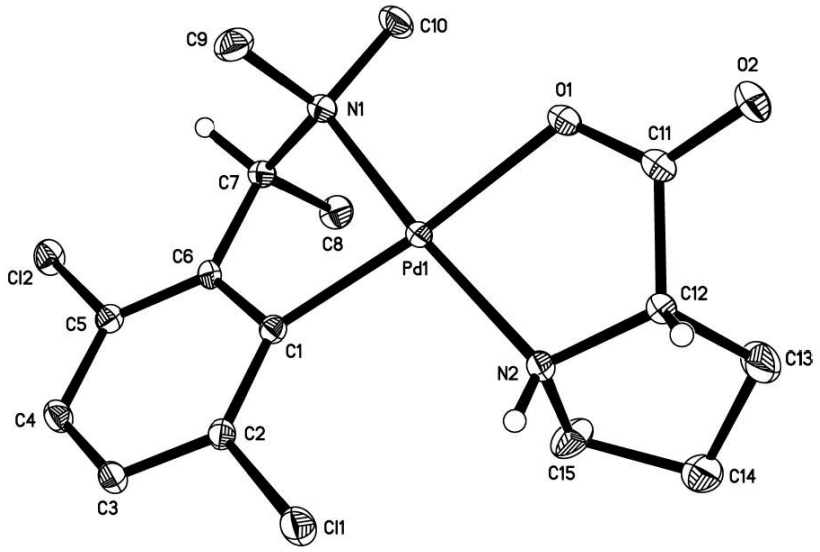

Figure 4.6 Molecular structure of complex (S_C,S_CS_N)-**124**. All hydrogen atoms except H(C7), H(C12) and H(N2) were omitted for clarity.

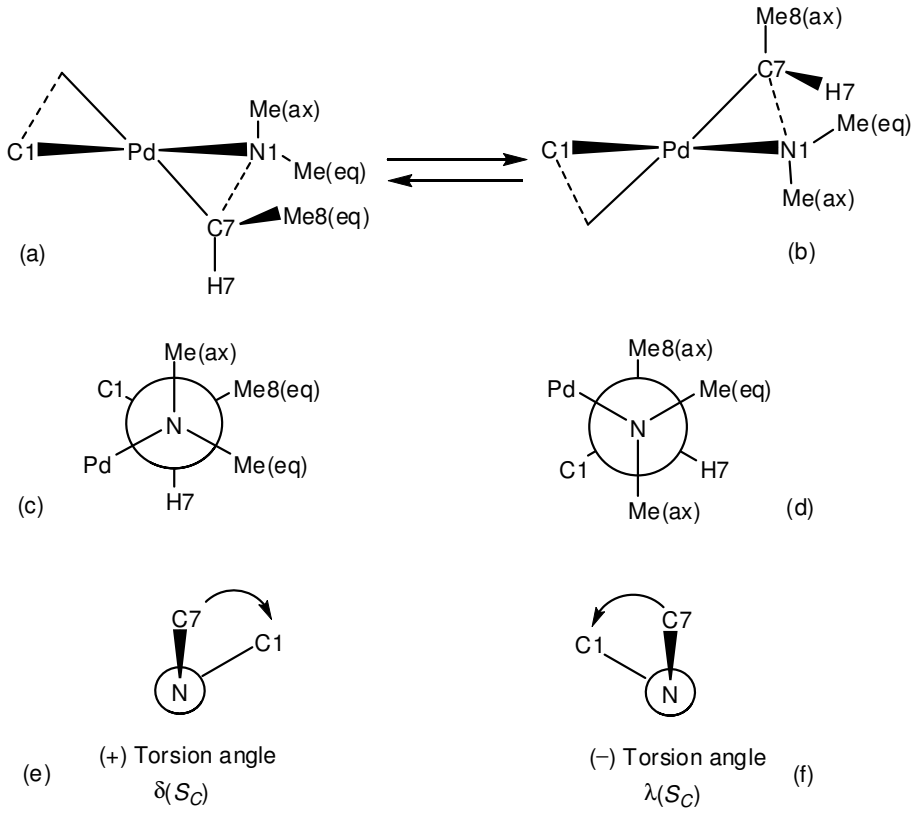

Figure 4.7 Chiral δ(S_C) (**a**, **c, e**) and λ(S_C) (**b**, **d, f**) conformations of the (S_C,S_CS_N)-**124** five-membered ring in projections to the plane orthogonal to the {C(1)–Pd(1)–N(1)} plane (**a**, **b**); in the Newman projections relative the N(1)–C(7) bond (**c**, **d**) and in the Newman projections relative the N(1)–Pd(1) bond (**e**, **f**).

Table 4.3: Selected bond lengths (Å) and angles (°) for complex (S_C,S_CS_N)-**124**

Pd(1)-C(1)	2.0034(2)	Pd(1)-N(1)	2.070(2)
Pd(1)-N(2)	2.0544(2)	Pd(1)-O(1)	2.069(2)
C(11)-O(1)	1.284(3)	C(11)-O(2)	1.238(2)
C(1)-Pd(1)-N(1)	81.5(1)	C(1)-Pd(1)-N(2)	102.4(1)
O(1)-Pd(1)-N(1)	94.1(1)	N(2)-Pd(1)-O(1)	82.4(1
C(1)-Pd(1)-O(1)	174.7(1)	N(2)-Pd(1)-N(1)	170.5(1)

4.3.2.4 Solution Structure of Diastereomer (S_C,S_CS_N)-124

The solution structure and signal assignment of the diastereomer (S_C,S_CS_N)-**124** is determined by the ^{1}H NMR and 2D ^{1}H-^{1}H ROESY NMR experiments. Similar to diastereomer (R_C,S_CS_N)-**124**, the ^{1}H NMR spectrum of the complex (S_C,S_CS_N)-**124** conducted at room temperature in $CDCl_3$, also shows only one geometric isomer in solution. The numbering scheme of the diastereomer (S_C,S_CS_N)-**124** use for NMR assignment and the 2D ^{1}H-^{1}H ROESY NMR spectrum is presented in Figure 4.8 and Figure 4.9, respectively.

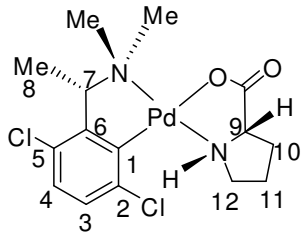

Figure 4.8 Numbering scheme of complex (S_C,S_CS_N)-**124** for NMR assignment

In the expanded 2D ^{1}H-^{1}H ROESY NMR spectrum of the complex (S_C,S_CS_N)-**124**, strong NOE signals between the Me8 and NMe(eq) denoted as A, and interactions between H7 with Me8, NMe(eq) and NMe(ax) are clearly recorded as signals B, C, D respectively and illustrate that the Me8 occupies an axial position (Figure 4.7). These signals, in conjunction with the confirmed *S* configuration at its chiral carbon center, leads to the conclusion that the five-membered organometallic ring adopts the λ conformation, as observed in the solid state investigation where the distance between the Me8 carbon, C(8) and the NMe(*eq*) carbon, C(10) is (2.889 Å) is smaller than the summation of the Van der Waals radii.[86] Similarly the interactions within the prolinate fragments are also clearly observed: signals E, F and G

correspond to the interactions of H9 with both H10 and H10'; NH–H12' and NH–H9 respectively indicated that the nitrogen donors retained the *trans*-(*N*,*N*)-geometry in solution.

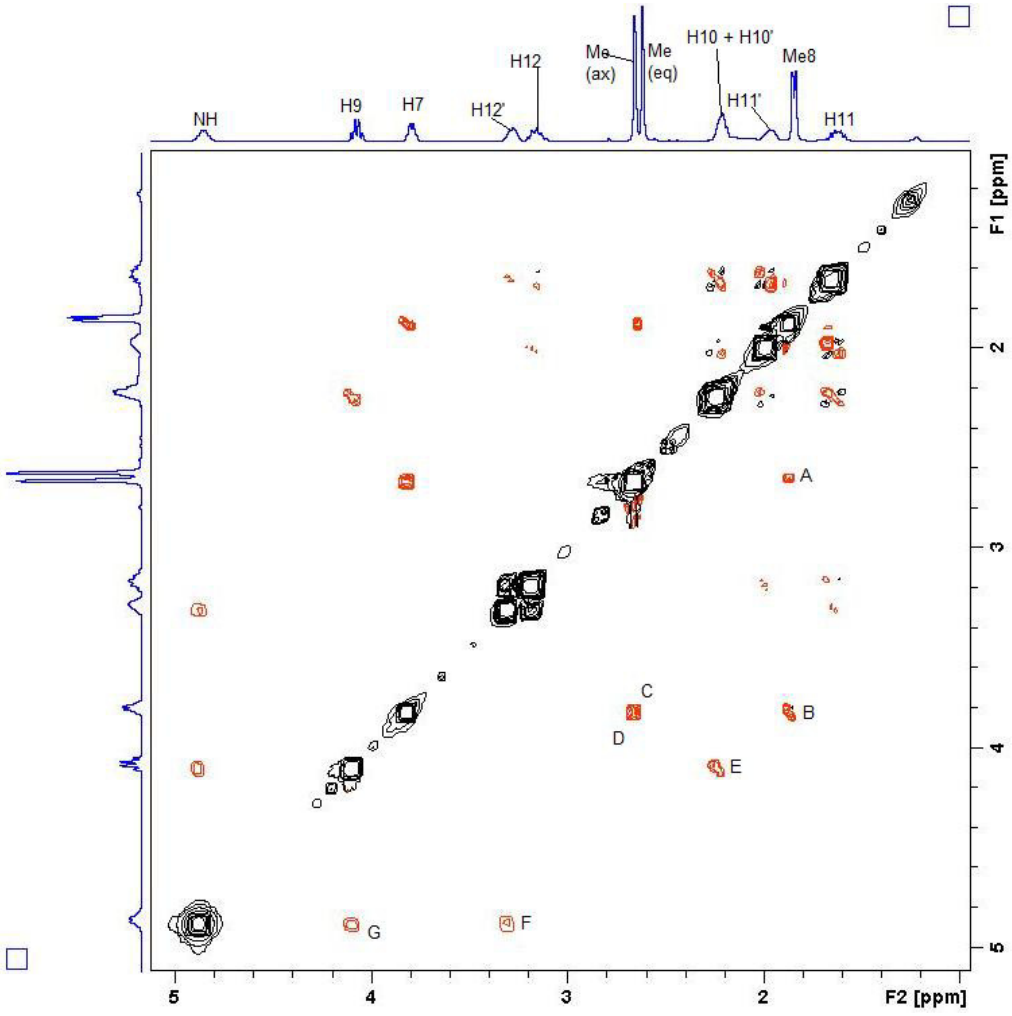

Figure 4.9 Expanded 2D ^{1}H-^{1}H ROESY NMR spectrum of the complex (S_C,$S_C S_N$)-**124** in $CDCl_3$. ROESY Interactions: (A) Me8−NMe(eq); (B) H7–Me8; (C) H7–NMe(eq); (D) H7–NMe(ax); (E) H9−H10 and H10'; (F) NH−H12'; (G) NH−H9

4.3.3 Synthesis of Optically Active Dimeric Complex

The removal of the prolinate ligand from (R_C,S_CS_N)-**124** by 1M aqueous hydrochloric acid in two-phase conditions resulted in the optically active dimeric complex, (*R*)-**118** in 90% isolated yield with $[\alpha]_D$ -326.0° (*c* 0.01, DCM) (Scheme 4.3).

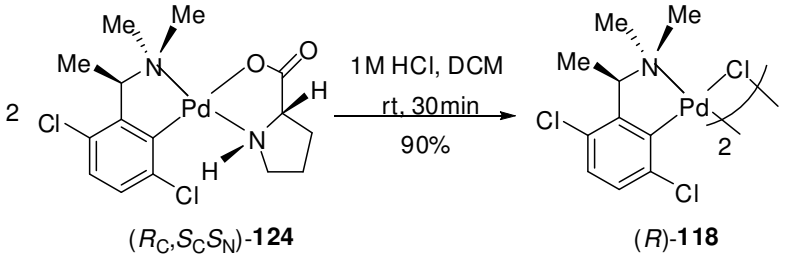

(R_C,S_CS_N)-**124** (*R*)-**118**

Scheme 4.3

The other pure dimeric complex, (*S*)-**118** is also prepared in same way by treating the diastereomer (S_C,S_CS_N)-**124** with 1M aqueous hydrochloric acid to give the dimeric complex (*S*)-**118** in 89% yield, $[\alpha]_D$ +345.0° (*c* 0.01, DCM). The chloro bridge dimeric complex (*S*)-**118** can be converted to acetate bridged (*S*)-**119** with the use of silver acetate in MeOH in 75% yield (Scheme 4.4).

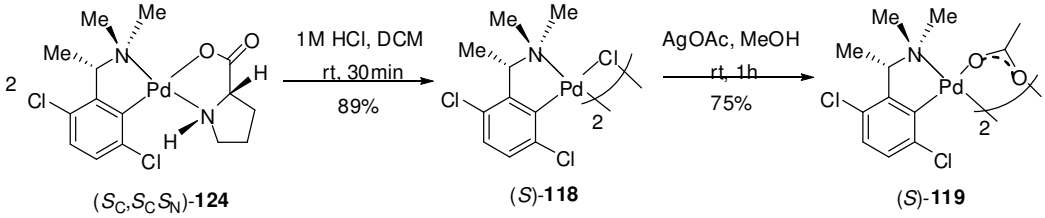

(S_C,S_CS_N)-**124** (*S*)-**118** (*S*)-**119**

Scheme 4.4

4.3.3.1 Molecular Structure Optically Active Complex (*R*)-118

The yellow plate-like single crystals were formed from a DCM/ *n*-hexane solution and the structure of complex (*R*)-**118** was confirmed crystallographically. The X-ray study confirms the absolute *R* configuration of the α-carbon stereocenter of the palladacycle and the molecular structure of complex (*R*)-**118** is depicted in Figure 4.10.

Selected bond lengths and angles are tabulated in Table 4.4. The coordination geometry of both palladium centers are slightly distorted square planar. The dihedral angle of distortion on Pd(1) and Pd(2) is 6.4° and 4.3°, respectively. The chloro bridging ligands and palladium centers formed a four-membered ring that is bent 8.3° along the Cl(3)–Cl(4) axis. The two nitrogen donor atoms are *cis* to each other, unlike the acetate bridged dimeric complex (±)**-119**.

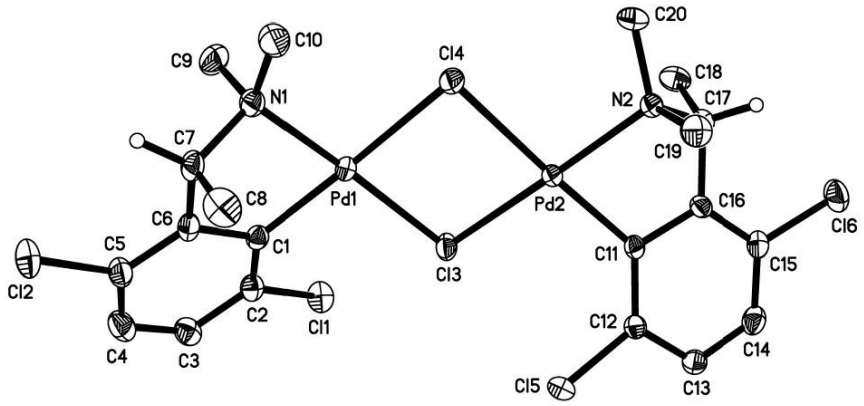

Figure 4.10 Molecular structure of complex (*R*)-**118**. All hydrogen atoms except H(C7), and H(C17) in were omitted for clarity.

Table 4.4: Selected bond lengths (Å) and angles (°) for complex (*R*)-**118**

Pd(1)-C(1)	2.000(3)	Pd(1)-N(1)	2.069(3)
Pd(1)-Cl(3)	2.326(8)	Pd(1)-Cl(4)	2.416(8)
Pd(2)-C(11)	1.992(3)	Pd(2)-N(2)	2.080(2)
Pd(2)-Cl(3)	2.333(7)	Pd(2)-Cl(4)	2.415(8)
C(1)-Pd(1)-N(1)	81.2(1)	C(1)-Pd(1)-Cl(3)	98.8(1)
N(1)-Pd(1)-Cl(3)	173.7(1)	C(1)-Pd(1)-Cl(4)	176.6(1)
N(1)-Pd(1)-Cl(4)	95.8(1)	Cl(3)-Pd(1)-Cl(4)	84.0(1)
C(11)-Pd(2)-N(2)	80.9(1)	C(11)-Pd(2)-Cl(3)	98.1(1)
N(2)-Pd(2)-Cl(3)	173.9()	C(11)-Pd(2)-Cl(4)	177.6(1)
N(2)-Pd(2)-Cl(4)	97.0(1)	Cl(3)-Pd(2)-Cl(4)	83.9(1)

4.3.3.2 Molecular Structure Optically Active Dimeric Complex (*S*)-118

Yellow block-like single crystals were obtained from a DCM/ *n*-hexane solution of (*S*)-**118** and the solid-state structure is determined by X-ray crystallography (Figure 4.11). Selected bond lengths and angles are presented in Table 4.5. Both (*R*)-**118** and (*S*)-**118** have the same the coordination geometry about the metal center and the two nitrogen groups are also in *cis*-(*N*,*N*) arrangement. The tetrahedral distortion of Pd(1) and Pd(2) is 6.6° and 6.3° correspondingly.

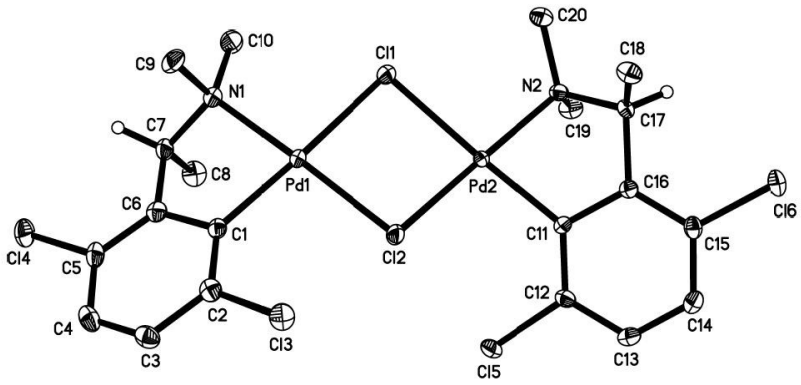

Figure 4.11 Molecular structure of complex (*S*)-**118**. All hydrogen atoms except H(C7), and H(C17) in were omitted for clarity.

Table 4.5: Selected bond lengths (Å) and angles (°) for complex (*S*)-**118**

Pd(1)-C(1)	2.002(3)	Pd(1)-N(1)	2.068(2)
Pd(1)-Cl(2)	2.328(1)	Pd(1)-Cl(1)	2.418(1)
Pd(2)-C(11)	1.984(2)	Pd(2)-N(2)	2.077(2)
Pd(2)-Cl(2)	2.335(1)	Pd(2)-Cl(1)	2.417(1)
C(1)-Pd(1)-N(1)	81.4(1)	C(1)-Pd(1)-Cl(2)	98.6(1)
N(1)-Pd(1)-Cl(2)	173.6(1)	C(1)-Pd(1)-Cl(1)	176.5(1)
N(1)-Pd(1)-Cl(1)	95.7(1)	Cl(2)-Pd(1)-Cl(1)	84.1 (1)
C(11)-Pd(2)-N(2)	80.8(1)	C(11)-Pd(2)-Cl(2)	97.9(1)
N(2)-Pd(2)-Cl(2)	173.7(1)	C(11)-Pd(2)-Cl(1)	177.7(1)
N(2)-Pd(2)-Cl(1)	97.2(1)	Cl(2)-Pd(2)-Cl(1)	84.0(1)

4.3.3.3 Molecular Structure Optically Active Dimeric Complex (*S*)-119

The solid-state structure of bright yellow block-like single crystals obtained from DCM/ *n*-hexane solution of (*S*)-**119** is confirmed *via* X-ray crystallography (Figure 4.12). Selected bond lengths and angles of (*S*)-**119** are shown in Table 4.6. Similarly, the complex (*S*)-**119** adopted distorted square planar coordination geometry about the palladium center and both five-member rings are in an envelope-like conformation. The dihedral angle of distortion about Pd(1) is 8.4° and 11.6° for Pd(2). The two nitrogen atoms have a *trans*-(*N*,*N*) disposition. The palladium centers together with the bridging ligands form an eight-membered ring of boat-boat conformation that bent 86.6° along the C(11)–C(13) axis and the two bridging ligands are positioned 89.3° away from each other and all the C–O bonds are delocalized C–O bonds. The Pd(1)–Pd(2) distance in the solid state is 3.191 Å.

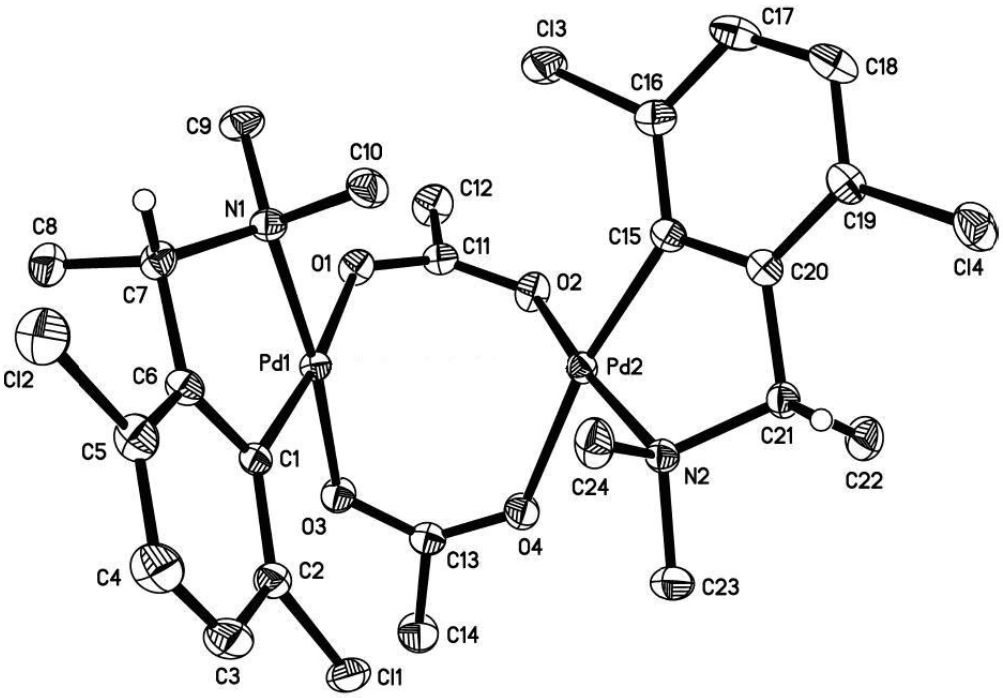

Figure 4.12 Molecular structure of complex (*S*)-**119**. All hydrogen atoms except H(C7), and H(C21) in were omitted for clarity.

Table 4.6: Selected bond lengths (Å) and angles (°) for complex (*S*)-**119**

Pd(1)-C(1)	2.011(2)	Pd(1)-O(3)	2.035(2)
Pd(1)-N(1)	2.058(2)	Pd(1)-O(1)	2.131(2)
Pd(2)-O(2)	2.031(2)	Pd(2)-C(15)	1.995(2)
Pd(2)-O(4)	2.099(2)	Pd(2)-N(2)	2.065(2)
C(11)-O(1)	1.255(3)	C(11)-O(2)	1.274(3)
C(13)-O(4)	1.253(3)	C(13)-O(3)	1.269(3)
C(1)-Pd(1)-O(3)	97.5(1)	C(1)-Pd(1)-N(1)	82.3(1)
O(3)-Pd(1)-N(1)	172.7(1)	C(1)-Pd(1)-O(1)	173.7(1)
O(3)-Pd(1)-O(1)	86.4(1)	N(1)-Pd(1)-O(1)	93.3(1)
C(15)-Pd(2)-O(2)	96.3(1)	C(15)-Pd(2)-N(2)	82.2(1)
O(2)-Pd(2)-N(2)	171.4(1)	C(15)-Pd(2)-O(4)	170.5(1)
O(2)-Pd(2)-O(4)	87.2(1)	N(2)-Pd(2)-O(4)	93.0(1)

4.3.4 Regio-selective Formation of the DMPP Complex (*S*)-125 and its *endo*-Cycloaddition Reactions with Ethyl Vinyl Ketone

In order to assess the effectiveness and the effect of the chloro withdrawing group of the new palladacycle (*S*)-**118** synthesized, the asymmetric [4+2] *endo*-cycloaddition reaction between DMPP and ethyl vinyl ketone promoted by the new palladacycle (*S*)-**118** was conducted. The DMPP-coordinated complex (*S*)-**125** is obtained by cleavage of the optically pure dimeric complex (*S*)-**118** with two molar equivalents of DMPP in 96% yield, $[\alpha]_D$ +511.2° (*c* 0.02, DCM). (Scheme 4.5)

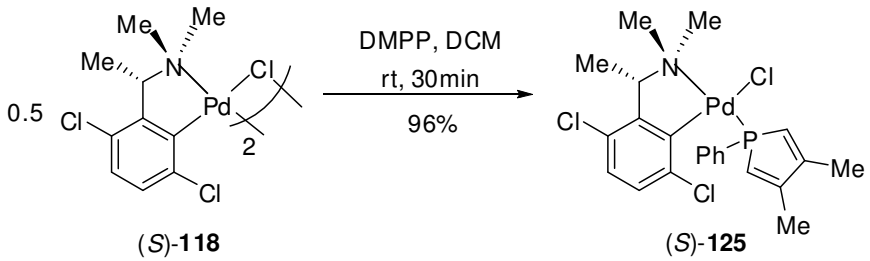

(*S*)-**118** (*S*)-**125**

Scheme 4.5

4.3.4.1 Molecular Structure of DMPP Complex (*S*)-125

The solid-state structural study on the yellow single crystal obtained from slow evaporation of the complex (*S*)-**125** in DCM/ *n*-hexane solution is investigated using X-ray crystallography (Figure 4.13). Selected bond lengths and angles of (*S*)-**125** are presented in Table 4.7. The complex (*S*)-**125** is in distorted square planar coordination geometry with tetrahedral distortion of 12.0° and the nitrogen group is *trans to* phosphole group. The Pd(1)–P(1) bond length is slightly longer than that of DMPP-coordinated complex (*S*)-**88**.[13c] This is shows that the Pd–P bond is weaker than the DMPP complex (*S*)-**88**. The bond angle of C(1)-Pd(1)-P(1) is also bigger than DMPP complex (*S*)-**88** which shows the steric repulsion between the chloro group and the DMPP group in complex (*S*)-**125** is larger. [13c]

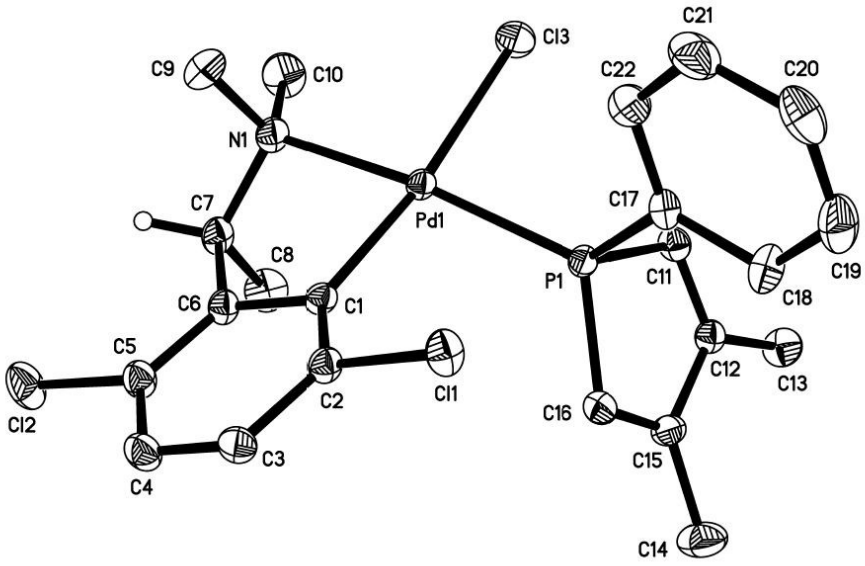

Figure 4.11 Molecular structure of DMPP complex (*S*)-**125**. All hydrogen atoms except H(C7) in were omitted for clarity.

Table 4.7: Selected bond lengths (Å) and angles (°) for complex (*S*)-**125**

Pd(1)-C(1)	2.014(2)	Pd(1)-N(1)	2.145(2)
Pd(1)-P(1)	2.250(1)	Pd(1)-Cl(3)	2.375(1)
C(2)-Cl(1)	1.744(2)	C(5)-Cl(2)	1.751(3)
C(1)-Pd(1)-N(1)	80.4(1)	C(1)-Pd(1)-P(1)	98.3(1)
N(1)-Pd(1)-P(1)	169.7(1)	C(1)-Pd(1)-Cl(3)	172.0(1)
N(1)-Pd(1)-Cl(3)	94.2(1)	P(1)-Pd(1)-Cl(3)	88.0(1)

4.3.4.2 Solution Structure of DMPP Complex (*S*)-125

The $^{31}P\{^{1}H\}$ NMR spectrum of DMPP complex (*S*)-**125** in $CDCl_3$ at room temperature gave only one singlet at δ 28.9, indicating the presence of only one isomer in the solution. The ^{1}H NMR and 2D ^{1}H-^{1}H ROESY NMR experiments were conducted to determine the solution structure of complex (*S*)-**125**. The numbering scheme of the DMPP complex (*S*)-**125** use for NMR study and the 2D ^{1}H-^{1}H ROESY NMR spectrum is presented in Figure 4.14 and Figure 4.15, respectively.

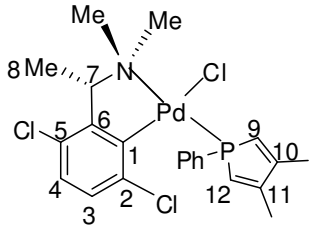

Figure 4.14: Numbering scheme of DMPP complex (*S*)-**125**

As shown in Figure 4.15, the interaction between the Me8 and NMe(eq) denoted as A, justified that the five-membered organometallic ring is locked in λ configuration in solution. And ROESY correlations B to D correspond to the interactions between H7 with Me8, NMe(eq) and NMe(ax), respectively. The absence

of interactions between the proton on the phosphole and the NMe groups further confirm that the two nitrogen groups are *trans* to each other.

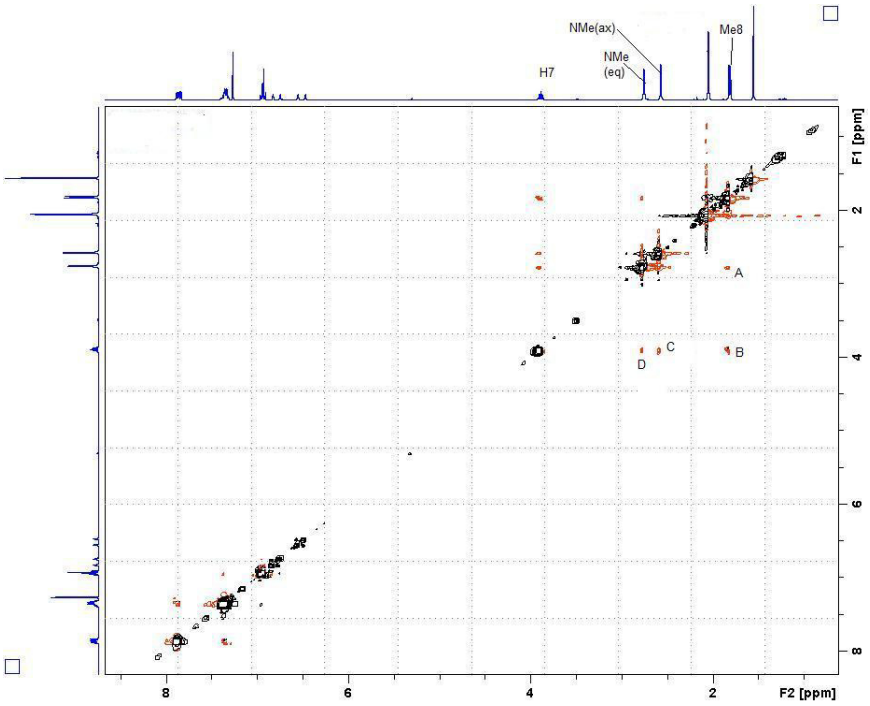

Figure 4.15 2D ^{1}H-^{1}H ROESY NMR spectrum of the complex (*S*)-**125** in $CDCl_3$. Selected ROESY Interactions: (A) Me8 - NMe(eq); (B) H7– Me8; (C) H7–NMe(ax); (D) H7–NMe(eq)

4.3.4.3 Asymmetric Intramolecular *endo*- Cycloaddition Reactions between DMPP Complex (*S*)- 125 and Ethyl Vinyl Ketone

Complex (*S*)-**125** was treated with excess of ethyl vinyl ketone in chloroform and stirred at room temperature. The reaction was monitored using ^{31}P{^{1}H} NMR. After ten days, the reaction was completed and a diastereomeric ratio of 2.1:1 was observed. In order to increase the reactivity of the reaction, the reaction temperature was increased to 50^{o}C. The reaction was completed after 4 days, the peak at δ 28.9 disappeared and two new sharp singlets 117.6 and 118.0 ppm in a 1:1.9 diastereomeric ratio. The stereoselectivity of the cycloaddition at 50 ^{o}C is approximately the same as

the reaction at room temperature. However, both reactions show that the chloro group does not exert much stereochemical influence on the reaction site. Unfortunately after several attempt of column chromatography the diastereomeric isomers could not be separated. The identities of the products were deduced with reference to previous published related works (Scheme 4.6).[13c,71]

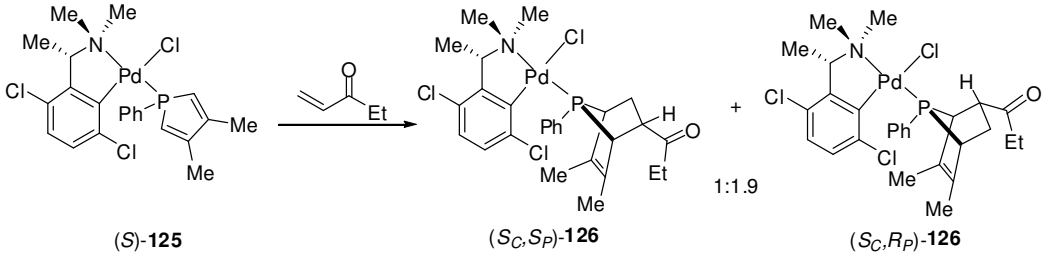

(*S*)-**125** (S_C,S_P)-**126** (S_C,R_P)-**126**

Scheme 4.6

4.3.5 Hydrophosphination Reaction of Diphenylphosphine and DMAD Promoted by Complex (*S*)-127

Since the stereoselectivity of the complex (*S*)-**118** was poor in the asymmetric intramolecular *endo*-cycloaddition reaction, the investigation of complex (*S*)-**118** on another asymmetric reaction was carried out. The complex (*S*)-**118** was used to promote asymmetric hydrophosphination between diphenylphosphine and DMAD. The dimeric complex (*S*)-**118** was first treated with slight excess of silver perchlorate in acetonitrile to give the cationic complex (*S*)-**127**. The neighboring coordination sites were free for coordination of the diphenylphosphine by replacing the chloro group with labile ligand (NCMe). Then the cationic complex (*S*)-**127** undergoes 1,2-addition of DMAD with two molar equivalents of diphenylphosphine in presence of a base, NEt_3 in DCM at -78°C. The $^{31}P\{^1H\}$ NMR spectrum of crude (*S*,*RR*)-**128** in $CDCl_3$ exhibited only a pair of doublets at δ 34.8 and 45.2 with J_{PP} = 39.7 Hz. This result obtained is much better compared with the naphthylamine template (*S*)-**83**,

under same reaction conditions. The naphthylamine template (*S*)-**91** promoted hydrophosphination reaction to give mixture of diastereomers (*S*,*RR*)-**92** and (*S*,*SS*)-**92** in ratio of 6:1.[78a] After column chromatography, the product (*S*,*RR*)-**128** was obtained as yellow oil in quantitative yield with presence of unknown by-product at δ 51.0 (dd). In order to obtain the pure product (*S*,*RR*)-**128**, crystallization method was employed. However, after several attempts with various solvents no crystals were obtained. Next, the chiral amine moiety was removed *via* concentrated HCl to give the dichloro palladium complex (*RR)*-**129**. The $^{31}P\{^{1}H\}$ NMR spectrum of (*RR*)-**129** in $CDCl_3$ shows a single sharp peak at δ 58.0 with optical rotation of [α]D = +140.0° (*c* = 0.1, $CHCl_3$) The enantiomerically pure ligand (*RR*)-**130** was obtained after liberation with aqueous potassium cyanide, giving a singlet at δ -6.3 in $CHCl_3$ (Scheme 4.7).

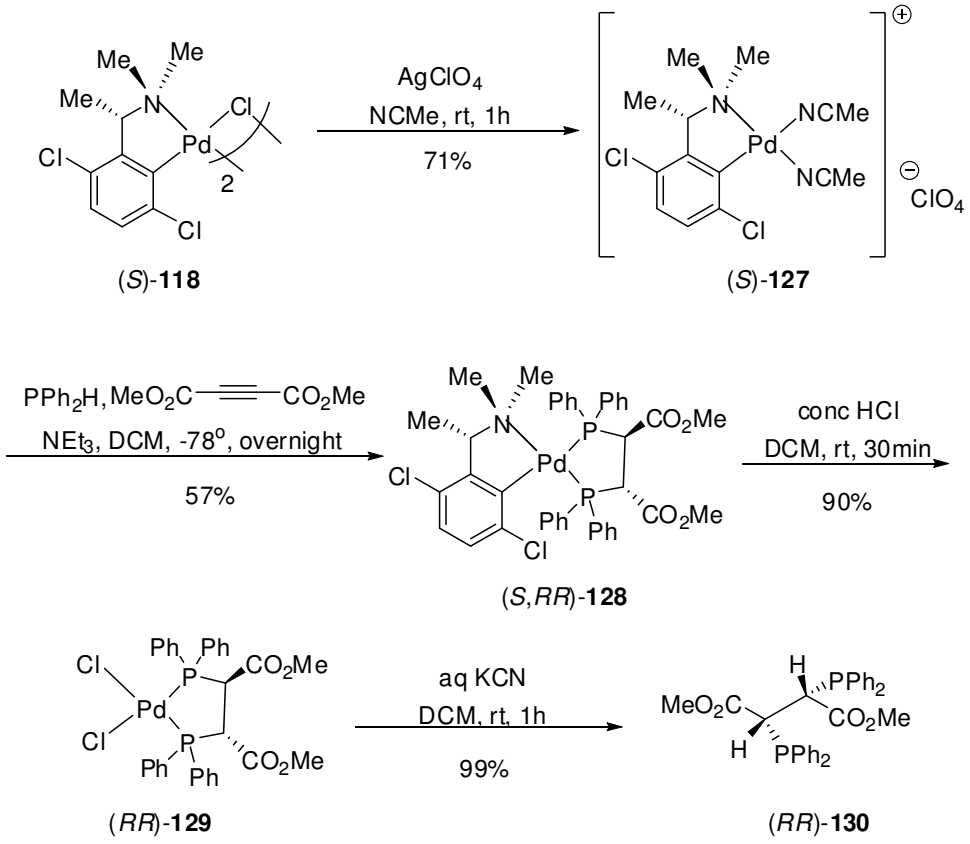

Scheme 4.7

4.3.5.1 Molecular Structure of Complex (*S*)-128

The pale yellow needle-like crystal is obtained from slow evaporation of complex (*S*)-**128** in DCM/ *n*-hexane solution. The structure is confirmed using X-ray crystallography (Figure 4.16) and selected bond lengths and angles of (*S*)-**128** are presented in Table 4.8. The coordination geometry of the palladium center is distorted square planar with the dihedral angle of the planes {N(1)−Pd(1)−C(1)} and {N(3)−Pd(1)−N(2)} is 5.3°. The five membered ring is in envelop conformation with N(1) is 0.774 Å above the plane {C(1)−C(6)−C(7))−Pd(1)}. The distance between the Cl(1) and the N(3) of the acetonitrile ligand is 3.032 Å which is smaller than the sum of van der Waals of the two groups,[86] showing the steric interaction between the protruding chloro group and the acetonitrile ligand.

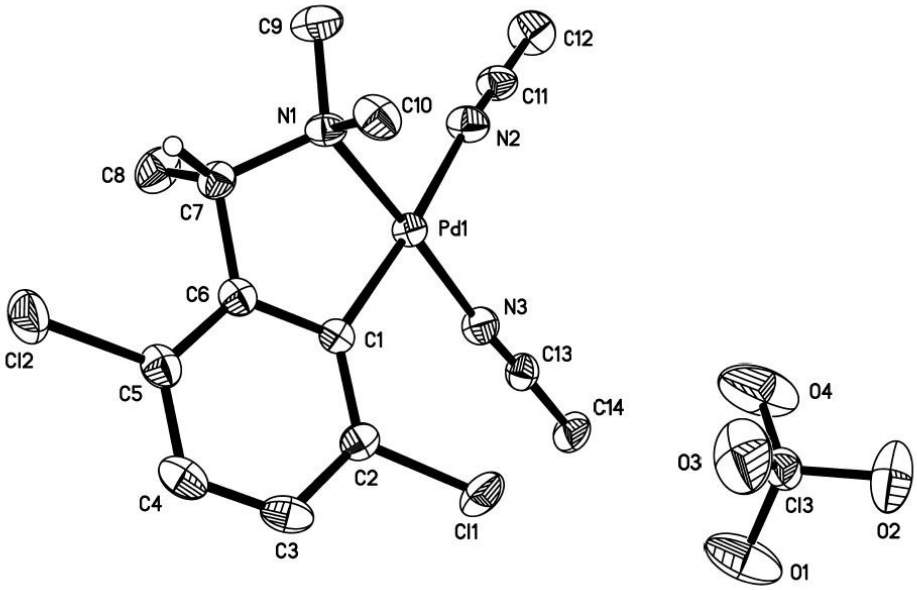

Figure 4.16 Molecular structure of complex (*S*)-**128**. All hydrogen atoms except H(C7) in were omitted for clarity.

Table 4.8: Selected bond lengths (Å) and angles (°) for complex (*S*)-**128**

Pd(1)-C(1)	1.993(3)	Pd(1)-N(3)	2.005(3)
Pd(1)-N(1)	2.051(3)	Pd(1)-N(2)	2.108(3)
C(1)-Pd(1)-N(3)	96.16(12)	C(1)-Pd(1)-N(1)	80.89(11)
N(3)-Pd(1)-N(1)	176.92(11)	C(1)-Pd(1)-N(2)	174.49(13)
N(3)-Pd(1)-N(2)	85.23(12)	N(1)-Pd(1)-N(2)	97.62(11)

4.3.6 Conclusion

The complex (*S*)-**118** was successfully synthesized. The racemic dimeric complex (±)-**119** was obtained from *ortho*-palladation of the amine ligand. The amine ligand was synthesized *via* three steps, the synthetic route starting from 1-(2,5-dichlorophenyl)ethanone. The complex (±)-**119** was successfully resolved using optically active (*S*)-sodium prolinate. It was found that the five-membered ring of the (*S*)-prolinate diastereomeric derivatives exist in one conformation, (*R*)-δ or (*S*)-λ, in both solid state and in solution. Investigation on the effectiveness and the effect of the chloro withdrawing group of the complex (*S*)-**118** on asymmetric [4+2] *endo*-cycloaddition reaction, resulted in poorer stereoselectivity than the methyl substituted benzyl chiral palladacycle. This suggested that the electronic effect of the electron withdrawing chloro group will also affect the stereoselectivity in asymmetric Diels-Alder reaction. The complex (*S*)-**118** is more effective in promoting the asymmetric hydrophosphination reaction giving one diastereomeric product (*S*,*RR*)-**128**. Since, (*S*,*RR*)-**128** could not be crystallized out after several attempts, it was converted to the dichloro complex (*RR*)-**129**. The crystal of the complex (*RR*)-**129** have a flack parameter of -0.0(0) and the value of δ P in the $^{31}P\{^{1}H\}$ NMR spectrum matched the published value.

4.4 Experimental

Reactions involving air-sensitive compounds were performed under positive pressure of purified nitrogen by using standard Schlenk techniques. Proton nuclear magnetic resonance (^{1}H NMR) and carbon nuclear magnetic resonance (^{13}C{^{1}H} NMR) spectroscopy were performed on a Bruker Avance III 400 Spectrometer (^{1}H at 400 MHz, ^{13}C{^{1}H} at 100 MHz). The and phosphorus nuclear magnetic resonance (^{31}P{^{1}H} NMR) spectroscopy is performed on a Bruker Avance 300, 500 and a Bruker Avance III 400 NMR Spectrometers Multiplicities are given as: s (singlet); br s (broad singlet); d (doublet); t (triplet); q (quartet); qn (quintet); dd (doublets of doublet); m (multiplets); etc. The number of protons (n) for a given resonance is indicated by nH. Coupling constants are reported as a *J* value in Hz. Chemical shifts are reported as δ in units of parts per million (ppm) downfield from tetramethylsilane (δ 0.0) and referenced to the chemical shifts of residual resonances of the respective deutero-solvent, chloroform-*d* (^{1}H at δ 7.26, singlet and ^{13}C{^{1}H} NMR δ 77.00, triplet), unless otherwise stated. All NMR spectroscopic experiments were performed at room temperature (300 K). Mass spectra were recorded on a JOEL AccuTOF-DART HRMS. Melting points were determined on SRS-Optimelt MPA-100 apparatus and were uncorrected. Melting points were determined with a SRS-Optimelt MPA-100 apparatus. Optical rotations were measured using a 0.1-dm cell at 589 nm with a Perkin-Elmer polarimeter (model 341) at 20 °C or Atago automatic polarimeter model (AP-300).

4.4.1 Synthesis of *1-(2,5-dichlorophenyl)ethanol*, (±)-122

A solution of $NaBH_4$ (3.15 g, 83.3 mmol) in MeOH (100 mL) was added dropwise into 1-(2,5-dichlorophenyl)ethanone **121** (8.00 mL, 10.5g, 55.5 mmol) in the same solvent (50 mL) at 0°C. The mixture was stirred rapidly at 0°C for 3 hours. Then a

solution of 6 wt% NaOH (20 mL) was added and the mixture was stirred for an hour. The resulting mixture was concentrated *via* reduced pressure. This was followed by extraction with DCM (3 x 100 mL). The organic layers were combined over anhydrous $MgSO_4$ and removal of solvent under reduced pressure to yield a white solid (10.5 g, 99 %). M.p. 59-61 °C. ^{1}H NMR (400 MHz): δ = 1.48 (d, $^3J_{H,H}$ = 6.0 Hz, 3H, CHCH_3), 2.03 (d, $^4J_{H,H}$ = 3.2 Hz 1H, O*H*), 5.23 (m, $^3J_{H,H}$ = 6.4 Hz, $^4J_{H,H}$ = 3.6 Hz 1H, C*H*CH$_3$), 7.17 (dd, $^3J_{H,H}$ = 8.4 Hz, $^3J_{H,H}$ = 2.4 Hz, 1H, aromatic), 7.25 (d, $^3J_{H,H}$ = 8.4 Hz, 1H, aromatic), 7.60(d, $^3J_{H,H}$ = 2.8 Hz, 1H, aromatic). ^{13}C{^{1}H} NMR (100 MHz): δ = 23.74 (CH***C***H$_3$), 67.04 (***C***HCH$_3$), 126.94 (Ar-C6), 128.60 (Ar-C4), 129.88 (Ar-C1), 130.73 (Ar-C3), 133.48 (Ar-C5), 145.09 (Ar-C2). HRMS (m/z (M − OH)]$^+$ calcd for $C_8H_7Cl_2$ 172.9925, found 172.9926.

4.4.2 Synthesis of *1-(1-bromoethyl)-2,5-dichlorobenzene*, (±)-123

A solution of PBr_3 (40.0 mL, 112 g, 413 mmol) in DCM (75mL) was added dropwise to the alcohol, **(±)-122** (19.7 g, 103mmol) dissolved in DCM (150 mL). The mixture was stirred at 0 °C for 14 h followed by the addition of water. The organic layer was separated and washed with water (3 x 200 mL), dried over anhydrous $MgSO_4$ and the solvent was removed under reduced pressure to yield (±)-**123** as colourless oil, Yield: 23.7 g (91 %). ^{1}H NMR (400 MHz): δ = 2.00 (d, $^3J_{H,H}$ = 7.2 Hz, 3H, CHCH_3), 5.53 (q, $^3J_{H,H}$ = 6.9 Hz, 1H, C*H*CH$_3$), 7.17 (dd, $^3J_{H,H}$ = 8.4 Hz, $^3J_{H,H}$ = 2.4 Hz, 1H, aromatic), 7.27 (d, $^3J_{H,H}$ = 8.4 Hz, 1H, aromatic), 7.60 (d, $^3J_{H,H}$ = 2.4 Hz, 1H, aromatic). ^{13}C{^{1}H} NMR (100 MHz): δ = 25.85 (CH***C***H$_3$), 43.36 (***C***HCH$_3$), 128.44 (Ar-C6), 129.60 (Ar-C4), 130.97 (Ar-C1), 131.01 (Ar-C3), 133.46 (Ar-C5), 142.093 (Ar-C2). HRMS (m/z (M − Br)]$^+$ calcd for $C_8H_7Cl_2$ 172.9925, found 172.9925.

4.4.3 Synthesis of *1-(2,5-dichlorophenyl)-N,N-dimethylethanamine*, (±)-**120**

A aqueous solution of 40 wt.% dimethylamine (375 mL) was added to a solution of bromo species, (±)-**123** (23.7 g, 93.5mmol) in DCM (200 mL) and stirred vigorously overnight at room temperature. After which, the solvents were removed. The residue was dissolved in DCM and washed with water (3 x 200 mL). The organic layer was dried over anhydrous MgSO4. Removal of solvent under reduced pressure yielded colorless oil. Yield: 18.7 g (92 %). ^{1}H NMR (400 MHz): δ = 1.28 (d, $^{3}J_{H,H}$ = 6.4 Hz, 3H, CHCH_3), 2.23 (s, 6H, N(CH_3)$_2$), 3.70 (q, $^{3}J_{H,H}$ = 6.7 Hz, 1H, CHCH$_3$), 7.12 (dd, $^{3}J_{H,H}$ = 8.6 Hz, $^{3}J_{H,H}$ = 2.6 Hz, 1H, aromatic), 7.27 (d, $^{3}J_{H,H}$ = 8.4 Hz, 1H, aromatic), 7.56 (d, $^{3}J_{H,H}$ = 2.4 Hz, 1H, aromatic). ^{13}C{^{1}H} NMR (100 MHz): δ = 20.15 (CH***C***H$_3$), 43.45 (N(***C***H$_3$)$_2$), 61.41 (***C***HCH$_3$), 127.76 (Ar-C4), 128.34 (Ar-C3), 130.45 (Ar-C6), 131.29 (Ar-C5), 133.02 (Ar-C1), 144.42 (Ar-C2). HRMS (m/z (M + H)]$^{+}$ calcd for $C_{10}H_{14}Cl_2N$ 218.0503, found 218.0511.

4.4.4 Synthesis of *(±)-μ-acetobis-{1-(2,5-dichlorophenyl)-N,N-dimethylethanamineC,N} dipalladium (II),* (±)-**119**

The palladium agent, Pd(OAc)$_2$ (2.13 g, 9.48 mmol) was added to a solution of amine (±)-**120** (2.06, 9.44 mmol), in MeOH (50 mL). The mixture was heated to 55 °C and stirred overnight. The mixture was filtered through celite and concentrated *via* reduced pressure. The residue was dissolved in DCM, followed by washing with water (3 x 50 mL), dried over anhydrous $MgSO_4$ and concentrated to give bright yellow solid. The bright yellow solid was recrystallized from DCM/ *n*-hexane solution and gave bright yellow crystals. Yield: 3.44 g (95 %). M.p. 172-174 °C. ^{1}H NMR (400 MHz): δ =1.95 (s, 3H, CH_3COO-), 2.04 (d, $^{3}J_{H,H}$ = 6.3 Hz, 3H, CHCH_3), 2.560 (s, 3H, NCH_3 (eq)), 2.87 (s, 3H, NCH_3 (ax)), 3.79 (q, $^{3}J_{H,H}$ = 6.3 Hz, 1H, CHCH$_3$), 6.81 (d, $^{3}J_{H,H}$ = 8.4 Hz,

1H, aromatic), 6.88 (d, $^{3}J_{H,H}$ = 8.5 Hz, 1H, aromatic). $^{13}C\{^{1}H\}$ NMR (100 MHz): δ = 22.13 (CH***C***H_3), 24.39 (***C***H_3COO-), 48.32 (N***C***H_3 (eq)), 54.30 (N***C***H_3 (ax)), 76.43 (***C***HCH_3), 125.47(Ar-C6), 126.54 (Ar-C3), 129.40 (Ar-C4), 138.63 (Ar-C1), 139.21 (Ar-C5), 152.56 (Ar-C2), 181.78 (C=O). HRMS (m/z (M - OAc)]$^{+}$ calcd for $C_{22}H_{27}Cl_4N_2O_2Pd_2$ 706.8880, found 706.8905.

4.4.5 Synthesis of *(R_C,$S_C$$S_N$)-Prolinato-{1-(2,5-dichlorophenyl)-N,N-dimethylethanamine-C,N} dipalladium (II),* (***R_C,$S_C$$S_N$***)-**124**

Firstly, the racemic dimer, (±)-**119** (13.18 g, 17.2 mmol) was dissolved in MeOH (100 mL). Then a solution of sodium prolinate (4.97 g, 36.3 mmol) in the same solvent (50 mL) was added. The mixture was stirred for 1 h, and the solvent was removed under reduced pressure. The residue was dissolved in DCM (100 mL) and washed with water (3 x 100 mL). The organic layer was dried over anhydrous $MgSO_4$. The diastereomeric compound (R_C,$S_C$$S_N$)-**124** adduct was separated by flash column chromatography over silica (eluent acetone: *n*-hexane, v/v: 1:1). The solvent was removed and the residue was recrystallized from ethyl acetate/diethyl ether yielding pale yellow flakes. Yield: 5.52 g (73%). M.p. 174-177 °C (dec). (73%) $[\alpha]^{23.2}$ +28.5° (*c* 0.0281, DCM). ^{1}H NMR (400 MHz): δ =1.62−1.67 (m, 1H, $CH_2CH_2CH_2$), 1.71 (d, $^{3}J_{H,H}$ = 6.4 Hz, 3H, $CHCH_3$), 1.84−1.94 (m, 2H, $CH_2CH_2CH_2$, $COCHCH_2$), 2.38−2.45 (m, 1H, $COCHCH_2$), 2.55 (s, 1H, NCH_3 (eq)), 2.78 (s, 1H, NCH_3 (ax)), 3.18−3.23 (m, 1H, $NHCH_2$), 3.72−3.77 (m, 1H, $NHCH_2$), 3.81 (q, $^{3}J_{H,H}$ = 6.4 Hz, 1H, $CHCH_3$), 4.05−4.08 (m, 1H, N*H*), 4.14−4.18 (m, 1H, $COCHCH_2$), 6.84 (d, $^{3}J_{H,H}$ = 8.8 Hz, 1H, aromatic), 6.90 (d, $^{3}J_{H,H}$ = 8.8 Hz, 1H, aromatic). $^{13}C\{^{1}H\}$ NMR (100 MHz): δ =22.00 (CH***C***H_3), 23.13 (CH_2***C***H_2CH_2), 28.79 ($COCHCH_2$), 47.91 (N***C***H_3 (eq)), 51.33 ($NHCH_2$), 53.47 (N***C***H_3 (ax)), 66.27 (CO***C***HCH_2), 74.70 (***C***HCH_3), 126.37 (Ar-C6),

126.75 (Ar-C3), 128.50 (Ar-C4), 140.04 (Ar-C5), 143.12 (Ar-C1), 153.38 (Ar-C2), 179.19 (C=O). HRMS (m/z (M + H)]$^+$ calcd for $C_{15}H_{21}Cl_2N_2O_2Pd$ 439.0019, found 439.0020.

4.4.6 Synthesis of *(S_C,$S_C$$S_N$)-Prolinato-{1-(2,5-dichlorophenyl)-N,N-dimethylethanamine-C,N}dipalladium (II),* (S_C,$S_C$$S_N$)-124

The other diastereomeric adduct, (S_C,$S_C$$S_N$)-**124** was separated using acetone as mobile phase. The solvent was removed and the residue was recrystallized from acetone/ *n*-heptane yielding pale yellow needle-like crystals. Yield: 5.80 g (77%). $[\alpha]^{22.8}$ +306.4° (*c* 0.0183, DCM). ^{1}H NMR (400 MHz): δ =1.60−1.67 (m, 1H, $CH_2CH_2CH_2$), 1.84 (d, $^3J_{H,H}$ = 6.4 Hz, 3H, $CHCH_3$), 1.96−1.98 (m, 1H, $CH_2CH_2CH_2$,), 2.17−2.23 (m, 2H, $COCHCH_2$), 2.61 (s, 1H, NCH_3 (eq)), 2.65 (s, 1H, NCH_3 (ax)), 3.11−3.19 (m, 1H, $NHCH_2$), 3.24−3.31 (m, 1H, $NHCH_2$), 3.78 (q, $^3J_{H,H}$ = 6.4 Hz, 1H, $CHCH_3$), 4.04−4.09 (q, 1H, $COCHCH_2$), 4.85−4.87 (m, 1H, NH), 6.83 (d, $^3J_{H,H}$ = 8.8 Hz, 1H, aromatic), 6.90 (d, $^3J_{H,H}$ = 8.4 Hz, 1H, aromatic). ^{13}C{^{1}H} NMR (100 MHz): δ = 22.05 ($CHCH_3$), 25.60 ($CH_2CH_2CH_2$), 30.20 ($COCHCH_2$), 47.78 (NCH_3 (eq)), 52.98 ($NHCH_2$), 53.09 (NCH_3 (ax)), 64.91 ($COCHCH_2$), 74.93 ($CHCH_3$), 126.46 (Ar-C6), 126.51 (Ar-C3), 128.59 (Ar-C4), 140.14 (Ar-C5), 144.61 (Ar-C1), 152.79 (Ar-C2), 181.10 (C=O). HRMS (m/z (M + H)]$^+$ calcd for $C_{15}H_{21}Cl_2N_2O_2Pd$ 439.0019, found 439.0020.

4.4.7 Synthesis of *R-μ-chloro-{1-(2,5-dichlorophenyl)-N,N-dimethylethanamine-C,N}dipalladium(II),* (*R*)-118

Hydrochloric acid (1 M, 20 mL) was added into the solution of (R_C,$S_C$$S_N$)-**124** (2.34 g, 5.34 mmol) complex in DCM (40 mL) and stirred at room temperature. After

vigorous stirring for 30 min, the organic layer was separated, washed with water, dried over $MgSO_4$ and followed by removal of solvent under vacuum to give the dimeric complex (*R*)-**118**. Yield: 1.73 g (90%). M.p. 170-173°C (dec). $[\alpha]_D$ -326° (*c* 0.0136, DCM).

The optically pure (*S*)-**118**, was prepared from the complex (S_C,$S_C$$S_N$)-**124** (2.51g, 5.74 mmol) using the same method in 89% yield (1.83 g) $[\alpha]_D$ +345 (*c* 0.0104, DCM) ^{1}H NMR (400 MHz): δ = 2.07−2.11 (m, 6H, CHCH_3), 2.49 (d, 6H, NCH_3 (eq)), 2.68 (6, 6H, NCH_3(ax)), 3.73−3.76 (m, 2H, CHCH$_3$), 6.78−6.87 (m, 2H, aromatic) . ^{13}C{^{1}H} NMR (100 MHz): δ = 21.69 (CH***C***H$_3$), 49.05 (N***C***H$_3$ (eq)), 50.01 (N***C***H$_3$ (eq)), 53.72 (N***C***H$_3$ (ax)), 53.99 (N***C***H$_3$ (ax)), 76.62 (***C***HCH$_3$), 124.69 (Ar-C6), 124.83 (Ar-C6), 126.23 (Ar-C3), 126.28 (Ar-C3), 128.99 (Ar-C4), 129.12 (Ar-C4), 139.09 (Ar-C5), 139.20 (Ar-C5), 139.95(Ar-C1), 140.10 (Ar-C1), 150.66 (Ar-C2), 150.79 (Ar-C2). HRMS (m/z (M − Cl)]$^+$ calcd for $C_{20}H_{24}Cl_5N_2Pd_2$ 678.8433, found 678.8452.

4.4.8 Synthesis of *S-μ-acetato-{1-(2,5-dichlorophenyl)-N,N-dimethylethanamine-C,N}dipalladium(II),* (*S*)-119.

A solution of silver acetate (59.5 mg, 0.36 mmol) in MeOH (5 mL) was added to the optically pure (*S*)-**118** (103.5 mg, 0.14 mol) dissolved in MeOH (10 mL) and the mixture vigorously in dark at room temperature for 1 h. The resulting solution was filtered and the filtrate was washed with water (15 mL) once. The organic layer was dried over anhydrous $MgSO_4$ and concentrated to give yellow solid. The yellow solid was recrystallized from DCM/ *n*-hexane yielding yellow crystals. Yield: 82.7 mg (75 %). ^{1}H NMR (400 MHz): δ =1.95 (s, 3H, CH_3COO-), 2.04 (d, $^3J_{H,H}$ = 6.4 Hz, 3H, CHCH_3), 2.59 (s, 3H, NCH_3 (eq)), 2.87 (s, 3H, NCH_3 (ax)), 3.79 (q, $^3J_{H,H}$ = 6.4 Hz, 1H, CHCH$_3$), 6.80 (d, $^3J_{H,H}$ = 8.4 Hz, 1H, aromatic), 6.87 (d, $^3J_{H,H}$ = 8.5 Hz, 1H,

aromatic) . $^{13}C\{^1H\}$ NMR (100 MHz): δ = 24.11 (CH***C***H_3), 29.63 (***C***H_3COO-), 48.06 (NCH_3 (ax)), 54.04 (NCH_3 (eq)), 76.18 (***C***HCH$_3$), 125.22 (Ar-C6), 126.23 (Ar-C3), 129.14 (Ar-C4), 138.36 (Ar-C1), 138.96 (Ar-C5), 152.31 (Ar-C6), 181.52 (C=O). HRMS (m/z (M − OAc)]$^+$ calcd for $C_{22}H_{27}Cl_4N_2O_2Pd_2$ 706.8880, found 706.8905.

4.4.9 Synthesis of *S-chloro-{1-{1-(2,5-dichlorophenyl)-N,N-dimethylethanamine-C,N}{3,4-dimethyl-1-phenylphosphole-P}palladium(II),* (*S*)-125.

The optically pure (*S*)-**118** (0.96 g, 1.33 mmol) was added to a solution of DMPP (0.49 g, 2.6 mmol) in degassed DCM, under positive pressure of nitrogen. The mixture was stirred at room temperature for 30 min, and then the solvent was removed under vacuum to give bright yellow solid. Yield: 1.37 g (96%). M.p. 188-190 °C. $[\alpha]_D$ = +511.2^o (c = 0.01, DCM). $^{31}P\{^1H\}$ NMR (162 MHz): δ = 28.9 (s) . ^1H NMR (400 MHz): δ = 1.80 (d, $^3J_{H,H}$ = 6.4 Hz, 3H, CHCH_3), 2.03 (s, 3H, C=CCH_3), 2.034 (s, 6H, C=CCH_3), 2.56 (d, $^4J_{P,H}$ =2.4 Hz , 3H, NCH_3 (ax)), 2.74 (d, $^4J_{P,H}$ =3.2 Hz , 3H, NCH_3 (eq)), 3.88 (qn, $^3J_{H,H}$ = 6.5 Hz, 1H, C*H*CH$_3$), 6.50 (d, $^2J_{P,H}$ = 32.4 Hz, 1H,), 6.78 (d, $^2J_{P,H}$ = 31.2 Hz, 1H, C=CC*H*), 6.90–6.95 (m, 2H, aromatic), 7.32–7.37 (m, 3H, aromatic), 7.82–7.87 (m, 2H, aromatic). $^{13}C\{^1H\}$ NMR (100 MHz): δ =17.31 (d, $J_{C,P}$ = 12.9 Hz, CH=C***C***H$_3$), 17.85 (d, $J_{C,P}$ = 12.9 Hz, CH=C***C***H$_3$), 21.49 (CH***C***H$_3$), 48.11 (d, $J_{C,P}$ = 2.4 Hz, N***C***H$_3$(eq)), 50.65 (d, $J_{C,P}$ = 2.9 Hz, N***C***H$_3$(ax)), 75.34 (d, $J_{C,P}$ = 3.0 Hz, ***C***HCH$_3$), 126.33 (Ar-C4), 127.15 (d, $J_{C,P}$ = 53.6 Hz, ***C***H=CCH$_3$), 127.57 (Ar-C3), 127.61-130.42 (6H, Ph), 129.47 (d, $J_{C,P}$ = 52.7 Hz, ***C***H=CCH$_3$), 140.03, 140.08, 148.29 (d, $J_{C,P}$ = 10.8 Hz, CH=***C***CH$_3$), 151.79, 151. 81, 153.87 (d, $J_{C,P}$ = 11.0 Hz, CH=***C***CH$_3$). HRMS (m/z (M − Cl)]$^+$ calcd for $C_{22}H_{25}Cl_2NPPd$ 510.0133, found 510.0137.

4.4.10 Asymmetric *endo*- Cycloaddition Reactions between Complex (*S*)-125 and Ethyl Vinyl Ketone Formation of Complex (*S*C,*Rp*)-126 and (*S*C,*Sp*)-126.

The optically pure DMPP complex (*S*)-**125** (0.19 g, 0.35 mmol) was dissolved in $CHCl_3$ (3 mL), then ethyl vinyl ketone (0.2 mL) was added and the solution was stirred at room temperature for 10 days. The resulting solution was filtered through celite and concentrated to give yellow oil. The mixture was unsuccessfully separated *via* column chromatography. The reaction was repeated at 50°C. $^{31}P\{^1H\}$ NMR (161 MHz): δ = 117.6 (s), 118.0 (s).

4.4.11 Synthesis of *(S)-[1-[1-(2,5-dichlorophenyl)-N,N-dimethylethanamine-C,N]palladium(II) perchlorate,* (*S*)-127.

Solution silver perchlorate (0.18 g, 0.87 mmol) in acetonitrile (5 mL) was added into the optically pure (*S*)-**118** (0.28 g, 0.38 mmol) dissolved in acetonitrile (5 mL) and the mixture stirred vigorously in dark at room temperature for 1 h. The resulting solution was filtered and the filtrate was washed with water (10 mL) once. The organic layer was dried over anhydrous $MgSO_4$ and concentrated to give pale yellow solid. The pale yellow solid was recrystallized from DCM/ *n*-hexane yielding pale yellow crystals. Yield: 0.28 g (71 %). M.p. 198-201 °C (dec). $[\alpha]^{21.9}$ = +151.4 (c = 0.0159, DCM). ^1H NMR (400 MHz): δ = 1.75 (s, 3H, N≡CCH_3), 1.98 (d, $^3J_{H,H}$ = 6.4 Hz, 3H, CHCH_3), 2.35 (s, 3H, N≡CCH_3), 2.62 (s, 3H, NCH_3 (eq)), 2.76 (s, 3H, NCH_3 (ax)), 3.83 (q, $^3J_{H,H}$ = 6.4 Hz, 1H, CHCH$_3$), 6.90 (d, $^3J_{H,H}$ = 8.5 Hz, 1H, aromatic), 6.98 (d, $^3J_{H,H}$ = 8.5 Hz, 1H, aromatic). $^{13}C\{^1H\}$ NMR (100 MHz): δ = 2.20 (N≡C***C***H$_3$), 3.24 (N≡C***C***H$_3$), 21.81 (CH***C***H$_3$), 50.05 (N***C***H$_3$(eq)), 53.88 (N***C***H$_3$(ax)), 77.00 (***C***HCH$_3$), 118.57 (N≡***C***CH$_3$), 122.40 (N≡***C***CH$_3$), 125.48 (Ar-C6), 127.50 (Ar-C3), 129.01 (Ar-

C4), 137.84 (Ar-C1), 139.39 (Ar-C5), 151.35 (Ar-C2). HRMS (m/z (M – ClO_4)]$^+$ calcd for $C_{14}H_{18}Cl_2N_3Pd$ 405.9878, found 405.9915.

4.4.11 Asymmetric Hydrophosphination between Diphenylphosphine and Dimethyl Acetylenedicarboxylate Promoted by Complex (*S*)-127

The asymmetric hydrophosphination was performed according to a previously published method.[78a] Diphenylphosphine (114.5 mg, 0.62 mmol) was dissolved in degassed DCM (5 mL) and added to the complex (*S*)-**127** (149.0 mg, 0.31 mmol) with dimethyl acetylenedicarboxylate (43.4 mg, 0.31 mmol) dissolved in degassed DCM (5 mL) under positive pressure of nitrogen. The solution was cooled to -78 ^oC, followed by addition of NEt_3 (62.2 mg, 0.62 mmol). The reaction mixture was allowed to stir at -78 ^oC for 24 hours and gradually warmed to room temperature. The crude product was purified with silica column chromatography using DCM/acetone (V/V = 1: 0.02) as eluent in 57% yield. (Calculated yield of complex with respect to $^{31}P\{^1H\}$ NMR) $^{31}P\{^1H\}$ NMR (202 MHz): δ = 34.8 (1P, d, J_{PP} = 39.7 Hz, P_2CHCOOMe), 45.2 (1P, d, J_{PP} = 39.7 Hz, P_2CHCOOMe). Unknown by-product δ 51.0 was also observed. Concentrated HCl (1 mL) was added dropwise to a solution of (*S*,*RR*)-**128** (165 mg, 0.18 mmol) in DCM (20 mL), the mixture was stirred vigorously at room temperature for 30 min. The resulting mixture was washed with H_2O (5 x 50 mL), the organic layer obtained was dried with $MgSO_4$, filter and concentrated under vacuum to give (*RR*)-**129** as yellow solid in 90% yield. (0.11 g) $^{31}P\{^1H\}$ NMR (121 MHz, $CDCl_3$): δ 58.0. $[\alpha]_{436}$ = +140.0^o (*c* 0.1, $CHCl_3$) The diphosphine (*RR*)-**130** was librated using aq KCN (excess), under the positive pressure of nitrogen as white solid with 99% yield (8.0 mg). $^{31}P\{^1H\}$ NMR (121 MHz, $CHCl_3$): δ -6.3.

Summary

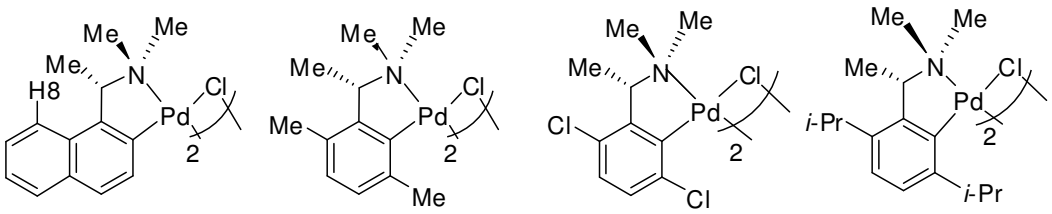

(*S*)-**13** (*S*)-**16** (*S*)-**118** (*S*)-**106**

Table Summary: The Stereoselectivity of Asymmetric Intramolecular *endo*-Cycloaddition

T/°C	(*S*)-**13**	(*S*)-**16**	(*S*)-**118**	(*S*)-**106**
Room temperature	1:2.5	-	2.1:1	1:5.6
50	1:1[a]	1:3.5	1:1.9	1:4.4

[a] The reaction temperature is 70°C.

The chiral arylamine palladacycles are arranged according to the size (from smallest to biggest) of the R group adjacent to the Pd–C bond and the stereoselectivity of the Asymmetric Intramolecular *endo*- Cycloaddition of their DMPP species with ethyl vinyl ketone was presented in Table Summary. From the result obtained, the more bulky the R groups the higher the stereoselectivity for the cycloaddition reaction. The present of the electron withdrawing chloro group will decrease the stereoselectivity, showing electronic factor do play a part, even though the chloro groups are slightly bigger than the methyl group. However, more investigation works need to be carry out on other R groups such as methoxy, trifluoromethyl etc. to confirm the electronic effects of the R groups on the arylamine on the stereoselectivity of the Asymmetric Intramolecular *endo*- Cycloaddition.

References

1. Dupont, J.; Consorti, C. S.; Spencer, J. *Chem. Rev.* **2005,** *105*, 2527–2571.
2. Cope, A. C.; Siekman, R. W. *J. Am. Chem. Soc.* **1965**, *87***,** 3272–3273.
3. Herrmann, W. A.; Bogdanovi, S.; Priermeier, T.; Poli, R.; Fettinger, J. *Angew. Chem. Int. Ed. Engl.* **1995**, 1844–1848.
4. (a) Chatterjee, S.; George, M. D.; Salem, G.; Willis, A. C. *J. Chem. Soc., Dalton Trans.* **2001** 1890–1896. (b) Roberts, N. K.; Wild, S. B. *J. Am. Chem. Soc.* **1979**, *101*, 6254–6260. (c) Roberts, N. K.; Wild, S. B. *J. Chem. Soc., Dalton Trans.* **1979**, 2015–2021. (d) He, G.; Mok, K. F.; Leung, P.-H. *Organometallics,* **1999**, *18*, 4027–4031.
5. Evans, D. W.; Baker, G. R.; Newkome, G. R. *Coord. Chem. Rev.* **1989**, *93*, 155–183.
6. Beletskaya, I. P.; Cheprakov, A. V. *Chem. Rev.* **2000,** *100,* 3009–3066.
7. Lyons, T. W.; Sanford, M. S. *Chem. Rev.* **2010** *110,* 1147–1169.
8. Cope, A. C.; Friedrich, E.C. *J. Am. Chem. Soc.* **1968**, 909–913.
9. Otsuka, S.; Nakamura, A.; Kano, T.; Tani, K. *J. Am. Chem. Soc*. **1971**, 4301–4303.
10. Julia, M.; Duteil, M.; Lallemand, J.Y. *J. Organomet. Chem.* **1977**, 239–243.
11. Tani, K.; Brown, L. D.; Ahmed, J.; Ibers, J. A.; Nakamura, A.; Otsuka, S.; Yokota, M. *J. Am. Chem. Soc.* **1977**, 7876–7886.
12. Allen, D. G.; McLaughlin, G. M.; Robertson, G. B.; Steffen, W. L.; Salem, G.; Wild, S. B. *Inorg. Chem.* **1982,** *21*, 1007-1014.
13. (a) Li, Y.; Ng, K.-H.; Selvaratnam, S.; Tan, G.-K.; Vittal, J. J.; Leung, P.-H. *Organometallics* **2003**, *22*, 834–842. (b) Ding, Y.; Li, Y.; Pullarkat, S. A.; Yap, S. L.; Leung, P.-H. *Eur. J. Inorg. Chem.* **2009**, 267–276. (c) Li, Y.; Selvaratnam,

S.; Vittal, J. J.; Leung, P.-H. *Inorg. Chem.* **2003***, 42,* 3229−3236. (d) Ding, Y.; Zhang, Y.; Li, Y.; Pullarkat, S.A.; Andrews, P.; Leung, P.-H. *Eur. J. Inorg. Chem.* **2010**, 4427–4437.

14. Hartwell, G.E.; Lawrence, R. V.; Smas, M. J. *J. Chem. Soc. D* **1970**, 912–912.
15. Vicente, J.; Saura-Llamas, I. *Comments on Inorganic Chemistry* **2007**, *28*, 39–72.
16. Cockburn, B. N.; Howe, D. V.; Keating, T.; Johnson B. F. G.; Lewis, J. *J. Chem. Soc., Dalton Trans.* **1973**, 404–410.
17. Avshu, A.; O'Sullivan, R. D.; Parkins, A. W.; Alcock, N. W.; Countryman, R. M. *J. Chem. Soc., Dalton Trans.* **1983**, 1619–1624.
18. Baba, S.; Kawaguchi, S. *Inorg. Nucl. Chem. Lett.* **1975**, *11*, 415–420.
19. Fuchita, Y.; Tsuchiya, H. *Polyhedron* **1993**, *12*, 2079–2080
20. Vicente, J.; Saura-Llamas, I.; Palin, M. G.; Jones, P.G. *J. Chem. Soc., Dalton Trans.* **1995**, 2535–2539.
21. (a) Vicente, J.; Saura-Llamas, I.; Bautista, D. *Organometallics* **2005**, *24*, 6001−6004. (b) Vicente, J.; Saura-Llamas, I.; Garcia-Lopez, J.-A.; Calmuschi-Cula, B. *Organometallics* **2007,** *26,* 2768−2776. (c) Oliva-Madrid, M.-J.; Garcia -Lopez, J.-A.; Saura-Llamas, I.; Bautista, D.; Vicente, J. *Organometallics* **2012**, *31*, 3647−3660.
22. Alper, H. *J. Organomet. Chem.* **1977**, *127*, 385–389.
23. Vicente, J.; Abad, J. A.; Clemente, R.; Lopez-Serrano, J.; Ramírez de Arellano, M. C.; Jones, P. G.; Bautista, D. *Organometallics* **2003**, *22*, 4248–4259.
24. Bielsa, R.; Larrea, A.; Navarro, R.; Soler, T.; Urriolabeitia, E. P. *Eur. J. Inorg. Chem.* **2005**, 1724–1736.
25. Moulton, C. J.; Shaw, B. L. *J. Chem. Soc., Dalton Trans.* 1976, 1020–1024.

26. van Koten, G.; Timmer, K.; Noltes, J. G.; Spek, A. L. *J. Chem. Soc., Chem. Commun.* 1978, 250−252.

27. (a) Albrecht, M.; van Koten, G. *Angew. Chem. Int. Ed.* **2001**, *40*, 3750–3781. (b) Dijkstra, H. P.; Slagt, M. Q.; McDonald, A.; Kruithof, C. A.; Kreiter, R.; Mills, A. M.; Lutz, M.; Spek, A. L.; Klopper, W.; van Klink, G. P. M.; van Koten, G. *Eur. J. Inorg. Chem.* **2003**, 830–838. (c) Morales-Morales, D. *J. Mex. Chem. Soc.* **2004**, *48*, 338−346. (d) Takenaka, K.; Uozumi, Y. *Adv. Synth. Catal.* **2004**, 346, 1693–1696. (e) Takenaka, K.; Minakawa, M.; Uozumi, Y. *J. Am. Chem. Soc.* **2005**, *127*, 12273–12281. (f) Li, P.; Zhou, H.-F.; Liu, F.; Hu, Z.-X.; Wang, H.-X. *Inorg. Chem. Comm.* **2013**, 78–81. (g) Arai, T.; Oka, I.; Morihata, T.; Awata, A.; Masu, H. *Chem. Eur. J.* **2013**, *19*, 1554–1557.

28. Sokolov, V. I.; Troitskaya, L. L.; Reutov, O. A. *J. Organomet. Chem.* **1979**, *182*, 537−546.

29. Nonoyama, M. *Inorg. Nucl. Chem. Lett*. **1976**, *12*, 709−712.

30. Benito, M.; Lopez, C.; Solans, X.; Font-Bardia, M. *Tetrahedron: Asymmetry* **1998**, *9*, 4219−4238.

31. Albert, J.; D'Andrea, L.; Bautista, J.; Gonzalez, A.; Granell, J.; Font-Bardia, M.; Calvet, T. *Organometallics* **2008**, *27*, 5108−5117.

32. Selbin, J.; Gutierrez, M. A. *J. Organomet. Chem.* **1983**, *246*, 95−104.

33. Braunstein, P.; Matt, D.; Dusausoy, Y.; Fischer, J.; Mitschler, A.; Ricard, L. *J. Am. Chem. Soc.* **1981**, *103*, 5115−5125.

34. Garber, A. R.; Garrou, P. E.; Hartwell, Smas, M. J.; Wilkinson, J. R.; Todd, L. J. *J. Organomet. Chem.* **1975**, *86*, 219−227.

35. (a) Giordano, T. J.; Rasmussen, P.G. *Inorg. Chem.* **1975,** *14*, 1628−1634. (b) Nonoyama, M.; Kajita, S. *Transition Met. Chem.* **1981**, *6*, 163−165.

36. Hiraki, K.; Fuchita, Y.; Nakaya, H.; Takakura, S. *Bull. Chem. Soc. Jpn.* 1979, *52*, 2531−2534.

37. Hiraki, K.; Fuchita, Y.; Takakura, S. *J. Organomet. Chem.* **1981**, *210*, 273−280.

38. Hiraki, K.; Fuchita, Y.; Takechi, K. *Inorg. Chem.* **1981**, *20*, 4316−4320.

39. Molnar, S. P.; Orchinad, M. *J. Organomet. Chem.* **1969**, *16*, 196−200.

40. Cameron, N. D.; Kilner, M. *J. Chem. Soc., Chem. Commun.* **1975**, 687−688.

41. Roiban, G.-D.; Serrano, E.; Soler, T.; Contel, M.; Grosu, I.; Cativiela, C.; Urriolabeitia, E. P. *Organometallics* **2010**, *29*, 1428–1435.

42. Cuesta, L.; Prat, D.; Soler, T.; Navarro, R.; Urriolabeitia, E. P. *Inorg. Chem.* **2011**, *50*, 8598–8607.

43. Roiban, G.-D.; Soler, T.; Grosu, I.; Cativiela, C.; Urriolabeitia, E. P. *Inorganica Chimica Acta* **2011**, 247–251.

44. Vicente, J.; Chicote, M.-T.; Abellan-Lopez, A.; Bautista, D. *Dalton Trans.* **2012**, *41*, 752–762.

45. Hajipour, A. R.; Rafiee, F. *Tetrahedron Lett.* **2012**, 4661–4664.

46. Ryabov, A. D. *Inorg. Chem.* **1987**, *26*, 1252−1260.

47. Dupont, J.; Beydoun, N.; Pfeffer, M. *J. Chem. Soc., Dalton Trans.* **1989**, 1715–1720.

48. Wehman, E.; Koten, G.; Jastrzebski, J. T. B. H. *J. Chem. Soc., Dalton Trans.* **1988**, 2975–2981.

49. Sokolov, V. I.; Reutov, O. A. *Coord. Chem. Rev.* **1978**, *27*, 89–107.

50. Sole, D.; Vallverdu, L.; Solans, X.; Font-Bardia, M.; Bonjoch, J. *J. Am. Chem. Soc.* **2003**, *125*, 1587–1594.

51. Lewis, L. N. *J. Am. Chem. Soc.* **1986**, *108*, 743–749.

52. Le Bras, J.; Muzart, J. *Chem. Rev.* **2011**, *111*, 1170–1214.

53. Ohff, M.; Ohff, A.; Milstein, D. *Chem. Commun.* **1999**, 357–358.

54. (a) Iyer, S.; Ramesh, C.; *Tetrahedron Lett.* **2000**, *41*, 8981–8984. (b) Alonso, D. A.; Najera, C.; Pacheco, M. C. *Org. Lett*. **2000**, *13*, 1823–1826.

55. Gai, Xi.; Grigg, R.; Ramzan, M. I.; Sridharan, V.; Collardb, S.; Muirb, J. E. *Chem. Commun,* **2000**, 2053–2054.

56. (a) Vyvyan, J. R.; Peterson, E. A.; Stephan, M. L. *Tetrahedron Lett.* **1999**, 4947–4949. (b) Marshall, J. A.; Johns, B. A. *J. Org. Chem.* **1998**, *63*, 7885–7892. (c) Evans, D. A.; Ng, H. P.; Rieger, D. L. *J. Am. Chem. Soc.* **1993**, *115*, 11446–11459.

57. Weissman, H.; Milstein, D. *Chem. Commun.* **1999**, 1901–1902.

58. Zhou, W.-J.; Wang, K.-H.; Wang, J.-X. *J. Org. Chem.* **2009**, *74*, 5599–5602.

59. Li, X.; Yang, F.; Wu, Y. *J. Org. Chem.* **2013**, *78*, 4543–4550.

60. Dieguez, M.; Pamies, O.; Clave, C. *Chem. Rev*. **2004**, *104*, 3189–3215.

61. Fernandez-Perez, H.; Etayo, P.; Panossian, A.; Vidal-Ferran, A. *Chem. Rev*. **2011**, *111*, 2119–2176.

62. Wild, S. B. *Coord. Chem. Rev.* **1997**, *166*, 291–311.

63. (a) Roberts, N. K.; Wild, S. B. *J. Am. Chem. Soc.* **1979**, 6254–6260. (b) Allen, D. G.; McLaughlin, G. M.; Robertson, G. B.; Steffen, W. L.; Salem, G.; Wild, S. B. *Inorg. Chem.* **1982,** *21*, 1007–1014.

64. Leung, P.- H.; McLaughlin, G. M.; Martin, J. W. L.; Wild, S. B. *Inorg. Chem.* **1986,** *25,* 3392–3395.

65. Pabel, M.; Willis, A.C.; Wild, S. B. *Tetrahedron: Asymmetry* 1995, 6, 2369–2374.

66. Pabel, M.; Willis, A.C.; Wild, S. B. *Inorg. Chem.* **1996**, *35*, 1244–1249.

67. Chooi, S. Y. M.; Siah, S.-Y.; Leung, P.-H.; Mok, K. F. *Inorg. Chem.* **1993**, *32*, 4812–4818.

68. He, G.; Mok, K. F.; Leung, P.-H. *Organometallics* **1999**, *18*, 4027–4031.

69. Leung, P.-H.; Quek, G. H.; Lang, H.; Liu, A. M.; Mok, K. F.; White, A. J. P.; Williams, D J.; Rees, N. H.; McFarlane, W. *J. Chem. Soc., Dalton Trans.* **1998**, 1639–1644

70. Huang, Y.; Pullarkat, S. A.; Li, Y.; Leung, P.-H. *Inorg. Chem.* **2012**, *51*, 2533−2540.

71. Leung, P.-H. *Acc. Chem. Res.* **2004**, *37*, 169−177.

72. (a) Sawamura, M.; Ito, Y. *Chem. Rev.*, **1992**, *92*, 857; (b) Gladiali, S.; Alberico, E. *Phosphorus Ligands in Asymmetric Catalysis; Synthesis and Applications*; Boerner, A., Ed., Wiley-VCH; 2008; p. 73; (c) Luhr, S.; Holz, J.; Borner, A. *ChemCatChem*, **2011**, 1708.

73. (a) Mann, F. G.; Millar, I. T. *J. Chem. Soc.*, **1952**, 4453; (b) Weiner, M. A.; Pasternack, G. *J. Org. Chem.*, **1969**, *34*, 1130.

74. (a) Hoff, M. C.; Hill, P. *J. Org. Chem.* **1959**, *24*, 356; (b) Dombek, B. D. *J. Org. Chem.*, **1978**, *43*, 3408.

75. Rauhut, M. M.; Hechenbleikner, I.; Currier, H. A.; Schaefer, F. C.; Wystrach, V. P. *J. Am. Chem. Soc.* **1959**, 1103–1107.

76. Rauhut, M. M.; Currier, H. A.; Semsel, A. M.; Wystrach, V. P. *J. Org. Chem.* **1961**, *26*, 5138−5145.

77. For example: (a) Shulyupin, M. O.; Kazankova, M. A.; Beletskaya, I. P. *Org. Lett.* **2002**, *4*, 761. (b) Kondoh, A.; Yorimitsu, H.; Oshima, K. *J. Am. Chem. Soc.* **2007**, *129*, 4099. (c) Sadow, A. D.; Haller, I.; Fadini, L.; Togni, A. *J. Am. Chem. Soc.* **2004**, *126*, 1470. (d) Behrle, A. C.; Schmidt, J. A. R. *Organometallics* **2013**,

32, 1141. (e) Rosenberg, L. *ACS Catal.* **2013**, *3*, 2845. (f) Kawaguchia, S.-i.; Ogawa, A. *Synlett.* **2013**; *24*, 2199. (f) Huang, Y.; Pullarkat, S. A.; Li, Y.; Leung, P.-H. *Inorg. Chem*., 2012, *5*1, 2533; (g) Chew, R. J.; Huang, Y.; Li, Y.; Pullarkat, S. A.; Leung, P.-H. *Adv. Synth. Catal.*, **2013**, *355*, 1403 and references cited therein.

78. (a) Tang, L.; Zhang, Y.; Ding, L.; Li, Y.; Mok, K.-F.; Yeo, W.-C.; Leung, P.-H. *Tetrahedron Lett.* **2007**, *48*, 33–35. (b) Zhang, Y.; Pullarkat, S. A.; Li, Y.; Leung, P.-H. *Inorg. Chem*., **2009**, *48*, 5535 and references cited therein; (c) Chen, K.; Pullarkat, S. A.; Ma, M.; Y Li, Y.; Leung, P.-H. *Dalton Trans*., **2012**, *41*, 539; (d) Pullarkat, S. A.; Leung, P.-H. *Chiral Metal Complex Promoted Asymmetric Hydrophosphinations*, Topics in Organometallic Chemistry: Hydrofunctionalization; Springer: Berlin Heidelberg, 2013; Vol. 43, pp. 145−166. (e) Ding, Y.; Zhang, Y.; Li, Y.; Pullarkat, S. A.; Andrews, P.; Leung, P.-H. *Eur. J. Inorg. Chem.* **2010**, 4427.

79. Pearson, D. E. *Synthesis*, **1976**, *9*, 621−623.

80. (a) Ritter, J. J.; Minieri, P. P. *J. Am. Chem. Soc.* **1948**, *70*, 4045. (b) Ritter, J. J.; Kalish, J. J. *J. Am. Chem. Soc.* **1948**, *70*, 4048.

81. Claisen L.; Eisleb, O. *Liebigs Ann. Chem.* **1913**, *401*, 21–119.

82. Balderman, D.; Kalir, A. *Synthesis* **1978**, *1*, 24−25.

83. (a) Vicente, J.; Saura-Llamas, I. *Comments on Inorganic Chemistry*, **2007**, *28*, 39−72. (b) Muzart, J. *J. Mol. Catal. A: Chem.* **2009**, *308*, 15 and references therein. (c) Carroll, J.; Gagnier, J. P.; Garner, A. W.; Moots, J. G.; Pike, R. D.; Li, Y.; Huo, S. *Organometallics* **2013**, *32*, 4828. (d) Dunina, V. V.; Golovan, E. B. *Inorg. Chem. Commun.* **1998**, *1*, 12. (e) Trzeciak, A. M.; Ciunik, Z.; Ziolkowski, J. J. *Organometallic*, **2002**, *21*, 132−137.

84. Hopf, H.; Hucker, J.; Ernst, L. *Pol. J. Chem.* **2007**, *81*, 947.

85. Kuzmina, L. G.; Struchkov, Yu. T.; Dunina, V. V.; Zalevskaya, O. A.; Potapov, V. M. *Zh. Obshch. Khim.* **1987**, *57*, 599.

86. Bondi, A. *J. Phys. Chem.* **1964**, *68*, 441.

87. (a) Hockless, D. C. R.; Gugger, P. A.; Leung, P.-H. Mayadunne, R. C.; Pabel, M.; Wild; S. B. *Tetrahedron* **1997**, *53*, 4083. (b) Ng, J. K.-P.; Chen, S.; Tan, G.-K., Leung, P.-H. *Eur. J. Inorg. Chem.* **2007**, 3124–3134.

88. (a) Dunina, V. V.; Gorunova, O. N. *Russ. Chem. Rev.* **2005**, *74*, 871. (b) Vicente, J.; Abad, J.-A.; Martıinez-Viviente, E. *Organometallics* **2002**, *21*, 4454. (c) Vicente, J.; Arcas, A.; Bautista, D. *Organometallics* **1997**, *16*, 2127. (d) Vicente, J.; Arcas, A.; Bautista, D.; Ramirez de Arellano, M. C. *J. Organomet. Chem.* **2002**, *663*, 164.

89. (a) Dunina, V. V. ; Razmyslova, E. D.; Kuzmina, L.G.; Churakov, A. V.; Rubina, M. Y.; Grishina, Y. K. *Tetrahedron: Asymmetry* **1999**, *10*, 3147. (b) Dunina, V. V. *Curr. Org. Chem.* **2011**, *15*, 3415.

90. Allen, F. H.; Kennard, O.; Watson, D. G.; Brammer, L.; Orpen, A. G.; Taylor, R. *Journal of the Chemical Society, Perkin Transactions 2* **1987**, *12*, S1–S19.

APPENDICES

Table A 1-1 Crystallographic data for complex **103**

Empirical formula	$C_{34}H_{58}Cl_2N_2Pd$	
Formula weight	672.12	
Temperature	173(2) K	
Wavelength	0.71073 Å	
Crystal system	Monoclinic	
Space group	P2(1)/c	
Unit cell dimensions	a = 11.9173(5) Å	a= 90°.
	b = 17.6622(8) Å	b= 92.555(2)°.
	c = 17.0830(8) Å	g = 90°.
Volume	3592.2(3) $Å^3$	
Z	4	
Density (calculated)	1.243 Mg/m^3	
Absorption coefficient	0.688 mm^{-1}	
F(000)	1424	
Crystal size	0.30 x 0.12 x 0.06 mm^3	
Theta range for data collection	1.66 to 25.93°.	
Index ranges	-13<=h<=14, -21<=k<=21, -20<=l<=20	
Reflections collected	65159	
Independent reflections	6983 [R(int) = 0.0471]	
Completeness to theta = 25.93°	99.7 %	
Absorption correction	Semi-empirical from equivalents	
Max. and min. transmission	0.9599 and 0.8201	
Refinement method	Full-matrix least-squares on F^2	
Data / restraints / parameters	6983 / 425 / 587	
Goodness-of-fit on F^2	1.080	
Final R indices [I>2sigma(I)][ab]	R1 = 0.0430, wR2 = 0.1105	
R indices (all data)[ab]	R1 = 0.0682, wR2 = 0.1356	
Largest diff. peak and hole	0.455 and -0.660 $e.Å^{-3}$	

a $R_1 = \Sigma||F_o| - |F_c||/\Sigma|F_o|$.

b $wR_2 = \sqrt{\{\Sigma[w(F_o^2 - F_c^2)^2] / \Sigma [(w(F_o^2)^2]\}}$, $w^{-1} = \sigma^2(F_o^2) + (aP)^2 + bP$.

Table A 1-2 Atomic coordinates (x 10^4) and equivalent isotropic displacement parameters (Å^{2}x 10^3) for **103**. U(eq) is defined as one third of the trace of the orthogonalized U^{ij} tensor.

	x	y	z	U(eq)
Pd1	10000	0	0	51(1)
Pd2	5000	0	10000	46(1)
C1	8929(6)	1152(4)	2486(3)	34(2)
C1A	9356(12)	1026(9)	2680(7)	44(5)
C2	8803(3)	1342(2)	3274(2)	41(1)
C3	8081(3)	877(2)	3821(2)	47(1)
C4	7237(4)	384(3)	3358(3)	56(1)
C5	8867(5)	388(4)	4323(3)	86(2)
C6	7403(5)	1401(3)	4341(3)	94(2)
C7	9383(11)	1986(6)	3513(7)	42(3)
C8	10040(10)	2413(6)	3053(5)	46(3)
C9	10224(9)	2205(5)	2274(5)	51(1)
C10	10972(9)	2691(4)	1781(4)	52(2)
C11	11429(10)	3378(6)	2244(6)	110(5)
C12	10292(11)	3025(8)	1070(7)	68(3)
C13	12013(8)	2239(7)	1520(8)	78(3)
C14	9605(7)	1557(5)	2004(4)	42(2)
C15	9675(4)	1271(3)	1154(3)	39(2)
C16	8538(8)	1368(5)	704(6)	48(2)
C17	11108(9)	254(6)	1530(5)	57(2)
C7A	9080(30)	2073(10)	3516(15)	37(8)
C8A	9670(20)	2446(14)	2983(13)	58(11)
C9A	10110(20)	2172(11)	2276(13)	51(1)
C10A	10640(20)	2763(13)	1770(15)	111(17)
C11A	10720(20)	3568(14)	2181(15)	130(12)
C12A	10020(30)	2910(20)	968(17)	117(17)
C13A	11870(30)	2550(20)	1630(20)	117(14)
C14A	9966(14)	1420(9)	2126(10)	33(5)
C15A	10389(12)	977(10)	1434(8)	53(5)
C16A	11280(30)	413(18)	1718(17)	57(2)
C17A	8449(19)	1006(13)	812(17)	55(7)
C18	4406(9)	2481(5)	8896(7)	45(2)

C18A	4030(11)	2398(6)	8767(8)	36(4)
C19	3956(3)	3174(2)	8617(2)	41(1)
C20	3267(4)	3702(2)	9114(2)	50(1)
C21	2640(8)	3282(4)	9717(5)	103(4)
C22	2467(5)	4182(4)	8608(4)	62(2)
C23	4122(5)	4252(4)	9537(4)	68(2)
C21A	2043(14)	3368(13)	9191(18)	99(11)
C22A	3080(30)	4494(11)	8785(17)	97(14)
C23A	3750(20)	3750(17)	9951(10)	69(8)
C24	4291(11)	3375(7)	7875(6)	32(3)
C25	4932(12)	2905(5)	7434(7)	34(3)
C24A	4542(17)	3450(12)	7993(9)	27(4)
C25A	5160(20)	2968(8)	7542(14)	33(5)
C26	5300(3)	2189(2)	7693(2)	38(1)
C27	5982(4)	1697(2)	7145(3)	53(1)
C28	5292(5)	1006(3)	6865(3)	70(1)
C29	7113(4)	1449(3)	7524(4)	85(2)
C30	6260(5)	2128(3)	6395(3)	83(2)
C31	5040(8)	1980(4)	8465(5)	36(2)
C31A	4670(11)	1910(7)	8325(7)	33(4)
C32	5421(5)	1249(3)	8863(3)	32(2)
C33	6342(12)	1430(11)	9461(7)	54(3)
C34	3580(14)	592(11)	8643(12)	67(6)
C32A	4684(10)	1098(5)	8650(6)	37(3)
C33A	3603(16)	650(14)	8540(20)	36(6)
C34A	6105(17)	1462(17)	9701(13)	47(6)
N1	10042(5)	462(4)	1118(4)	46(2)
N1A	9484(12)	537(10)	1000(10)	52(5)
N2	4457(5)	848(3)	9228(3)	33(1)
N2A	5021(9)	1060(6)	9473(6)	40(3)
Cl1	10883(1)	1042(1)	-506(1)	77(1)
Cl2	4150(1)	635(1)	10988(1)	66(1)

Table A 2-1 Crystallographic data for complex **104**

Empirical formula	C21 H40 Cl2 N2 Pd	
Formula weight	497.85	
Temperature	173(2) K	
Wavelength	0.71073 Å	
Crystal system	Monoclinic	
Space group	P2(1)/c	
Unit cell dimensions	a = 10.7196(2) Å	a= 90°.
	b = 20.1379(4) Å	b= 103.7510(10)°.
	c = 11.9190(2) Å	g = 90°.
Volume	2499.21(8) Å^3	
Z	4	
Density (calculated)	1.323 Mg/m^3	
Absorption coefficient	0.964 mm^{-1}	
F(000)	1040	
Crystal size	0.34 x 0.30 x 0.16 mm^3	
Theta range for data collection	1.96 to 34.59°.	
Index ranges	-17<=h<=17, -32<=k<=30, -19<=l<=19	
Reflections collected	62068	
Independent reflections	10593 [R(int) = 0.0465]	
Completeness to theta = 34.59°	99.4 %	
Absorption correction	None	
Max. and min. transmission	0.8611 and 0.7353	
Refinement method	Full-matrix least-squares on F^2	
Data / restraints / parameters	10593 / 51 / 276	
Goodness-of-fit on F^2	1.130	
Final R indices [I>2sigma(I)][ab]	R1 = 0.0511, wR2 = 0.1276	
R indices (all data)[ab]	R1 = 0.0760, wR2 = 0.1544	
Largest diff. peak and hole	2.655 and -2.228 e.Å^{-3}	

a $R_1 = \Sigma||F_o| - |F_c||/\Sigma|F_o|$.

b $wR_2 = \sqrt{\{\Sigma[w(F_o^2 - F_c^2)^2] / \Sigma [(w(F_o^2)^2]\}}$, $w^{-1} = \sigma^2(F_o^2) + (aP)^2 + bP$.

Table A 2-2 Atomic coordinates (x 10^4) and equivalent isotropic displacement parameters ($Å^2$x 10^3) for **104**. U(eq) is defined as one third of the trace of the orthogonalized U^{ij} tensor.

	x	y	z	U(eq)
Pd1	7154(1)	7745(1)	11184(1)	25(1)
C1	2387(4)	8350(2)	11382(4)	46(1)
C2	3569(4)	9432(3)	11949(3)	47(1)
C3	1242(4)	9420(2)	11153(4)	46(1)
C4	2498(3)	9079(2)	11049(3)	34(1)
C5	2703(3)	9139(2)	9812(3)	31(1)
C6	1760(3)	9448(2)	8954(3)	35(1)
C7	1859(3)	9511(2)	7819(3)	39(1)
C8	2913(4)	9271(2)	7459(3)	40(1)
C9	2990(5)	9311(2)	6191(3)	55(1)
C10	4326(15)	9394(12)	6040(20)	99(8)
C11	2422(17)	8631(7)	5695(14)	52(3)
C12	1870(20)	9778(9)	5491(9)	88(7)
C10A	4378(9)	9187(6)	6063(11)	42(2)
C11A	2173(16)	8783(9)	5466(13)	97(8)
C12A	2796(18)	10047(6)	5763(11)	79(5)
(13	3885(4)	8991(2)	8317(3)	45(1)
C14	3814(3)	8924(2)	9474(3)	37(1)
C15	5047(3)	8674(2)	10334(3)	33(1)
C16)	6106(3)	9195(2)	10517(4)	41(1)
C17	4521(4)	7524(2)	9578(3)	37(1)
C18	9284(4)	6798(2)	12111(3)	44(1)
C19	8348(6)	6237(3)	11774(5)	67(1)
C20	9630(3)	7914(2)	12938(3)	37(1)
C21	9034(5)	8513(2)	13363(4)	56(1)
Cl1	8520(1)	8069(1)	10051(1)	35(1)
Cl2	5840(1)	7460(1)	12371(1)	45(1)
N1	5585(3)	8066(2)	9942(2)	36(1)
N2	8663(2)	7402(1)	12445(2)	27(1)

Table A 3-1 Crystallographic data for complex (±)-**106**

Empirical formula	$C_{33}H_{54}Cl_4N_2Pd_2$	
Formula weight	833.38	
Temperature	153(2) K	
Wavelength	0.71073 Å	
Crystal system	Monoclinic	
Space group	C2/c	
Unit cell dimensions	a = 29.2325(5) Å	a= 90°.
	b = 10.4096(2) Å	b= 95.8530(10)°.
	c = 12.0601(2) Å	g = 90°.
Volume	3650.74(11) $Å^3$	
Z	4	
Density (calculated)	1.516 Mg/m^3	
Absorption coefficient	1.302 mm^{-1}	
F(000)	1704	
Crystal size	0.40 x 0.30 x 0.20 mm^3	
Theta range for data collection	2.80 to 26.39°.	
Index ranges	-36<=h<=36, -13<=k<=13, -14<=l<=15	
Reflections collected	22878	
Independent reflections	3733 [R(int) = 0.0233]	
Completeness to theta = 26.39°	99.9 %	
Absorption correction	Semi-empirical from equivalents	
Max. and min. transmission	0.7807 and 0.6239	
Refinement method	Full-matrix least-squares on F^2	
Data / restraints / parameters	3733 / 0 / 193	
Goodness-of-fit on F^2	1.067	
Final R indices [I>2sigma(I)][ab]	R1 = 0.0187, wR2 = 0.0426	
R indices (all data)[ab]	R1 = 0.0212, wR2 = 0.0444	
Largest diff. peak and hole	0.514 and -0.450 $e.Å^{-3}$	

a $R_1 = \Sigma||F_o| - |F_c||/\Sigma|F_o|$.

b $wR_2 = \sqrt{\{\Sigma[w(F_o^2 - F_c^2)^2] / \Sigma [(w(F_o^2)^2]\}}$, $w^{-1} = \sigma^2(F_o^2) + (aP)^2 + bP$.

Table A 3-2 Atomic coordinates (x 10^4) and equivalent isotropic displacement parameters ($Å^2$x 10^3) for (±)-**106**. U(eq) is defined as one third of the trace of the orthogonalized U^{ij} tensor.

	x	y	z	U(eq)
Pd1	583(1)	6890(1)	2322(1)	16(1)
C1	1195(1)	6628(2)	3178(2)	19(1)
C2	1407(1)	7370(2)	4062(2)	20(1)
C3	1194(1)	8609(2)	4439(2)	25(1)
C4	1223(1)	9643(2)	3567(2)	41(1)
C5	1404(1)	9096(2)	5572(2)	43(1)
C6	1840(1)	6970(2)	4530(2)	26(1)
C7	2061(1)	5910(2)	4140(2)	29(1)
C8	1869(1)	5216(2)	3224(2)	26(1)
C9	2131(1)	4104(2)	2762(2)	33(1)
C10	2342(1)	3211(3)	3682(3)	70(1)
C11	2508(1)	4597(3)	2099(2)	46(1)
C12	1436(1)	5613(2)	2737(2)	21(1)
C13	1204(1)	5019(2)	1683(2)	24(1)
C14	895(1)	3901(2)	1935(2)	34(1)
C15	634(1)	5599(2)	112(2)	33(1)
C16	1261(1)	7020(2)	643(2)	32(1)
C17	0	323(3)	2500	42(1)
Cl1	150(1)	7302(1)	3819(1)	20(1)
Cl2	21(1)	1252(1)	1297(1)	69(1)
N1	937(1)	6101(2)	1084(1)	22(1)

Table A 4-1 Crystallographic data for complex (±)-**113**

Empirical formula	$C_{30}H_{50}Cl_2N_2Pd$	
Formula weight	616.02	
Temperature	103(2) K	
Wavelength	0.71073 Å	
Crystal system	Monoclinic	
Space group	P2(1)/c	
Unit cell dimensions	a = 5.9168(3) Å	a= 90°.
	b = 15.5434(8) Å	b= 98.270(4)°.
	c = 17.0110(8) Å	g = 90°.
Volume	1548.19(13) $Å^3$	
Z	2	
Density (calculated)	1.321 Mg/m^3	
Absorption coefficient	0.792 mm^{-1}	
F(000)	648	
Crystal size	0.40 x 0.10 x 0.10 mm^3	
Theta range for data collection	1.78 to 26.41°.	
Index ranges	-7<=h<=7, -19<=k<=18, -21<=l<=21	
Reflections collected	13618	
Independent reflections	3178 [R(int) = 0.0566]	
Completeness to theta = 26.41°	99.7 %	
Absorption correction	Semi-empirical from equivalents	
Max. and min. transmission	0.9250 and 0.7423	
Refinement method	Full-matrix least-squares on F^2	
Data / restraints / parameters	3178 / 0 / 166	
Goodness-of-fit on F^2	1.116	
Final R indices [I>2sigma(I)][ab]	R1 = 0.0557, wR2 = 0.1381	
R indices (all data)[ab]	R1 = 0.0755, wR2 = 0.1657	
Largest diff. peak and hole	2.255 and -1.096 $e.Å^{-3}$	

a $R_1 = \Sigma||F_o| - |F_c||/\Sigma|F_o|$.

b $wR_2 = \sqrt{\{\Sigma[w(F_o^2 - F_c^2)^2] / \Sigma [(w(F_o^2)^2]\}}$, $w^{-1} = \sigma^2(F_o^2) + (aP)^2 + bP$.

Table A 4-2 Atomic coordinates (x 10^4) and equivalent isotropic displacement parameters (Å^{2}x 10^3) for (±)-**113**. U(eq) is defined as one third of the trace of the orthogonalized U^{ij} tensor.

	x	y	z	U(eq)
Pd1	5000	0	0	26(1)
C1	12651(9)	1524(4)	3871(3)	32(1)
C2	9415(10)	1168(4)	4623(3)	34(1)
C3	10207(9)	1186(3)	3803(3)	25(1)
C4	8581(8)	1703(3)	3216(3)	22(1)
C5	8156(8)	2569(3)	3351(2)	21(1)
C6	6677(8)	3033(3)	2817(3)	22(1)
C7	5519(8)	2673(3)	2118(2)	20(1)
C8	3936(8)	3244(3)	1561(3)	23(1)
C9	5106(10)	4065(4)	1337(3)	36(1)
C10	1784(10)	3455(4)	1924(3)	37(1)
C11	5887(8)	1801(3)	1986(3)	24(1)
C12	7404(9)	1335(3)	2542(3)	25(1)
C13	4600(9)	1300(3)	1290(3)	26(1)
C14	3056(9)	591(3)	1555(3)	30(1)
C15	7566(10)	1601(4)	453(3)	34(1)
Cl1	2420(2)	930(1)	-694(1)	32(1)
N1	6263(8)	928(3)	808(2)	27(1)

Table A 5-1 Crystallographic data for complex (±)-**114**

Chemical formula	$C_{36.38}H_{46.50}Cl_{1.25}NPPd$	
Formula weight	679.43	
Temperature	103(2) K	
Wavelength	0.71073 Å	
Crystal size	0.020 x 0.400 x 0.420 mm	
Crystal system	triclinic	
Space group	P -1	
Unit cell dimensions	a = 14.6326(9) Å	α = 75.523(3)°
	b = 17.0098(9) Å	β = 87.301(3)°
	c = 29.5372(17) Å	γ = 76.835(3)°
Volume	6930.8(7) $Å^3$	
Z	8	
Density (calculated)	1.302 g/cm^3	
Absorption coefficient	0.702 mm^{-1}	
F(000)	2832	
Theta range for data collection	1.27 to 29.00°	
Reflections collected	37042	
Absorption correction	multi-scan	
Max. and min. transmission	0.9900 and 0.7600	
Structure solution technique	direct methods	
Structure solution program	SHELXS-97 (Sheldrick, 2008)	
Refinement method	Full-matrix least-squares on F^2	
Refinement program	SHELXL-2013 (Sheldrick, 2013)	
Function minimized	$\Sigma\, w(F_o^2 - F_c^2)^2$	
Data / restraints / parameters	37042 / 50 / 1509	
Goodness-of-fit on F^2	1.131	
Δ/σ_{max}	0.002	
Final R indices 26558 data; >2σ(I)	R1 = 0.0822, wR2 = 0.1989	
Final R indices all data	R1 = 0.1345, wR2 = 0.2513	
Weighting scheme	$w=1/[\sigma^2(F_o^2)+(0.0742P)^2+72.7403P]$ where $P=(F_o^2+2F_c^2)/3$	
Largest diff. peak and hole	2.573 and -2.761 $eÅ^{-3}$	

Table A 5-2 Atomic coordinates and equivalent isotropic displacement parameters ($Å^2$) for (±)-**114**. U(eq) is defined as one third of the trace of the orthogonalized U^{ij} tensor.

	x	y	z	U(eq)
Pd1	0.64036(5)	0.34058(4)	0.89460(2)	0.01823(14)
Pd2	0.48236(5)	0.61611(4)	0.65665(2)	0.02253(15)
Pd3	0.06144(5)	0.65047(4)	0.35268(2)	0.02195(15)
Pd4	0.04381(5)	0.39319(4)	0.18731(2)	0.01762(14)
C1	0.7449(6)	0.2416(5)	0.8955(3)	0.0193(17)
C2	0.7462(7)	0.1765(5)	0.8742(3)	0.0237(18)
C3	0.6660(8)	0.1789(5)	0.8423(3)	0.027(2)
C4	0.6696(8)	0.2445(6)	0.7965(4)	0.032(2)
C5	0.6670(8)	0.0948(6)	0.8322(4)	0.034(2)
C6	0.8281(7)	0.1134(5)	0.8798(4)	0.030(2)
C7	0.9064(7)	0.1146(6)	0.9052(4)	0.032(2)
C8	0.9090(6)	0.1844(5)	0.9206(4)	0.0248(19)
C9	0.9996(7)	0.1892(6)	0.9424(4)	0.035(2)
C10	0.0735(8)	0.2040(9)	0.9045(5)	0.046(3)
C11	0.0364(10)	0.1135(8)	0.9825(5)	0.058(4)
C12	0.8285(6)	0.2482(5)	0.9143(3)	0.0205(17)
C13	0.8270(6)	0.3332(5)	0.9225(3)	0.0228(18)
C14	0.7976(7)	0.3381(6)	0.9725(4)	0.030(2)
C15	0.7435(7)	0.4798(5)	0.8945(4)	0.028(2)
C16	0.8005(7)	0.3991(6)	0.8388(3)	0.027(2)
C17	0.5021(6)	0.2928(5)	0.9861(3)	0.0212(17)
C18	0.4820(8)	0.2326(6)	0.0242(4)	0.030(2)
C19	0.4563(9)	0.2522(6)	0.0671(4)	0.037(2)
C20	0.4483(8)	0.3321(7)	0.0711(4)	0.033(2)
C21	0.4695(9)	0.3924(6)	0.0331(4)	0.039(3)
C22	0.4961(8)	0.3721(6)	0.9912(4)	0.033(2)
C23	0.4199(6)	0.2981(5)	0.8977(3)	0.0206(17)
C24	0.3340(7)	0.3042(5)	0.9198(3)	0.0261(19)
C25	0.2512(7)	0.3264(6)	0.8939(4)	0.028(2)
C26	0.2552(8)	0.3425(7)	0.8456(4)	0.037(2)
C27	0.3409(7)	0.3374(8)	0.8235(4)	0.038(3)
C28	0.4230(7)	0.3160(6)	0.8489(4)	0.033(2)

C29	0.5616(6)	0.1559(5)	0.9438(3)	0.0212(17)
C30	0.6454(7)	0.1133(5)	0.9679(3)	0.0265(19)
C31	0.6729(8)	0.0274(6)	0.9781(4)	0.035(2)
C32	0.6172(9)	0.9813(6)	0.9651(4)	0.043(3)
C33	0.5335(8)	0.0220(6)	0.9408(4)	0.038(2)
C34	0.5051(8)	0.1080(6)	0.9309(4)	0.032(2)
C35	0.4770(8)	0.7198(6)	0.6779(3)	0.029(2)
C36	0.5159(8)	0.7886(6)	0.6573(4)	0.030(2)
C37	0.5805(8)	0.7869(6)	0.6166(4)	0.035(2)
C38	0.5911(11)	0.8717(8)	0.5879(4)	0.050(3)
C39	0.6753(8)	0.7313(8)	0.6331(5)	0.043(3)
C40	0.5018(8)	0.8540(6)	0.6792(4)	0.033(2)
C41	0.4490(8)	0.8528(6)	0.7197(4)	0.036(2)
C42	0.4197(7)	0.7819(6)	0.7438(3)	0.029(2)
C43	0.3675(8)	0.7782(7)	0.7899(4)	0.033(2)
C44	0.2686(10)	0.8321(9)	0.7835(5)	0.055(4)
C45	0.4189(9)	0.8052(11)	0.8253(5)	0.062(4)
C46	0.4361(7)	0.7140(6)	0.7230(3)	0.0253(19)
C47	0.4236(7)	0.6278(6)	0.7485(3)	0.0245(19)
C48	0.3256(7)	0.6174(7)	0.7408(4)	0.034(2)
C49	0.4862(8)	0.4812(6)	0.7491(4)	0.032(2)
C50	0.5938(7)	0.5706(6)	0.7486(4)	0.030(2)
C51	0.3874(8)	0.7913(6)	0.5624(3)	0.030(2)
C52	0.4142(11)	0.8320(8)	0.5185(4)	0.052(3)
C53	0.3848(13)	0.9182(8)	0.5030(5)	0.067(5)
C54	0.3310(14)	0.9642(8)	0.5304(5)	0.079(6)
C55	0.3039(12)	0.9238(8)	0.5745(5)	0.067(5)
C56	0.3307(10)	0.8387(7)	0.5906(4)	0.045(3)
C57	0.4842(7)	0.6414(6)	0.5370(3)	0.026(2)
C58	0.4415(8)	0.6246(8)	0.5011(4)	0.040(3)
C59	0.4967(10)	0.5962(8)	0.4655(4)	0.045(3)
C60	0.5912(8)	0.5853(8)	0.4665(4)	0.040(3)
C61	0.6363(8)	0.6029(7)	0.5024(4)	0.038(3)
C62	0.5816(7)	0.6308(6)	0.5383(3)	0.029(2)
C63	0.3021(7)	0.6547(6)	0.5805(3)	0.0266(19)
C64	0.2779(8)	0.5842(7)	0.6105(4)	0.033(2)

C65	0.1917(8)	0.5654(7)	0.6064(4)	0.037(2)
C66	0.1276(7)	0.6177(7)	0.5728(4)	0.035(2)
C67	0.1492(7)	0.6869(7)	0.5435(4)	0.034(2)
C68	0.2343(9)	0.7057(7)	0.5474(4)	0.037(2)
C69	0.1089(7)	0.7518(5)	0.3245(3)	0.028(2)
C70	0.0699(7)	0.8144(5)	0.2833(3)	0.027(2)
C71	0.9906(7)	0.8028(6)	0.2558(4)	0.031(2)
C72	0.0317(9)	0.7436(8)	0.2249(4)	0.040(3)
C73	0.9302(9)	0.8834(7)	0.2259(5)	0.052(3)
C74	0.1140(8)	0.8813(5)	0.2688(4)	0.032(2)
C75	0.1920(8)	0.8851(6)	0.2904(4)	0.037(2)
C76	0.2373(8)	0.8207(6)	0.3272(4)	0.034(2)
C77	0.3290(9)	0.8219(7)	0.3488(5)	0.043(3)
C78	0.4118(9)	0.7889(8)	0.3197(5)	0.046(3)
C79	0.3329(11)	0.9103(8)	0.3515(6)	0.063(4)
C80	0.1950(8)	0.7518(5)	0.3417(4)	0.029(2)
C81	0.2413(7)	0.6716(5)	0.3748(3)	0.026(2)
C82	0.2149(9)	0.6671(7)	0.4263(4)	0.036(2)
C83	0.2407(8)	0.5218(6)	0.3901(4)	0.032(2)
C84	0.2526(8)	0.5986(6)	0.3120(4)	0.030(2)
C85	0.8819(8)	0.8316(6)	0.3512(3)	0.032(2)
C86	0.9447(10)	0.8758(6)	0.3613(4)	0.041(3)
C87	0.9253(12)	0.9620(7)	0.3494(5)	0.058(4)
C88	0.8416(13)	0.0055(7)	0.3267(6)	0.077(6)
C89	0.7786(13)	0.9626(8)	0.3181(5)	0.072(5)
C90	0.7985(10)	0.8752(7)	0.3287(5)	0.053(4)
C91	0.8204(7)	0.6847(5)	0.3471(3)	0.0253(19)
C92	0.8344(7)	0.6532(5)	0.3069(3)	0.0270(19)
C93	0.7611(8)	0.6274(6)	0.2899(4)	0.037(2)
C94	0.6759(8)	0.6326(6)	0.3119(4)	0.034(2)
C95	0.6615(7)	0.6626(7)	0.3516(4)	0.035(2)
C96	0.7329(7)	0.6880(7)	0.3695(4)	0.031(2)
C97	0.8977(7)	0.6964(6)	0.4321(3)	0.027(2)
C98	0.8595(10)	0.7593(7)	0.4546(4)	0.044(3)
C99	0.8457(10)	0.7398(7)	0.5017(4)	0.049(3)
C100	0.8705(8)	0.6582(7)	0.5278(4)	0.038(3)

C101	0.9068(7)	0.5960(7)	0.5059(4)	0.035(2)
C102	0.9198(7)	0.6146(6)	0.4581(4)	0.031(2)
C103	0.0880(6)	0.2850(5)	0.2352(3)	0.0180(16)
C104	0.1563(6)	0.2153(5)	0.2318(3)	0.0211(17)
C105	0.2219(7)	0.2166(6)	0.1891(4)	0.029(2)
C106	0.2954(9)	0.2653(8)	0.1922(4)	0.044(3)
C107	0.2667(9)	0.1300(6)	0.1818(5)	0.045(3)
C108	0.1700(8)	0.1460(5)	0.2697(4)	0.034(2)
C109	0.1213(8)	0.1475(6)	0.3109(4)	0.034(2)
C110	0.0611(7)	0.2196(5)	0.3171(3)	0.0248(19)
C111	0.0128(8)	0.2208(6)	0.3637(4)	0.031(2)
C112	0.9291(10)	0.1790(8)	0.3674(4)	0.047(3)
C113	0.0774(11)	0.1815(9)	0.4054(4)	0.053(3)
C114	0.0503(7)	0.2900(5)	0.2794(3)	0.0212(18)
C115	0.0002(6)	0.3755(5)	0.2834(3)	0.0207(17)
C116	0.8945(7)	0.3943(6)	0.2740(4)	0.030(2)
C117	0.9962(8)	0.5231(5)	0.2458(3)	0.029(2)
C118	0.1427(7)	0.4271(5)	0.2671(3)	0.0260(19)
C119	0.0548(7)	0.3706(5)	0.0732(3)	0.0224(19)
C120	0.1467(7)	0.3782(5)	0.0712(3)	0.0246(19)
C121	0.1902(8)	0.4000(6)	0.0286(4)	0.030(2)
C122	0.1399(9)	0.4142(6)	0.9882(4)	0.035(3)
C123	0.0484(9)	0.4063(6)	0.9898(3)	0.034(2)
C124	0.0051(8)	0.3847(6)	0.0316(3)	0.026(2)
C125	0.0214(6)	0.2267(5)	0.1404(3)	0.0200(17)
C126	0.0617(7)	0.1851(5)	0.1070(3)	0.0252(19)
C127	0.0645(8)	0.1008(5)	0.1128(3)	0.031(2)
C128	0.0284(8)	0.0578(5)	0.1534(4)	0.034(2)
C129	0.9886(7)	0.0985(5)	0.1865(4)	0.032(2)
C130	0.9846(6)	0.1827(5)	0.1811(3)	0.0221(17)
C131	0.8746(6)	0.3664(5)	0.1216(3)	0.0191(16)
C132	0.8335(8)	0.3171(5)	0.1006(3)	0.028(2)
C133	0.7371(7)	0.3371(6)	0.0926(4)	0.030(2)
C134	0.6819(7)	0.4041(6)	0.1048(4)	0.028(2)
C135	0.7215(7)	0.4526(6)	0.1260(4)	0.028(2)
C136	0.8179(7)	0.4342(5)	0.1340(3)	0.0240(19)

C137	0.1430(15)	0.8950(11)	0.4435(6)	0.089(6)
C138	0.1165(14)	0.9401(9)	0.4807(6)	0.083(6)
C139	0.0102(15)	0.9739(9)	0.4830(5)	0.091(7)
C140	0.7895(14)	0.0974(9)	0.0800(7)	0.094(6)
C141	0.7785(15)	0.0246(13)	0.1221(8)	0.121(6)
C142	0.6975(16)	0.9913(14)	0.1189(7)	0.138(7)
C143	0.6866(18)	0.9147(13)	0.1548(7)	0.138(7)
C144	0.6446(19)	0.9297(13)	0.1996(7)	0.121(6)
C145	0.6111(17)	0.8566(11)	0.2299(7)	0.111(7)
C146	0.615(2)	0.925(2)	0.3934(17)	0.100(15)
Cl1	0.52995(16)	0.47213(12)	0.87664(8)	0.0236(4)
Cl2	0.50513(17)	0.48259(14)	0.63899(8)	0.0260(5)
Cl3	0.02481(17)	0.51471(13)	0.37316(8)	0.0264(5)
Cl4	0.99649(15)	0.52972(12)	0.13509(7)	0.0205(4)
Cl5	0.5686(5)	0.9183(5)	0.3391(4)	0.083(3)
Cl6	0.5950(9)	0.8482(8)	0.4377(5)	0.127(5)
N1	0.7597(5)	0.3951(4)	0.8865(3)	0.0213(15)
N2	0.5002(6)	0.5673(4)	0.7307(3)	0.0246(16)
N3	0.2103(6)	0.6041(5)	0.3577(3)	0.0241(16)
N4	0.0470(6)	0.4356(4)	0.2494(3)	0.0216(15)
P1	0.53213(16)	0.26906(13)	0.92901(8)	0.0192(4)
P2	0.41683(19)	0.67778(15)	0.58457(8)	0.0249(5)
P3	0.91593(18)	0.71757(14)	0.36836(8)	0.0235(5)
P4	0.00277(16)	0.33866(12)	0.13090(8)	0.0180(4)

Table A 6-1 Crystallographic data for complex (R_C,$S_C$$S_N$)-**115**

Chemical formula	$C_{21}H_{34}N_2O_2Pd$	
Formula weight	452.90	
Temperature	103(2) K	
Wavelength	0.71073 Å	
Crystal size	0.040 x 0.360 x 0.420 mm	
Crystal habit	yellow plate	
Crystal system	monoclinic	
Space group	P 1 21 1	
Unit cell dimensions	a = 9.9067(5) Å	α = 90°
	b = 11.0700(5) Å	β = 117.0575(9)°
	c = 10.6301(5) Å	γ = 90°
Volume	1038.18(9) $Å^3$	
Z	2	
Density (calculated)	1.449 g/cm^3	
Absorption coefficient	0.911 mm^{-1}	
F(000)	472	
Theta range for data collection	2.33 to 31.11°	
Index ranges	-14<=h<=14, -16<=k<=16, -15<=l<=15	
Reflections collected	20323	
Independent reflections	6662 [R(int) = 0.0347]	
Coverage of independent reflections	99.7%	
Absorption correction	multi-scan	
Max. and min. transmission	0.9640 and 0.7010	
Refinement method	Full-matrix least-squares on F^2	
Refinement program	SHELXL-2013 (Sheldrick, 2013)	
Function minimized	$\Sigma\, w(F_o^2 - F_c^2)^2$	
Data / restraints / parameters	6662 / 1 / 245	
Goodness-of-fit on F^2	1.031	
Δ/σ_{max}	0.001	
Final R indices 6372 data; I>2σ(I)	R1 = 0.0228, wR2 = 0.0518	
Final R indices all data	R1 = 0.0248, wR2 = 0.0531	
Weighting scheme	$w=1/[\sigma^2(F_o^2)+(0.0262P)^2]$ where $P=(F_o^2+2F_c^2)/3$	
Absolute structure parameter	0.0(0)	
Largest diff. peak and hole	0.781 and -0.605 $eÅ^{-3}$	
R.M.S. deviation from mean	0.075 $eÅ^{-3}$	

Table A 6-2 Atomic coordinates and equivalent isotropic displacement parameters ($Å^2$) for (R_C,$S_C$$S_N$)-**115**. U(eq) is defined as one third of the trace of the orthogonalized U^{ij} tensor.

	x	y	z	U(eq)
Pd1	0.80767(2)	0.60064(3)	0.56477(2)	0.00795(5)
C1	0.0189(3)	0.5493(2)	0.7020(2)	0.0084(4)
C2	0.0681(3)	0.4552(2)	0.8023(3)	0.0098(4)
C3	0.9578(3)	0.3844(2)	0.8368(3)	0.0104(5)
C4	0.9040(3)	0.4650(3)	0.9229(3)	0.0171(5)
C5	0.0222(3)	0.2662(3)	0.9166(3)	0.0143(5)
C6	0.2241(3)	0.4342(2)	0.8777(3)	0.0123(5)
C7	0.3300(3)	0.5049(3)	0.8609(3)	0.0132(5)
C8	0.2850(2)	0.6040(4)	0.7702(2)	0.0109(4)
C9	0.4004(3)	0.6904(3)	0.7608(3)	0.0139(5)
C10	0.4230(3)	0.8007(3)	0.8563(3)	0.0203(6)
C11	0.5540(3)	0.6318(3)	0.7988(3)	0.0206(7)
C12	0.1287(3)	0.6244(2)	0.6921(2)	0.0094(5)
C13	0.0671(3)	0.7284(2)	0.5904(3)	0.0104(5)
C14	0.0452(3)	0.6939(3)	0.4432(3)	0.0145(5)
C15	0.8365(3)	0.8543(3)	0.4785(3)	0.0139(5)
C16	0.9491(3)	0.8187(3)	0.7261(3)	0.0147(5)
C17	0.5535(3)	0.4409(3)	0.4692(3)	0.0118(5)
C18	0.4767(3)	0.5637(2)	0.4203(3)	0.0111(5)
C19	0.3387(3)	0.5606(3)	0.2713(3)	0.0154(5)
C20	0.3713(3)	0.6602(3)	0.1901(3)	0.0164(5)
C21	0.5437(3)	0.6656(3)	0.2620(3)	0.0153(5)
N1	0.9185(2)	0.7623(2)	0.5890(2)	0.0094(4)
N2	0.5847(3)	0.6546(2)	0.4145(2)	0.0104(4)
O1	0.6989(2)	0.43797(17)	0.5328(2)	0.0132(4)
O2	0.4718(2)	0.35117(19)	0.4472(2)	0.0169(4)

Table A 7-1 Crystallographic data for complex (S_C,$S_C S_N$)-**115**

Chemical formula	$C_{23.40}H_{40}N_2O_{2.60}Pd$	
Formula weight	497.37	
Temperature	103(2) K	
Wavelength	0.71073 Å	
Crystal size	0.060 x 0.080 x 0.400 mm	
Crystal habit	colorless needle	
Crystal system	monoclinic	
Space group	P 1 21 1	
Unit cell dimensions	a = 15.002(2) Å	α = 90°
	b = 32.905(4) Å	β = 110.553(4)°
	c = 15.089(2) Å	γ = 90°
Volume	6974.4(17) $Å^3$	
Z	10	
Density (calculated)	1.184 g/cm^3	
Absorption coefficient	0.685 mm^{-1}	
F(000)	2612	
Theta range for data collection	1.24 to 28.05°	
Index ranges	-19<=h<=19, -43<=k<=43, -19<=l<=19	
Reflections collected	120576	
Independent reflections	33642 [R(int) = 0.1005]	
Coverage of independent reflections	99.7%	
Absorption correction	multi-scan	
Max. and min. transmission	0.9601 and 0.7712	
Structure solution technique	direct methods	
Structure solution program	SHELXS-97 (Sheldrick, 2008)	
Refinement method	Full-matrix least-squares on F^2	
Refinement program	SHELXL-97 (Sheldrick, 2008)	
Function minimized	$\Sigma\, w(F_o^2 - F_c^2)^2$	
Data / restraints / parameters	33642 / 598 / 1458	
Goodness-of-fit on F^2	1.024	
Δ/σ_{max}	0.003	
Final R indices 24330 data; I>2σ(I)	R1 = 0.0574, wR2 = 0.1399	
Final R indices all data	R1 = 0.0946, wR2 = 0.1798	
Weighting scheme	$w=1/[\sigma^2(F_o^2)+(0.0975P)^2+0.0000P]$ where $P=(F_o^2+2F_c^2)/3$	
Absolute structure parameter	0.0(0)	
Largest diff. peak and hole	1.963 and -1.366 $eÅ^{-3}$	
R.M.S. deviation from mean	0.276 $eÅ^{-3}$	

Table A 7-2 Atomic coordinates and equivalent isotropic displacement parameters (Å2) for (S_C,$S_C S_N$)-**115**. U(eq) is defined as one third of the trace of the orthogonalized U^{ij} tensor.

	x	y	z	U(eq)
Pd1	0.58860(4)	0.352425(15)	0.21527(4)	0.02316(12)
Pd2	0.66663(4)	0.248119(16)	0.94899(4)	0.02257(12)
Pd3	0.34211(4)	0.147156(16)	0.86686(4)	0.02138(12)
Pd4	0.28705(4)	0.445523(16)	0.94242(4)	0.02193(12)
Pd5	0.52084(4)	0.546288(15)	0.80707(4)	0.02171(12)
C1	0.5648(6)	0.3474(2)	0.3385(5)	0.0279(16)
C2	0.5177(6)	0.3738(2)	0.3809(6)	0.0286(17)
C3	0.4703(6)	0.4133(2)	0.3329(6)	0.0349(19)
C4	0.3802(7)	0.4027(3)	0.2501(7)	0.045(2)
C5	0.4489(7)	0.4452(3)	0.3971(7)	0.046(2)
C6	0.5075(7)	0.3613(3)	0.4664(6)	0.038(2)
C7	0.5412(7)	0.3249(3)	0.5067(6)	0.044(2)
C8	0.5838(7)	0.2966(3)	0.4643(6)	0.040(2)
C9	0.6108(8)	0.2528(3)	0.5038(7)	0.054(3)
C10	0.5268(10)	0.2239(3)	0.4677(8)	0.068(4)
C11	0.6534(10)	0.2493(5)	0.6125(8)	0.098(5)
C12	0.5928(6)	0.3086(2)	0.3787(5)	0.0280(16)
C13	0.6279(7)	0.2800(3)	0.3213(6)	0.040(2)
C14	0.7361(8)	0.2831(4)	0.3456(8)	0.061(3)
C15	0.6052(8)	0.2674(2)	0.1531(7)	0.044(2)
C16	0.4675(7)	0.2797(2)	0.1963(7)	0.039(2)
C17	0.6505(5)	0.3844(2)	0.0690(5)	0.0265(16)
C18	0.6519(6)	0.4226(2)	0.1271(6)	0.0285(18)
C19	0.7511(6)	0.4404(3)	0.1703(6)	0.0407(19)
C20	0.7859(8)	0.4277(4)	0.2744(8)	0.045(3)
C20A	0.747(4)	0.4595(11)	0.258(3)	0.035(5)
C21	0.6969(6)	0.4295(3)	0.2968(6)	0.0355(18)
C22	0.8090(5)	0.2438(2)	0.9786(6)	0.0281(16)
C23	0.8814(6)	0.2719(2)	0.0190(7)	0.036(2)
C24	0.8648(6)	0.3121(3)	0.0567(7)	0.038(2)
C25	0.9209(8)	0.3473(3)	0.0365(8)	0.054(3)
C26	0.8906(9)	0.3116(4)	0.1668(8)	0.071(3)

C27	0.9746(6)	0.2586(3)	0.0318(9)	0.057(3)
C28	0.9961(7)	0.2199(3)	0.0095(10)	0.061(3)
C29	0.9257(6)	0.1919(3)	0.9766(8)	0.044(2)
C30	0.9498(7)	0.1489(3)	0.9586(8)	0.053(3)
C31	0.0308(9)	0.1472(4)	0.9222(12)	0.088(4)
C32	0.9712(8)	0.1252(3)	0.0497(9)	0.059(3)
C33	0.8324(6)	0.2038(2)	0.9588(6)	0.0324(18)
C34	0.7501(6)	0.1740(2)	0.9263(6)	0.0316(18)
C35	0.7019(7)	0.1735(3)	0.8199(7)	0.047(2)
C36	0.5943(6)	0.1631(2)	0.9431(7)	0.039(2)
C37	0.7305(6)	0.1790(2)	0.0790(6)	0.0324(18)
C38	0.4744(5)	0.2778(2)	0.8748(6)	0.0266(16)
C39	0.5315(5)	0.3148(2)	0.8649(6)	0.0275(16)
C40	0.5091(6)	0.3279(3)	0.7606(6)	0.0322(18)
C41	0.6005(6)	0.3490(2)	0.7655(6)	0.0324(17)
C42	0.6775(6)	0.3220(2)	0.8322(6)	0.0318(18)
C43	0.2673(5)	0.1432(2)	0.7295(6)	0.0286(16)
C44	0.2530(6)	0.1717(3)	0.6559(6)	0.0333(18)
C45	0.3086(6)	0.2105(3)	0.6688(7)	0.047(2)
C46	0.4110(15)	0.1998(9)	0.668(3)	0.058(6)
C47	0.260(2)	0.2457(9)	0.598(3)	0.071(7)
C46A	0.391(2)	0.2047(8)	0.629(3)	0.052(6)
C47A	0.238(2)	0.2467(8)	0.620(2)	0.057(6)
C48	0.1910(7)	0.1607(3)	0.5616(7)	0.052(3)
C49	0.1445(7)	0.1243(3)	0.5451(6)	0.047(2)
C50	0.1607(6)	0.0948(3)	0.6157(7)	0.043(2)
C51	0.1070(12)	0.0542(5)	0.5968(9)	0.040(4)
C52	0.9999(10)	0.0638(8)	0.530(2)	0.044(6)
C53	0.148(2)	0.0252(6)	0.538(2)	0.040(6)
C51A	0.1170(12)	0.0521(5)	0.5925(10)	0.053(5)
C52A	0.0090(14)	0.0509(9)	0.568(3)	0.054(6)
C53A	0.155(2)	0.0287(8)	0.524(3)	0.054(7)
C54	0.2252(5)	0.1051(3)	0.7074(5)	0.0304(18)
C55	0.2606(6)	0.0730(3)	0.7894(6)	0.0338(19)
C56	0.1958(7)	0.0711(3)	0.8467(7)	0.043(2)
C57	0.3984(7)	0.0627(2)	0.9346(5)	0.0339(19)

C58	0.4235(6)	0.0795(2)	0.7912(6)	0.0311(18)
C59	0.4013(5)	0.1772(2)	0.0580(5)	0.0228(15)
C60	0.3517(5)	0.2133(2)	0.0019(5)	0.0232(15)
C61	0.2626(6)	0.2278(2)	0.0233(6)	0.0353(19)
C62	0.2015(6)	0.2474(3)	0.9324(6)	0.040(2)
C63	0.2106(6)	0.2180(3)	0.8590(7)	0.042(2)
C64	0.1618(5)	0.4368(2)	0.8398(5)	0.0254(16)
C65	0.1041(6)	0.4627(2)	0.7689(6)	0.0314(17)
C66	0.1390(6)	0.5047(3)	0.7538(6)	0.037(2)
C67	0.1807(8)	0.5031(3)	0.6740(7)	0.049(2)
C68	0.0608(8)	0.5372(3)	0.7368(7)	0.052(3)
C69	0.0195(5)	0.4468(3)	0.7028(6)	0.0349(18)
C70	0.9906(6)	0.4074(3)	0.7019(7)	0.046(2)
C71	0.0482(6)	0.3802(2)	0.7698(7)	0.0350(19)
C72	0.0202(6)	0.3348(3)	0.7666(8)	0.047(2)
C73	0.0560(8)	0.3120(3)	0.6963(10)	0.070(4)
C74	0.9142(7)	0.3272(3)	0.7394(10)	0.068(4)
C75	0.1315(5)	0.3956(2)	0.8370(6)	0.0324(18)
C76	0.2020(6)	0.3677(2)	0.9079(6)	0.0334(18)
C77	0.1868(7)	0.3659(3)	0.0029(7)	0.045(2)
C78	0.3168(6)	0.3779(2)	0.8273(6)	0.0309(18)
C79	0.3761(5)	0.3648(2)	0.9930(6)	0.0330(18)
C80	0.4340(5)	0.4803(2)	0.1059(5)	0.0246(15)
C81	0.3652(6)	0.5148(2)	0.0714(6)	0.0271(17)
C82	0.3256(6)	0.5307(3)	0.1451(7)	0.043(2)
C83	0.2240(7)	0.5446(3)	0.0858(7)	0.049(2)
C84	0.1927(6)	0.5146(3)	0.0081(7)	0.039(2)
C85	0.6165(5)	0.5409(2)	0.7409(5)	0.0211(14)
C86	0.6825(6)	0.5695(2)	0.7313(6)	0.0327(18)
C87	0.6925(7)	0.6121(2)	0.7750(7)	0.039(2)
C88	0.7500(8)	0.6073(3)	0.8829(8)	0.057(3)
C89	0.7421(10)	0.6434(3)	0.7333(10)	0.076(4)
C90	0.7419(7)	0.5564(3)	0.6848(7)	0.041(2)
C91	0.7428(6)	0.5179(3)	0.6526(6)	0.038(2)
C92	0.6827(6)	0.4881(2)	0.6679(6)	0.0281(16)
C93	0.6870(6)	0.4437(2)	0.6384(6)	0.0312(17)

C94	0.7569(6)	0.4199(2)	0.7207(6)	0.0336(19)
C95	0.7159(7)	0.4391(3)	0.5496(6)	0.043(2)
C96	0.6201(5)	0.5009(2)	0.7120(5)	0.0245(15)
C97	0.5576(5)	0.4712(2)	0.7417(5)	0.0233(15)
C98	0.4574(6)	0.4681(2)	0.6653(6)	0.0343(19)
C99	0.4912(6)	0.4634(2)	0.8676(6)	0.0333(19)
C100	0.6525(6)	0.4806(2)	0.9085(6)	0.0289(18)
C101	0.3639(5)	0.5762(2)	0.8570(5)	0.0231(15)
C102	0.3860(5)	0.6117(2)	0.8048(5)	0.0252(16)
C103	0.3055(6)	0.6258(3)	0.7160(6)	0.0376(19)
C104	0.3546(8)	0.6434(4)	0.6530(9)	0.037(3)
C4A	0.3356(11)	0.6090(7)	0.6371(13)	0.038(4)
C105	0.4384(6)	0.6157(3)	0.6706(6)	0.0355(18)
N1	0.5714(6)	0.2909(2)	0.2197(5)	0.0333(16)
N2	0.6202(4)	0.41365(19)	0.2100(4)	0.0244(13)
N3	0.6849(4)	0.18642(19)	0.9762(5)	0.0297(15)
N4	0.6374(4)	0.30805(18)	0.9058(5)	0.0253(13)
N5	0.3591(5)	0.08620(19)	0.8460(5)	0.0280(14)
N6	0.3150(4)	0.20603(18)	0.8959(5)	0.0243(13)
N7	0.2988(5)	0.38466(19)	0.9179(5)	0.0254(13)
N8	0.2786(4)	0.50448(19)	0.9843(4)	0.0243(13)
N9	0.5567(5)	0.48585(18)	0.8342(5)	0.0252(14)
N10	0.4699(5)	0.60442(19)	0.7727(4)	0.0259(14)
O1	0.6187(4)	0.35127(15)	0.0895(3)	0.0268(11)
O2	0.6815(4)	0.38712(16)	0.0032(4)	0.0319(13)
O3	0.5175(3)	0.24606(16)	0.9140(4)	0.0294(11)
O4	0.3858(4)	0.28137(15)	0.8462(4)	0.0304(12)
O5	0.4126(4)	0.14557(16)	0.0147(4)	0.0294(11)
O6	0.4332(4)	0.18015(16)	0.1457(4)	0.0331(13)
O7	0.4194(4)	0.44871(15)	0.0537(3)	0.0260(11)
O8	0.5011(4)	0.48461(16)	0.1804(4)	0.0292(12)
O9	0.4171(3)	0.54475(16)	0.8705(3)	0.0277(11)
O10	0.2953(4)	0.57913(15)	0.8836(4)	0.0285(12)
O11	0.4081(8)	0.5702(4)	0.4176(11)	0.151(4)
C106	0.5815(9)	0.5879(6)	0.4588(12)	0.123(5)
C107	0.4807(10)	0.5996(5)	0.4183(13)	0.123(5)

C108	0.3118(10)	0.5869(5)	0.3729(14)	0.129(5)
C109	0.2314(11)	0.5588(6)	0.3657(16)	0.165(7)
O12	0.9829(10)	0.4674(4)	0.0852(9)	0.139(4)
C110	0.9155(11)	0.4929(5)	0.9135(10)	0.105(4)
C111	0.9435(11)	0.5013(5)	0.0180(9)	0.099(4)
C112	0.0091(13)	0.4757(5)	0.1870(11)	0.123(5)
C113	0.0583(17)	0.4440(6)	0.2624(14)	0.176(7)
O13	0.2287(11)	0.3411(4)	0.4441(11)	0.075(4)
C114	0.194(2)	0.3898(7)	0.5560(17)	0.086(7)
C115	0.1578(14)	0.3585(6)	0.4808(14)	0.061(4)
C116	0.1975(14)	0.3102(6)	0.3688(14)	0.063(5)
C117	0.2641(15)	0.2861(7)	0.3343(17)	0.067(5)
O14	0.0494(12)	0.7077(5)	0.5672(11)	0.085(4)
C118	0.9977(15)	0.7029(6)	0.7137(13)	0.062(5)
C119	0.0637(16)	0.6974(8)	0.6636(14)	0.079(5)
C120	0.1130(13)	0.6943(6)	0.5193(12)	0.055(4)
C121	0.0987(19)	0.7077(8)	0.4230(13)	0.082(6)

Table A 8-1 Crystallographic data for complex (*R*)-**106**

Chemical formula	$C_{32}H_{52}Cl_2N_2Pd_2$
Formula weight	748.46
Temperature	103(2) K
Wavelength	0.71073 Å
Crystal size	0.040 x 0.120 x 0.400 mm
Crystal habit	yellow plate
Crystal system	monoclinic
Space group	C 1 2 1
Unit cell dimensions	a = 24.861(2) Å α = 90°
	b = 9.4149(7) Å β = 110.369(2)°
	c = 15.2513(10) Å γ = 90°
Volume	3346.6(4) $Å^3$
Z	4
Density (calculated)	1.485 g/cm^3
Absorption coefficient	1.257 mm^{-1}
F(000)	1536
Theta range for data collection	1.42 to 31.02°
Index ranges	-36<=h<=27, -13<=k<=13, -22<=l<=22
Reflections collected	20693
Independent reflections	10439 [R(int) = 0.0409]
Coverage of independent reflections	99.7%
Absorption correction	multi-scan
Max. and min. transmission	0.9514 and 0.6333
Structure solution technique	direct methods
Structure solution program	SHELXS-97 (Sheldrick, 2008)
Refinement method	Full-matrix least-squares on F^2
Refinement program	SHELXL-97 (Sheldrick, 2008)
Function minimized	$\Sigma\, w(F_o^2 - F_c^2)^2$
Data / restraints / parameters	10439 / 2 / 357
Goodness-of-fit on F^2	1.060
Δ/σ_{max}	0.001
Final R indices 9192 data; I>2σ(I)	R1 = 0.0387, wR2 = 0.0847
Final R indices all data	R1 = 0.0490, wR2 = 0.1140
Weighting scheme	$w=1/[\sigma^2(F_o^2)+(0.0566P)^2+0.0000P]$ where $P=(F_o^2+2F_c^2)/3$
Absolute structure parameter	-0.0(0)
Largest diff. peak and hole	0.771 and -0.987 $eÅ^{-3}$
R.M.S. deviation from mean	0.258 $eÅ^{-3}$

Table A 8-2 Atomic coordinates and equivalent isotropic displacement parameters (Å2) for (*R*)-**106**. U(eq) is defined as one third of the trace of the orthogonalized U^{ij} tensor.

	x	y	z	U(eq)
Pd1	0.920041(15)	0.18860(3)	0.67665(2)	0.01396(8)
Pd2	0.824653(14)	0.31169(3)	0.47693(2)	0.01217(7)
C1	0.91806(19)	0.0429(5)	0.7697(3)	0.0135(8)
C2	0.8925(2)	0.0507(5)	0.8385(3)	0.0171(9)
C3	0.8665(2)	0.1867(6)	0.8609(3)	0.0193(9)
C4	0.8999(3)	0.2339(6)	0.9618(4)	0.0321(13)
C5	0.8022(2)	0.1685(6)	0.8440(4)	0.0289(12)
C6	0.8935(2)	0.9284(6)	0.8899(3)	0.0211(10)
C7	0.9180(2)	0.8043(6)	0.8760(3)	0.0219(10)
C8	0.9469(2)	0.7961(5)	0.8130(3)	0.0169(9)
C9	0.9771(2)	0.6597(6)	0.8031(4)	0.0243(11)
C10	0.9454(3)	0.5268(7)	0.8071(6)	0.0448(18)
C11	0.0362(3)	0.6513(7)	0.8766(4)	0.0379(15)
C12	0.9477(2)	0.9190(5)	0.7621(3)	0.0157(9)
C13	0.9813(2)	0.9299(6)	0.6969(3)	0.0185(9)
C14	0.9467(3)	0.8825(6)	0.5969(3)	0.0254(12)
C15	0.0261(3)	0.1193(7)	0.6319(4)	0.0336(14)
C16	0.0411(2)	0.1194(7)	0.7936(4)	0.0266(12)
C17	0.82363(19)	0.3350(4)	0.3464(3)	0.0133(9)
C18	0.8515(2)	0.4367(5)	0.3104(3)	0.0140(9)
C19	0.8845(2)	0.5627(5)	0.3658(3)	0.0152(9)
C20	0.8582(3)	0.7024(6)	0.3222(5)	0.0391(15)
C21	0.9473(2)	0.5597(7)	0.3755(4)	0.0287(12)
C22	0.8461(2)	0.4242(5)	0.2165(3)	0.0178(9)
C23	0.8150(2)	0.3153(6)	0.1603(3)	0.0202(9)
C24	0.7843(2)	0.2178(5)	0.1933(3)	0.0149(9)
C25	0.7504(2)	0.0980(5)	0.1304(3)	0.0189(10)
C26	0.7927(3)	0.9955(7)	0.1094(5)	0.0321(13)
C27	0.7048(3)	0.1514(6)	0.0391(4)	0.0332(13)
C28	0.78796(19)	0.2324(4)	0.2862(3)	0.0126(8)
C29	0.7535(2)	0.1436(5)	0.3311(3)	0.0147(9)
C30	0.7865(2)	0.0086(5)	0.3735(4)	0.0206(10)

C31	0.7142(2)	0.1563(5)	0.4586(3)	0.0185(10)
C32	0.7023(2)	0.3534(5)	0.3553(3)	0.0167(9)
Cl1	0.92214(5)	0.36007(15)	0.55553(9)	0.0248(3)
Cl2	0.82503(5)	0.26479(13)	0.63639(8)	0.0179(2)
N1	0.74286(16)	0.2375(4)	0.4034(3)	0.0118(7)
N2	0.99837(18)	0.0866(5)	0.7002(3)	0.0206(9)

Table A 9-1 Crystallographic data for complex (*S*)-**116**

Chemical formula	$C_{28}H_{39}ClNPPd$	
Formula weight	562.42	
Temperature	103(2) K	
Wavelength	0.71073 Å	
Crystal size	0.100 x 0.180 x 0.400 mm	
Crystal habit	yellow block	
Crystal system	orthorhombic	
Space group	P 21 21 21	
Unit cell dimensions	a = 9.0815(3) Å	α = 90°
	b = 15.2127(5) Å	β = 90°
	c = 19.8010(7) Å	γ = 90°
Volume	2735.59(16) $Å^3$	
Z	4	
Density (calculated)	1.366 g/cm^3	
Absorption coefficient	0.850 mm^{-1}	
F(000)	1168	
Theta range for data collection	7.54 to 43.26°	
Index ranges	-8<=h<=17, -26<=k<=29, -37<=l<=38	
Reflections collected	45409	
Independent reflections	20209 [R(int) = 0.0595]	
Coverage of independent reflections	98.4%	
Absorption correction	multi-scan	
Max. and min. transmission	0.9200 and 0.7270	
Refinement method	Full-matrix least-squares on F^2	
Refinement program	SHELXL-2013 (Sheldrick, 2013)	
Function minimized	$\Sigma\, w(F_o^2 - F_c^2)^2$	
Data / restraints / parameters	20209 / 0 / 298	
Goodness-of-fit on F^2	0.976	
Δ/σ_{max}	0.002	
Final R indices 15516 data; I>2σ(I)	R1 = 0.0484, wR2 = 0.0798	
Final R indices all data	R1 = 0.0732, wR2 = 0.0897	
Weighting scheme	$w=1/[\sigma^2(F_o^2)+(0.0272P)^2]$ where $P=(F_o^2+2F_c^2)/3$	
Absolute structure parameter	-0.0(0)	
Largest diff. peak and hole	1.234 and -1.011 $eÅ^{-3}$	
R.M.S. deviation from mean	0.123 $eÅ^{-3}$	

Table A 9-2 Atomic coordinates and equivalent isotropic displacement parameters ($Å^2$) for (*S*)-**116**. U(eq) is defined as one third of the trace of the orthogonalized U^{ij} tensor.

	x	y	z	U(eq)
Pd1	0.66945(2)	0.57094(2)	0.11398(2)	0.01242(3)
C1	0.8338(3)	0.48524(14)	0.09423(12)	0.0137(3)
C2	0.8336(3)	0.39283(15)	0.09868(12)	0.0160(4)
C3	0.6998(3)	0.33907(16)	0.11891(18)	0.0220(5)
C4	0.6185(4)	0.3114(3)	0.0546(2)	0.0373(8)
C5	0.7364(4)	0.2588(2)	0.1623(2)	0.0394(9)
C6	0.9574(3)	0.34720(18)	0.07587(16)	0.0205(5)
C7	0.0782(3)	0.38963(18)	0.04862(16)	0.0206(5)
C8	0.0786(3)	0.48051(17)	0.04041(14)	0.0164(4)
C9	0.2059(3)	0.52552(19)	0.00423(16)	0.0211(5)
C10	0.1719(4)	0.5341(2)	0.92895(16)	0.0291(6)
C11	0.3528(3)	0.4772(2)	0.01392(18)	0.0263(6)
C12	0.9555(3)	0.52693(16)	0.06348(13)	0.0137(4)
C13	0.9431(3)	0.62535(16)	0.05427(15)	0.0165(4)
C14	0.9946(3)	0.67334(17)	0.11747(18)	0.0233(5)
C15	0.7543(3)	0.73873(19)	0.03715(19)	0.0275(6)
C16	0.7525(3)	0.6098(2)	0.96886(15)	0.0251(6)
C17	0.4435(3)	0.45242(17)	0.22991(14)	0.0159(4)
C18	0.3104(3)	0.48304(19)	0.20338(15)	0.0203(5)
C19	0.1821(3)	0.4362(2)	0.21320(15)	0.0238(5)
C20	0.1850(3)	0.3576(2)	0.24925(16)	0.0240(5)
C21	0.3162(3)	0.32689(18)	0.27575(15)	0.0224(5)
C22	0.4459(3)	0.37424(18)	0.26659(15)	0.0189(5)
C23	0.5988(3)	0.60837(19)	0.27218(15)	0.0201(5)
C24	0.7094(3)	0.6054(2)	0.31707(15)	0.0238(5)
C25	0.7376(5)	0.6733(3)	0.3702(2)	0.0394(9)
C26	0.9435(4)	0.5177(3)	0.35016(19)	0.0343(8)
C27	0.8048(3)	0.5271(2)	0.30970(14)	0.0218(5)
C28	0.7601(3)	0.47036(19)	0.26171(15)	0.0191(5)
Cl1	0.46543(6)	0.67292(4)	0.11997(4)	0.01915(11)
N1	0.7840(2)	0.64307(14)	0.03745(12)	0.0170(4)
P1	0.60966(7)	0.51679(4)	0.21548(3)	0.01377(11)

Table A 10-1 Crystallographic data for complex (±)-**119**

Empirical formula	$C_{25.5}H_{33.5}Cl_4N_2O_4Pd_2$	
Formula weight	786.64	
Temperature	103(2) K	
Wavelength	0.71073 Å	
Crystal system	Monoclinic	
Space group	C2/c	
Unit cell dimensions	a = 16.5309(3) Å	a= 90°.
	b = 25.6674(4) Å	b= 94.7660(10)°.
	c = 15.1461(3) Å	g = 90°.
Volume	6404.3(2) $Å^3$	
Z	8	
Density (calculated)	1.632 Mg/m^3	
Absorption coefficient	1.488 mm^{-1}	
F(000)	3140	
Crystal size	0.40 x 0.24 x 0.04 mm^3	
Theta range for data collection	3.85 to 37.20°.	
Index ranges	-28<=h<=28, -43<=k<=43, -25<=l<=9	
Reflections collected	55693	
Independent reflections	16434 [R(int) = 0.0448]	
Completeness to theta = 37.20°	99.5 %	
Absorption correction	Semi-empirical from equivalents	
Max. and min. transmission	0.9429 and 0.5874	
Refinement method	Full-matrix least-squares on F^2	
Data / restraints / parameters	16434 / 77 / 388	
Goodness-of-fit on F^2	1.024	
Final R indices [I>2sigma(I)][ab]	R1 = 0.0347, wR2 = 0.0761	
R indices (all data)[ab]	R1 = 0.0596, wR2 = 0.0875	
Largest diff. peak and hole	0.912 and -1.181 e.$Å^{-3}$	

a $R_1 = \Sigma||F_o| - |F_c||/\Sigma|F_o|$.

b $wR_2 = \sqrt{\{\Sigma[w(F_o^2 - F_c^2)^2] / \Sigma [(w(F_o^2)^2]\}}$, $w^{-1} = \sigma^2(F_o^2) + (aP)^2 + bP$.

Table A 10-2 Atomic coordinates (x 10^4) and equivalent isotropic displacement parameters ($Å^2$x 10^3) for (±)-**119**. U(eq) is defined as one third of the trace of the orthogonalized U^{ij} tensor.

	x	y	z	U(eq)
Pd1	3496(1)	697(1)	3641(1)	15(1)
Pd2	2267(1)	580(1)	5121(1)	15(1)
C1	3803(1)	1426(1)	3381(1)	19(1)
C2	4154(1)	1824(1)	3918(2)	24(1)
C3	4290(1)	2321(1)	3601(2)	31(1)
C4	4076(2)	2444(1)	2726(2)	34(1)
C5	3738(2)	2057(1)	2169(2)	29(1)
C6	3602(1)	1561(1)	2484(2)	22(1)
C7	3269(1)	1125(1)	1896(1)	21(1)
C8	3960(1)	831(1)	1506(2)	26(1)
C9	2568(1)	286(1)	2027(1)	21(1)
C10	2021(1)	1062(1)	2635(2)	22(1)
C11	2831(1)	-363(1)	4248(1)	16(1)
C12	2862(1)	-952(1)	4170(2)	24(1)
C13	4142(1)	558(1)	5490(1)	19(1)
C14	4847(1)	503(1)	6178(2)	28(1)
C15	2644(1)	1509(1)	6284(2)	28(1)
C16	2006(1)	1706(1)	4840(2)	23(1)
C17	1210(1)	1286(1)	5918(1)	17(1)
C18	1218(1)	1013(1)	6816(1)	23(1)
C19	686(1)	985(1)	5237(1)	15(1)
C20	1083(1)	607(1)	4745(1)	14(1)
C21	588(1)	328(1)	4126(1)	16(1)
C22	-250(1)	394(1)	4005(1)	19(1)
C23	-628(1)	756(1)	4514(1)	20(1)
C24	-148(1)	1051(1)	5115(1)	18(1)
C25	6371(13)	2244(7)	6627(11)	74(5)
C26	5950(13)	2739(6)	6501(12)	87(6)
C27	5434(12)	2935(7)	7157(15)	103(6)
C28	4791(12)	2552(8)	7511(15)	93(6)
C29	4474(8)	2791(7)	8349(9)	54(4)
C30	3610(9)	2562(9)	8495(14)	73(5)

Cl1	4452(1)	1740(1)	5042(1)	32(1)
Cl2	3506(1)	2209(1)	1056(1)	44(1)
Cl3	978(1)	-144(1)	3442(1)	19(1)
Cl4	-629(1)	1517(1)	5734(1)	25(1)
N1	2790(1)	788(1)	2476(1)	18(1)
N2	2039(1)	1319(1)	5579(1)	18(1)
O1	3210(1)	-103(1)	3721(1)	19(1)
O2	2410(1)	-188(1)	4843(1)	19(1)
O3	4317(1)	592(1)	4695(1)	21(1)
O4	3446(1)	573(1)	5757(1)	21(1)

Table A 11-1 Crystallographic data for complex (R_C,$S_C$$S_N$)-**124**

Empirical formula	$C_{15}H_{20}Cl_2N_2O_2Pd$	
Formula weight	437.63	
Temperature	103(2) K	
Wavelength	0.71073 Å	
Crystal system	Tetragonal	
Space group	P4(1)	
Unit cell dimensions	a = 8.8546(3) Å	a= 90°.
	b = 8.8546(3) Å	b= 90°.
	c = 22.2760(9) Å	g = 90°.
Volume	1746.53(11) $Å^3$	
Z	4	
Density (calculated)	1.664 Mg/m^3	
Absorption coefficient	1.375 mm^{-1}	
F(000)	880	
Crystal size	0.40 x 0.20 x 0.14 mm^3	
Theta range for data collection	2.30 to 31.09°.	
Index ranges	-12<=h<=11, -11<=k<=12, -27<=l<=32	
Reflections collected	12460	
Independent reflections	5319 [R(int) = 0.0389]	
Completeness to theta = 31.09°	99.7 %	
Absorption correction	Semi-empirical from equivalents	
Max. and min. transmission	0.8308 and 0.6092	
Refinement method	Full-matrix least-squares on F^2	
Data / restraints / parameters	5319 / 1 / 202	
Goodness-of-fit on F^2	1.036	
Final R indices [I>2sigma(I)][ab]	R1 = 0.0307, wR2 = 0.0593	
R indices (all data)[ab]	R1 = 0.0343, wR2 = 0.0608	
Absolute structure parameter	-0.04(2)	
Largest diff. peak and hole	0.352 and -0.458 $e.Å^{-3}$	

a $R_1 = \Sigma||F_o| - |F_c||/\Sigma|F_o|$.

b $wR_2 = \sqrt{\{\Sigma[w(F_o^2 - F_c^2)^2] / \Sigma [(w(F_o^2)^2]\}}$, $w^{-1} = \sigma^2(F_o^2) + (aP)^2 + bP$.

Table A 11-2 Atomic coordinates (x 10^4) and equivalent isotropic displacement parameters (Å^{2}x 10^3) for (R_C,$S_C$$S_N$)-**124**. U(eq) is defined as one third of the trace of the orthogonalized U^{ij} tensor.

	x	y	z	U(eq)
Pd1	8093(1)	3661(1)	907(1)	9(1)
C1	7857(3)	5363(3)	322(1)	10(1)
C2	8658(3)	5769(3)	-195(1)	13(1)
C3	8327(3)	7042(3)	-535(1)	18(1)
C4	7162(4)	7974(3)	-374(1)	20(1)
C5	6333(3)	7616(3)	133(1)	18(1)
C6	6667(3)	6353(3)	480(1)	13(1)
C7	5765(3)	5963(3)	1032(1)	11(1)
C8	4329(3)	5085(4)	875(1)	21(1)
C9	5976(4)	4245(3)	1909(1)	20(1)
C10	7852(4)	6143(3)	1739(1)	19(1)
C11	8769(3)	698(3)	1374(1)	13(1)
C12	9177(3)	608(3)	708(1)	14(1)
C13	10605(3)	-305(3)	580(1)	19(1)
C14	11884(3)	880(4)	552(1)	21(1)
C15	11104(3)	2386(4)	679(1)	16(1)
Cl1	10149(1)	4674(1)	-469(1)	22(1)
Cl2	4841(1)	8799(1)	331(1)	34(1)
N1	6810(3)	5073(3)	1432(1)	13(1)
N2	9513(2)	2167(3)	486(1)	12(1)
O1	8203(2)	1962(2)	1554(1)	14(1)
O2	8958(2)	-409(2)	1701(1)	18(1)

Table A 12-1 Crystallographic data for complex (S_C,$S_C S_N$)-**124**

Empirical formula	$C_{15}H_{20}Cl_2N_2O_2Pd$	
Formula weight	437.63	
Temperature	103(2) K	
Wavelength	0.71073 Å	
Crystal system	Monoclinic	
Space group	P2(1)	
Unit cell dimensions	a = 6.7161(2) Å	a= 90°.
	b = 8.8109(3) Å	b= 102.6990(10)°.
	c = 14.4813(5) Å	g = 90°.
Volume	835.97(5) $Å^3$	
Z	2	
Density (calculated)	1.739 Mg/m^3	
Absorption coefficient	1.437 mm^{-1}	
F(000)	440	
Crystal size	0.40 x 0.16 x 0.14 mm^3	
Theta range for data collection	1.44 to 33.14°.	
Index ranges	-10<=h<=10, -13<=k<=5, -22<=l<=22	
Reflections collected	10095	
Independent reflections	4480 [R(int) = 0.0162]	
Completeness to theta = 33.14°	99.9 %	
Absorption correction	Semi-empirical from equivalents	
Max. and min. transmission	0.8242 and 0.5972	
Refinement method	Full-matrix least-squares on F^2	
Data / restraints / parameters	4480 / 1 / 206	
Goodness-of-fit on F^2	1.106	
Final R indices [I>2sigma(I)][ab]	R1 = 0.0181, wR2 = 0.0434	
R indices (all data)[ab]	R1 = 0.0187, wR2 = 0.0479	
Absolute structure parameter	0.002(18)	
Largest diff. peak and hole	1.433 and -0.665 $e.Å^{-3}$	

a $R_1 = \Sigma||F_o| - |F_c||/\Sigma|F_o|$.

b $wR_2 = \sqrt{\{\Sigma[w(F_o^2 - F_c^2)^2] / \Sigma [(w(F_o^2)^2]\}}$, $w^{-1} = \sigma^2(F_o^2) + (aP)^2 + bP$.

Table A 12-2 Atomic coordinates (x 10^4) and equivalent isotropic displacement parameters (Å^{2}x 10^3) for (S_C,$S_C S_N$)-**124**. U(eq) is defined as one third of the trace of the orthogonalized U^{ij} tensor.

	x	y	z	U(eq)
Pd1	9773(1)	9865(1)	1962(1)	10(1)
C1	11327(3)	9269(2)	3255(1)	11(1)
C2	12867(3)	8201(2)	3566(1)	12(1)
C3	13914(3)	8074(2)	4507(1)	14(1)
C4	13420(3)	9016(2)	5183(1)	14(1)
C5	11864(3)	10071(2)	4906(1)	12(1)
C6	10859(3)	10225(2)	3965(1)	11(1)
C7	9182(3)	11359(2)	3632(1)	12(1)
C8	7129(3)	10611(3)	3619(2)	18(1)
C9	11244(4)	12861(3)	2773(2)	19(1)
C10	7626(4)	12733(3)	2166(2)	20(1)
C11	8256(2)	9779(4)	-45(1)	13(1)
C12	8809(3)	8127(2)	188(1)	14(1)
C13	6946(4)	7088(3)	-121(2)	33(1)
C14	7166(4)	5893(3)	658(2)	23(1)
C15	8157(4)	6780(3)	1540(2)	22(1)
Cl1	13581(1)	6937(1)	2764(1)	18(1)
Cl2	11149(1)	11207(1)	5770(1)	17(1)
N1	9421(3)	11856(2)	2668(1)	14(1)
N2	9607(3)	7855(2)	1229(1)	12(1)
O1	8276(3)	10682(2)	654(1)	17(1)
O2	7784(2)	10154(2)	-889(1)	19(1)

Table A 13-1 Crystallographic data for complex (*R*)-**118**

Chemical formula	$C_{21}H_{26}Cl_8N_2Pd_2$	
Formula weight	802.84	
Temperature	153(2) K	
Wavelength	0.71073 Å	
Crystal size	0.080 x 0.400 x 0.400 mm	
Crystal habit	yellow plate	
Crystal system	monoclinic	
Space group	P 1 21 1	
Unit cell dimensions	a = 8.8703(8) Å	α = 90°
	b = 14.2235(13) Å	β = 95.270(2)°
	c = 11.1660(11) Å	γ = 90°
Volume	1402.8(2) $Å^3$	
Z	2	
Density (calculated)	1.901 g/cm^3	
Absorption coefficient	2.059 mm^{-1}	
F(000)	788	
Theta range for data collection	1.83 to 31.01°	
Index ranges	-12<=h<=12, -20<=k<=20, -16<=l<=16	
Reflections collected	34184	
Independent reflections	8961 [R(int) = 0.0335]	
Coverage of independent reflections	100.0%	
Absorption correction	multi-scan	
Max. and min. transmission	0.8526 and 0.4931	
Structure solution technique	direct methods	
Structure solution program	SHELXS-97 (Sheldrick, 2008)	
Refinement method	Full-matrix least-squares on F^2	
Refinement program	SHELXL-97 (Sheldrick, 2008)	
Function minimized	$\Sigma\, w(F_o^2 - F_c^2)^2$	
Data / restraints / parameters	8961 / 1 / 304	
Goodness-of-fit on F^2	1.173	
Δ/σ_{max}	0.002	
Final R indices8625 data; I>2σ(I)	R1 = 0.0214, wR2 = 0.0522	
Final R indices all data	R1 = 0.0240, wR2 = 0.0672	
Weighting scheme	$w=1/[\sigma^2(F_o^2)+(0.0317P)^2+0.3742P]$ where $P=(F_o^2+2F_c^2)/3$	
Absolute structure parameter	-0.0(0)	
Largest diff. peak and hole	0.618 and -0.708 $eÅ^{-3}$	
R.M.S. deviation from mean	0.172 $eÅ^{-3}$	

Table A 13-2 Atomic coordinates and equivalent isotropic displacement parameters ($Å^2$) for (*R*)-**118**. U(eq) is defined as one third of the trace of the orthogonalized U^{ij} tensor.

	x	y	z	U(eq)
Pd1	0.96779(2)	0.001125(13)	0.399312(18)	0.01547(5)
Pd2	0.23656(2)	0.982299(13)	0.650153(18)	0.01451(5)
C1	0.7550(3)	0.9620(2)	0.3484(3)	0.0173(5)
C2	0.6752(3)	0.8805(2)	0.3686(3)	0.0198(5)
C3	0.5217(3)	0.8714(2)	0.3306(3)	0.0242(6)
C4	0.4455(3)	0.9421(3)	0.2657(3)	0.0276(7)
C5	0.5249(3)	0.0204(2)	0.2373(3)	0.0244(6)
C6	0.6774(3)	0.0320(2)	0.2777(3)	0.0194(6)
C7	0.7658(3)	0.1183(2)	0.2537(3)	0.0224(6)
C8	0.7493(4)	0.1902(2)	0.3532(4)	0.0316(8)
C9	0.9413(4)	0.0310(3)	0.1386(3)	0.0319(7)
C10	0.0307(4)	0.1684(3)	0.2457(4)	0.0324(8)
C11	0.2585(3)	0.9196(2)	0.8103(3)	0.0155(5)
C12	0.1500(3)	0.8909(2)	0.8867(3)	0.0183(5)
C13	0.1892(3)	0.8402(2)	0.9912(3)	0.0218(6)
C14	0.3387(4)	0.8187(2)	0.0242(3)	0.0236(6)
C15	0.4485(3)	0.8520(2)	0.9552(3)	0.0202(6)
C16	0.4116(3)	0.9025(2)	0.8500(3)	0.0164(5)
C17	0.5277(3)	0.9412(2)	0.7725(3)	0.0181(5)
C18	0.5784(4)	0.8667(2)	0.6851(3)	0.0269(7)
C19	0.4518(4)	0.1050(2)	0.7951(3)	0.0248(6)
C20	0.5435(3)	0.0571(3)	0.6087(3)	0.0273(7)
C21	0.0238(4)	0.6631(3)	0.2742(4)	0.0372(8)
Cl1	0.75796(9)	0.78212(5)	0.44056(8)	0.02512(15)
Cl2	0.43183(10)	0.10732(7)	0.14839(9)	0.0364(2)
Cl3	0.00251(8)	0.91887(5)	0.57978(7)	0.02185(14)
Cl4	0.22142(8)	0.05749(6)	0.45547(7)	0.02250(14)
Cl5	0.95866(7)	0.91870(6)	0.85875(7)	0.02554(15)
Cl6	0.63773(9)	0.83001(7)	0.00328(8)	0.03077(17)
Cl7	0.91801(12)	0.67787(10)	0.13508(12)	0.0542(3)
Cl8	0.15185(13)	0.75406(9)	0.30821(11)	0.0502(3)
N1	0.9281(3)	0.08643(19)	0.2496(3)	0.0217(5)
N2	0.4554(3)	0.02521(18)	0.7079(2)	0.0179(5)

Table A 14-1 Crystallographic data for complex (*S*)-**118**

Chemical formula	$C_{10.50}H_{13}Cl_4NPd$	
Formula weight	401.42	
Temperature	103(2) K	
Wavelength	0.71073 Å	
Crystal size	0.120 x 0.300 x 0.400 mm	
Crystal habit	yellow block	
Crystal system	monoclinic	
Space group	P 1 21 1	
Unit cell dimensions	a = 8.8571(2) Å	α = 90°
	b = 14.1867(3) Å	β = 95.0910(10)°
	c = 11.1258(3) Å	γ = 90°
Volume	1392.48(6) $Å^3$	
Z	4	
Density (calculated)	1.915 g/cm^3	
Absorption coefficient	2.074 mm^{-1}	
F(000)	788	
Theta range for data collection	2.82 to 30.53°	
Index ranges	-12<=h<=12, -16<=k<=20, -15<=l<=15	
Reflections collected	14642	
Independent reflections	7623 [R(int) = 0.0255]	
Coverage of independent reflections	99.0%	
Absorption correction	multi-scan	
Max. and min. transmission	0.7889 and 0.4909	
Structure solution technique	direct methods	
Structure solution program	SHELXS-97 (Sheldrick, 2008)	
Refinement method	Full-matrix least-squares on F^2	
Refinement program	SHELXL-97 (Sheldrick, 2008)	
Function minimized	$\Sigma\, w(F_o^2 - F_c^2)^2$	
Data / restraints / parameters	7623 / 1 / 304	
Goodness-of-fit on F^2	1.010	
Δ/σ_{max}	0.001	
Final R indices 7393 data; I>2σ(I)	R1 = 0.0226, wR2 = 0.0460	
Final R indices all data	R1 = 0.0237, wR2 = 0.0466	
Weighting scheme	$w=1/[\sigma^2(F_o^2)+(0.0115P)^2+0.0000P]$ where $P=(F_o^2+2F_c^2)/3$	
Absolute structure parameter	-0.0(0)	
Largest diff. peak and hole	0.480 and -0.730 $eÅ^{-3}$	
R.M.S. deviation from mean	0.095 $eÅ^{-3}$	

Table A 14-2 Atomic coordinates and equivalent isotropic displacement parameters ($Å^2$) for (*S*)-**118**. U(eq) is defined as one third of the trace of the orthogonalized U^{ij} tensor.

	x	y	z	U(eq)
Pd1	0.031615(19)	0.980133(12)	0.601515(16)	0.01086(4)
Pd2	0.762896(19)	0.999243(13)	0.350211(16)	0.01003(4)
C1	0.2451(3)	0.01928(19)	0.6519(2)	0.0131(5)
C2	0.3257(3)	0.10137(19)	0.6318(2)	0.0154(5)
C3	0.4789(3)	0.1101(2)	0.6691(3)	0.0179(6)
C4	0.5549(3)	0.0393(2)	0.7340(3)	0.0191(6)
C5	0.4745(3)	0.9603(2)	0.7632(2)	0.0171(6)
C6	0.3228(3)	0.94949(19)	0.7228(2)	0.0141(5)
C7	0.2339(3)	0.8621(2)	0.7466(3)	0.0163(5)
C8	0.2517(3)	0.7901(2)	0.6471(3)	0.0221(6)
C9	0.0589(3)	0.9492(2)	0.8634(2)	0.0224(6)
C10	0.9693(3)	0.8112(2)	0.7552(3)	0.0229(6)
C11	0.7419(3)	0.06208(18)	0.1903(2)	0.0102(5)
C12	0.8506(3)	0.09021(19)	0.1135(2)	0.0139(5)
C13	0.8116(3)	0.1415(2)	0.0087(2)	0.0161(5)
C14	0.6632(3)	0.16357(19)	0.9754(2)	0.0163(5)
C15	0.5515(3)	0.13011(19)	0.0448(2)	0.0148(5)
C16	0.5887(3)	0.07945(18)	0.1503(2)	0.0116(5)
C17	0.4716(3)	0.04064(19)	0.2274(2)	0.0131(5)
C18	0.4203(3)	0.1146(2)	0.3144(3)	0.0193(6)
C19	0.5476(3)	0.8768(2)	0.2044(3)	0.0188(6)
C20	0.4548(3)	0.9249(2)	0.3915(3)	0.0205(6)
C21	0.9766(3)	0.3207(2)	0.7247(3)	0.0263(7)
Cl1	0.77766(7)	0.92347(5)	0.54551(6)	0.01620(13)
Cl2	0.99691(7)	0.06341(5)	0.42085(6)	0.01618(13)
Cl3	0.24179(8)	0.19998(5)	0.56019(7)	0.01894(14)
Cl4	0.56889(8)	0.87365(6)	0.85209(7)	0.02541(17)
Cl5	0.04235(7)	0.06232(5)	0.14094(6)	0.01854(13)
Cl6	0.36265(7)	0.15202(5)	0.99546(6)	0.02135(14)
Cl7	0.08294(9)	0.30430(7)	0.86346(8)	0.0368(2)
Cl8	0.84800(10)	0.22758(6)	0.69070(8)	0.03422(19)
N1	0.0715(2)	0.89386(17)	0.7508(2)	0.0156(5)
N2	0.5444(2)	0.95642(16)	0.2919(2)	0.0129(5)

Table A 15-1 Crystallographic data for complex (*S*)-**119**

Chemical formula	$C_{25}H_{32}Cl_6N_2O_4Pd_2$
Formula weight	850.03
Temperature	153(2) K
Wavelength	0.71073 Å
Crystal size	0.140 x 0.400 x 0.420 mm
Crystal habit	yellow block
Crystal system	orthorhombic
Space group	P 21 21 21
Unit cell dimensions	a = 12.2303(15) Å α = 90°
	b = 12.5092(16) Å β = 90°
	c = 20.828(3) Å γ = 90°
Volume	3186.5(7) $Å^3$
Z	4
Density (calculated)	1.772 g/cm^3
Absorption coefficient	1.665 mm^{-1}
F(000)	1688
Theta range for data collection	1.90 to 37.15°
Index ranges	-20<=h<=8, -21<=k<=21, -35<=l<=35
Reflections collected	41684
Independent reflections	16228 [R(int) = 0.0393]
Coverage of independent reflections	99.2%
Absorption correction	multi-scan
Max. and min. transmission	0.8003 and 0.5414
Structure solution technique	direct methods
Structure solution program	SHELXS-97 (Sheldrick, 2008)
Refinement method	Full-matrix least-squares on F^2
Refinement program	SHELXL-97 (Sheldrick, 2008)
Function minimized	$\Sigma\, w(F_o^2 - F_c^2)^2$
Data / restraints / parameters	16228 / 0 / 360
Goodness-of-fit on F^2	1.056
Δ/σ_{max}	0.003
Final R indices 14427 data; I>2σ(I)	R1 = 0.0319, wR2 = 0.0679
Final R indices all data	R1 = 0.0400, wR2 = 0.0799
Weighting scheme	$w=1/[\sigma^2(F_o^2)+(0.0342P)^2+0.1632P]$ where $P=(F_o^2+2F_c^2)/3$
Absolute structure parameter	-0.0(0)
Largest diff. peak and hole	0.923 and -1.364 $eÅ^{-3}$
R.M.S. deviation from mean	0.154 $eÅ^{-3}$

Table A 15-2 Atomic coordinates and equivalent isotropic displacement parameters ($Å^2$) for (*S*)-**119**. U(eq) is defined as one third of the trace of the orthogonalized U^{ij} tensor.

	x	y	z	U(eq)
Pd1	0.134623(13)	0.159971(13)	0.942831(8)	0.01272(3)
Pd2	0.232438(14)	0.964643(14)	0.86276(8)	0.01462(3)
C1	0.13944(19)	0.13376(17)	0.03806(10)	0.0146(3)
C2	0.0973(2)	0.05189(19)	0.07635(12)	0.0182(4)
C3	0.1186(2)	0.0419(2)	0.14196(12)	0.0258(5)
C4	0.1829(2)	0.1170(2)	0.17238(13)	0.0272(5)
C5	0.2246(2)	0.2009(2)	0.13602(12)	0.0215(4)
C6	0.20343(18)	0.21142(19)	0.07073(11)	0.0164(4)
C7	0.2411(2)	0.30458(18)	0.03110(11)	0.0171(4)
C8	0.1534(2)	0.3915(2)	0.03166(13)	0.0223(5)
C9	0.2747(2)	0.3495(2)	0.91691(12)	0.0225(4)
C10	0.3678(2)	0.2020(2)	0.96566(13)	0.0216(4)
C11	0.14199(19)	0.15264(19)	0.79378(11)	0.0171(4)
C12	0.1137(2)	0.2056(2)	0.73115(13)	0.0267(5)
C13	0.99055(19)	0.98225(19)	0.90086(12)	0.0175(4)
C14	0.8778(2)	0.9334(2)	0.89840(15)	0.0271(5)
C15	0.39082(18)	0.97601(19)	0.84084(10)	0.0159(4)
C16	0.4511(2)	0.0546(2)	0.80865(12)	0.0195(4)
C17	0.5619(2)	0.0418(3)	0.79386(12)	0.0240(5)
C18	0.61718(19)	0.9519(2)	0.81349(12)	0.0242(5)
C19	0.56160(19)	0.8758(2)	0.84874(12)	0.0191(4)
C20	0.45065(18)	0.88623(18)	0.86181(12)	0.0162(4)
C21	0.38616(18)	0.79885(18)	0.89478(11)	0.0165(4)
C22	0.3526(2)	0.7156(2)	0.84524(13)	0.0244(5)
C23	0.2064(2)	0.7727(2)	0.94656(15)	0.0266(5)
C24	0.3300(2)	0.9059(2)	0.98635(13)	0.0250(5)
C25	0.4971(3)	0.5612(3)	0.31561(16)	0.0328(6)
Cl1	0.01310(5)	0.95128(5)	0.04511(3)	0.02382(12)
Cl2	0.30886(6)	0.29399(6)	0.17526(3)	0.02771(13)
Cl3	0.39480(6)	0.17592(5)	0.78411(3)	0.02702(13)
Cl4	0.63485(5)	0.76640(5)	0.87785(3)	0.02612(12)
Cl5	0.38272(8)	0.49245(8)	0.28391(5)	0.0467(2)

Cl6	0.53302(9)	0.51211(9)	0.39161(4)	0.0521(3)
N1	0.26214(16)	0.26127(15)	0.96418(9)	0.0156(3)
N2	0.29045(16)	0.85258(16)	0.92714(10)	0.0167(3)
O1	0.13102(15)	0.20609(14)	0.84438(8)	0.0188(3)
O2	0.17717(15)	0.05708(15)	0.78944(9)	0.0204(3)
O3	0.99576(14)	0.07594(14)	0.92401(9)	0.0186(3)
O4	0.06843(14)	0.92594(15)	0.88120(10)	0.0221(4)

Table A 16-1 Crystallographic data for complex (*S*)-**125**

Chemical formula	$C_{22}H_{25}Cl_3NPPd$	
Formula weight	547.15	
Temperature	153(2) K	
Wavelength	0.71073 Å	
Crystal size	0.300 x 0.320 x 0.420 mm	
Crystal habit	yellow block	
Crystal system	orthorhombic	
Space group	P 21 21 21	
Unit cell dimensions	a = 8.8195(2) Å	α = 90°
	b = 10.4714(2) Å	β = 90°
	c = 24.7931(5) Å	γ = 90°
Volume	2289.71(8) $Å^3$	
Z	4	
Density (calculated)	1.587 g/cm^3	
Absorption coefficient	1.239 mm^{-1}	
F(000)	1104	
Theta range for data collection	1.64 to 38.27°	
Index ranges	-15<=h<=14, -17<=k<=18, -43<=l<=43	
Reflections collected	45563	
Independent reflections	12489 [R(int) = 0.0561]	
Coverage of independent reflections	99.2%	
Absorption correction	multi-scan	
Max. and min. transmission	0.7075 and 0.6242	
Structure solution technique	direct methods	
Structure solution program	SHELXS-97 (Sheldrick, 2008)	
Refinement method	Full-matrix least-squares on F^2	
Refinement program	SHELXL-97 (Sheldrick, 2008)	
Function minimized	$\Sigma\, w(F_o^2 - F_c^2)^2$	
Data / restraints / parameters	12489 / 0 / 258	
Goodness-of-fit on F^2	1.070	
Δ/σ_{max}	0.002	
Final R indices 10607 data; I>2σ(I)	R1 = 0.0407, wR2 = 0.0862	
Final R indices all data	R1 = 0.0545, wR2 = 0.1063	
Weighting scheme	$w=1/[\sigma^2(F_o^2)+(0.0499P)^2+0.0000P]$ where $P=(F_o^2+2F_c^2)/3$	
Absolute structure parameter	-0.0(0)	
Largest diff. peak and hole	1.401 and -1.161 $eÅ^{-3}$	
R.M.S. deviation from mean	0.248 $eÅ^{-3}$	

Table A 16-2 Atomic coordinates and equivalent isotropic displacement parameters ($Å^2$) for (*S*)-**125**. U(eq) is defined as one third of the trace of the orthogonalized U^{ij} tensor.

	x	y	z	U(eq)
Pd1	0.73104(2)	0.408448(16)	0.098063(7)	0.01468(4)
C1	0.7398(3)	0.5996(2)	0.08968(9)	0.0153(4)
C2	0.7424(3)	0.6984(2)	0.12760(9)	0.0169(4)
C3	0.7572(3)	0.8262(2)	0.11396(10)	0.0193(5)
C4	0.7742(3)	0.8600(2)	0.06062(10)	0.0216(5)
C5	0.7823(3)	0.7643(2)	0.02215(10)	0.0202(5)
C6	0.7663(3)	0.6366(2)	0.03552(9)	0.0172(4)
C7	0.7777(4)	0.5305(2)	0.99457(10)	0.0197(4)
C8	0.6202(4)	0.4998(3)	0.97341(12)	0.0286(6)
C9	0.0136(3)	0.4511(3)	0.03233(14)	0.0297(6)
C10	0.8452(5)	0.3044(3)	0.98908(14)	0.0350(8)
C11	0.4369(3)	0.2672(2)	0.16375(11)	0.0180(4)
C12	0.2928(3)	0.3082(2)	0.16672(10)	0.0178(4)
C13	0.1562(3)	0.2228(3)	0.16654(13)	0.0251(5)
C14	0.1271(4)	0.5129(3)	0.17683(17)	0.0339(7)
C15	0.2794(3)	0.4494(2)	0.17153(10)	0.0188(4)
C16	0.4128(3)	0.5112(2)	0.17278(11)	0.0190(5)
C17	0.6493(3)	0.3840(2)	0.23451(10)	0.0180(4)
C18	0.5622(3)	0.4026(3)	0.28067(11)	0.0244(5)
C19	0.6297(4)	0.3902(3)	0.33088(12)	0.0306(6)
C20	0.7818(4)	0.3635(3)	0.33543(12)	0.0300(6)
C21	0.8677(4)	0.3454(3)	0.29002(13)	0.0309(6)
C22	0.8013(4)	0.3538(3)	0.23946(12)	0.0269(6)
Cl1	0.73597(9)	0.66631(5)	0.19658(2)	0.02118(12)
Cl2	0.81589(11)	0.80958(7)	0.95521(3)	0.03077(16)
Cl3	0.75731(9)	0.18339(5)	0.10518(3)	0.02744(14)
N1	0.8520(3)	0.4204(2)	0.02317(9)	0.0203(4)
P1	0.56680(7)	0.39964(6)	0.16742(3)	0.01538(11)

Table A 17-1 Crystallographic data for complex (*S*)-**127**

Chemical formula	$C_{14}H_{18}Cl_3N_3O_4Pd$	
Formula weight	505.06	
Temperature	153(2) K	
Wavelength	0.71073 Å	
Crystal size	0.080 x 0.120 x 0.400 mm	
Crystal habit	yellow needle	
Crystal system	monoclinic	
Space group	P 1 21 1	
Unit cell dimensions	a = 10.8357(8) Å	α = 90°
	b = 6.3586(4) Å	β = 108.798(2)°
	c = 14.7427(11) Å	γ = 90°
Volume	961.59(12) $Å^3$	
Z	2	
Density (calculated)	1.744 g/cm^3	
Absorption coefficient	1.405 mm^{-1}	
F(000)	504	
Theta range for data collection	1.46 to 35.66°	
Index ranges	-17<=h<=17, -10<=k<=10, -24<=l<=23	
Reflections collected	21041	
Independent reflections	8531 [R(int) = 0.0396]	
Coverage of independent reflections	99.7%	
Absorption correction	multi-scan	
Max. and min. transmission	0.8959 and 0.6034	
Structure solution technique	direct methods	
Structure solution program	SHELXS-97 (Sheldrick, 2008)	
Refinement method	Full-matrix least-squares on F^2	
Refinement program	SHELXL-97 (Sheldrick, 2008)	
Function minimized	$\Sigma\, w(F_o^2 - F_c^2)^2$	
Data / restraints / parameters	8531 / 1 / 231	
Goodness-of-fit on F^2	1.095	
Δ/σ_{max}	0.001	
Final R indices 7247 data; I>2σ(I)	R1 = 0.0370, wR2 = 0.0805	
Final R indices all data	R1 = 0.0505, wR2 = 0.1045	
Weighting scheme	$w=1/[\sigma^2(F_o^2)+(0.0482P)^2+0.0000P]$ where $P=(F_o^2+2F_c^2)/3$	
Absolute structure parameter	-0.0(0)	
Largest diff. peak and hole	0.806 and -0.665 $eÅ^{-3}$	
R.M.S. deviation from mean	0.165 $eÅ^{-3}$	

Table A 17-2 Atomic coordinates and equivalent isotropic displacement parameters ($Å^2$) for (*S*)-**127**. U(eq) is defined as one third of the trace of the orthogonalized U^{ij} tensor.

	x	y	z	U(eq)
Pd1	0.623812(19)	0.56797(4)	0.27885(14)	0.01996(5)
C1	0.6223(3)	0.7852(5)	0.1810(2)	0.0190(5)
C2	0.5291(3)	0.9300(5)	0.1320(2)	0.0228(6)
C3	0.5424(3)	0.0523(7)	0.0574(2)	0.0297(7)
C4	0.6530(4)	0.0318(5)	0.0303(2)	0.0301(8)
C5	0.7513(3)	0.8978(6)	0.0816(2)	0.0263(6)
C6	0.7383(3)	0.7775(5)	0.1565(2)	0.0214(6)
C7	0.8437(3)	0.6308(5)	0.2144(2)	0.0230(6)
C8	0.8349(4)	0.4208(6)	0.1632(3)	0.0349(8)
C9	0.9022(4)	0.4373(7)	0.3681(3)	0.0356(9)
C10	0.8613(4)	0.8071(6)	0.3661(3)	0.0301(7)
C11	0.6163(4)	0.1752(6)	0.4148(3)	0.0294(7)
C12	0.5979(5)	0.9908(7)	0.4671(3)	0.0407(9)
C13	0.3214(3)	0.5118(5)	0.2258(2)	0.0252(6)
C14	0.1813(3)	0.4913(7)	0.2033(3)	0.0347(8)
Cl1	0.39002(9)	0.98121(14)	0.16421(8)	0.0350(2)
Cl2	0.89276(10)	0.8855(2)	0.05100(7)	0.0423(2)
Cl3	0.19937(9)	0.01473(14)	0.35849(6)	0.03104(19)
N1	0.8210(2)	0.6091(4)	0.31055(18)	0.0222(6)
N2	0.6309(3)	0.3173(5)	0.3740(2)	0.0296(6)
N3	0.4298(3)	0.5353(5)	0.2410(2)	0.0268(7)
O1	0.1049(4)	0.0192(6)	0.2658(2)	0.0657(13)
O2	0.1510(4)	0.1163(6)	0.4250(3)	0.0624(11)
O3	0.3110(3)	0.1381(8)	0.3567(3)	0.0707(13)
O4	0.2282(6)	0.8053(6)	0.3852(3)	0.104(2)